Quantitative Analysis of Cubic and Quintic Nonlinear Schrodinger Equations

By

Eng. **Sherif Eid Nasr**

A thesis submitted to the

Faculty of Engineering at Cairo University

In Partial Fulfillment of the Requirements for the Degree of

Doctor of Philosophy

In

Engineering Mathematics

FACULTY OF ENGINEERING

CAIRO UNIVERSITY,

GIZA, EGYPT

April, 2010

Quantitative Analysis of Cubic and Quintic Nonlinear Schrodinger Equations

By

Eng. **Sherif Eid Nasr**

A thesis submitted to the Faculty of Engineering at Cairo University

In Partial Fulfillment of the Requirements for the Degree of

Doctor of Philosophy

In

Engineering Mathematics

Under Supervision of:

Prof. Dr. Magdy A. El Tawil

Prof. Dr. Hanafy El Zoheiry **Prof. Dr. Labib Iskander**

Engineering Mathematics & Physics Department

Faculty of Engineering

Cairo University

FACULTY OF ENGINEERING

CAIRO UNIVERSITY,

GIZA, EGYPT

April, 2010

Acknowledgments

First of all, I thank Allah for helping me to finish this work.

I would like to first than my principal advisor, Prof. Dr. Magdy A. El-Tawil, who encourage me to start working on Nonlinear Schrodinger equation. His experiences were tremendously helpful in this thesis.

I would like to thank (Prof. Dr. Hanafy El-Zoheiry and Prof. Dr. Labib iskander) for their encouragement, guidance and insight that have been invaluable with this thesis. I would like also to thank them for their fatherly support. I am forever indebted to them for revealing to me true spiritual wisdom and mathematical insight.

Finally, I would like to express my deepest gratitude to whole of my family; father, mother, wife and children.

Abstract

In this thesis and through a quantitative analysis, the cubic and quintic nonlinear Schrodinger equations had been solved approximately using two independent techniques, the Perturbation technique and the Picard approximation technique. At first, a lemma proved that the solution exists as a power series in the perturbation parameter (ε). Then, the approximate solution was obtained up to the third order using both techniques according to the computation limits in Mathematica 5.1 code. Both homogeneous and non-homogeneous cases had been studied showing the effect of the complex nonhomogenity and under the effect of complex initial conditions. Comparisons were made under the results of the two techniques for a lot of case studies which showed semi-identical results. The solution was obtained under finite time interval T. Then, a T-study was obtained under increasing T values to study the stability of the solution which showed that instability has high chances, when the parameter of dissipation (γ) vanishes.

We used a computer with core 2Duo processor 3 GHz, 3 GB RAM to perform all calculations for both Cubic (homogeneous and non-homogeneous) and Quintic Nonlinear Schrodinger Equations.

Contents

List of Figures

Chapter 1 Schrodinger Equations, Types and Applications

1.0 Introduction

The Schrodinger Wave Equation, developed by the Austrian theoretical physicist Erwin Schrodinger in 1925, defines the quantum mechanical characteristics of the electrons orbiting the nucleus and can be used to define the positions of the protons and neutrons within the "gravitational potential well of attraction" of the nucleus. The Schrodinger Wave Equation assumes the particle and wave duality characteristic of the electrons, protons, and neutrons.
It defines the total energy of the system analyzed. In words, the Schrodinger wave equation states that the kinetic energy (energy of motion of the particle) plus the potential energy (stored energy within the particle) equals the total energy of the particle. The Schrodinger wave Equation, therefore, provides a quantum mechanical approach to evaluate the total energy of the proton or neutron in the nucleus or the electron orbiting the nucleus. It is a spatial dependent and time dependent differential equations.

Analytical solutions of the time-independent Schrodinger equation can be obtained for a variety of relatively simple conditions. These solutions provide insight into the nature of quantum phenomena and sometimes provide a reasonable approximation of the behavior of more complex systems (e.g., in statistical mechanics, molecular vibrations are often approximated as harmonic oscillators). Many of the more common analytical solutions include, the free particle, the particle in a box, the finite potential well, the Delta function potential, the particle in a ring, the particle in a spherically symmetric potential, the quantum harmonic oscillator, the hydrogen atom or hydrogen-like atom, the ring wave guide and the particle in a one-dimensional lattice (periodic potential).

The one dimensional nonlinear Schrodinger equation (NLS) emerges as a first order model in a variety of fields – from high intensity laser beam propagation to Bose-Einstein condensation to water waves theory. The NLS is completely integrable, hence solvable, in one dimension on the infinite line or with periodic boundary conditions. The realization that the integrable structure might not persist under small perturbations led to the investigation of the forced and damped NLS [Cazenave and Lions, 1982].

1.1 Nonlinear Schrodinger Systems: Continuous and discrete

The Nonlinear Schrodinger (NLS) equation is a prototypical dispersive nonlinear partial differential equation (PDE) that has been derived in many areas of physics and analyzed mathematically for over 40 years. Historically the essence of NLS equations can be found in the early work of Ginzburg and Landau [Ginzburg and Landau, 1950] and Ginzburg [Ginzburg, 1956] in their study of the macroscopic theory of superconductivity, and also of Ginzburg and Pitaevskii [Ginzburg and Pitaevskii, 1958] who subsequently investigated the theory of superfluidity. Nonetheless, it was not until the works of Chiao *et al* [Chiao, 1964] and Talanov [Talanov, 1964] that the wider physical importance of NLS equation became evident, especially in connection with the phenomenon of self-focusing and the conditions under which an electromagnetic beam can propagate without spreading in nonlinear media. In the general situation, an optical beam in a dielectric broadens due to diffraction. However, in materials whose dielectric constant increases with the field intensity, the critical angle for internal reflection at the beam's boundary can become greater than the angular divergence due to diffraction and as a consequence the beam does not spread and can, in some situations, continue to focus into extremely high intensity spots.

Starting from the electromagnetic wave equation in the presence of nonlinearities and assuming a linearly polarized wave propagating along the z -axis, after a suitable rescaling of the dependent and independent variables, one can derive for the propagation of the electromagnetic field the NLS equation in standard non-dimensional form

$$i\partial_z\psi + \Delta_\perp\psi + 2|\psi|^2\psi = 0 \qquad (1.1)$$

Where ψ is proportional to the slowly varying complex envelope of the electromagnetic field, z is the propagation variable, and $\Delta_\perp$ denotes the Laplacian with respect to the transverse coordinates.

Beside the fact that NLS systems have direct applications in many physical problems, the importance of the NLS equation is also due to its universal character [Benney and Newell, 1967]. Generally speaking, most weakly nonlinear, dispersive, energy-preserving systems give rise, in an appropriate limit, to the NLS

equation. Specifically, the NLS equation provides a "canonical" description for the envelope dynamics of a quasi-monochromatic plane wave propagating in a weakly nonlinear dispersive medium when dissipation can be neglected.

Mathematically, the NLS equation attains broad significance since, in one transverse dimension; it is integrable via the Inverse Scattering Transform (IST) which is a nonlinear Fourier Transform. It admits multisoliton solutions, it has an infinite number of conserved quantities, and it possesses many other interesting properties.

There has been a vast amount of literature involving the NLS equation over the years, but recently there has been additional interest, mainly due to the developments in nonlinear optics and soft-condensed matter physics. In the optical context, the experimental developments involving localized pulses in arrays of coupled optical waveguides [Eisenberg, 1998] have drawn attention to discrete NLS models (where the fields are substituted by appropriate finite differences). Related problems involving NLS equations on a lattice background [Efremidis, 2003] have also generated considerable interest. The vector generalization of the NLS equation has been also proved to be particularly valuable from the point of view of nonlinear optics. On the other hand, the experimental realization of Bose-Einstein condensates (BECs) and their mean field modeling by the so-called Gross-Pitaevskii [Pethick and Smith, 2002] equation which, like optical pulses on a lattice background, is an NLS equation with an external potential, has opened new avenues for the study of NLS-type equations.

The following sections elucidate some of the physical and the mathematical aspects of NLS systems, both continuous and discrete, scalar and vector, in one or more spatial dimensions.

1.1.1 Scalar (1+1)-dimensional systems

The nonlinear propagation of wave packets is governed by Nonlinear Schrodinger-type systems in such diverse fields as fluid dynamics [Ablowitz and Segur, 1981], nonlinear optics [Agrawal, 2001], magnetic spin waves [Zvedzin and Popkov, 1983]and [Chen, 1994], plasma physics [Zakharov, 1972] etc.

For example, the Nonlinear Schrodinger equation describes self-compression and self-modulation of electromagnetic wave packets in weakly nonlinear media. Hasegawa and Tappert [Hasegawa and Tappert, 1973] first derived the NLS equation in fiber optics, taking into account both dispersion and nonlinearity. Detailed derivations can be found in texts [Hasegawa and Kodama, 1995].

The Nonlinear Schrodinger equation in "standard" form is given by

$$i\, q_z + q_{tt} \pm 2|q|^2 q = 0 \qquad (1.2)$$

In these notations, the focusing case is given by the (+) sign in equation (1.2), and it corresponds to anomalous dispersion. The defocusing case is obtained when the dispersion is normal, and it corresponds to the (-) sign in equation (1.2).

The Nonlinear Schrodinger equation possesses soliton solutions, which are exact solutions decaying to a background state. The focusing (+) NLS equation admits so-called "bright" solitons (namely, solutions that are localized travelling "humps"). A pure one-soliton solution of the focusing Nonlinear Schrodinger equation has the form

$$q(z,t) = \eta\, \mathrm{sech}[\eta(t + 2\xi z - t_0)]\, e^{-i\theta(z,t)} \qquad (1.3)$$

where $\theta(z,t) = \xi t + (\xi^2 - \eta^2)z + \theta_0$.

It is worth noting that in nonlinear optics and many other areas of physics solitary waves are usually called solitons, despite the fact that they generally do not interact elastically. Indeed today, most physicists and engineers use the word soliton in this broader sense.

The defocusing (-) NLS equation does not admit solitons that vanish at infinity. However, it does admit soliton solutions on a nontrivial background, called "dark" and "gray" solitons. A dark soliton is a solution of the form

$$q(z,t) = q_0 \tanh(\mathrm{q_0 t})\, e^{2iq_0{}^2 z} \qquad (1.4)$$

A gray soliton solution is

$$q(z,t) = q_0 e^{2iq_0{}^2 z}[cos\alpha + i\, sin\alpha\, tanh[sin\alpha q_0(t - 2q_0 cos\alpha z - t_0)]] \qquad (1.5)$$

Importantly, the solution of the nonlinear Schrodinger equation for both decaying initial data and for data which tend to constant amplitude at infinity were obtained by the method of the Inverse Scattering Transform (see below for a brief description) by [Zakharov and Shabat, 1972]and [Zakharov and Shabat, 1973].

One of the most remarkable properties of soliton solutions is that interacting scalar solitons affect each other only by a phase shift, that depends only on the soliton powers and velocities, but of which are conserved quantities. Thus, when two soliton collisions occur sequentially, the outcome of the first collision does not affect the second collision, except for a uniform phase shift.

In the context of small-amplitude water waves, the nonlinear Schrodinger equation was derived by Zakharov [Zakharov, 1968] for the case of infinite depth and Benney and Roskes [Benney and Roskes, 1969] for finite depth. Basically, the nonlinear Schrodinger equation is obtained from the Euler-Bernoulli equations for the dynamics of an ideal (i.e., incompressible, irrotational and inviscid) fluid under the assumption of a small amplitude quasi-monochromatic wave expansion.

Finally, it should also be mentioned that Ablowitz *et al* [Ablowitz, 1997]and [Ablowitz, 2001] have shown that, in quadratically nonlinear optical materials, more complicated nonlinear Schrodinger -type equations can arise.

1.1.2 Vector (1+1)-dimensional systems

In many applications, vector NLS (VNLS) systems are the key governing equations. Physically, the VNLS arises under conditions similar to those described by NLS whenever there are suitable multiple wave trains moving with nearly the same group velocity [Roskes, 1976]. Moreover, VNLS also models systems where the electromagnetic field has more than one component. For example, in optical fibers and waveguides, the propagating electric field has two polarized components transverse to the direction of propagation.

$$i\, u_z + u_{tt} + (|u|^2 + |v|^2)u = 0 \qquad (1.6)$$

$$i\, v_z + v_{tt} + (|u|^2 + |v|^2)v = 0 \qquad (1.7)$$

The dimensionless system in equations (1.6) and (1.7) was considered by Manakov [Manakov, 1974] as an asymptotic model governing the propagation of the electric field in a waveguide. where z is the normalized distance along the waveguide, t is a transverse coordinate and $(u, v)^T$ (the superscript T denotes matrix transpose) are the transverse components of the complex electromagnetic field envelope. Manakov was able to integrate the above Vector Nonlinear Schrodinger system by the IST method.

Subsequently, Menyuk [Menyuk, 1987] showed that in optical fibers with constant birefringence, the two polarization components $(u, v)^T$ of the complex electromagnetic field envelope orthogonal to direction of propagation along a fiber satisfy asymptotically the following non-dimensional equations

$$i\left(u_z + \delta u_t) + \frac{d}{2}u_{tt} + \ (|u|^2 + \alpha|v|^2)\right)u = 0 \tag{1.8}$$

$$i\left(v_z - \delta v_t) + \frac{d}{2}v_{tt} + \ (\alpha|u|^2 + |v|^2)\right)v = 0 \tag{1.9}$$

where δ represents the group velocity "mismatch" between the components u and v , d is the group velocity dispersion and α is a constant depending on the polarization properties of the fiber.

The physical phenomenon of birefringence implies that the phase and group velocities of the electromagnetic wave are different for each polarization component. It is important to realize, however, that the derivation of the above equations assumes that certain nonlinear (four-wave mixing) terms are neglected. In the general case, i.e. when $\delta \neq 1$, the vector Nonlinear Schrodinger system is unlikely to be integrable. However, in a communications environment, due to the distances involved, not only does the birefringence evolve, but it does so randomly and on a scale much faster than the distances required for communication transmission. In this case, Menyuk [Menyuk, 1999] showed, after averaging over the fast birefringence fluctuations, the relevant equation is the above but with $\alpha = 1$ and $\delta = 0$ that is, it reduces to the integrable Vector Nonlinear Schrodinger system derived by Manakov, which therefore attains broader relevance.

As indicated above, the Manakov system (1.8) and (1.9) is integrable, and it possesses vector soliton solutions. In the focusing case that is, with a plus sign in front of the cubic nonlinear terms. These are bright solitons whose shape is the same as that of the bright solitons of the scalar NLS equation, multiplied by a constant polarization vector. Unlike scalar solitons, however, the collision of solitons with internal degrees of freedom (e.g. vector or matrix solitons) can be highly nontrivial: even though the collision is elastic, in the sense that the total energy of each soliton is conserved, there can be a significant redistribution of energy among the components. It has been shown by Soljacic *et al* [Soljacic, 1998] that the parameters controlling the energy switching between components exhibit nontrivial transformation of information. This set forth the experimental foundations of computation with solitons. Despite the vector nature of the problem, one can show that the multisoliton interaction process is nevertheless pair-wise and the net result of the interaction is independent of the order in which such collisions occur. This interaction property can be related to the fact that the map determining the interaction of two solitons satisfies the Yang-Baxter relation [Ablowitz, 2004].

The defocusing vector nonlinear Schrodinger equation(VNLS) (1.8) and (1.9) with a (-) sign in front of the nonlinear terms admits "dark-dark soliton" solutions; i.e., solitons which have dark solitonic behavior in both components, as well as "dark-bright" soliton solutions, which contain one dark and one bright component [Kivshar and Turitsyn, 1993]. Although the mathematical properties of VNLS have been investigated for decades, the IST for the vector system under non-vanishing boundary conditions has been developed only recently.

1.1.3 Scalar multidimensional systems

The nonlinear Schrodinger equation in two spatial dimensions,

$$i\psi_t + \Delta\psi + 2|\psi|^2\psi = 0, \quad X = (x, y) \in \mathbb{R}^2 \tag{1.10}$$

has been investigated shortly after the early studies on the one-dimensional equation. Note that in optics, the transverse Laplacian, here simply indicated by Δ , describes wave diffraction. Remarkable early direct numerical simulations and scaling arguments by Kelley [Kelley, 1965] indicated that wave collapse could occur. Vlasov [Vlasov, 1971] showed that for a purely cubic nonlinearity in a self-

focusing nonlinear medium, the phenomenon of wave collapse takes place and the light beam blows up in a finite time. The proof that a finite-time singularity can occur in Eq. (1.10) is remarkably straightforward [Vlasov, 1971] and it is based on the virial theorem, see also [Ablowitz and Segur, 1979]. One can also prove rigorously [C Sulem and P L Sulem, 1999] that, for initial conditions for which the

Hamiltonian

$$H = \int \left(|\nabla\psi|^2 - \left(\frac{1}{2}\right)|\psi|^4 \right) dx \qquad (1.11)$$

is negative, there exists a time t_0 such that the quantity $\int |\nabla\psi|^2 dx$ becomes infinite as t approaches t_0, which in turn implies that ψ valso becomes infinite as $t \to t_0$ (blowup in finite time). It is worth mentioning that near blowup the solution displays universal scaling properties.

Results are also available for the more general Nonlinear Schrodinger equation in $d$spatial dimensions and with generic power nonlinearity:

$$i\psi_t + \Delta_{\mathrm{d}}\psi + 2|\psi|^{2}\psi = 0, \quad X \in \mathbb{R}^d \qquad (1.12)$$

where Δ_{d} is the Laplacian d -dimensional.

The first proof of global existence of solutions to the focusing nonlinear Schrodinger equation in the sub-critical dimension was given by Ginibre and Velo [Ginibre and Velo, 1979]. There are many references to this interesting subject; see for example [Papanicolau, 1994], [Sulem C. and Sulem PL. , 1999] and [Merle and Raphael, 2004].

Finally, we mention the Zakharov system for Langmuir turbulence in plasmas, where the mean field obeys a dynamical equation [Zakharov, 1972].

1.2 Nonlinear Schrodinger equation: Types and solutions

In general there are two types of solutions of the Schrodinger equation: travelling waves and standing waves. Linear superpositions of travelling waves are used to form wave packets describing the motions of “free” particles while standing waves (superpositions of waves travelling in opposite directions) are used to describe the states of particles bound in potential wells, e.g. of electrons in atoms, molecules and solids and of protons and neutrons in atomic nuclei.

The nonlinear Schrodinger equation (NLS) is also the second nonlinear partial differential equation (PDE) whose initial value problem was discovered to be solvable via IST method[Ablowitz Clarkson, 1991], [Emmanuel, 2008].
In the last ten decades, there are a lot of NLS problems depending on additive or multiplicative noise in the random case [Debussche and Menza, 2002] or a lot of solution methodologies in the deterministic case.

Wang M. and et al [Wang and et al, 2007] obtained the exact solutions to NLS using what they called the sub-equation method. They got four kinds of exact solutions of the equation.

$$i\,\frac{\partial u}{\partial t}+\frac{1}{2}\,\frac{\partial^2 u}{\partial z^2}+\,\alpha|u|^{P}u+\,\beta|u|^{2P}u=0 \qquad (1.13)$$

for which no sign to the initial or boundary conditions type is made.

Xu L. and Zhang J. [Xu and Zhang, 2007] followed the same previous technique in solving the higher order NLS:

$$i\,\frac{\partial u}{\partial x}-\frac{1}{2}\alpha\,\frac{\partial^2 u}{\partial t^2}+\,\beta|u|^2u+i\varepsilon\,\frac{\partial^3 u}{\partial t^3}+\,i\delta|u|^2u\frac{\partial u}{\partial t}+\,i\gamma u^2\frac{\partial u}{\partial t}=0 \qquad (1.14)$$

Sweilam N. [Sweilam, 2006] solved

$$i\,\frac{\partial u}{\partial t}+\,\frac{\partial^2 u}{\partial x^2}+\,q|u|^2u=0\,,t>0,L_0<x<\,L_1 \qquad (1.15)$$

with initial condition $u(x,0)=g(x)$ and boundary conditions $u_x(L_0,t)=u_x(L_1,t)=0$ which gives rise to solitary solutions using variational iteration method.

By using the extended hyperbolic auxiliary equation method [Zhu, 2007] in getting the exact explicit solutions to the higher order Nonlinear Schrodinger equation (NLS):

$$iq_z-\frac{\beta_1}{2}q_{tt}+\,\gamma_1|q|^2q=i\frac{\beta_2}{6}q_{ttt}+\,\frac{\beta_3}{24}q_{tttt}-\,\gamma_2|q|^4q \qquad (1.16)$$

Without any boundary conditions Sun J. and et al [Sun and et al, 2007] solved the Nonlinear Schrodinger equation (NLS) :

$$i\frac{\partial\psi}{\partial t}+\frac{\partial^2\psi}{\partial x^2}+a|\psi|^2\psi=0 \qquad (1.17)$$

with the initial condition $\psi(x,0)=\psi_0(x)$ using Lie group method.
By using coupled amplitude phase formulation, Parsezian K. and Kalithasan B. [Parsezian and Kalithasan, 2007] constructed the quartic anharmonic oscillator equation from the coupled higher order Nonlinear Schrodinger equation (NLS).

Two-dimensional grey solitons to the NLS were numerically analyzed by Sakaguchi H. and Higashiuchi T. [Sakaguchi and Higashiuchi, 2006].

The generalized derivative NLS was studied by Huang D. and et al [Huang and et al, 2007] introducing a new auxiliary equation expansion method.

El-Tawil A. and El-Hazmy A. [El-Tawil and El-Hazmy, 2007], [El-Tawil and El-Hazmy, 2009] introduce a perturbative technique to solve the cubic nonlinear schrodinger equation(CNLS):

$$i\frac{\partial u}{\partial z}+\alpha\frac{\partial^2 u}{\partial t^2}+\varepsilon|u|^2u+\gamma u=0,(t,z)\in[0,T]\,x\,[0,\infty) \qquad (1.18)$$

where $u(t,z)$ is a complex valued function which is subjected to:
initial conditions: $u(t,0)=f_1(t)+i\,f_2(t)$, a complex valued function and boundary conditions : $u(0,z)=u(T,z)=0$. with proving that the solution –if exist- of (1.18) should be a power series in ε.

The nonlinear Schrodinger equation can be solved numerically by using split-step Fourier transform (SSFT); [Ismail, 2008], [Molleneauer and Gordon , 2006], [Ruiyu, Lu, Zhonghao, Wenrui and Guosheng, 2004].

1.3 Outline of Thesis

In chapter 2, we solve cubic homogeneous nonlinear Schrodinger equation (2.1) by using two different methods; perturbation and Picard approximation in sections (2.1), (2.2) and (2.4) respectively. We introduce the methodology by using many case studies; constant, sinusoidal and exponential for initial conditions function, for each method. In section (2.6), we also compare between two methods with the same initial conditions on the same graph. At the end of this chapter; section (2.7), we introduce T study for both methods, each method separately, at different values of time; 10, 20 and 60.

In chapter 3, we solve cubic non homogeneous nonlinear Schrodinger equation (3.1) by using the same two methods illustrated in chapter 2; perturbation and Picard approximation in sections (3.1), (3.2) and (3.4) respectively. We introduce the methodology by using many case studies; constant, sinusoidal and exponential with many combinations between non homogeneous terms and initial conditions functions, for each method. In section (3.6), we also compare between two methods with the same initial conditions and non homogeneous part on the same graph. At the end of this chapter; section (3.7), we introduce T study for both methods, each method separately, at different values of time; 10, 20 and 60.

In chapter 4, we solve quintic homogeneous nonlinear Schrodinger equation (QNLS) (4.1) by using two different methods; perturbation and Picard approximation in sections (4.1), (4.2) and (4.4) respectively. We introduce the methodology by using many case studies; constant, sinusoidal and exponential for initial conditions function, for each method. In section (4.6), we also compare between two methods with the same initial conditions on the same graph. At the end of this chapter; section (4.7), we introduce T study for both methods, each method separately, at different values of time; 10, 20 and 60.

In chapter 5, we introduce the thesis summary and conclusions.

Chapter 2 Homogeneous Nonlinear Cubic Schrodinger Equations

2.0 Introduction

In this chapter, a perturbing nonlinear Schrodinger equation is studied under limited time interval, complex excitation, complex initial conditions and zero Neumann conditions. The perturbation and Picard approximation method together with the eigenfunction expansion and variational parameters methods are used to introduce an approximate solution for the perturbative nonlinear case for which a power series solution is proved to exist. Using Mathematica, the solution algorithm is tested through computing the possible orders of approximations. The method of solution is illustrated through case studies and figures.

In this chapter, a straight forward solution algorithm is introduced using the transformation from a complex solution to a two coupled equations in two real solutions, eliminating one of the solutions to get separate independent and higher order equations, and finally introducing a perturbative approximate solution to the system.

2.1 The Non-linear case

Consider the homogeneous non-linear Schrodinger equation:

$$i\,\frac{\partial u(t,z)}{\partial z} + \alpha\,\frac{\partial^2 u(t,z)}{\partial t^2} + \varepsilon|u(t,z)|^2 u(t,z) + i\,\gamma u(t,z) = 0,$$

$$(t,z) \in (0,T)x\,(0,\infty) \tag{2.1}$$

where $u(t,z)$ is a complex valued function which is subjected to:

$$I.Cs.: u(t,0) = f_1(t) + i\,f_2(t), \tag{2.2}$$

$$B.Cs.: u(0,z) = u(T,z) = 0. \tag{2.3}$$

Lemma (2.1)

The solution of equation (2.1) with the constraints (2.2), (2.3) is a power series in ε if exists.

Proof

At $\varepsilon = 0$ ($u(t,z) = u_0(t,z)$), the following linear homogeneous equation is got:

$$i\,\frac{\partial u_0(t,z)}{\partial z} + \alpha\,\frac{\partial^2 u_0(t,z)}{\partial t^2} + i\,\gamma u_0(t,z) = 0, \quad (t,z) \in (0,T)\ x\ (0,\infty) \tag{2.4}$$

$$u_0(t\,,z) = \psi_0(t\,,z) + i\,\phi_0(t\,,z) \tag{2.5}$$

By following Appendix (A), the linear Schrodinger equation (2.4) has the following solution:

$$\psi_0(t\,,z) = e^{-\gamma z}\sum_{n=0}^{\infty} T_{0n}(z)\,\sin\left(\frac{n\,\pi}{T}\right)t, \tag{2.6}$$

$$\phi_0(t\,,z) = e^{-\gamma z}\sum_{n=0}^{\infty} \tau_{0n}(z)\sin\left(\frac{n\,\pi}{T}\right)t \tag{2.7}$$

where $T_{0n}(z)$ and $\tau_{0n}(z)$ can be calculated as illustrated in the general linear case, (Appendix (A), equations (A.12), (A.13) respectively).

By following Pickard approximation, equation (2.1) can be rewritten as:

$$i\frac{\partial u_n(t,z)}{\partial z} + \alpha\,\frac{\partial^2 u_n(t,z)}{\partial t^2} + i\,\gamma u_n(t,z) = -\varepsilon|u_{n-1}(t,z)|^2 u_{n-1}(t,z), n \geq 1 \tag{2.8}$$

at $n = 1$, the iterative equation (2.8) takes the form

$$i\frac{\partial u_1(t,z)}{\partial z} + \alpha\frac{\partial^2 u_1(t,z)}{\partial t^2} + i\,\gamma u_1(t,z) = -\varepsilon|u_0(t,z)|^2 u_0(t,z) = \varepsilon k_1(t\,,z) \tag{2.9}$$

which can be solved as a linear case with zero initial and boundary conditions. The following general solution can be obtained:

$$\psi_1(t\,,z) = e^{-\gamma z}\sum_{n=0}^{\infty}(T_{0n}(z) + \varepsilon T_{1n}(z))(z)\sin\left(\frac{n\,\pi}{T}\right)t, \tag{2.10}$$

$$\phi_1(t\,,z) = e^{-\gamma z}\sum_{n=0}^{\infty}(\tau_{0n}(z) + \varepsilon \tau_{1n}(z))(z)\sin\left(\frac{n\,\pi}{T}\right)t, \tag{2.11}$$

$$u_1(t,z) = \psi_1(t,z) + i\,\phi_1(t,z), \tag{2.12}$$

$$= u_1{}^{(0)} + \varepsilon\, u_1{}^{(1)}, \tag{2.13}$$

where $u_1{}^{(0)} = u_0$.

At $n = 2$, the following equation is obtained:

$$i\frac{\partial u_2(t,z)}{\partial z} + \alpha\,\frac{\partial^2 u_2(t,z)}{\partial t^2} + i\gamma u_2(t,z) = -\varepsilon|u_1(t,z)|^2 u_1(t,z)$$

$$= \varepsilon k_2(t,z) \tag{2.14}$$

which can be solved as a linear case with zero initial and boundary conditions. The following general solution can be obtained:

$$u_2(t,z) = u_2{}^{(0)} + \varepsilon\, u_2{}^{(1)} + \varepsilon^2 u_2{}^{(2)} + \varepsilon^3\, u_2{}^{(3)} + \varepsilon^4\, u_2{}^{(4)}, \tag{2.15}$$

where $u_2{}^{(0)} = u_0$. Continuing like this, one can get:

$$u_n(t,z) = u_n{}^{(0)} + \varepsilon\, u_n{}^{(1)} + \varepsilon^2 u_n{}^{(2)} + \varepsilon^3\, u_n{}^{(3)} + \ldots + \varepsilon^{m(n)}\, u_n{}^{m(n)}. \tag{2.16}$$

where $\mathrm{m(n)}$ is an increasing polynomial in n. As $n \to \infty$, the solution (if exists) can be reached as $u(t,z) = \lim_{n\to\infty} u_n(t,z)$. Accordingly the solution is a power series in ε.

According to the previous lemma, one can assume the solution of equation (2.1) as the following:

$$u(t,z) = \sum_{n=0}^{\infty} \varepsilon^n\, u_n(t,z) \tag{2.17}$$

Let $u(t,z) = \psi(t,z) + i\,\phi(t,z), \psi, \phi$: are real valued functions. The following coupled equations are got:

$$\frac{\partial \phi(t,z)}{\partial z} = \alpha\,\frac{\partial^2 \psi(t,z)}{\partial t^2} + \varepsilon(\psi^2 + \phi^2)\psi - \gamma\phi, \tag{2.18}$$

$$\frac{\partial \psi(t,z)}{\partial z} = -\alpha\,\frac{\partial^2 \phi(t,z)}{\partial t^2} - \varepsilon(\psi^2 + \phi^2)\phi - \gamma\psi, \tag{2.19}$$

where $\psi(t,0) = f_1(t),\ \phi(t,0) = f_2(t)$, and all corresponding other I.Cs. and B.Cs. are zeros.

As a third order perturbation solution, one can assume that:

$$\psi(t\,,z\;) = \psi_0 + \;\varepsilon\psi_1 + \;\varepsilon^2\psi_2 + \;\varepsilon^3\psi_3\,, \tag{2.20}$$

$$\phi(t\,,z\;) = \phi_0 + \;\varepsilon\phi_1 + \;\varepsilon^2\phi_2 + \;\varepsilon^3\phi_3\,, \tag{2.21}$$

where $\psi_0(t,0) = f_1(t),\ \phi_0(t,0) = f_2(t)$, and all corresponding other I.C. and B.C. are zeros.

Substituting from equations (2.20) and (2.21) into equations (2.18) and (2.19) and then equating the equal powers of ε, one can get the following set of coupled equations:

$$\frac{\partial\phi_0(t,z)}{\partial z} = \;\alpha\;\frac{\partial^2\psi_0(t,z)}{\partial t^2} - \;\gamma\phi_0, \tag{2.22}$$

$$\frac{\partial\psi_0(t,z)}{\partial z} = -\,\alpha\;\frac{\partial^2\phi_0(t,z)}{\partial t^2} - \;\gamma\psi_0, \tag{2.23}$$

$$\frac{\partial\phi_1(t,z)}{\partial z} = \;\alpha\;\frac{\partial^2\psi_1(t,z)}{\partial t^2} - \;\gamma\phi_1 + \left({\psi_0}^3 + \;\psi_0{\phi_0}^2\right), \tag{2.24}$$

$$\frac{\partial\psi_1(t,z)}{\partial z} = \;-\alpha\;\frac{\partial^2\phi_1(t,z)}{\partial t^2} - \;\gamma\psi_1 - \left({\phi_0}^3 + \;\phi_0{\psi_0}^2\right), \tag{2.25}$$

$$\frac{\partial\phi_2(t,z)}{\partial z} = \alpha\;\frac{\partial^2\psi_2(t,z)}{\partial t^2} - \gamma\phi_2 + \left(3{\psi_0}^2\psi_1 + 2\psi_0\phi_0\phi_1 + \psi_1{\phi_0}^2\right), \tag{2.26}$$

$$\frac{\partial\psi_2(t,z)}{\partial z} = -\,\alpha\;\frac{\partial^2\phi_2(t,z)}{\partial t^2} - \gamma\psi_2 - \left(3{\phi_0}^2\phi_1 + 2\phi_0\psi_0\psi_1 + \phi_1{\psi_0}^2\right), \tag{2.27}$$

$$\begin{aligned}\frac{\partial\phi_3(t,z)}{\partial z} = \;&\alpha\;\frac{\partial^2\psi_3(t,z)}{\partial t^2} - \;\gamma\phi_3\\ &+ \left(3{\psi_1}^2\psi_0 + 3{\psi_0}^2\psi_2 + \psi_2{\phi_0}^2 + 2\psi_1\phi_0\phi_1 + \psi_0{\phi_1}^2\right.\\ &\left.+\,2\psi_0\phi_0\phi_2\right)\end{aligned} \tag{2.28}$$

$$\begin{aligned}\frac{\partial\psi_3(t,z)}{\partial z} = -\,&\alpha\;\frac{\partial^2\phi_3(t,z)}{\partial t^2} - \;\gamma\psi_3\\ &- \left(3{\phi_1}^2\phi_0 + 3{\phi_0}^2\phi_2 + \;\phi_2{\psi_0}^2 + 2\phi_1\psi_0\psi_1 + \phi_0{\psi_1}^2\right.\\ &\left.+\,2\phi_0\psi_0\psi_2\right)\end{aligned} \tag{2.29}$$

and so on. The prototype equations, to be solved, are:

$$\frac{\partial \phi_i(t,z)}{\partial z} = \alpha \frac{\partial^2 \psi_i(t,z)}{\partial t^2} + G_{1i} \quad , \qquad i \geq 1 \tag{2.30}$$

$$\frac{\partial \psi_i(t,z)}{\partial z} = \alpha \frac{\partial^2 \phi_i(t,z)}{\partial t^2} + G_{2i} \quad , \qquad i \geq 1 \tag{2.31}$$

where $\psi_i(t,0) = \delta_{i,0} f_1(t)$, $\phi_i(t,0) = \delta_{i,0} f_2(t)$, and all other corresponding conditions are zeros. G_{1i} , G_{2i} are functions to be computed from previous steps.

By following the solution algorithm described in Appendix (A) for the linear case, the following final results are obtained.

2.2 The order of approximations

The following final expressions can be used to obtain different order of approximations.

2.2.1 The zero order approximation

The zero order approximation is the linear case illustrated in Appendix (A).

2.2.2 The first order approximation

$$u_1(t\,,z) = u_0(t,z) + \varepsilon\big(\,\psi_1(t,z) + \, i\,\phi_1(t,z)\big) \tag{2.32}$$

By following Appendix (A), for *n=1,* we can find that:

$$\psi_1(t\,,z) = e^{-\gamma z} \sum_{n=0}^{\infty} T_{1n}(z)\sin\left(\frac{n\,\pi}{T}\right)t, \tag{2.33}$$

$$\phi_1(t\,,z) = e^{-\gamma z} \sum_{n=0}^{\infty} \tau_{1n}(z)\sin\left(\frac{n\,\pi}{T}\right)t\,, \tag{2.34}$$

from equations (2.24) and (2.25), we can see that:

$$G_{11} = \, e^{-2\gamma z}\big({\psi_0}^3 + \, \psi_0{\phi_0}^2\big) \tag{2.35}$$

$$G_{21} = \, e^{-2\gamma z}\big(-{\phi_0}^3 - \, \phi_0{\psi_0}^2\big) \tag{2.36}$$

in which,

$$T_{1n}(z) = A_{11}(z)\sin\beta_n z + \left(C_{12} + B_{11}(z)\right)\cos\beta_n z, \quad (2.37)$$

$$\tau_{1n}(z) = A_{12}(z)\sin\beta_n z + \left(C_{14} + B_{12}(z)\right)\cos\beta_n z, \quad (2.38)$$

where $C_{12} = -B_{11}(0)$ and $C_{14} = -B_{12}(0)$. The rest constants A_{11} , B_{11} , A_{12} , B_{12} can be calculated in similar manner as illustrated in Appendix (A).

The absolute value of the zero order approximation can be got using

$$|u_1(t\,,z)|^2 = |u_0(t\,,z)|^2 + 2\varepsilon(\psi_0\psi_1 + \phi_0\phi_1) + \varepsilon^2\left({\psi_1}^2 + {\phi_1}^2\right) \quad (2.39)$$

2.2.3 The second order approximation

$$u_2(t\,,z) = u_1(t,z) + \varepsilon^2\left(\psi_2(t,z) + i\,\phi_2(t,z)\right) \quad (2.40)$$

By following Appendix (A), for *n=2,* we can find that:

$$\psi_2(t\,,z) = e^{-\gamma z}\sum_{n=0}^{\infty} T_{2n}(z)\sin\left(\frac{n\,\pi}{T}\right)t, \quad (2.41)$$

$$\phi_2(t\,,z) = e^{-\gamma z}\sum_{n=0}^{\infty} \tau_{2n}(z)\sin\left(\frac{n\,\pi}{T}\right)t\,, \quad (2.42)$$

from equations (2.26) and (2.27), we can see that:

$$G_{12} = e^{-2\gamma z}(3{\psi_0}^2\psi_1 + 2\psi_0\phi_0\phi_1 + \psi_1{\phi_0}^2) \quad (2.43a)$$

$$G_{22} = e^{-2\gamma z}\left(-3{\phi_0}^2\phi_1 - 2\phi_0\psi_0\psi_1 - \phi_1{\psi_0}^2\right) \quad (2.43b)$$

in which

$$T_{2n}(z) = A_{21}(z)\sin\beta_n z + \left(C_{22} + B_{21}(z)\right)\cos\beta_n z, \quad (2.44)$$

$$\tau_{2n}(z) = A_{22}(z)\sin\beta_n z + \left(C_{24} + B_{22}(z)\right)\cos\beta_n z, \quad (2.45)$$

where $C_{22} = -B_{21}(0)$ and $C_{24} = -B_{22}(0)$. The rest constants A_{21} , B_{21} , A_{22} , B_{22} can be calculated in similar manner as illustrated in Appendix (A).

The absolute value of the zero order approximation can be got using

$$|u_2(t\,,z)|^2 = |u_0(t\,,z)|^2 + 2\varepsilon^2(\psi_0\psi_2 + \phi_0\phi_2) + 2\varepsilon^3(\psi_1\psi_2 + \phi_1\phi_2) + \varepsilon^4\left({\psi_2}^2 + {\phi_2}^2\right) \quad (2.46)$$

2.2.4 The third order approximation

$$u_3(t\,,z) = u_2(t,z) + \varepsilon^3\big(\,\psi_3(t,z) + \,i\,\phi_3(t,z)\big) \tag{2.47}$$

By following Appendix (A), for *n=3,* we can find that:

$$\psi_3(t\,,z) = e^{-\gamma z}\sum_{n=0}^{\infty} T_{3n}(z)\sin\,(\frac{n\,\pi}{T})t, \tag{2.48}$$

$$\phi_3(t\,,z) = e^{-\gamma z}\sum_{n=0}^{\infty} \tau_{3n}(z)\sin\,(\frac{n\,\pi}{T})t\,, \tag{2.49}$$

from equations (2.28) and (2.29), we can see that:

$$G_{13} = \,e^{-2\gamma z}(3{\psi_0}^2\psi_1 + 3{\psi_0}^2\psi_2 + \psi_2{\phi_0}^2 + 2\psi_0\phi_0\phi_1 + \,\psi_0{\phi_1}^2 + 2\psi_0\phi_0\phi_2) \tag{2.50}$$

$$G_{23} = \,e^{-2\gamma z}\big(-3{\phi_0}^2\phi_1 - 3{\phi_0}^2\phi_2 - \phi_2{\psi_0}^2 - 2\phi_0\psi_0\psi_1 - \,\phi_0{\psi_1}^2 - 2\phi_0\psi_0\psi_2\big) \tag{2.51}$$

in which

$$T_{3n}(z) = A_{31}(z)\sin\beta_n z + \,\big(C_{32} + \,B_{31}(z)\big)\cos\beta_n z, \tag{2.52}$$

$$\tau_{3n}(z) = A_{32}(z)\sin\beta_n z + \,\big(C_{34} + \,B_{32}(z)\big)\cos\beta_n z, \tag{2.53}$$

where $C_{32} = -B_{31}(0)$ and $C_{34} = -B_{32}(0)$. The rest constants A_{31} , B_{31} , A_{32} , B_{32} can be calculated in similar manner as in Appendix (A).

The absolute value of the zero order approximation can be got using

$$|u_3(t\,,z)|^2 = |u_2(t\,,z)|^2 + 2\varepsilon^3(\psi_0\psi_3 + \phi_0\phi_3) + \,2\varepsilon^4(\psi_1\psi_3 + \phi_1\phi_3) + 2\varepsilon^5(\psi_2\psi_3 + \phi_2\phi_3) + \varepsilon^6\big({\psi_3}^2 + {\phi_3}^2\big) \tag{2.54}$$

2.3 Case Studies

To examine the proposed solution algorithm, some case studies are illustrated.

2.3.1 Case study 1

Taking the case $f_1(t) = \rho_1, f_2(t) = \rho_2$ where ρ_1 & ρ_2 are constants and following the algorithm, the following selected results for the first, second and third order approximations are got:

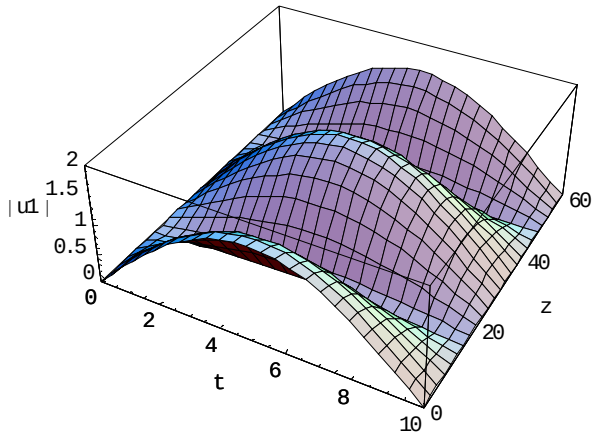

Fig. (2.1) the first order approximation of $\left|u^{(1)}\right|$ at $\varepsilon = 0, \gamma = 0$ and $\alpha, \rho_1, \ \rho_2 = 1, T = 10$ with considering only ten terms on the series (M=10)

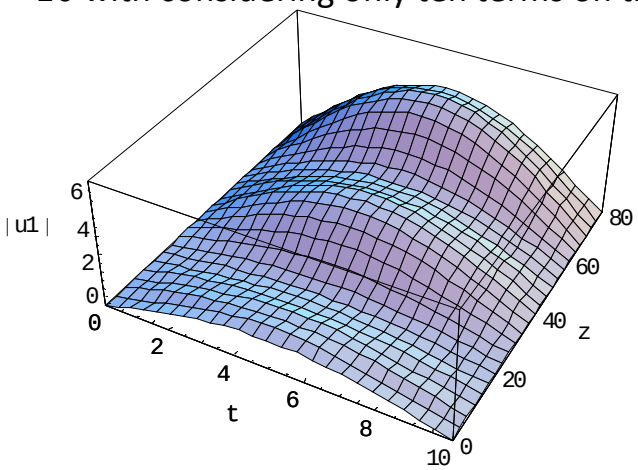

Fig. (2.2) the first order approximation of $\left|u^{(1)}\right|$ at $\varepsilon = 0.2$, $\gamma = 0$ and $\alpha, \rho_1, \ \rho_2 = 1, T = 10$ with considering only ten terms on the series (M=10)

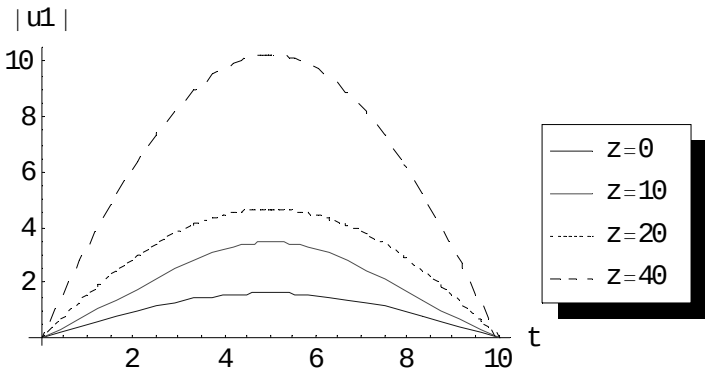

Fig. (2.3) the first order approximation of $\left|u^{(1)}\right|$ at $\varepsilon = 0.2$, $\gamma = 0$ and $\alpha, \rho_1, \rho_2 = 1, T = 10, M = 10$ for different values of z.

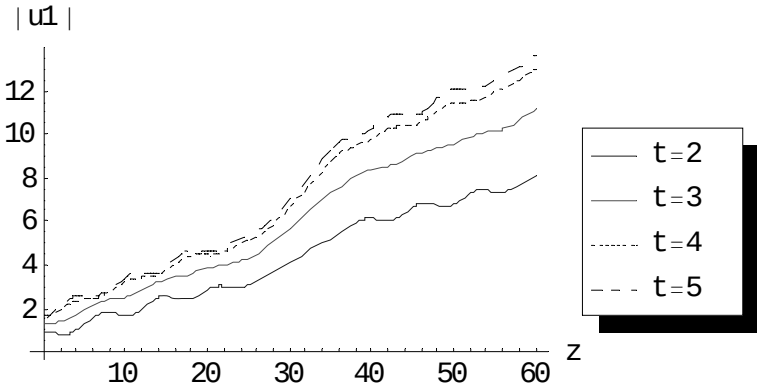

Fig. (2.4) the first order approximation of $\left|u^{(1)}\right|$ at $\varepsilon = 0.2$, $\gamma = 0$ and $\alpha, \rho_1, \rho_2 = 1, T = 10, M = 10$ for different values of t.

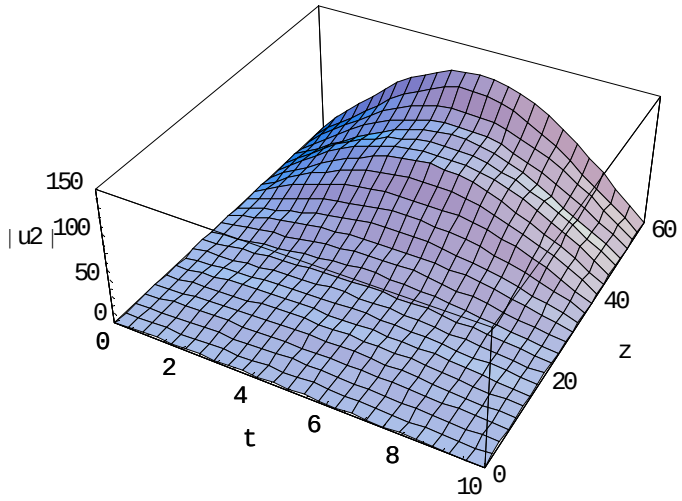

Fig. (2.5) the second order approximation of $\left|u^{(2)}\right|$ at $\varepsilon = 0.2$, $\gamma = 0$ and $\alpha, \rho_1, \rho_2 = 1, T = 10$ with considering only ten terms on the series (M=10)

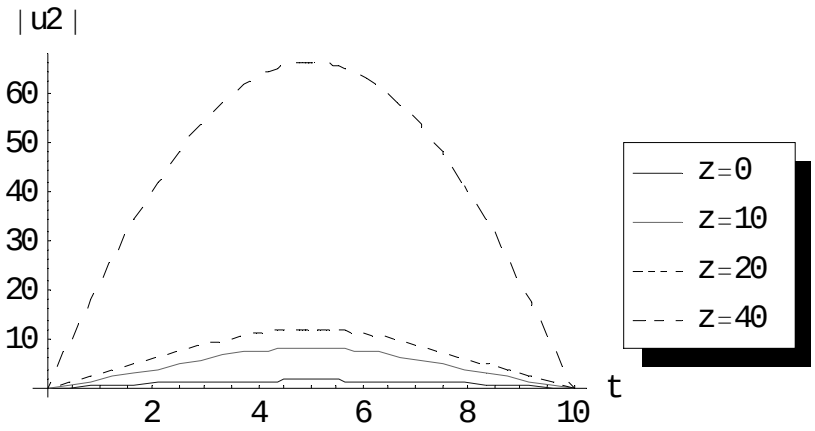

Fig. (2.6) the second order approximation of $\left|u^{(2)}\right|$ at $\varepsilon = 0.2$, $\gamma = 0$ and $\alpha, \rho_1, \rho_2 = 1, T = 10, M = 10$ for different values of z.

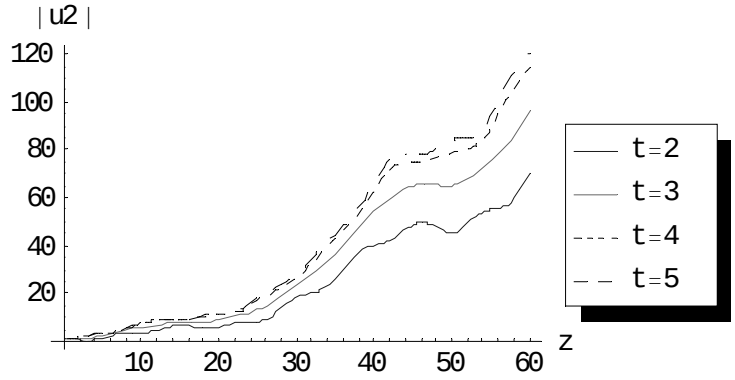

Fig. (2.7) the second order approximation of $\left|u^{(2)}\right|$ at $\varepsilon = 0.2$, $\gamma = 0$ and $\alpha, \rho_1, \rho_2 = 1, T = 10, M = 10$ for different values of t.

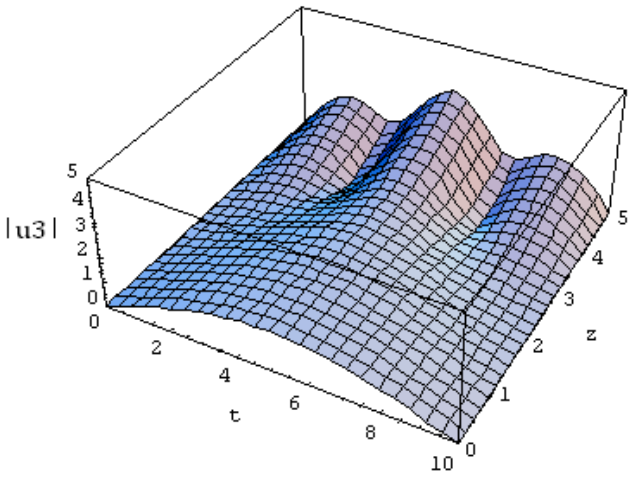

Fig. (2.8) the third order approximation of $\left|u^{(3)}\right|$ at $\varepsilon = 0.2$, $\gamma = 0$ and $\alpha, \rho_1, \rho_2 = 1, T = 10$ with considering only ten terms on the series (M=10).

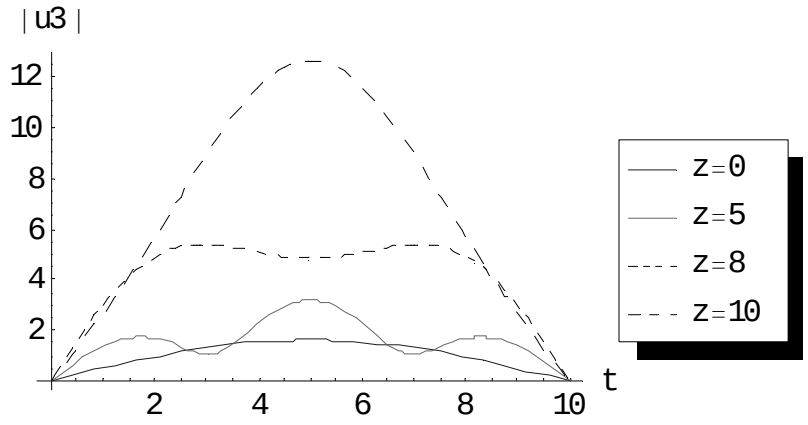

Fig. (2.9) the third order approximation of $\left|u^{(3)}\right|$ at $\varepsilon = 0.2$, $\gamma = 0$ and $\alpha, \rho_1, \rho_2 = 1, T = 10, M = 10$ for different values of z.

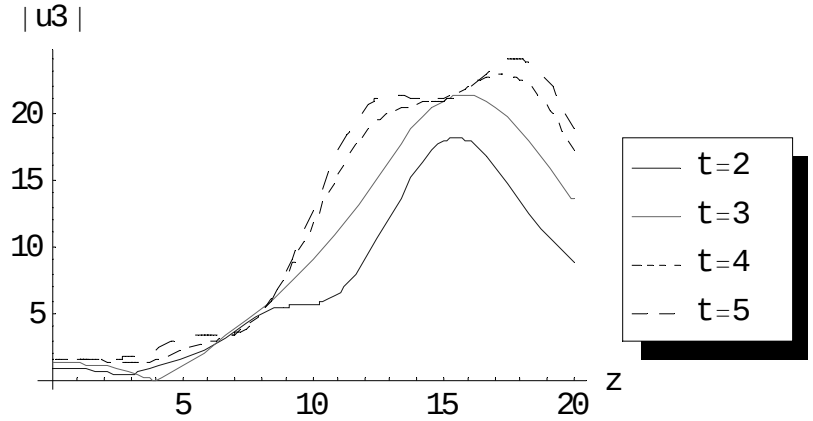

Fig. (2.10) the third order approximation of $\left|u^{(3)}\right|$ at $\varepsilon = 0.2$, $\gamma = 0$ and $\alpha, \rho_1, \rho_2 = 1, T = 10, M = 10$ for different values of t.

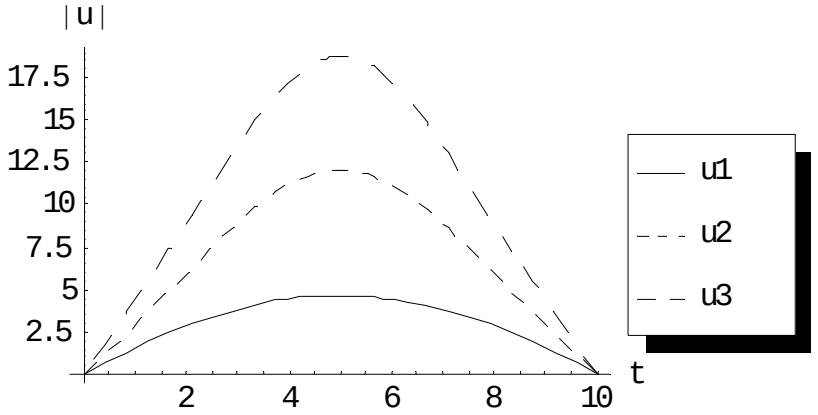

Fig. (2.11) comparison between first, second and third order approximation at $\varepsilon = 0.2$, $\gamma = 0$ and $\alpha, \rho_1, \rho_2 = 1, T = 10, M = 10, z = 20$.

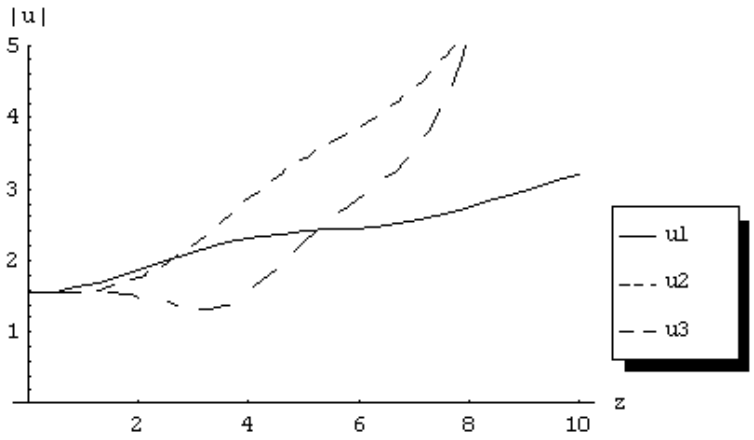

Fig. (2.12) comparison between first, second and third order approximations at $\varepsilon = 0.2, \gamma = 0$ and $\alpha, \rho_1, \rho_2 = 1, T = 10, M = 10, t = 4$.

Note: with constant initial conditions we calculated till third order which takes around 2 days continuously and we cannot calculate more since the machine gives "MATHEMATICA KERNEL OUT OF MEMORY".

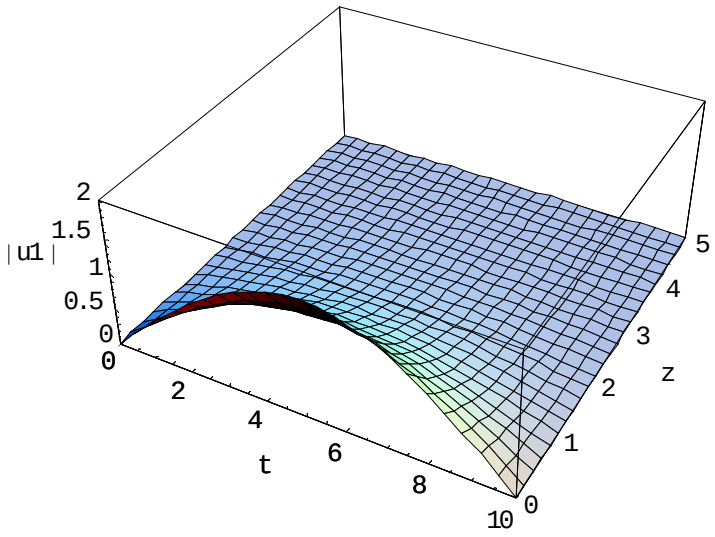

Fig. (2.13) the first order approximation of $\left|u^{(1)}\right|$ at $\varepsilon = 0.2,\ \alpha, \rho_1, \rho_2 = 1, T = 10, \gamma = 1$ with considering only ten terms on the series (M=10).

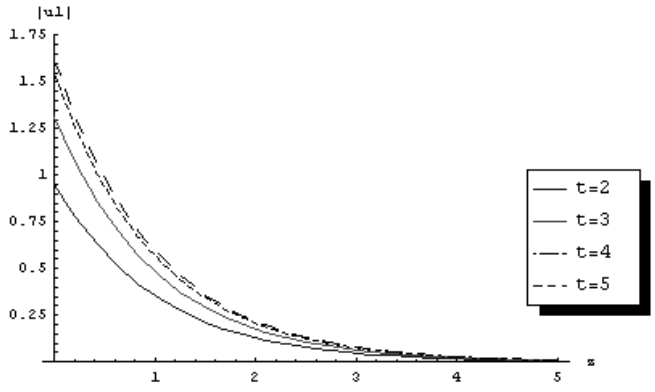

Fig. (2.14) the first order approximation of $\left|u^{(1)}\right|$ at $\varepsilon = 0.2, \gamma = 1$ and $\alpha, \rho_1, \rho_2 = 1, T = 10, M = 10$ for different values of t.

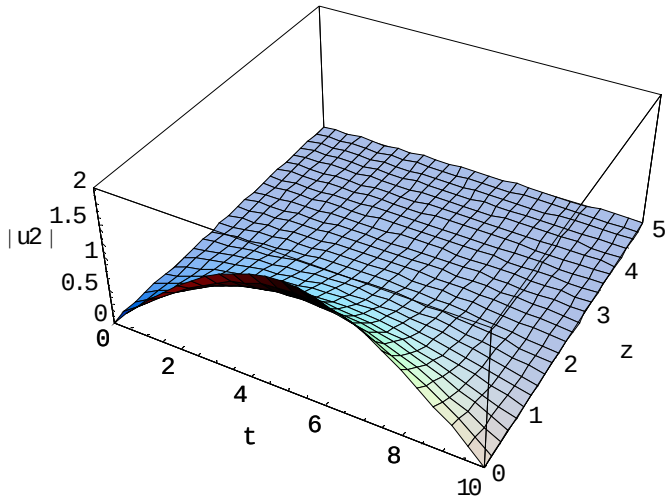

Fig.(2.15) the second order approximation of $\left|u^{(2)}\right|$ at $\varepsilon = 0.2$, $\gamma = 1$ and $\alpha, \rho_1, \rho_2 = 1, T = 10,$ with considering only ten terms on the series (M=10).

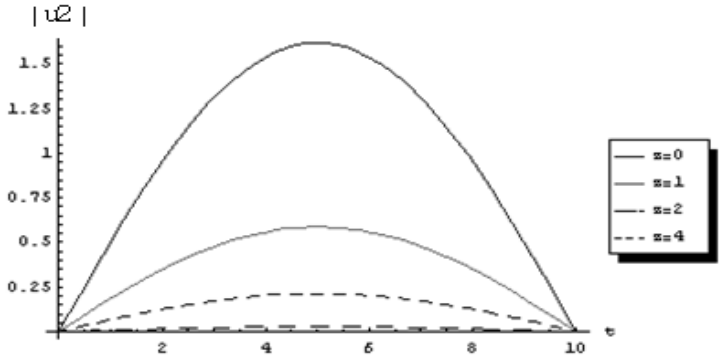

Fig.(2.16) the second order approximation of $\left|u^{(2)}\right|$ at $\varepsilon = 0.2, \gamma = 1$ and $\alpha, \rho_1, \rho_2 = 1, T = 10, M = 10$for different values of z.

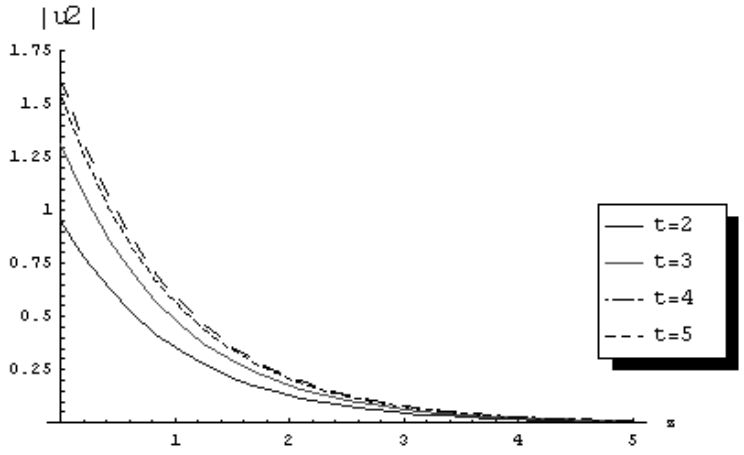

Fig.(2.17) the second order approximation of $\left|u^{(2)}\right|$ at $\varepsilon = 0.2, \gamma = 1$ and $\alpha, \rho_1, \rho_2 = 1, T = 10, M = 10$ for different values of t.

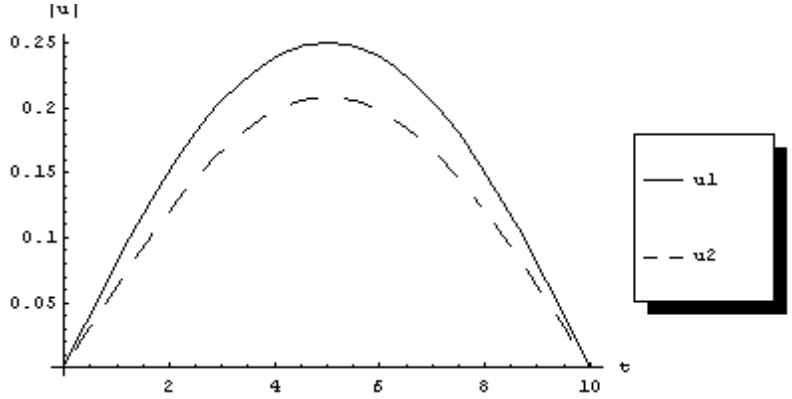

Fig.(2.18) comparison between first and second order approximations at $\varepsilon = 1, \gamma = 1$ and $\alpha, \rho_1, \rho_2 = 1, T = 10, M = 10, z = 2$.

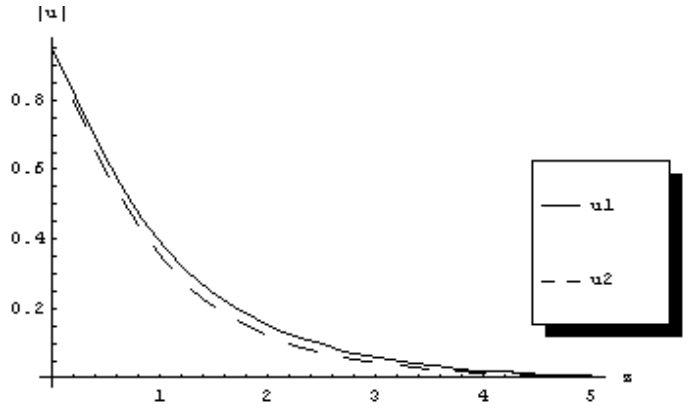

Fig.(2.19) comparison between first and second order approximations at $\varepsilon = 1, \gamma = 1$ and $\alpha, \rho_1, \rho_2 = 1, T = 10, M = 10, t = 2$.

Note: with constant initial conditions and γ exist we calculated till second order which takes around 3 days continuously and we cannot calculate more since the machine gives "MATHEMATICA KERNEL OUT OF MEMORY" .

2.3.2 Case study 2

Taking the case $f_1(t) = \rho_1 e^{-t}, f_2(t) = \rho_2 e^{-t}$ where ρ_1 & ρ_2 are constants and following the algorithm, the following selected results for the first and second order approximations are got:

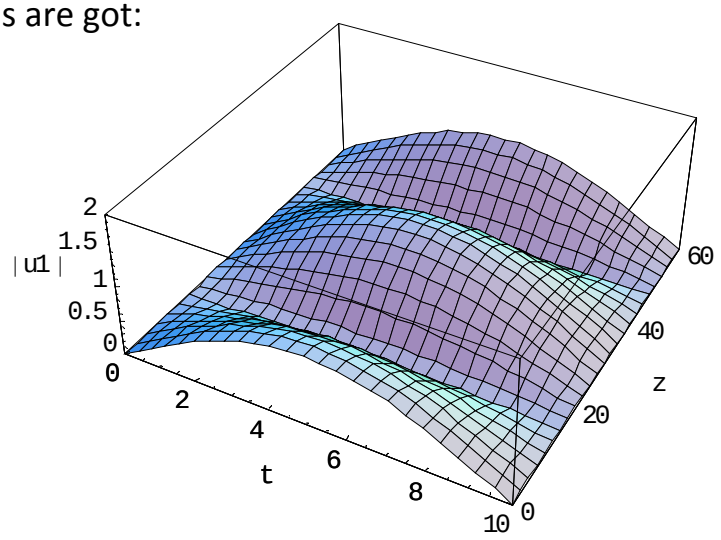

Fig.(2.20) the first order approximation of $\left|u^{(1)}\right|$ at $\varepsilon = 0, \gamma = 0$ and $\alpha, \rho_1, \rho_2 = 1, T = 10$ with considering only ten terms on the series (M=10).

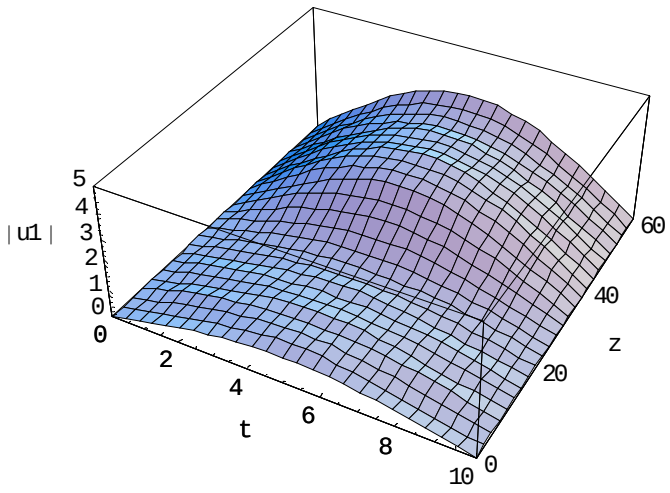

Fig. (2.21) the first order approximation of $\left|u^{(1)}\right|$ at $\varepsilon = 0.2, \gamma = 0$ and $\alpha, \rho_1, \rho_2 = 1, T = 10$ with considering only ten terms on the series (M=10).

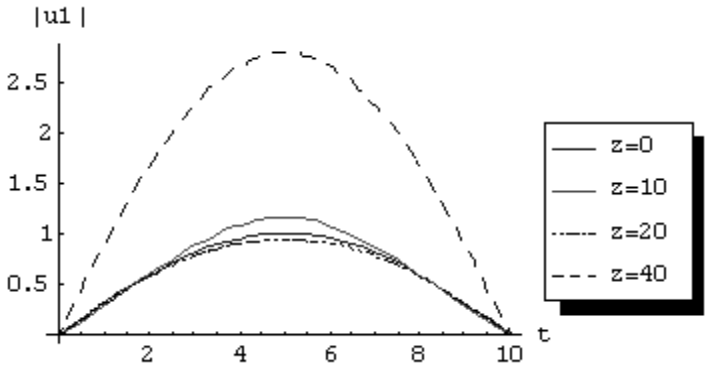

Fig.(2.22) the first order approximation of $\left|u^{(1)}\right|$ at $\varepsilon = 0.2, \gamma = 0$ and $\alpha, \rho_1, \rho_2 = 1, T = 10, M = 10$ for different values of z.

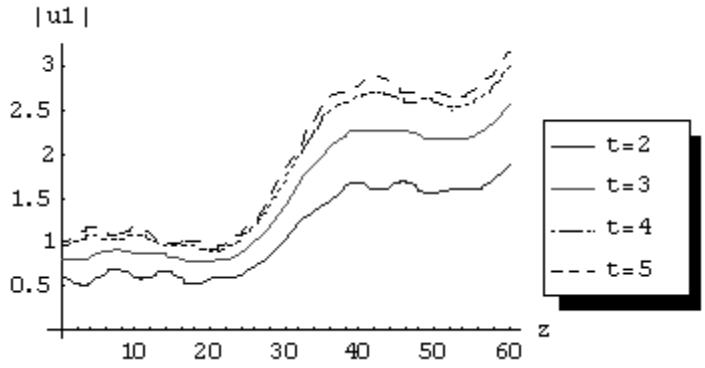

Fig. (2.23) the first order approximation of $\left|u^{(1)}\right|$ at $\varepsilon = 0.2, \gamma = 0$ and $\alpha, \rho_1, \rho_2 = 1, T = 10, M = 10$ for different values of t.

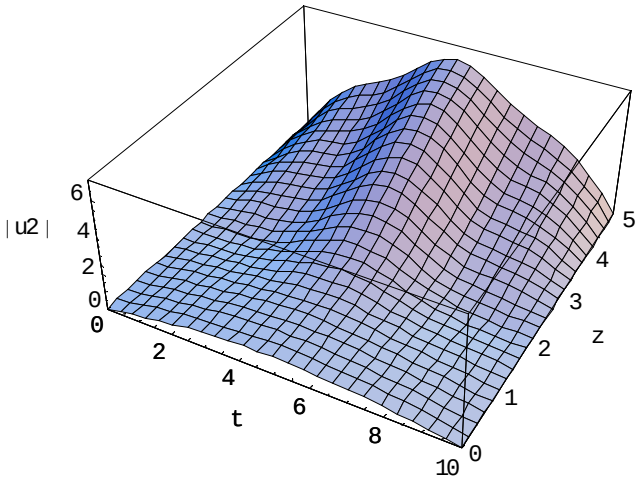

Fig. (2.24) the second order approximation of $\left|u^{(2)}\right|$ at $\varepsilon = 1,\ \gamma = 0$ and $\alpha, \rho_1, \rho_2 = 1, T = 10$ with considering only ten terms on the series (M=10).

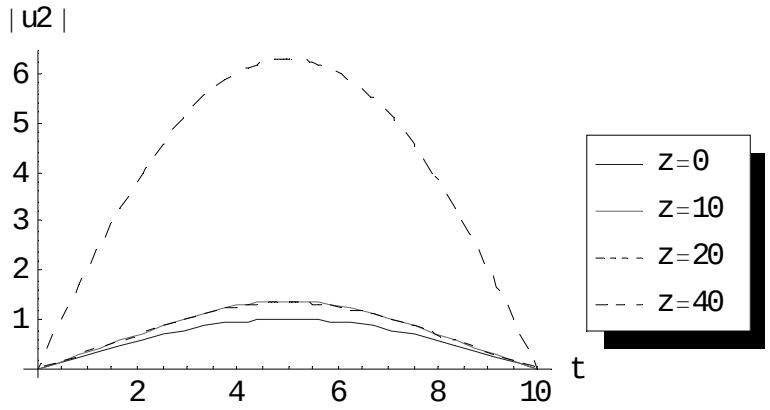

Fig. (2.25) the second order approximation of $\left|u^{(2)}\right|$ at $\varepsilon = 0.2,\ \gamma = 0$ and $\alpha, \rho_1, \rho_2 = 1, T = 10, M = 10$ for different values of z.

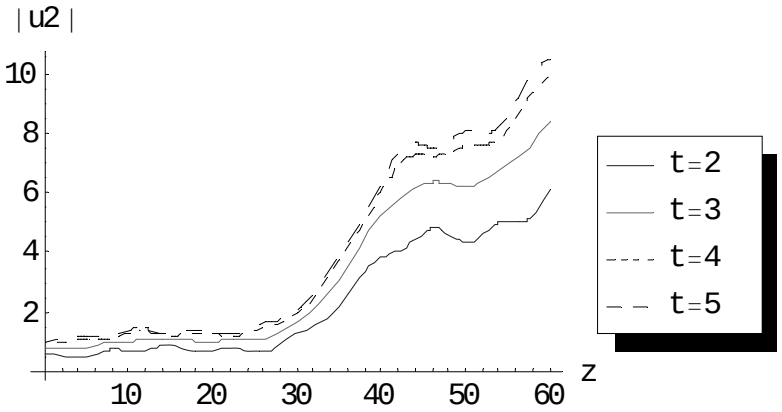

Fig.(2.26) the second order approximation of $\left|u^{(2)}\right|$ at $\varepsilon = 0.2,\ \gamma = 0$ and $\alpha, \rho_1, \rho_2 = 1, T = 10, M = 10$ for different values of t.

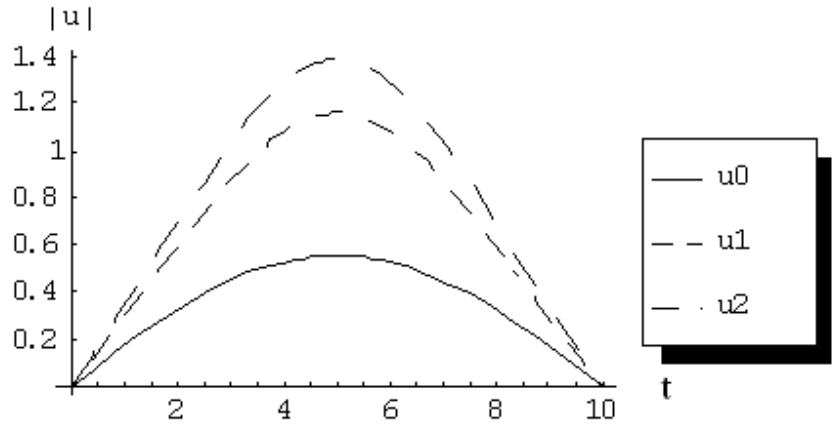

Fig.(2.27) comparison between zero, first and second order approximations at $\varepsilon = 0.2, \gamma = 0$ and $\alpha, \rho_1, \rho_2 = 1, T = 10, M = 10, z = 10$.

Note: the calculations for second order takes 3 and half day and we can not calculate more orders since the machine gives "MATHEMATICA KERNEL OUT OF MEMORY" .

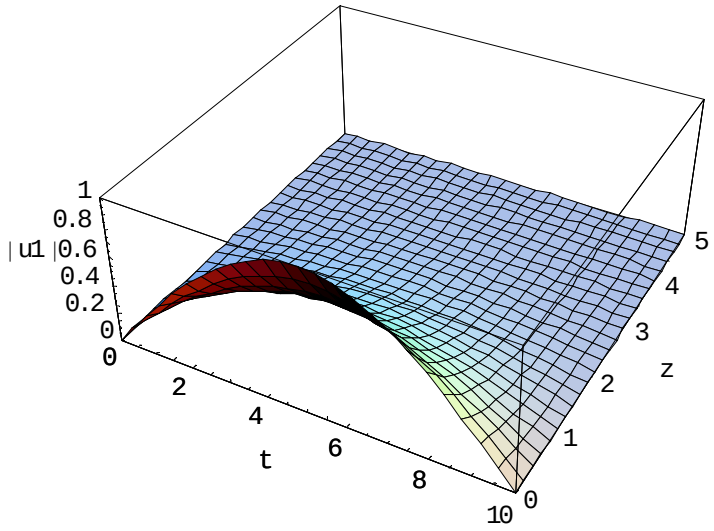

Fig.(2.28) the first order approximation of $\left|u^{(1)}\right|$ at $\varepsilon = 0.2,\ \gamma = 1$ and $\alpha, \rho_1, \rho_2 = 1, T = 10$ with considering only ten terms on the series (M=10).

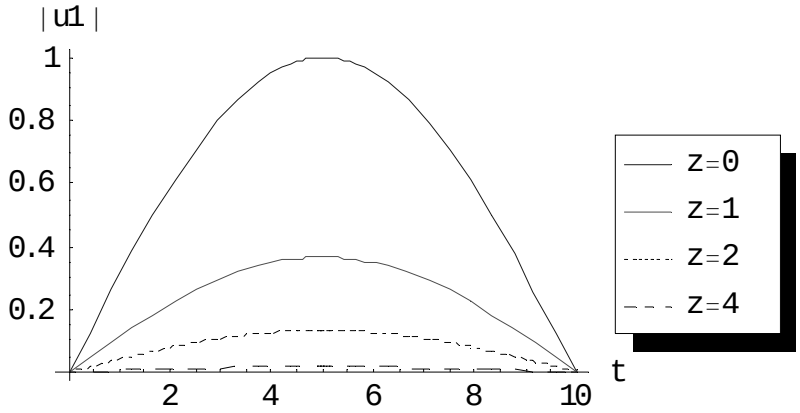

Fig.(2.29) the first order approximation of $\left|u^{(1)}\right|$ at $\varepsilon = 0.2, \gamma = 1$ and $\alpha, \rho_1, \rho_2 = 1, T = 10, M = 10$ for different values of z.

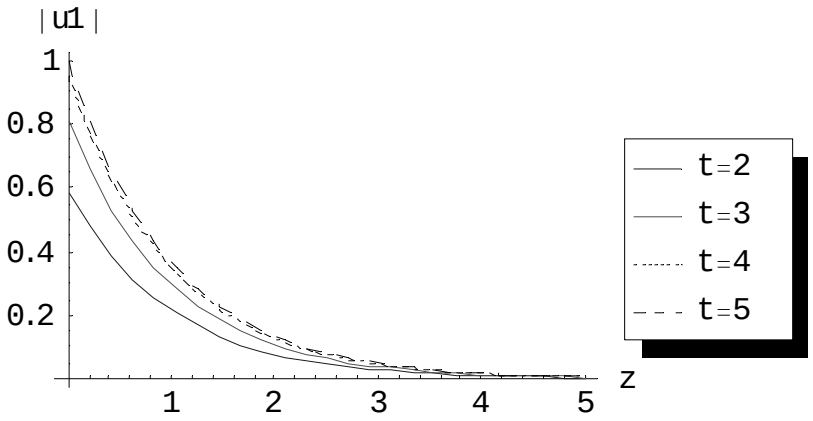

Fig. (2.30) the first order approximation of $\left|u^{(1)}\right|$ at $\varepsilon = 0.2, \gamma = 1$ and $\alpha, \rho_1, \rho_2 = 1, T = 10, M = 10$ for different values of t.

Note: the calculations for first order takes 3 days and we can not calculate more orders since the machine gives "MATHEMATICA KERNEL OUT OF MEMORY" .

2.3.3 Case study 3

Taking the case $f_1(t) = \rho_1, f_2(t) = \rho_2 \sin\left(\frac{m\pi}{T}\right) t$ where ρ_1 & ρ_2 are constants and following the algorithm, the following selected results for the first, second and third order approximations are got:

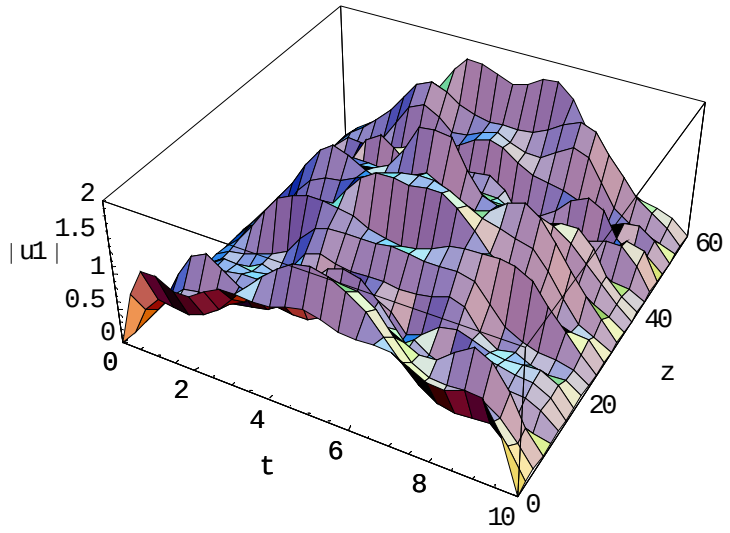

Fig.(2.31) the first order approximation of $\left|u^{(1)}\right|$ at $\varepsilon = 0, \gamma = 0$ and $\alpha, \rho_1, \rho_2 = 1, T = 10$ with considering only ten terms on the series (M=10).

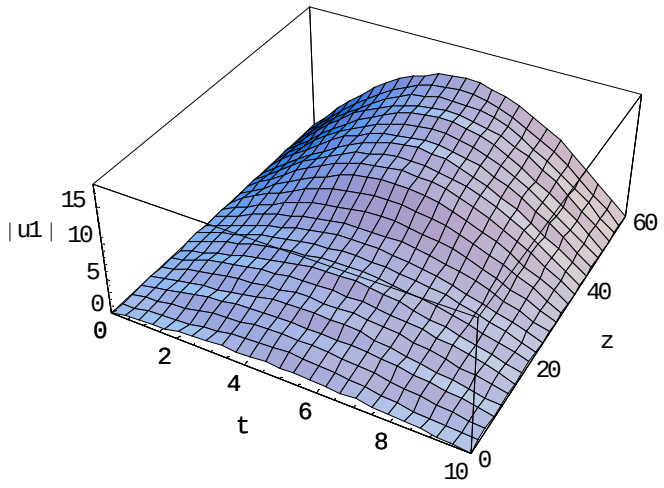

Fig. (2.32) the first order approximation of $\left|u^{(1)}\right|$ at $\varepsilon = 0.2, \gamma = 0$ and $\alpha, \rho_1, \rho_2 = 1, T = 10$ with considering only ten terms on the series (M=10).

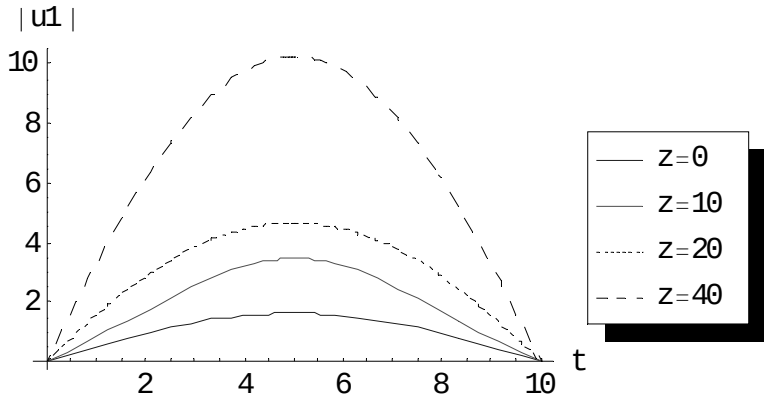

Fig. (2.33) the first order approximation of $\left|u^{(1)}\right|$ at $\varepsilon = 0.2,\ \gamma = 0$ and $\alpha, \rho_1, \rho_2 = 1, T = 10, M = 10$ for different values of z.

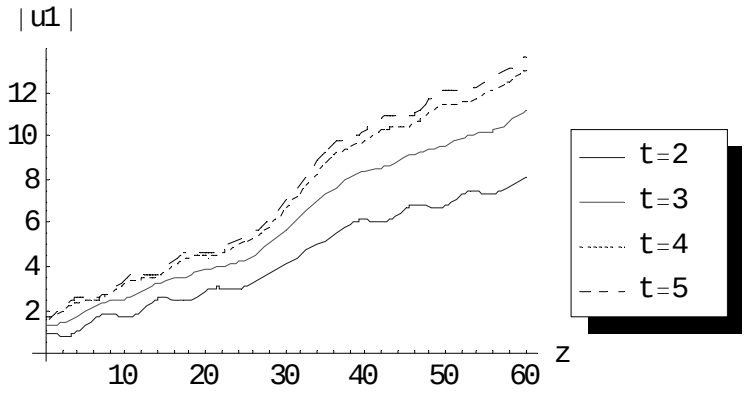

Fig. (2.34) the first order approximation of $\left|u^{(1)}\right|$ at $\varepsilon = 0.2, \gamma = 0$ and $\alpha, \rho_1, \rho_2 = 1, T = 10, M = 10$ for different values of t.

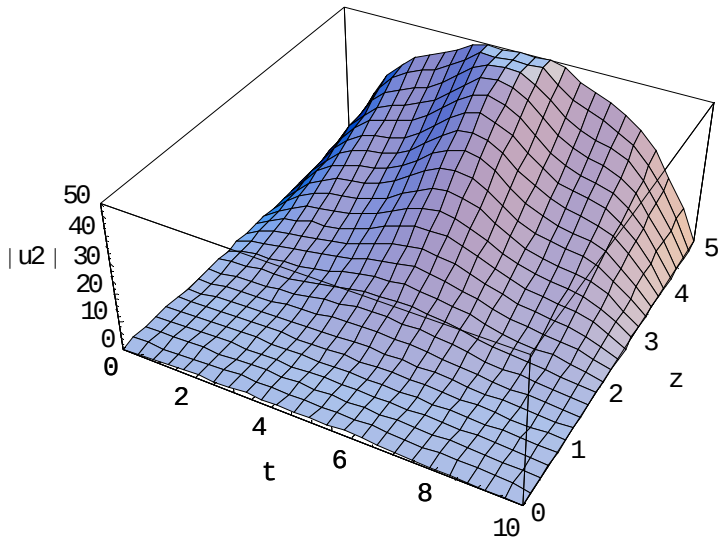

Fig.(2.35) the second order approximation of $\left|u^{(2)}\right|$ at $\varepsilon = 1,\ \gamma = 0$ and $\alpha, \rho_1, \rho_2 = 1, T = 10$ with considering only ten terms on the series (M=10).

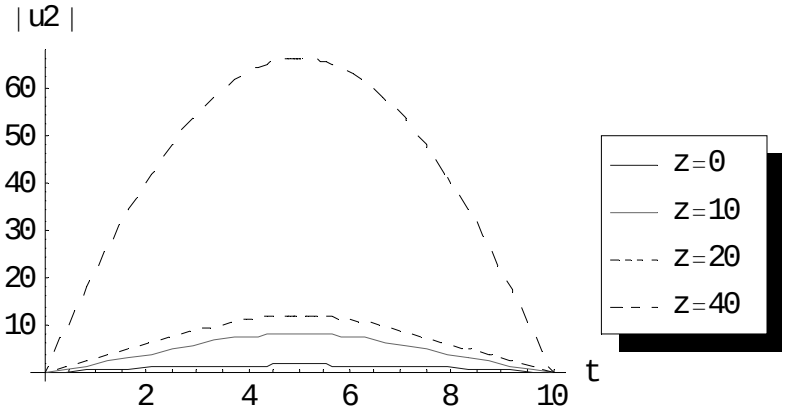

Fig. (2.36) the second order approximation of $\left|u^{(2)}\right|$ at $\varepsilon = 0.2, \gamma = 0$ and $\alpha, \rho_1, \rho_2 = 1, T = 10, M = 10$ for different values of z.

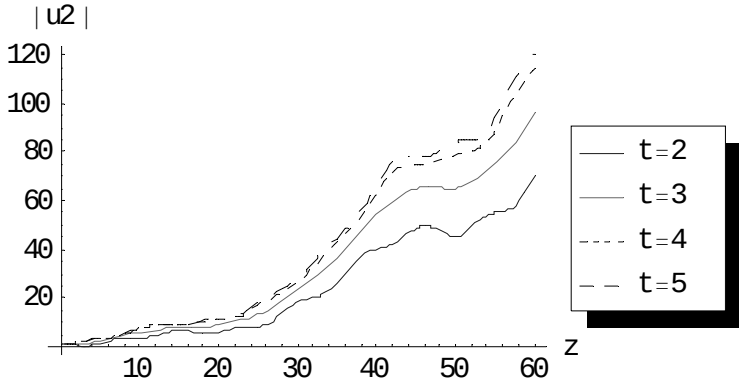

Fig. (2.37) the second order approximation of $\left|u^{(2)}\right|$ at $\varepsilon = 0.2,\ \gamma = 0$ and $\alpha, \rho_1, \rho_2 = 1, T = 10, M = 10$ for different values of t.

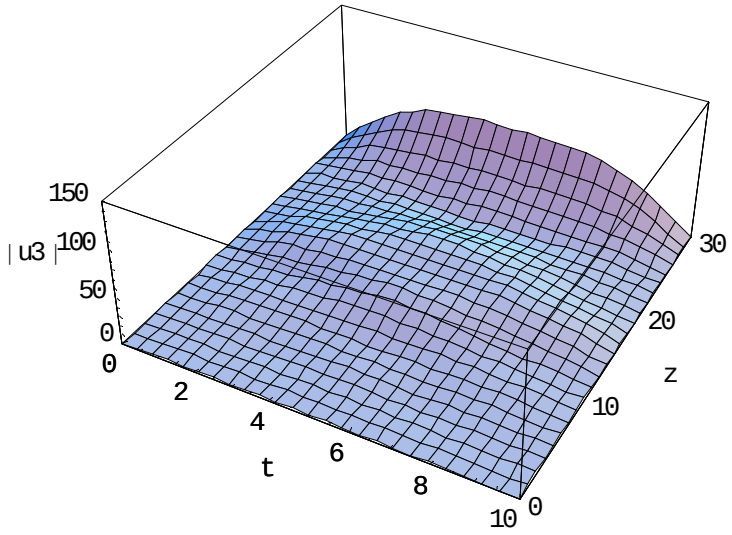

Fig. (2.38) the third order approximation of $\left|u^{(3)}\right|$ at $\varepsilon = 0.2,\ \gamma = 0$ and $\alpha, \rho_1, \rho_2 = 1, T = 10$ with considering only ten terms on the series (M=10).

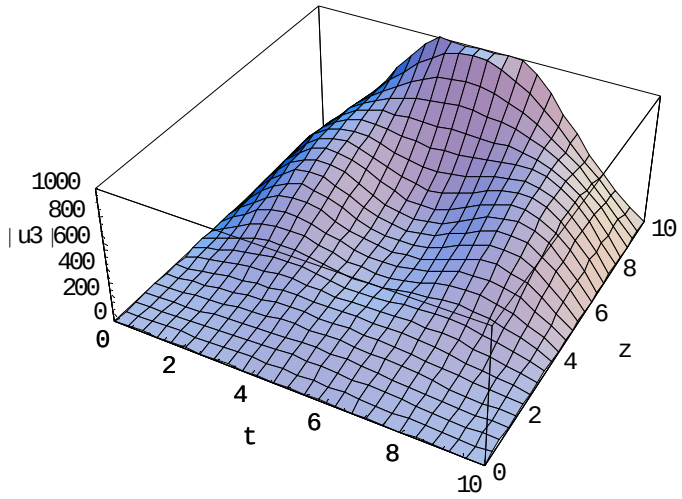

Fig. (2.39) the third order approximation of $\left|u^{(3)}\right|$ at $\varepsilon = 1, \gamma = 0$, and $\alpha, \rho_1, \rho_2 = 1, T = 10$ with considering only ten terms on the series (M=10).

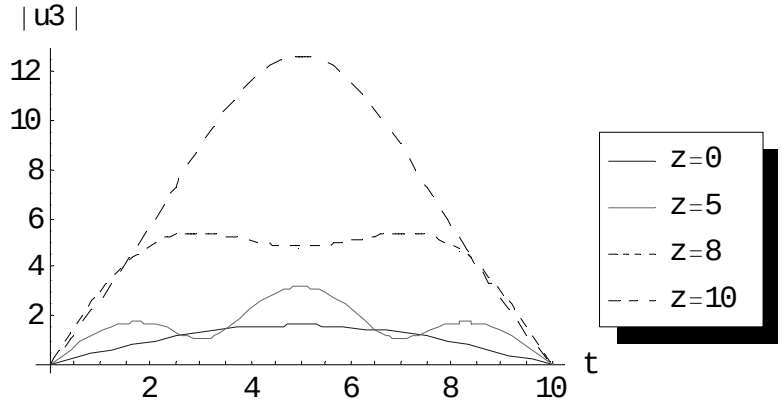

Fig. (2.40) the third order approximation of $\left|u^{(3)}\right|$ at $\varepsilon = 0.2,\ \gamma = 0$ and $\alpha, \rho_1, \rho_2 = 1, T = 10, M = 10$ for different values of z.

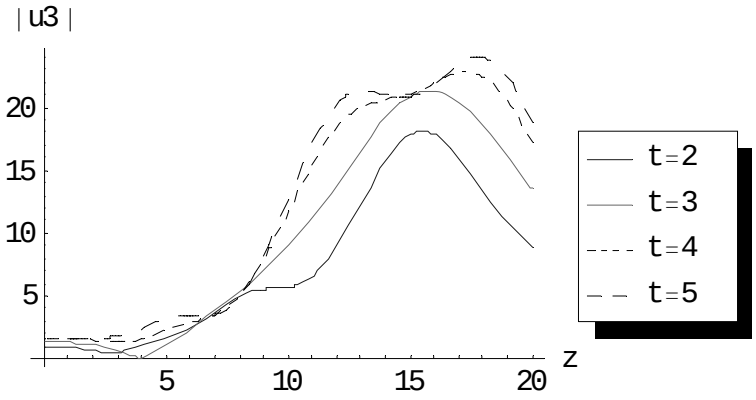

Fig. (2.41) the third order approximation of $\left|u^{(3)}\right|$ at $\varepsilon = 0.2,\ \gamma = 0$ and $\alpha, \rho_1, \rho_2 = 1, T = 10, M = 10$ for different values of t.

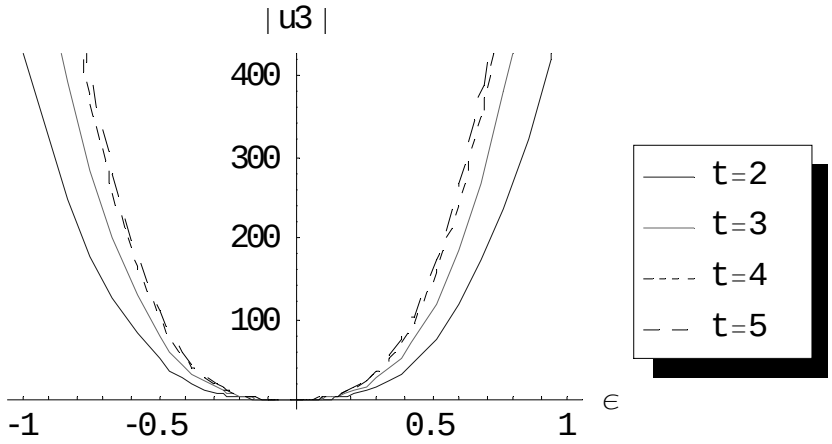

Fig. (2.42) the third order approximation of $\left|u^{(3)}\right|$ at z= $10, \gamma = 0$, and $\alpha, \rho_1, \rho_2 = 1, T = 10, M = 10$ for different values of t.

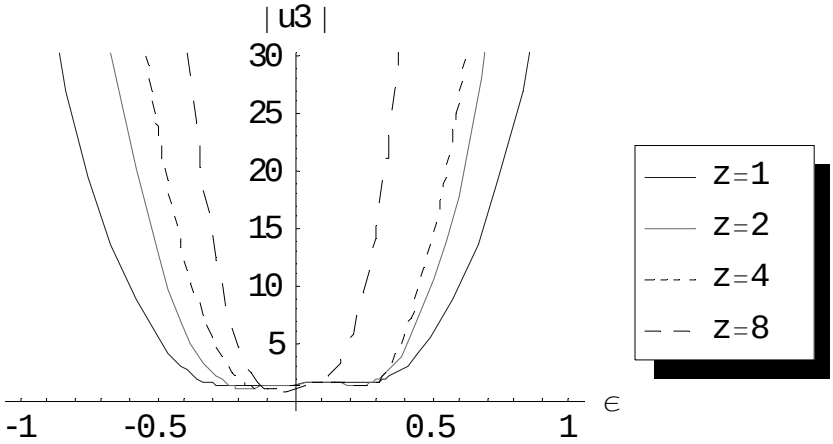

Fig. (2.43) the third order approximation of $\left|u^{(3)}\right|$ at t= $4, \gamma = 0$, and $\alpha, \rho_1, \rho_2 = 1, T = 10, M = 10$ for different values of z.

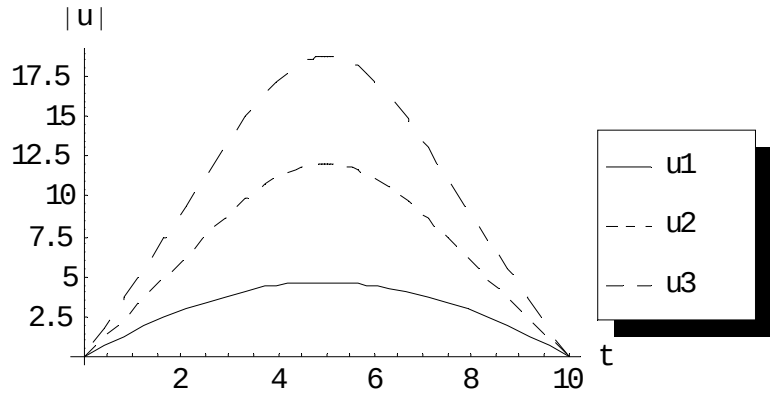

Fig. (2.44) comparison between first, second and third order approximations at $\varepsilon = 0.2$, $\gamma = 0$ and $\alpha, \rho_1, \rho_2 = 1, T = 10, M = 10, z = 20$.

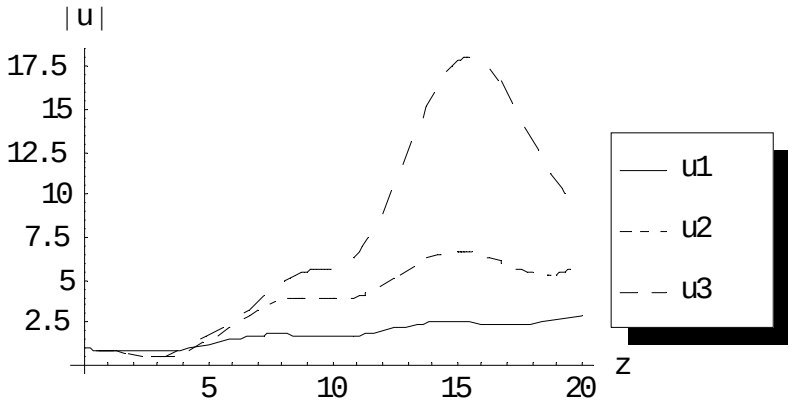

Fig. (2.45) comparison between first, second and third order approximations at $\varepsilon = 0.2$, $\gamma = 0$ and $\alpha, \rho_1, \rho_2 = 1, T = 10, M = 10, t = 2$.

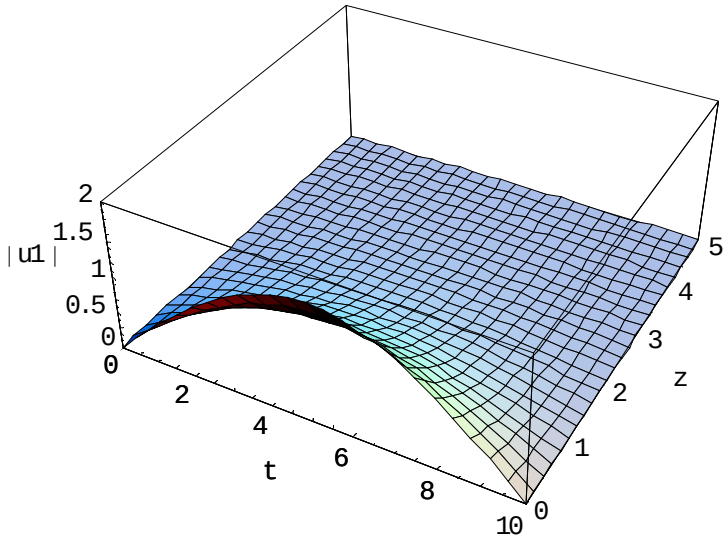

Fig. (2.46) the first order approximation of $\left|u^{(1)}\right|$ at $\varepsilon = 0.2, \gamma = 1$, and $\alpha, \rho_1, \rho_2 = 1, T = 10$ with considering only ten terms on the series (M=10).

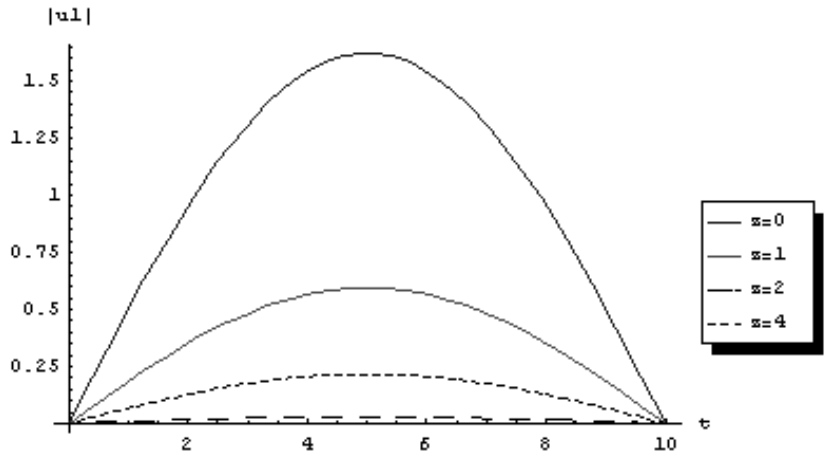

Fig. (2.47) the first order approximation of $\left|u^{(1)}\right|$ at $\varepsilon = 0.2, \alpha, \rho_1, \rho_2 = 1, T = 10, M = 10$ for different values of z.

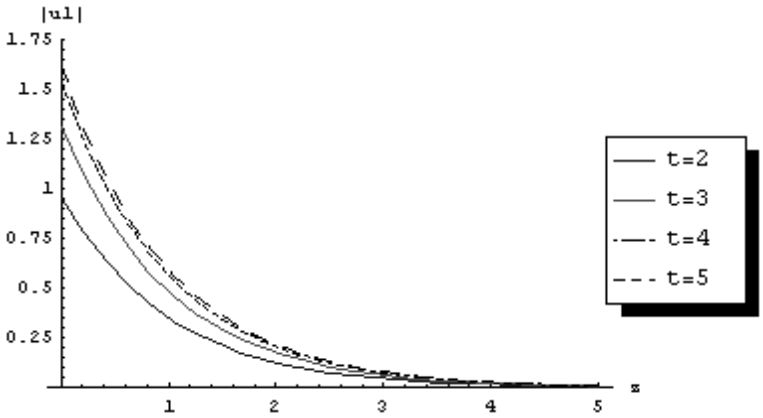

Fig. (2.48) the first order approximation of $\left|u^{(1)}\right|$ at $\varepsilon = 0.2, \gamma = 1$, and $\alpha, \rho_1, \rho_2 = 1, T = 10, M = 10$ for different values of t.

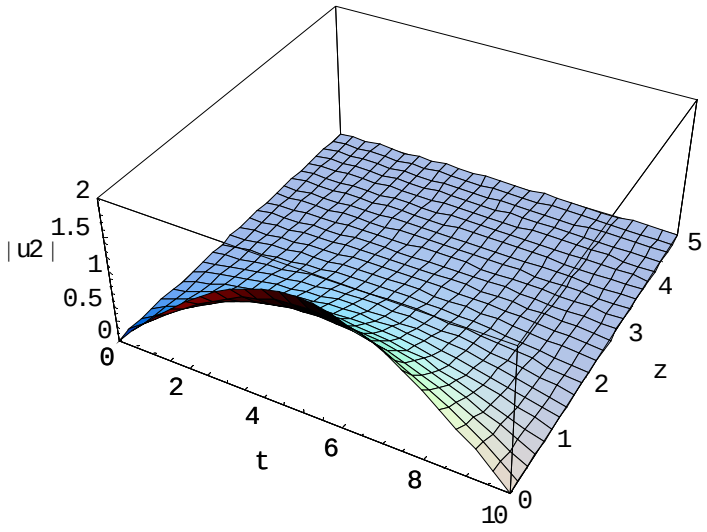

Fig. (2.49) the second order approximation of $\left|u^{(2)}\right|$ at $\varepsilon = 0.2, \gamma = 1$, and $\alpha, \rho_1, \rho_2 = 1, T = 10$ with considering only ten terms on the series (M=10).

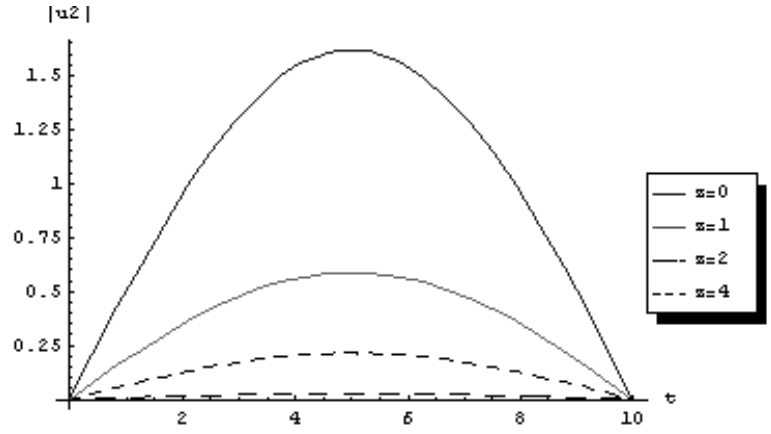

Fig. (2.50) the second order approximation of $\left|u^{(2)}\right|$ at $\varepsilon = 0.2$, $\alpha, \rho_1, \rho_2 = 1, T = 10, M = 10$ for different values of z.

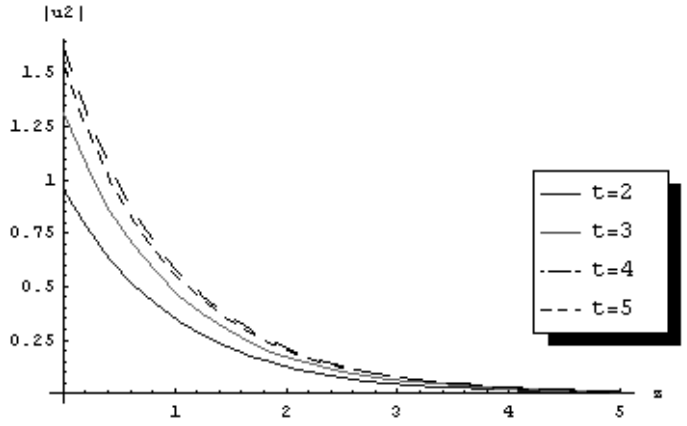

Fig. (2.51) the second order approximation of $\left|u^{(2)}\right|$ at $\varepsilon = 0.2, \gamma = 1$ and $\alpha, \rho_1, \rho_2 = 1, T = 10, M = 10$ for different values of t.

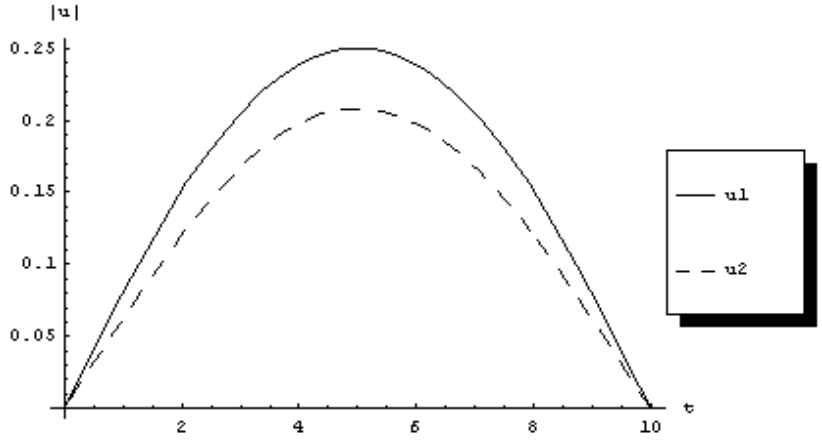

Fig. (2.52) comparison between first and second order approximation at $\varepsilon = 1$, $\gamma = 1$ and $\alpha, \rho_1, \rho_2 = 1, T = 10, M = 10, z = 2$.

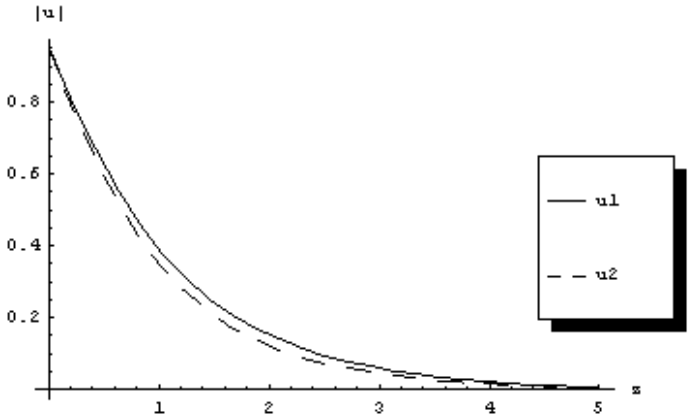

Fig. (2.53) comparison between first and second order approximation at $\varepsilon = 1, \gamma = 1$ and $\alpha, \rho_1, \rho_2 = 1, T = 10, M = 10, t = 2.$

Note: we cannot calculate further than second order since the machine gives "MATHEMATICA KERNEL OUT OF MEMORY" .

2.4 Picard Approximation

To validate our previous results, in the absence of the exact solution, let us follow another approximation technique. The Picard approximation is considered in this section.

Solving equation (2.1) with the same conditions (2.2) and (2.3) and following the Picard algorithm which puts the nonlinear terms in the right hand side of the equation evaluated at the previous step, which means that we solve the linear case iteratively [Zwillinger, 1997].

Let $u(t, z) = \psi(t, z) + i\,\phi(t, z), \psi, \phi$: are real valued functions. The following coupled equations are got:

$$\frac{\partial \phi(t,z)}{\partial z} = \alpha \frac{\partial^2 \psi(t,z)}{\partial t^2} + \varepsilon(\psi^2 + \phi^2)\psi - \gamma\phi, \tag{2.55}$$

$$\frac{\partial \psi(t,z)}{\partial z} = -\alpha \frac{\partial^2 \phi(t,z)}{\partial t^2} - \varepsilon(\psi^2 + \phi^2)\phi - \gamma\phi. \tag{2.56}$$

Where $\psi(t,0) = f_1(t)$, $\phi(t,0) = f_2(t)$, and all corresponding other I.Cs. and B.Cs. are zeros.

$$\frac{\partial \phi_i(t,z)}{\partial z} = \alpha \frac{\partial^2 \psi_i(t,z)}{\partial t^2} + H_{1i} \quad , \qquad i \geq 1 \tag{2.57}$$

$$\frac{\partial \psi_i(t,z)}{\partial z} = \alpha \frac{\partial^2 \phi_i(t,z)}{\partial t^2} + H_{2i} \quad , \qquad i \geq 1 \tag{2.58}$$

where $\psi_i(t,0) = f_1(t)$, $\phi_i(t,0) = f_2(t)$, and all other corresponding conditions are zeros. H_{1i}, H_{2i} are functions to be computed from previous steps.

2.4.1 Picard order of approximations

2.4.1.1 Zero order approximation

The zero order approximation is the linear case illustrated in Appendix (A).

2.4.1.2 First order approximation

$$i \frac{\partial u_1(t,z)}{\partial z} + \alpha \frac{\partial^2 u_1(t,z)}{\partial t^2} + \varepsilon |u_0(t,z)|^2 u_0(t,z) + i\,\gamma u_1(t,z) = 0,$$

$$(t,z) \in (0,T)x\,(0,\infty) \tag{2.59}$$

with initial condition $u_1(t,0) = f_1(t) + i\, f_2(t)$ and boundary conditions $u_1(0,z) = u_1(T,z) = 0$. By following Appendix (A), the linear Schrodinger equation (2.59) has the following solution:

$$u_1(t\,,z) = \psi_1 + i\,\phi_1\,, \tag{2.60}$$

$$\psi_1(t\,,z) = e^{-\gamma z} \sum_{n=0}^{\infty} T_{1n}(z) \sin\left(\frac{n\,\pi}{T}\right)t, \tag{2.61}$$

$$\phi_1(t\,,z) = e^{-\gamma z} \sum_{n=0}^{\infty} \tau_{1n}(z) \sin\left(\frac{n\,\pi}{T}\right)t \tag{2.62}$$

$$H_{11} = e^{-2\gamma z}\varepsilon({\psi_0}^3 + \psi_0{\phi_0}^2) \tag{2.63}$$

$$H_{21} = -e^{-2\gamma z}\varepsilon\left({\phi_0}^3 + \phi_0{\psi_0}^2\right) \tag{2.64}$$

in which,

$$T_{1n}(z) = A_{11}(z)\sin\beta_n z + \left(C_{12} + B_{11}(z)\right)\cos\beta_n z, \tag{2.65}$$

$$\tau_{1n}(z) = A_{12}(z)\sin\beta_n z + \left(C_{14} + B_{12}(z)\right)\cos\beta_n z, \quad (2.66)$$

where the constants and variables A_{11} , C_{12} , B_{11} , A_{12} , C_{14} , B_{12} can be calculated in similar manner as illustrated in Appendix (A).

The absolute value of the first order approximation is:

$$|u_1(t,z)|^2 = {\psi_1}^2 + {\phi_1}^2 \quad (2.67)$$

2.4.1.3 Second order approximation

$$i\frac{\partial u_2(t,z)}{\partial z} + \alpha\frac{\partial^2 u_2(t,z)}{\partial t^2} + \varepsilon|u_1(t,z)|^2 u_1(t,z) + i\gamma u_2(t,z) = 0,$$

$$(t,z) \in (0,T)x\,(0,\infty) \quad (2.68)$$

with initial conditions $u_2(t,0) = f_1(t) + i\,f_2(t)$ and boundary conditions $u_2(0,z) = u_2(T,z) = 0$. Following Appendix (A), the linear Schrodinger equation (2.68) has the following solution:

$$u_2(t,z) = \psi_2 + i\,\phi_2\,, \quad (2.69)$$

$$\psi_2(t,z) = e^{-\gamma z}\sum_{n=0}^{\infty} T_{2n}(z)\sin\left(\frac{n\pi}{T}\right)t, \quad (2.70)$$

$$\phi_2(t,z) = e^{-\gamma z}\sum_{n=0}^{\infty} \tau_{2n}(z)\sin\left(\frac{n\pi}{T}\right)t \quad (2.71)$$

$$H_{12} = e^{-2\gamma z}\varepsilon({\psi_1}^3 + \psi_1{\phi_1}^2) \quad (2.72)$$

$$H_{22} = -e^{-2\gamma z}\varepsilon\left({\phi_1}^3 + \phi_1{\psi_1}^2\right) \quad (2.73)$$

in which,

$$T_{2n}(z) = A_{21}(z)\sin\beta_n z + \left(C_{22} + B_{21}(z)\right)\cos\beta_n z, \quad (2.74)$$

$$\tau_{2n}(z) = A_{22}(z)\sin\beta_n z + \left(C_{24} + B_{22}(z)\right)\cos\beta_n z, \quad (2.75)$$

where the constants and variables A_{21} , C_{22} , B_{21} , A_{22} , C_{24} , B_{22} can be calculated in similar manner as illustrated in Appendix (A).

The absolute value of the second order approximation is:

$$|u_2(t\,,z)|^2 = \psi_2{}^2 + \phi_2{}^2 \tag{2.76}$$

2.4.1.4 Third order approximation

$$i\,\frac{\partial u_3(t,z)}{\partial z} + \alpha\,\frac{\partial^2 u_3(t,z)}{\partial t^2} + \varepsilon|u_2(t,z)|^2 u_2(t,z) + i\,\gamma u_3(t,z) = 0,$$

$$(t,z) \in (0,T)x\,(0,\infty) \tag{2.77}$$

with initial conditions $u_2(t,0) = f_1(t) + i\,f_2(t)$ and boundary conditions $u_2(0,z) = u_2(T,z) = 0$. Following Appendix (A), the linear Schrodinger equation (2.77) has the following solution:

$$u_3(t\,,z) = \psi_3 + i\,\phi_3\,, \tag{2.78}$$

$$\psi_3(t\,,z) = e^{-\gamma z}\sum_{n=0}^{\infty} T_{3n}(z)\sin\left(\frac{n\,\pi}{T}\right)t, \tag{2.79}$$

$$\phi_3(t\,,z) = e^{-\gamma z}\sum_{n=0}^{\infty} \tau_{3n}(z)\sin\left(\frac{n\,\pi}{T}\right)t \tag{2.80}$$

$$H_{13} = e^{-2\gamma z}\varepsilon\left(\psi_2{}^3 + \psi_2\phi_2{}^2\right) \tag{2.81}$$

$$H_{32} = -e^{-2\gamma z}\varepsilon\left(\phi_2{}^3 + \phi_2\psi_2{}^2\right) \tag{2.82}$$

where,

$$T_{3n}(z) = A_{31}(z)\sin\beta_n z + \left(C_{32} + B_{31}(z)\right)\cos\beta_n z, \tag{2.83}$$

$$\tau_{3n}(z) = A_{32}(z)\sin\beta_n z + \left(C_{34} + B_{32}(z)\right)\cos\beta_n z, \tag{2.84}$$

where the constants and variables $A_{31}\,, C_{32}\,,\ B_{31}\,,\ A_{32}\,, C_{34}\,, B_{32}$ can be calculated in similar manner as illustrated in Appendix (A).

The absolute value of the third order approximation is:

$$|u_3(t\,,z)|^2 = \psi_3{}^2 + \phi_3{}^2 \tag{2.85}$$

2.5 Case studies, Picard

To examine the proposed solution algorithm, some case studies are illustrated.

2.5.1 Case study 1

Taking the case $f_1(t) = \rho_1, f_2(t) = \rho_2 \sin\left(\frac{\pi}{T} t\right)$ where ρ_1 & ρ_2 are constants and following the algorithm, the following selected results for the first and second order approximations are got:

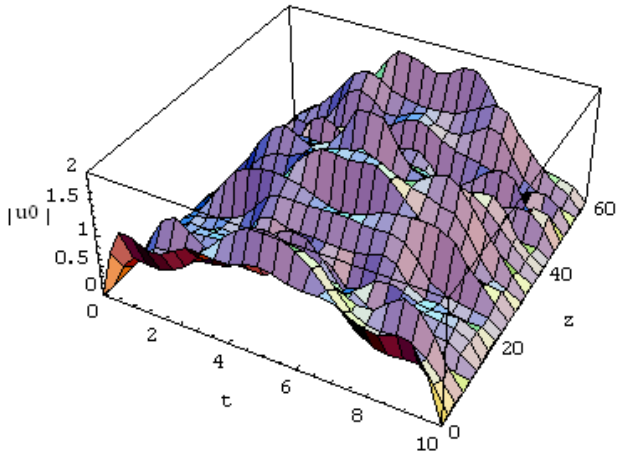

Fig.(2.54) the first order approximation of $\left|u^{(0)}\right|$ at $\varepsilon = 0$, $\gamma = 0$ and $\alpha, \rho_1, \rho_2 = 1, T = 10$ with considering only ten terms on the series (M=10)

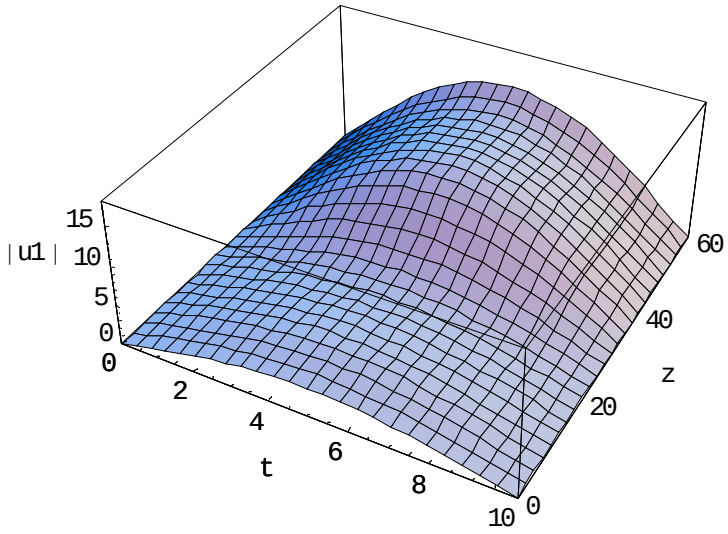

Fig. (2.55) the first order approximation of $\left|u^{(1)}\right|$ at $\varepsilon = 0.2$, $\gamma = 0$ and $\alpha, \rho_1, \rho_2 = 1, T = 10$ with considering only one term on the series (M=1)

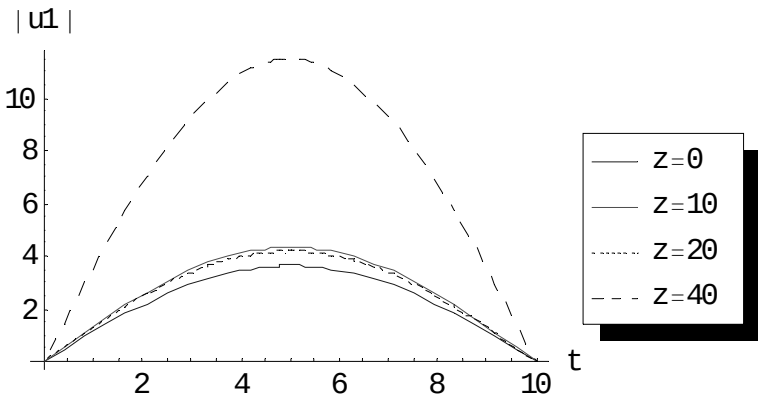

Fig. (2.56) the first order approximation of $\left|u^{(1)}\right|$ at $\varepsilon = 0.2$, $\gamma = 0$ and $\alpha, \rho_1, \rho_2 = 1, T = 10, M = 1$ for different values of z.

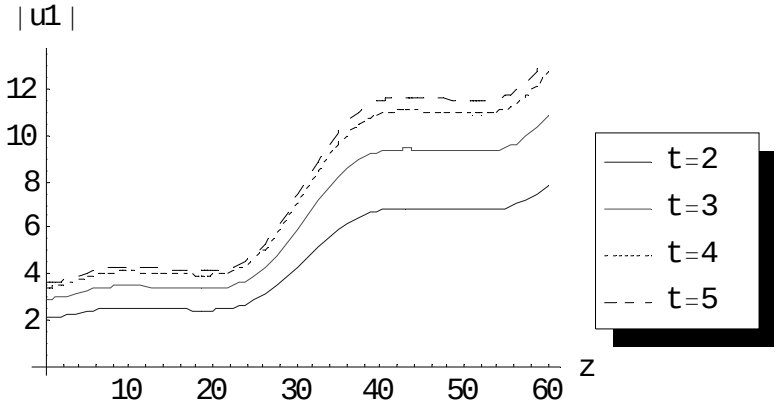

Fig. (2.57) the first order approximation of $\left|u^{(1)}\right|$ at $\varepsilon = 0.2$, $\gamma = 0$ and $\alpha, \rho_1, \rho_2 = 1, T = 10, M = 1$ for different values of t.

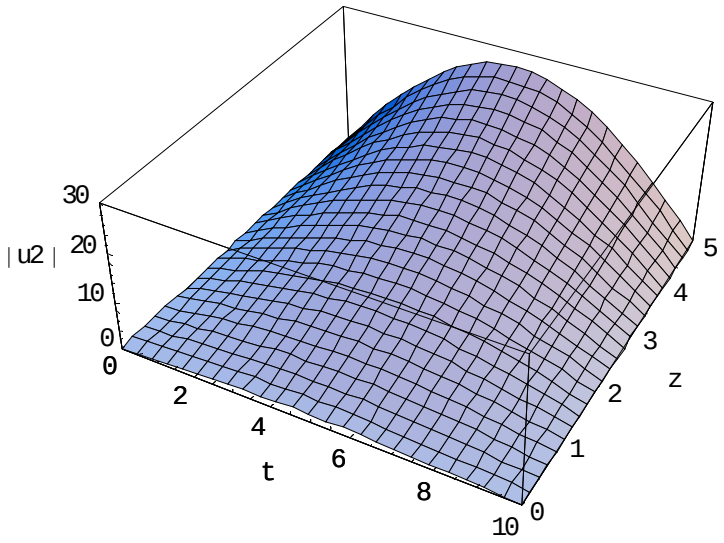

Fig. (2.58) the second order approximation of $\left|u^{(2)}\right|$ at $\varepsilon = 0.2$, $\gamma = 0$ and $\alpha, \rho_1, \rho_2 = 1, T = 10$ with considering only one term on the series (M=1)

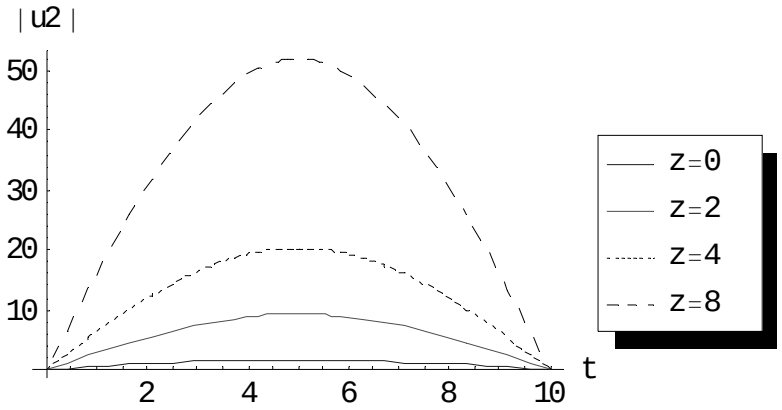

Fig. (2.59) the second order approximation of $\left|u^{(2)}\right|$ at $\varepsilon = 0.2$, $\gamma = 0$ and $\alpha, \rho_1, \rho_2 = 1, T = 10, M = 1$ for different values of z.

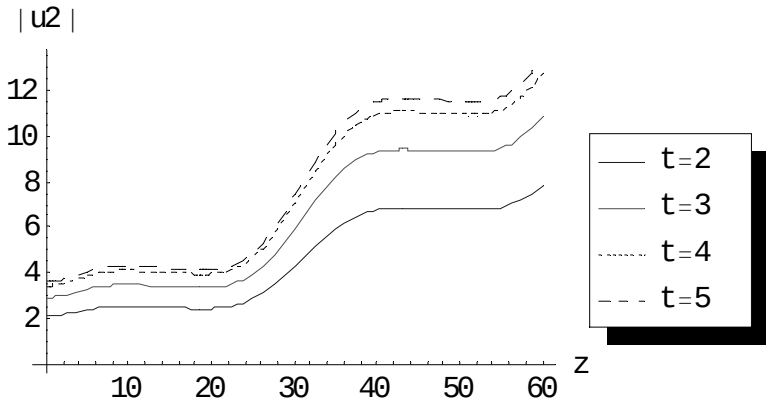

Fig. (2.60) the second order approximation of $\left|u^{(2)}\right|$ at $\varepsilon = 0.2$, $\gamma = 0$ and $\alpha, \rho_1, \rho_2 = 1, T = 10, M = 1$ for different values of t.

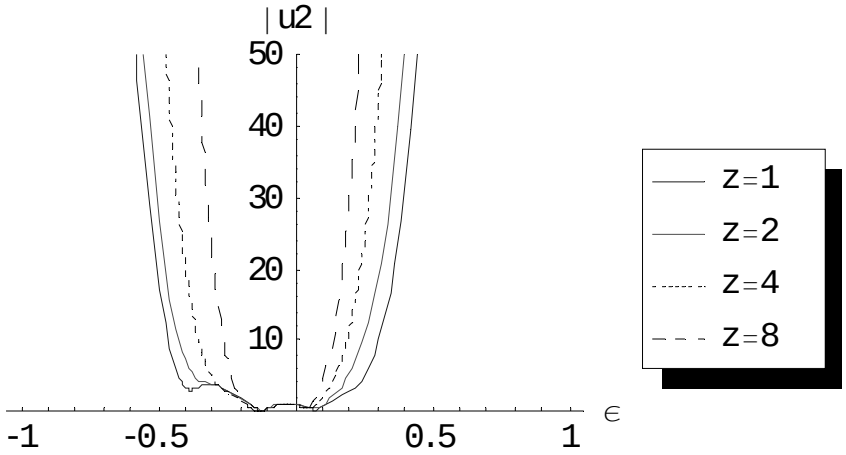

Fig. (2.61) the second order approximation of $\left|u^{(2)}\right|$ at $t = 2, \gamma = 0$ and $\alpha, \rho_1, \rho_2 = 1, T = 10, M = 1$ and t = 2 for different values of z.

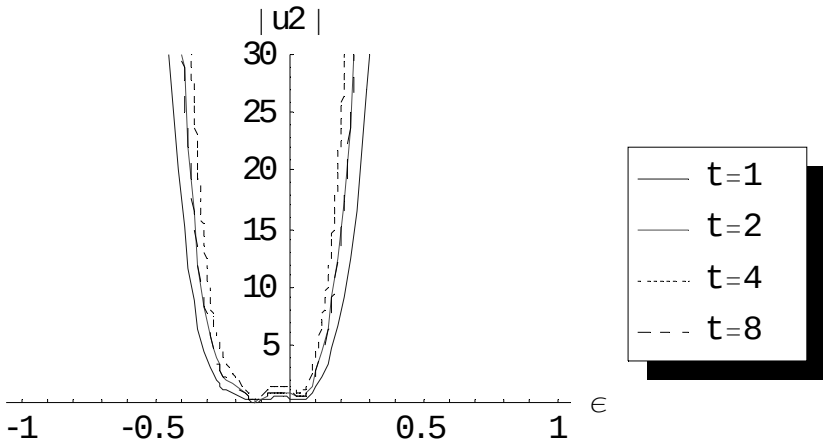

Fig. (2.62) the second order approximation of $\left|u^{(2)}\right|$ at $z = 5, \gamma = 0$ and $\alpha, \rho_1, \rho_2 = 1, T = 10, M = 1$ and z = 5 for different values of t.

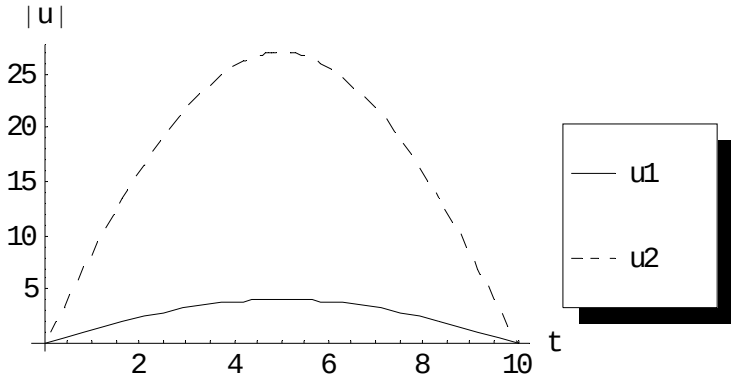

Fig. (2.63) comparison between first and second order approximations at $\varepsilon = 0.2$, $\gamma = 0$ and $\alpha, \rho_1, \rho_2 = 1, T = 10, M = 1, z = 5$.

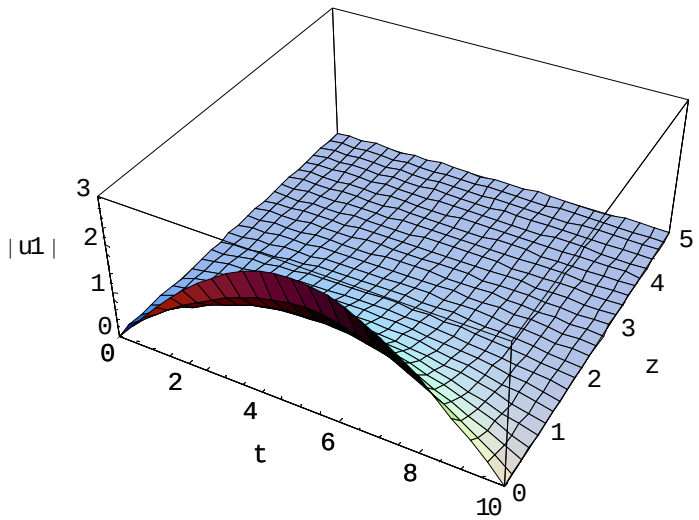

Fig. (2.64) the first order approximation of $\left|u^{(1)}\right|$ at $\varepsilon = 1, \gamma = 1$ and $\alpha, \rho_1, \rho_2 = 1, T = 10$ with considering only one term on the series (M=1)

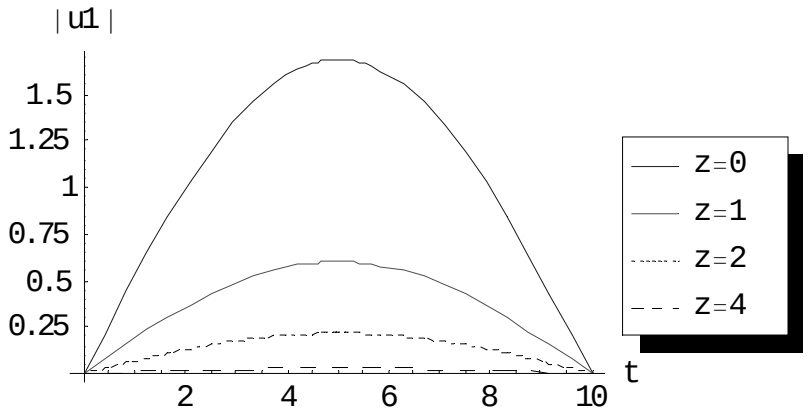

Fig. (2.65) the first order approximation of $\left|u^{(1)}\right|$ at $\varepsilon = 0.2,\ \gamma = 1$ and $\alpha, \rho_1, \rho_2, = 1, T = 10, M = 1$ for different values of z.

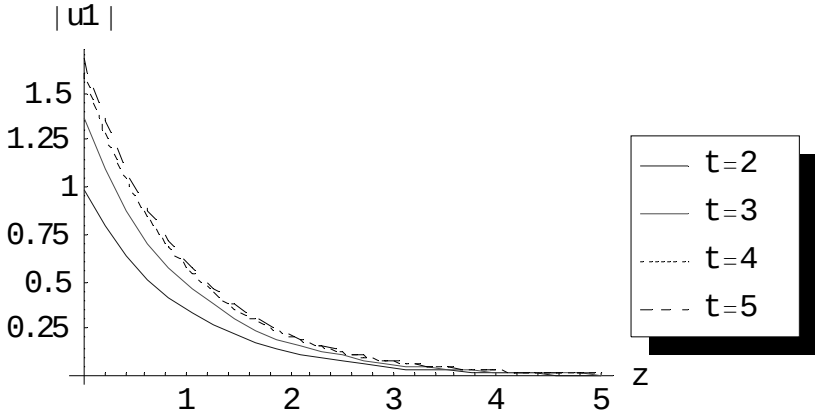

Fig. (2.66) the first order approximation of $\left|u^{(1)}\right|$ at $\varepsilon = 0.2\ , \gamma = 1$ and $\alpha, \rho_1, \rho_2 = 1, T = 10, M = 1$ for different values of t.

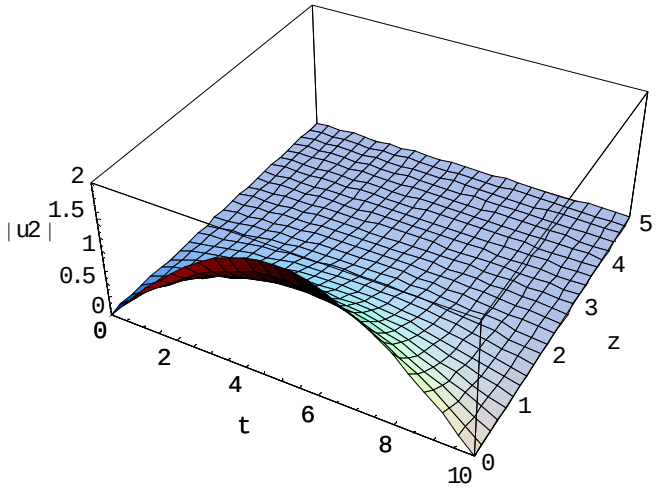

Fig. (2.67) the first order approximation of $\left|u^{(2)}\right|$ at $\varepsilon = 0.2$ and $\alpha, \rho_1, \rho_2, \gamma = 1, T = 10$ with considering only one term on the series (M=1)

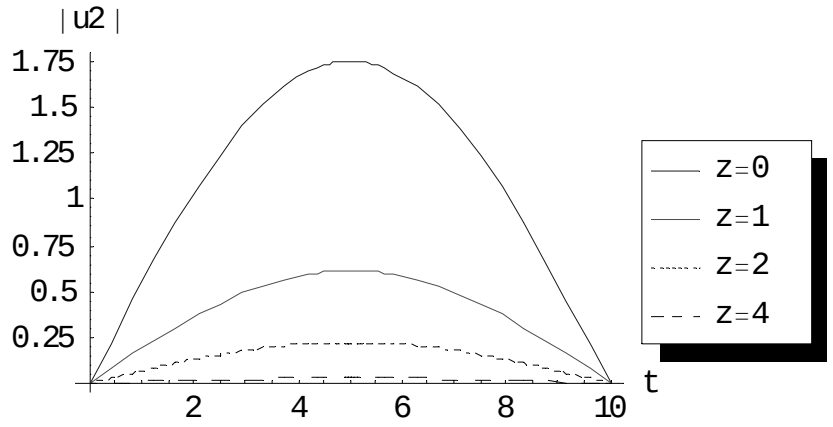

Fig. (2.68) the second order approximation of $\left|u^{(2)}\right|$ at $\varepsilon = 0.2, \gamma = 1$ and $\alpha, \rho_1, \rho_2 = 1, T = 10, M = 1$ for different values of z.

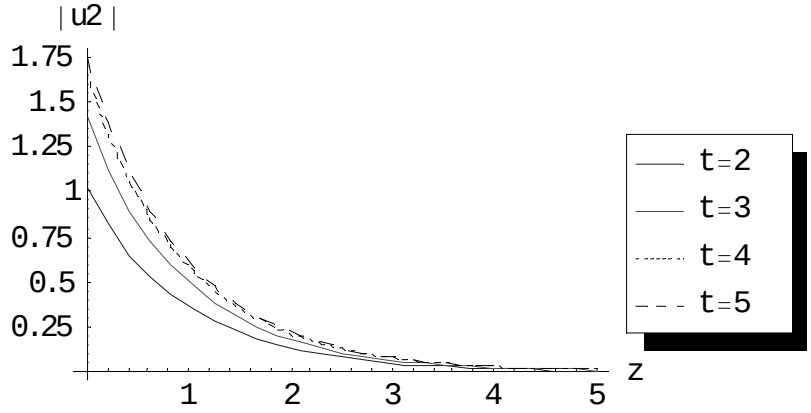

Fig. (2.69) the second order approximation of $\left|u^{(2)}\right|$ at $\varepsilon = 0.2, \gamma = 1$ and $\alpha, \rho_1, \rho_2 = 1, T = 10, M = 1$ for different values of t.

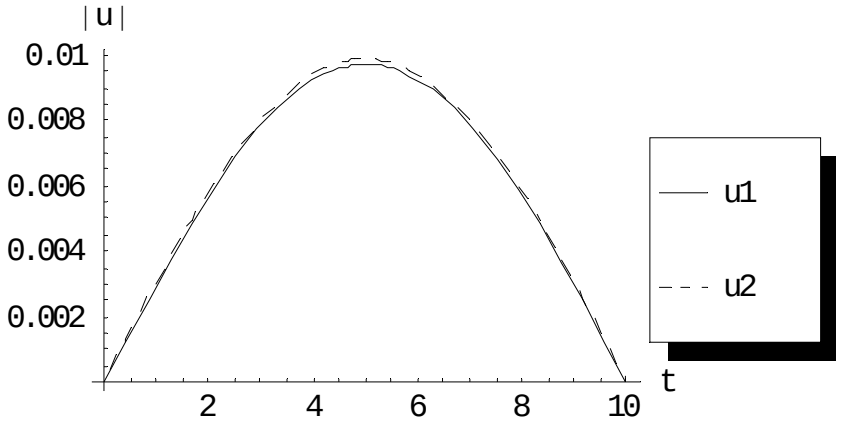

Fig. (2.70) comparison between first and second order approximations at $\varepsilon = 0.2, \gamma = 1$ and $\alpha, \rho_1, \rho_2 = 1, T = 10, M = 1, z = 5$.

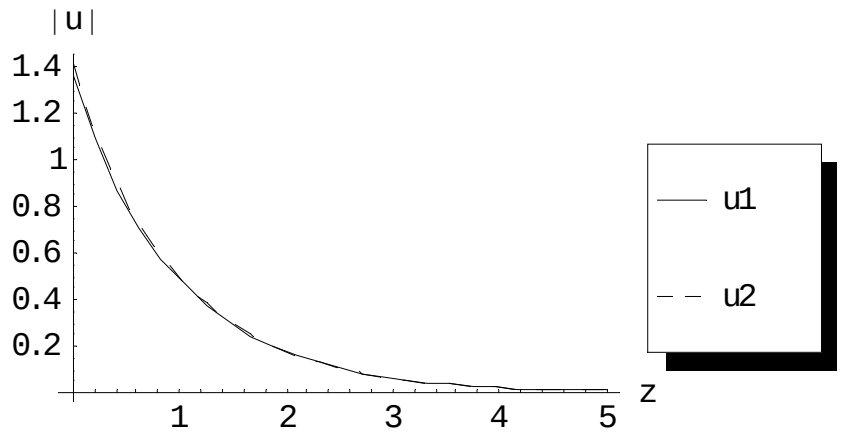

Fig. (2.71) comparison between first and second order approximations at $\varepsilon = 0.2, \gamma = 1$ and $\alpha, \rho_1, \rho_2 = 1, T = 10, M = 10, t = 3$.

2.5.2 Case study 2

Taking the case $f_1(t) = \rho_1 e^{-t}, f_2(t) = \rho_2 e^{-t}$ where ρ_1 & ρ_2 are constants and following the algorithm, the following selected results for the first and second order approximations are got:

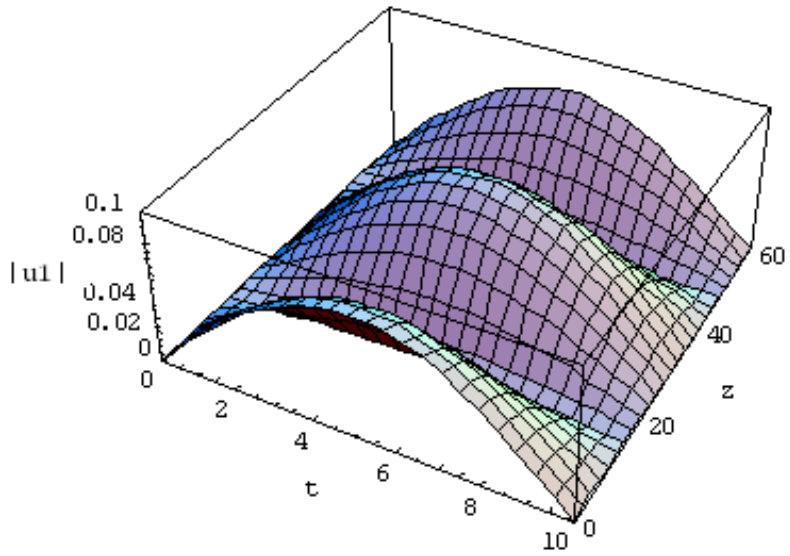

Fig. (2.72) the first order approximation of $\left|u^{(1)}\right|$ at $\varepsilon = 0.2$, $\gamma = 0$ and $\alpha, \rho_1, \rho_2 = 1, T = 10$ with considering only one term on the series (M=1)

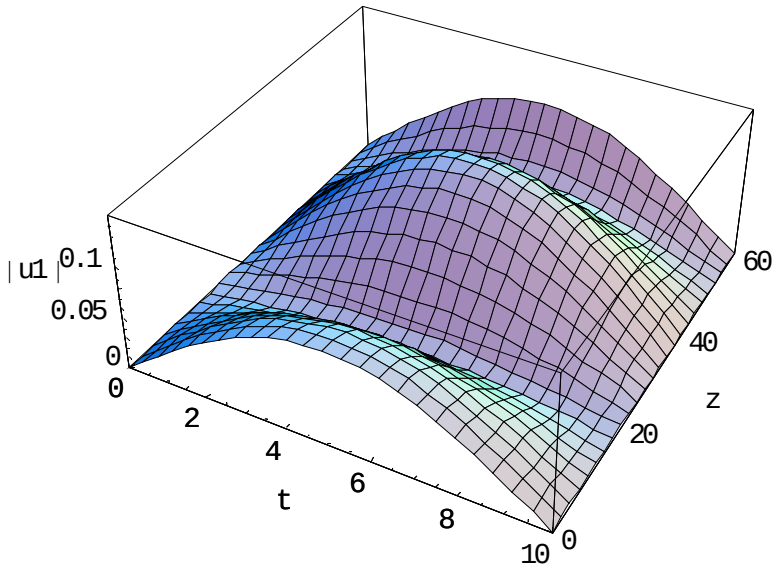

Fig. (2.73) the first order approximation of $\left|u^{(1)}\right|$ at $\varepsilon = 1$, $\gamma = 0$ and $\alpha, \rho_1, \rho_2 = 1, T = 10$ with considering only one term on the series (M=1)

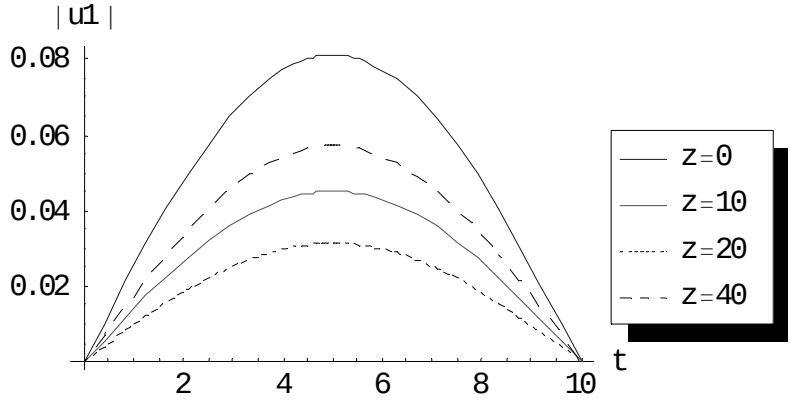

Fig. (2.74) the first order approximation of $\left|u^{(1)}\right|$ at $\varepsilon = 0.2$, $\gamma = 0$ and $\alpha, \rho_1, \rho_2 = 1, T = 10, M = 1$ for different values of z.

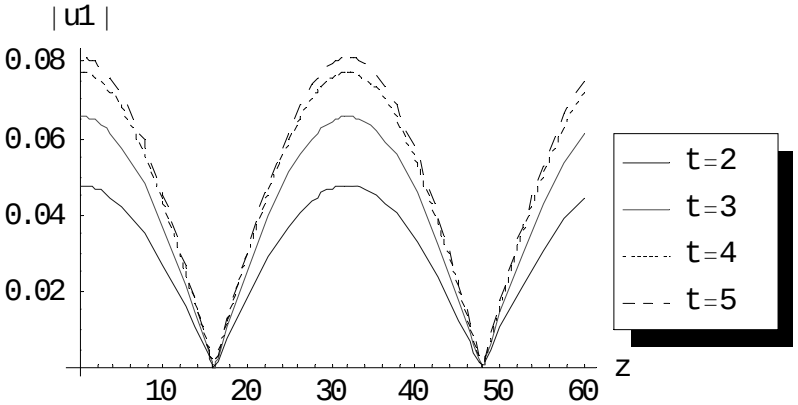

Fig. (2.75) the first order approximation of $\left|u^{(1)}\right|$ at $\varepsilon = 0.2$, $\gamma = 0$ and $\alpha, \rho_1, \rho_2 = 1, T = 10, M = 1$ for different values of t.

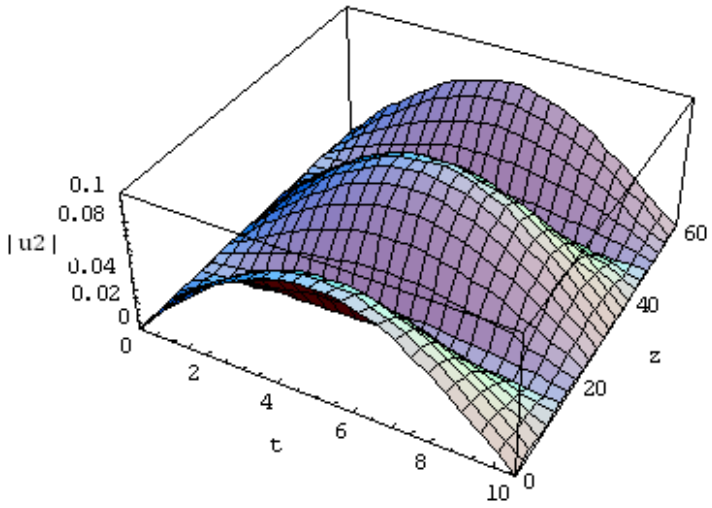

Fig. (2.76) the second order approximation of $\left|u^{(2)}\right|$ at $\varepsilon = 0.2$, $\gamma = 0$ and $\alpha, \rho_1, \rho_2 = 1, T = 10$ with considering only one term on the series (M=1)

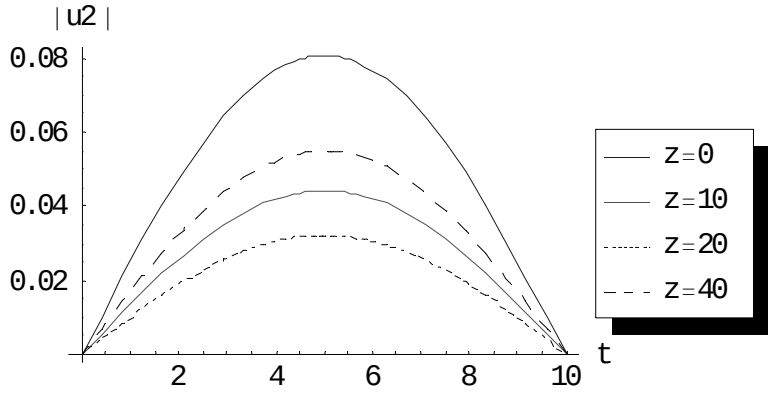

Fig. (2.77) the second order approximation of $\left|u^{(2)}\right|$ at $\varepsilon = 0.2$, $\gamma = 0$ and $\alpha, \rho_1, \rho_2 = 1, T = 10, M = 1$ for different values of z.

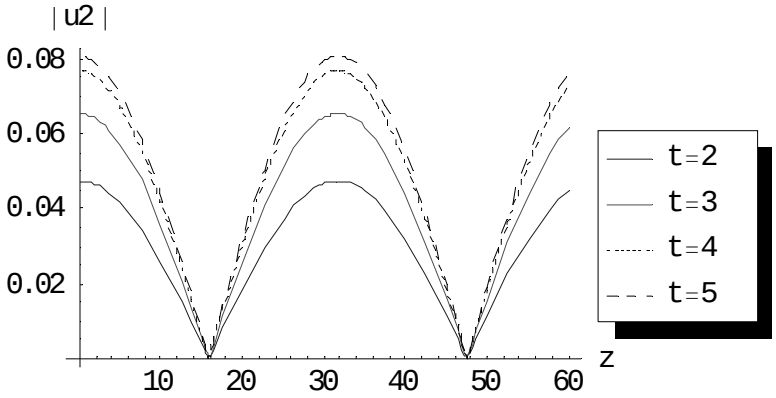

Fig. (2.78) the second order approximation of $\left|u^{(2)}\right|$ at $\varepsilon = 0.2$, $\gamma = 0$ and $\alpha, \rho_1, \rho_2 = 1, T = 10, M = 1$ for different values of t.

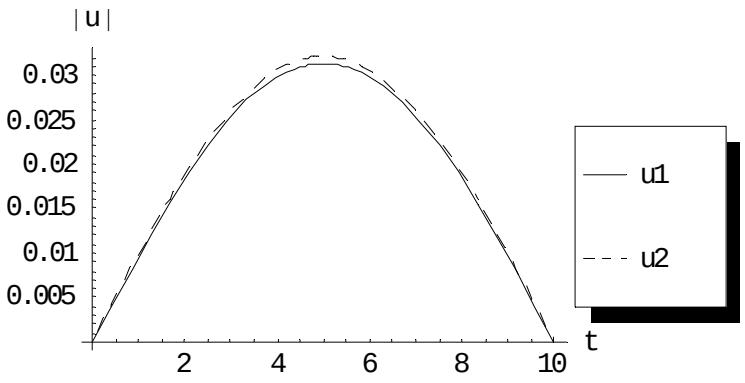

Fig. (2.79) comparison between first and second order approximations at $\varepsilon = 0.2$,$\gamma = 0$ and $\alpha, \rho_1, \rho_2 = 1, T = 10, M = 1, z = 2$.

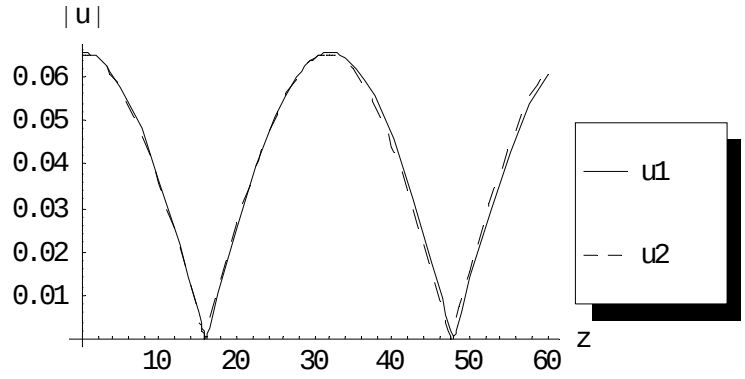

Fig. (2.80) comparison between first and second order approximations at $\varepsilon = 0.2$, $\gamma = 0$ and $\alpha, \rho_1, \rho_2 = 1, T = 10, M = 1, t = 3$.

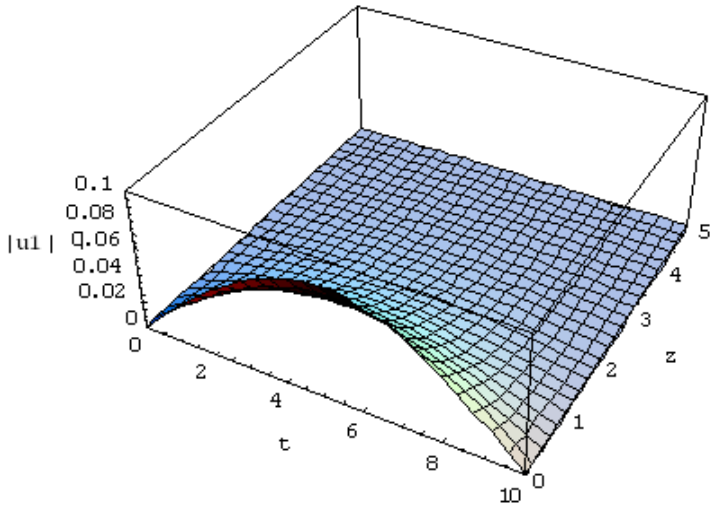

Fig. (2.81) the first order approximation of $\left|u^{(1)}\right|$ at $\varepsilon = 0.2$, $\gamma = 1$ and $\alpha, \rho_1, \rho_2 = 1, T = 10$ with considering only one term on the series (M=1)

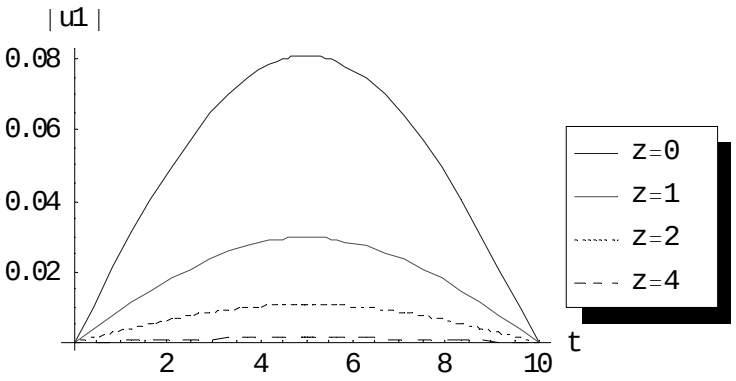

Fig. (2.82) the first order approximation of $\left|u^{(1)}\right|$ at $\varepsilon = 0.2$, $\gamma = 1$ and $\alpha, \rho_1, \rho_2 = 1, T = 10, M = 1$ for different values of z.

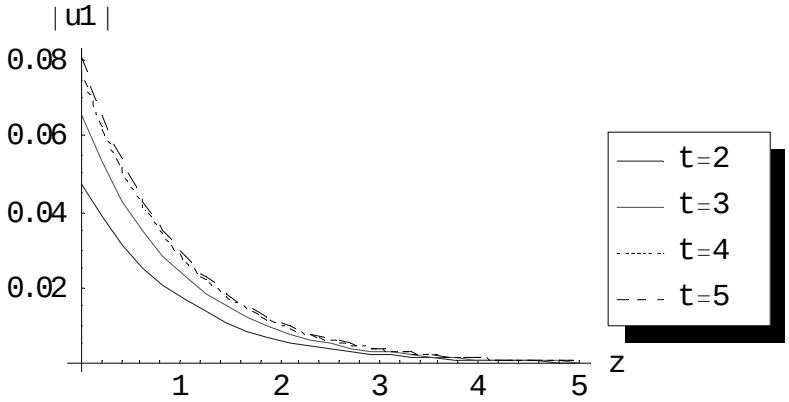

Fig. (2.83) the first order approximation of $\left|u^{(1)}\right|$ at $\varepsilon = 0.2$, $\gamma = 1$ and $\alpha, \rho_1, \rho_2 = 1, T = 10, M = 1$ for different values of t.

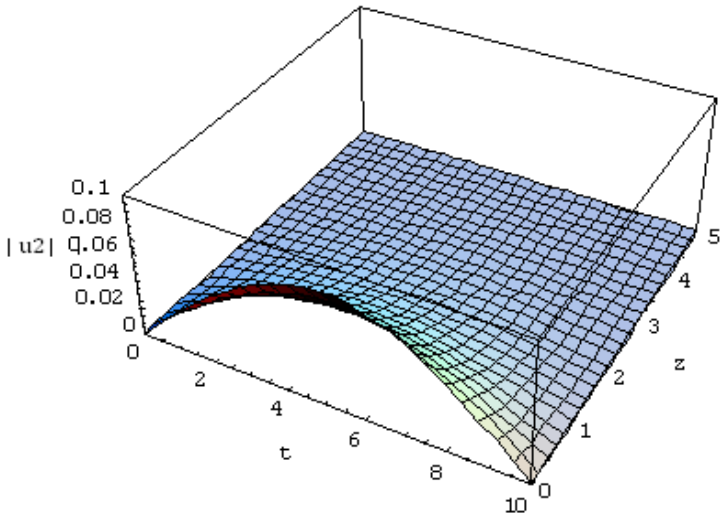

Fig. (2.84) the second order approximation of $\left|u^{(2)}\right|$ at $\varepsilon = 1$, $\gamma = 1$ and $\alpha, \rho_1, \rho_2 = 1, T = 10$ with considering only one term on the series (M=1)

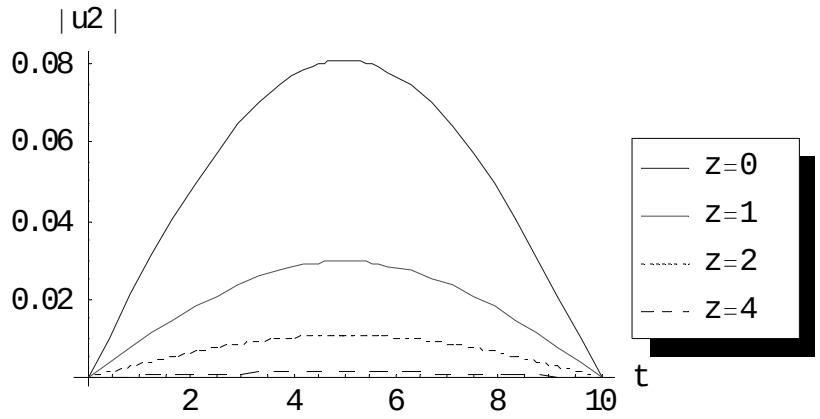

Fig. (2.85) the second order approximation of $\left|u^{(2)}\right|$ at $\varepsilon = 0.2$, $\gamma = 1$ and $\alpha, \rho_1, \rho_2 = 1, T = 10, M = 1$ for different values of z.

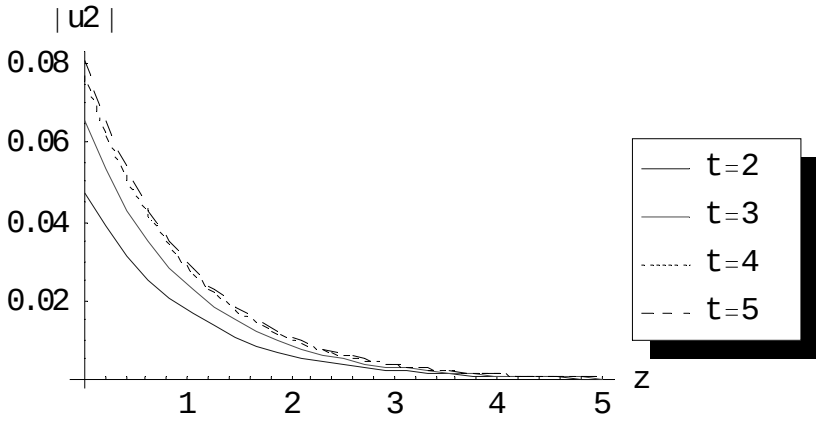

Fig. (2.86) the second order approximation of $\left|u^{(2)}\right|$ at $\varepsilon = 0.2$, $\gamma = 1$ and $\alpha, \rho_1, \rho_2 = 1, T = 10, M = 1$ for different values of t.

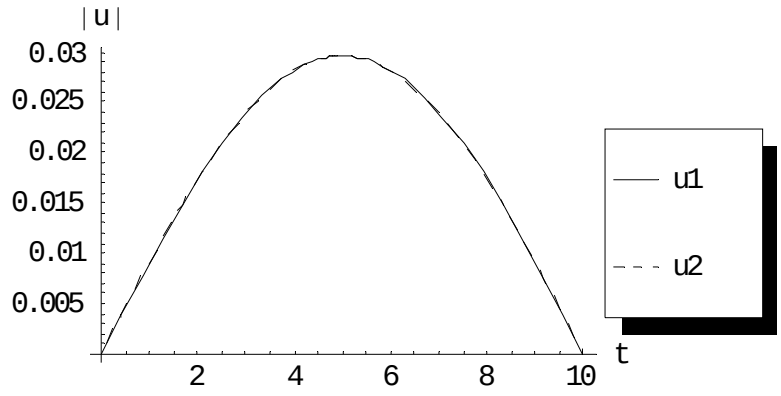

Fig. (2.87) comparison between first and second order approximations at $\varepsilon = 0.2, \gamma = 1$ and $\alpha, \rho_1, \rho_2 = 1, T = 10, M = 1, z = 5$.

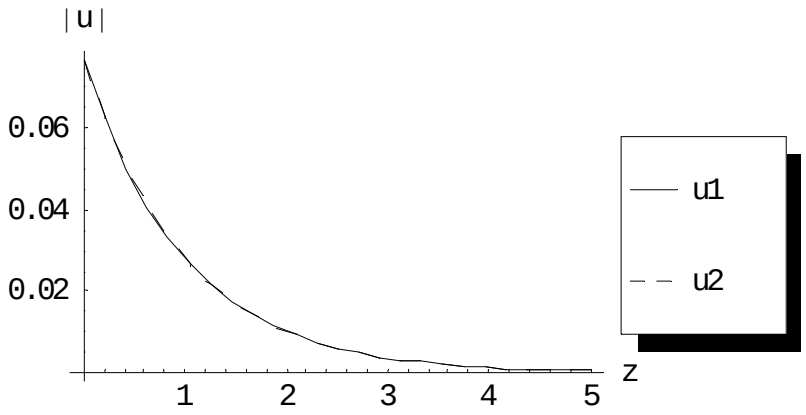

Fig. (2.88) comparison between first and second order approximations at $\varepsilon = 0.2, \gamma = 1$ and $\alpha, \rho_1, \rho_2 = 1, T = 10, M = 1, z = 5.$

2.5.3 Case study 3

Taking the case $f_1(t) = \rho_1, f_2(t) = \rho_2$ where ρ_1 & ρ_2 are constants and following the algorithm, the following selected results for the first and second order approximations are got:

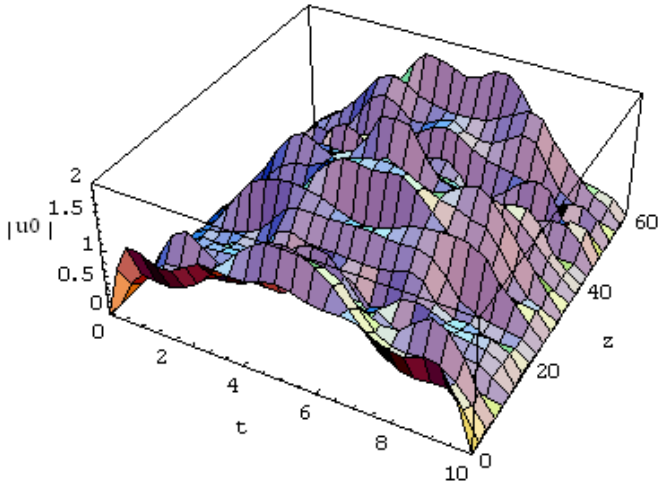

Fig. (2.89) the zero order approximation of $\left|u^{(0)}\right|$ at $\varepsilon = 0$, $\gamma = 0$ and $\alpha, \rho_1, \rho_2 = 1, T = 10$ with considering only ten terms on the series (M=10)

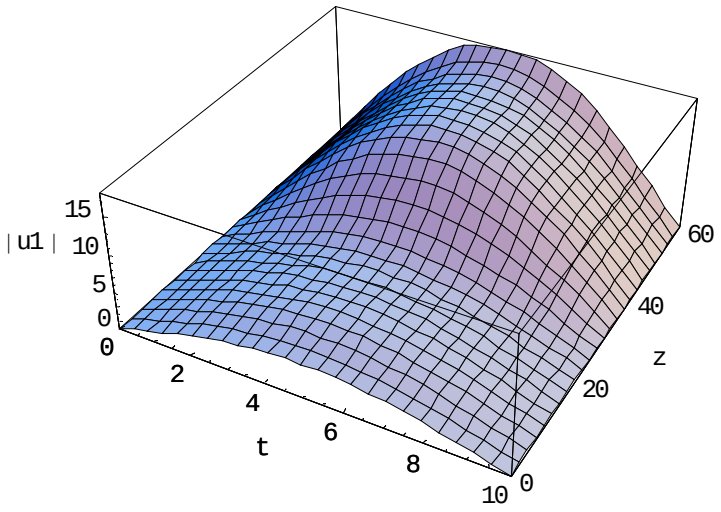

Fig. (2.90) the first order approximation of $\left|u^{(1)}\right|$ at $\varepsilon = 0$, $\gamma = 0$ and $\alpha, \rho_1, \rho_2 = 1, T = 10$ with considering only ten terms on the series (M=1)

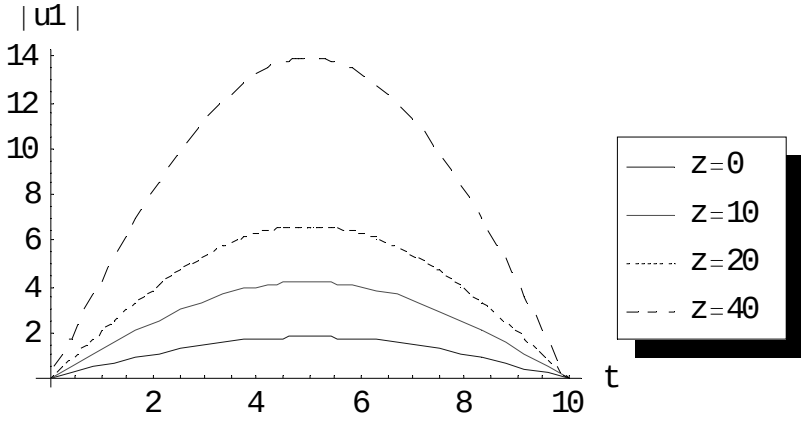

Fig. (2.91) the first order approximation of $\left|u^{(1)}\right|$ at $\varepsilon = 0.2, \gamma = 0$ and $\alpha, \rho_1, \rho_2 = 1, T = 10, M = 1$ for different values of z.

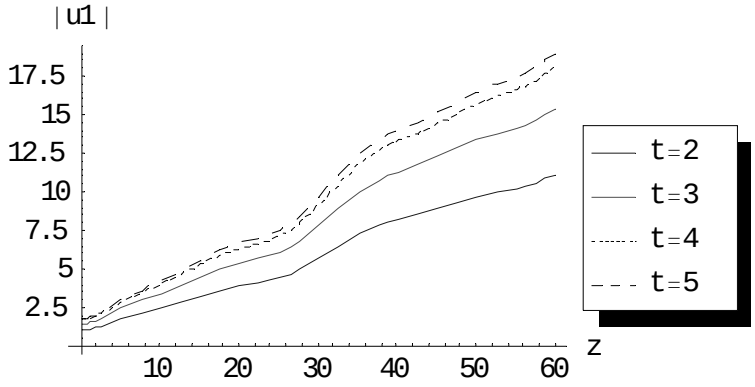

Fig. (2.92) the first order approximation of $\left|u^{(1)}\right|$ at $\varepsilon = 0.2$, $\gamma = 0$ and $\alpha, \rho_1, \rho_2 = 1, T = 10, M = 1$ for different values of t.

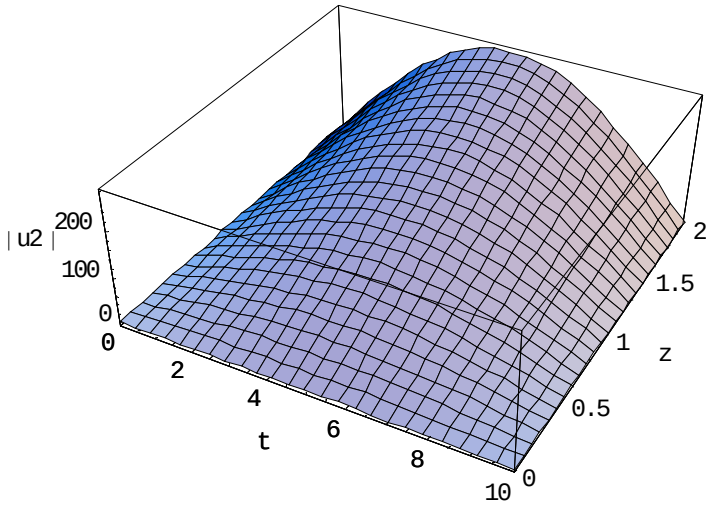

Fig. (2.93) the second order approximation of $\left|u^{(2)}\right|$ at $\varepsilon = 1, \gamma = 0$ and $\alpha, \rho_1, \rho_2 = 1, T = 10$ with considering only one term on the series (M=1)

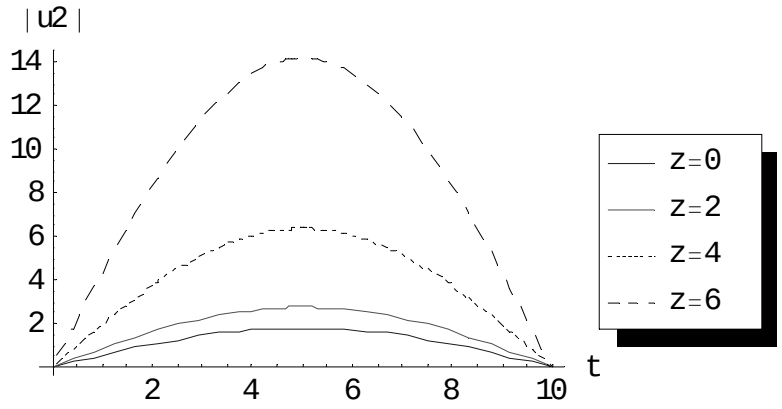

Fig. (2.94) the second order approximation of $\left|u^{(2)}\right|$ at $\varepsilon = 0.2, \gamma = 0$ and $\alpha, \rho_1, \rho_2 = 1, T = 10, M = 1$ for different values of z.

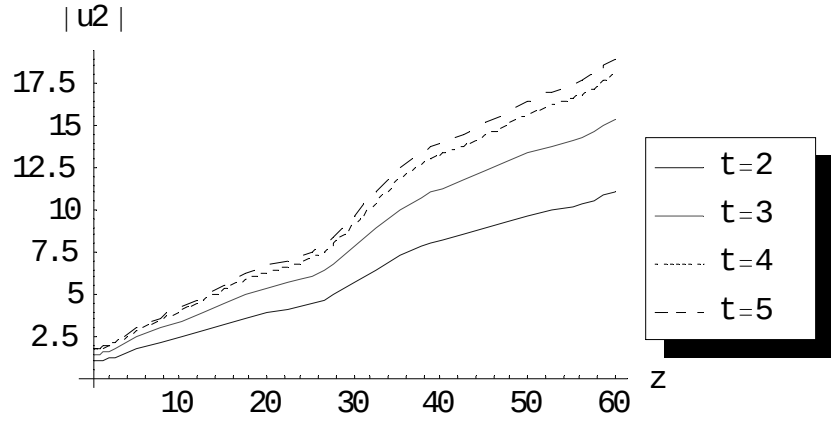

Fig. (2.95) the second order approximation of $\left|u^{(2)}\right|$ at $\varepsilon = 0.2, \gamma = 0$ and $\alpha, \rho_1, \rho_2 = 1, T = 10, M = 1$ for different values of t.

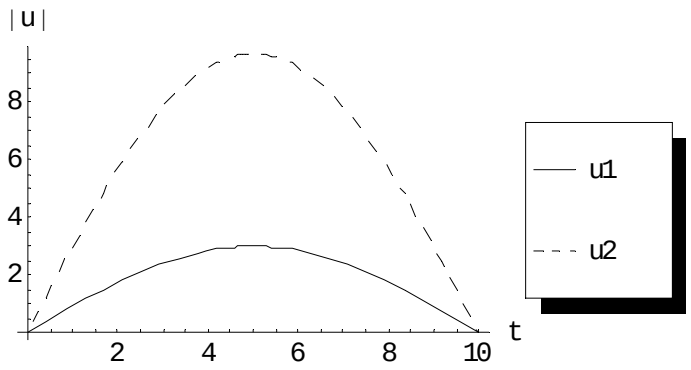

Fig. (2.96) comparison between first and second order approximations at $\varepsilon = 0.2, \gamma = 0$ and $\alpha, \rho_1, \rho_2 = 1, T = 10, M = 1, z = 5$.

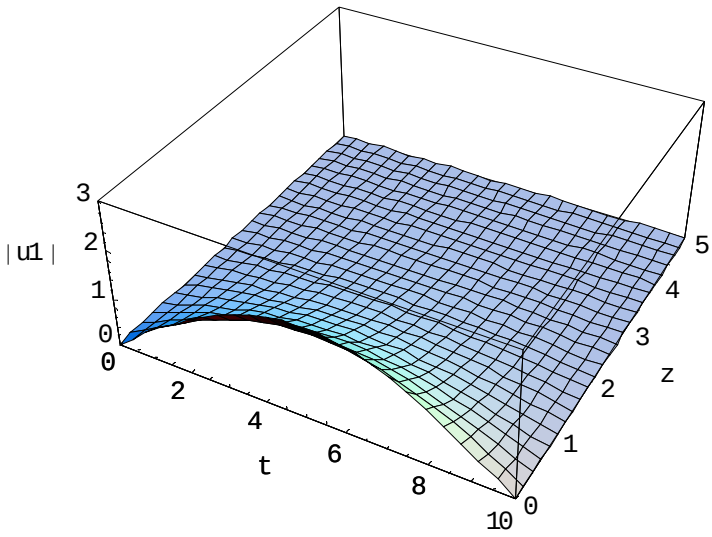

Fig. (2.97) the first order approximation of $\left|u^{(1)}\right|$ at $\varepsilon = 0.2, \gamma = 1$ and $\alpha, \rho_1, \rho_2 = 1, T = 10$ with considering only one term on the series (M=1)

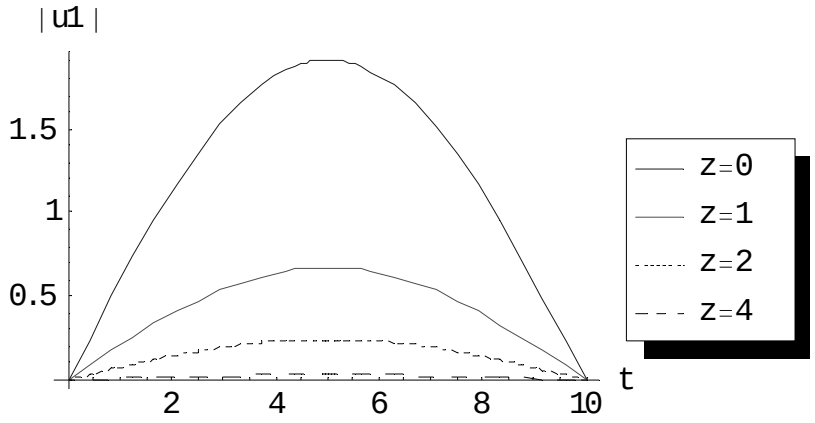

Fig. (2.98) the first order approximation of $\left|u^{(1)}\right|$ at $\varepsilon = 0.2$, $\gamma = 1$ and $\alpha, \rho_1, \rho_2 = 1, T = 10, M = 1$ for different values of z.

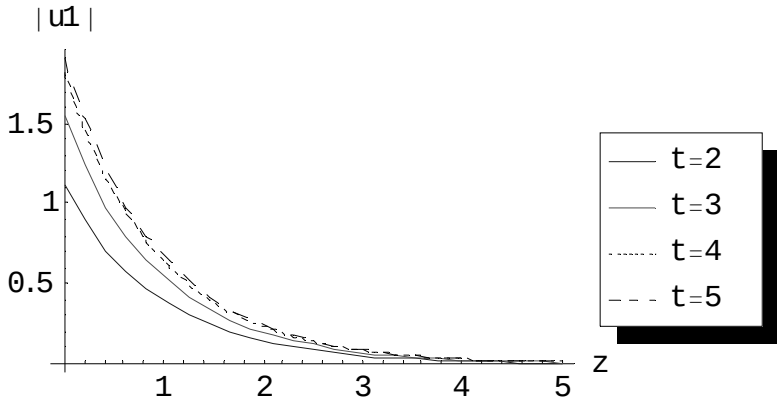

Fig. (2.99) the first order approximation of $\left|u^{(1)}\right|$ at $\varepsilon = 0.2, \gamma = 1$ and $\alpha, \rho_1, \rho_2 = 1, T = 10, M = 1$ for different values of t.

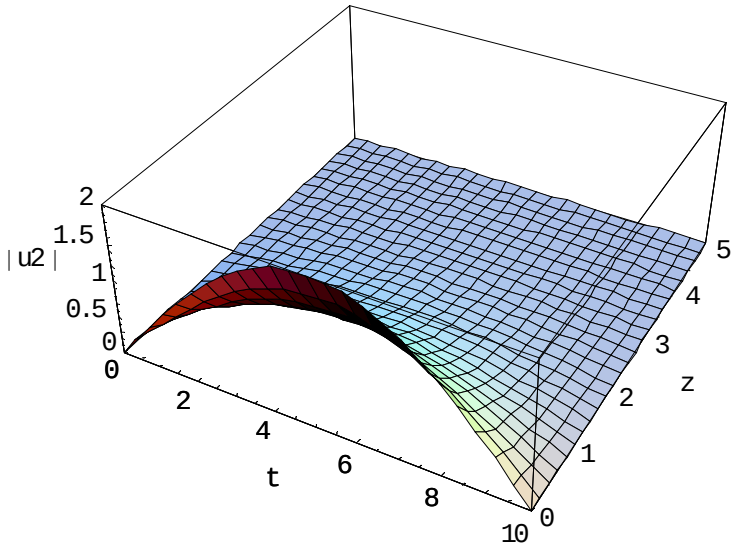

Fig. (2.100) the second order approximation of $\left|u^{(2)}\right|$ at $\varepsilon = 0.2$, $\gamma = 1$ and $\alpha, \rho_1, \rho_2 = 1, T = 10$ with considering only one term on the series (M=1)

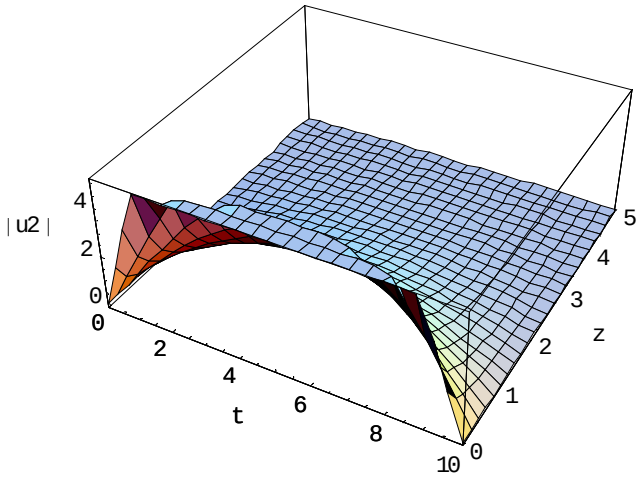

Fig. (2.101) the second order approximation of $\left|u^{(2)}\right|$ at $\varepsilon = 1$, $\gamma = 1$ and $\alpha, \rho_1, \rho_2 = 1, T = 10$ with considering only one term on the series (M=1)

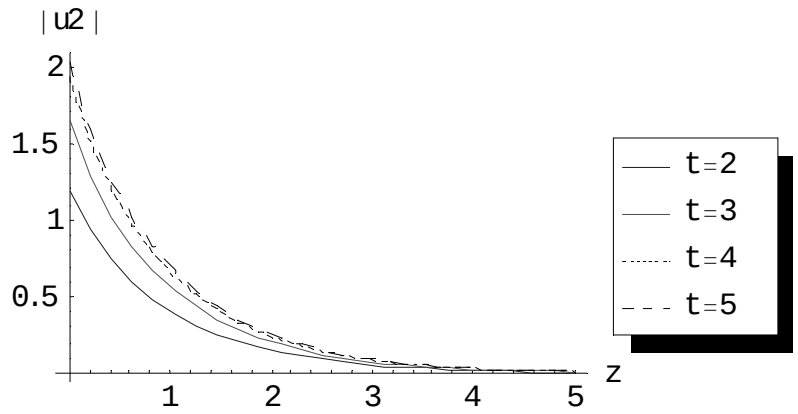

Fig. (2.102) the second order approximation of $\left|u^{(2)}\right|$ at $\varepsilon = 0.2, \gamma = 1$ and $\alpha, \rho_1, \rho_2 = 1, T = 10, M = 1$ for different values of t.

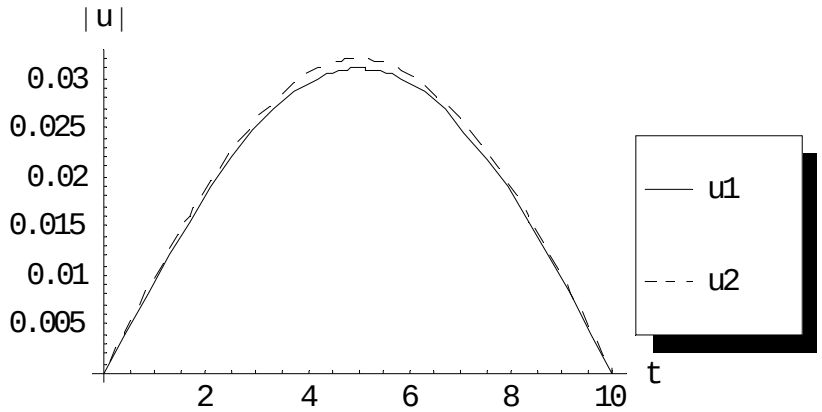

Fig. (2.103) comparison between first and second order approximations at $\varepsilon = 0.2, \gamma = 1$ and $\alpha, \rho_1, \rho_2 = 1, T = 10, M = 1, z = 4$.

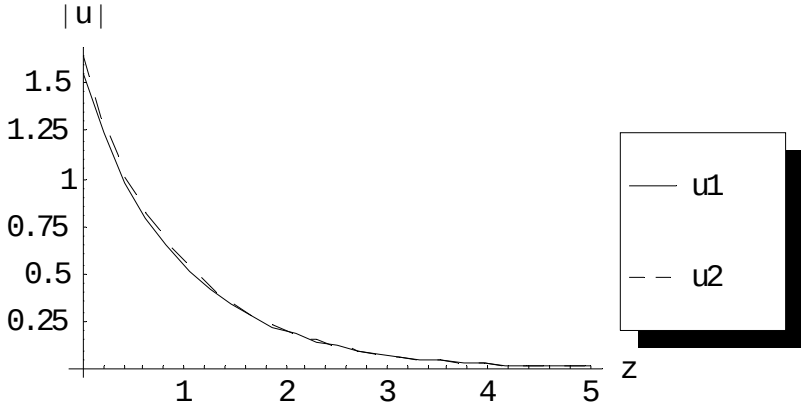

Fig. (2.104) comparison between first and second order approximations at $\varepsilon = 0.2, \gamma = 1$ and $\alpha, \rho_1, \rho_2 = 1, T = 10, M = 1, t = 3$.

2.6 Comparison between Perturbation & Picard Approximation

We are here giving both perturbation and Picard results in the same graph for some selected cases.

2.6.1 Case Study 1

Taking the case $f_1(t) = \rho_1, f_2(t) = \rho_2$ where ρ_1 & ρ_2 are constants, the following selected results are obtained.

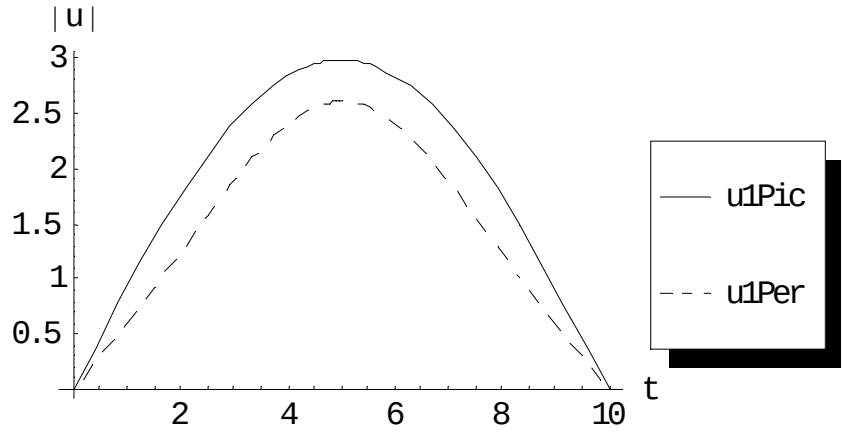

Fig. (2.105) comparison between Picard approximation and Perturbation method for first order at $\varepsilon = 0.2,\ \gamma = 0$ and $\alpha, \rho_1, \rho_2 = 1, T = 10, z = 5$.

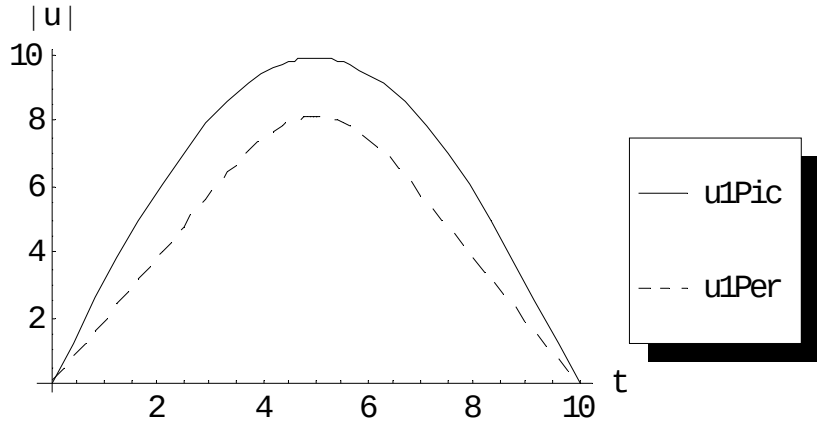

Fig. (2.106) comparison between Picard approximation and Perturbation method for first order at $\varepsilon = 1, \gamma = 0$ and $\alpha, \rho_1, \rho_2 = 1, T = 10, z = 5$.

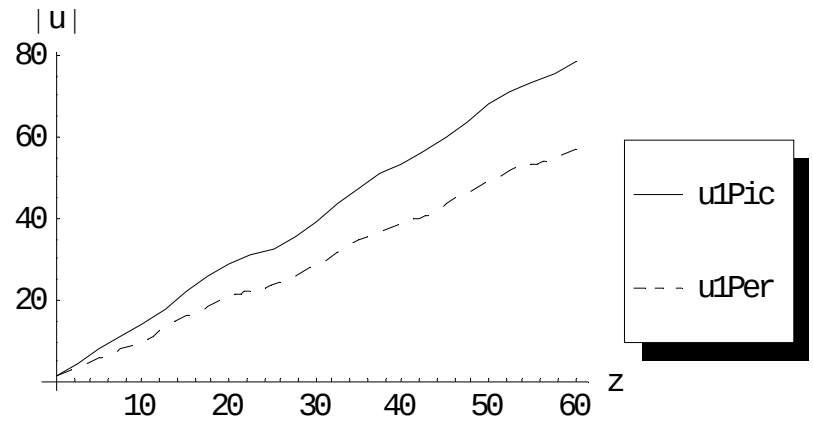

Fig. (2.107) comparison between Picard approximation and Perturbation method for first order at $\varepsilon = 1, \gamma = 0$ and $\alpha, \rho_1, \rho_2 = 1, T = 10, t = 3$.

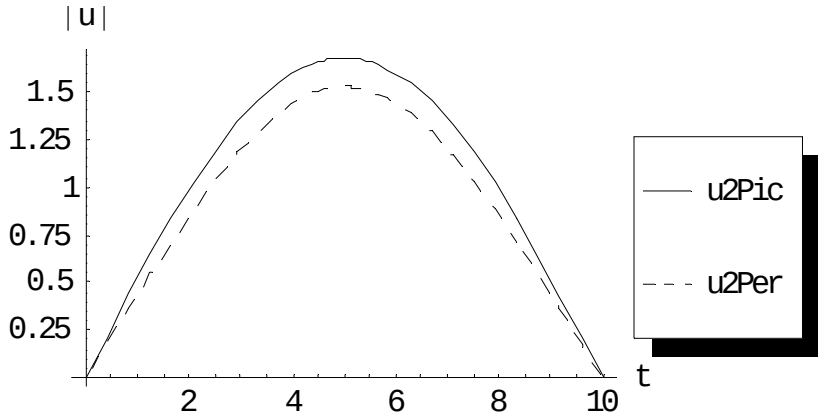

Fig. (2.108) comparison between Picard approximation and Perturbation method for second order at $\varepsilon = 0.02, \gamma = 0$ and $\alpha, \rho_1, \rho_2 = 1, T = 10, z = 5$.

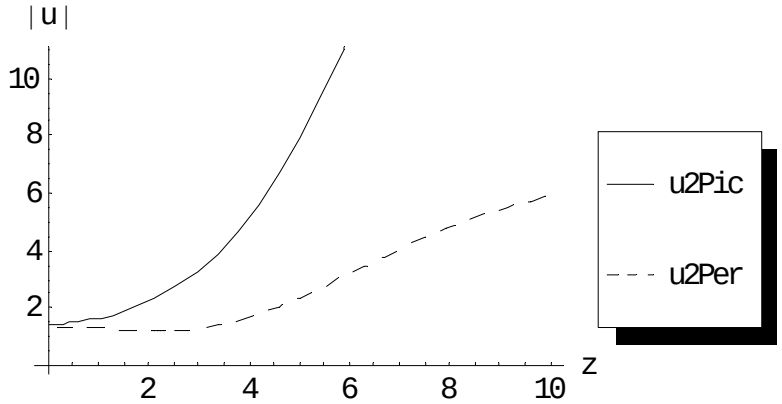

Fig. (2.109) comparison between Picard approximation and Perturbation method for second order at $\varepsilon = 0.2, \gamma = 0$ and $\alpha, \rho_1, \rho_2 = 1, T = 10, t = 3$.

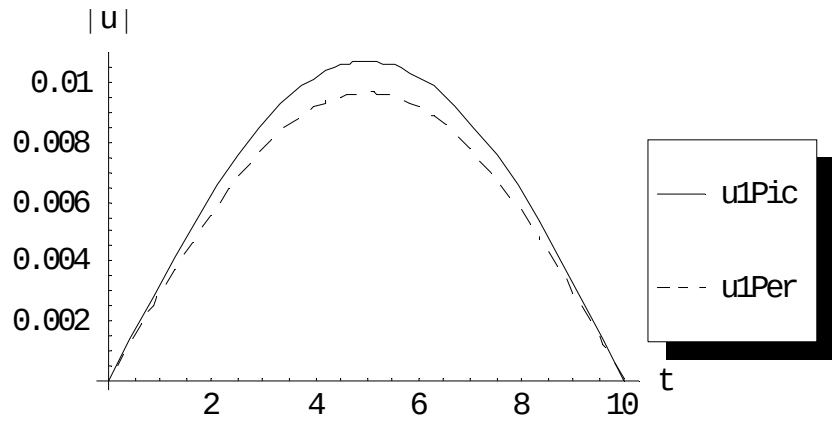

Fig. (2.110) comparison between Picard approximation and Perturbation method for first order at $\varepsilon = 0.2, \gamma = 1$ and $\alpha, \rho_1, \rho_2 = 1, T = 10, z = 5$.

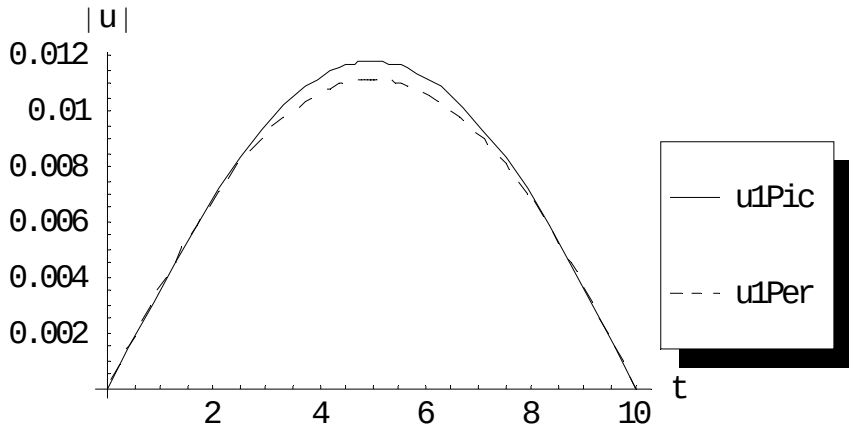

Fig. (2.111) comparison between Picard approximation and Perturbation method for first order at $\varepsilon = 1, \gamma = 1$ and $\alpha, \rho_1, \rho_2 = 1, T = 10, z = 5$.

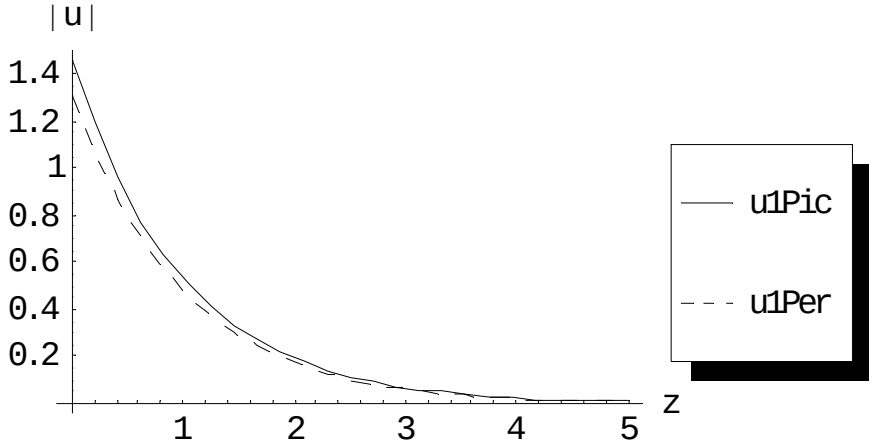

Fig. (2.112) comparison between Picard approximation and Perturbation method for first order at $\varepsilon = 0.2, \gamma = 1$ and $\alpha, \rho_1, \rho_2 = 1, T = 10, t = 3$.

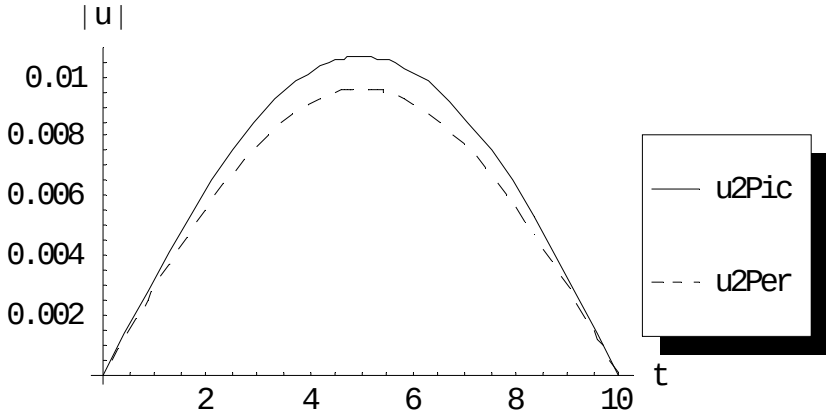

Fig. (2.113) comparison between Picard approximation and Perturbation method for second order at $\varepsilon = 0.2, \gamma = 1$ and $\alpha, \rho_1, \rho_2 = 1, T = 10, z = 5$.

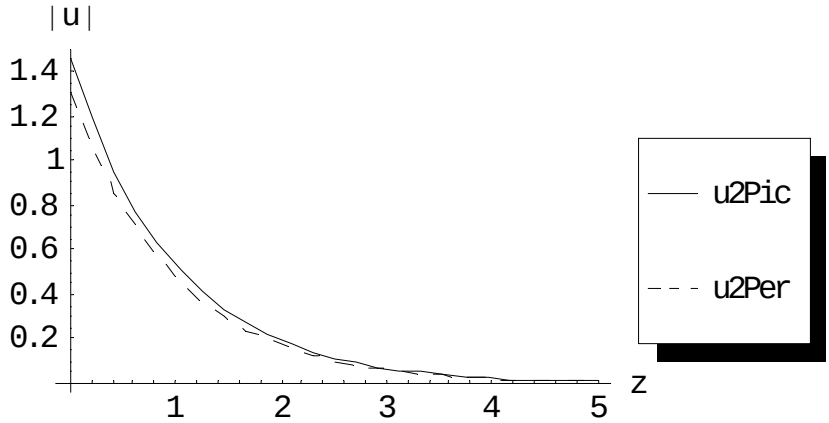

Fig. (2.114) comparison between Picard approximation and Perturbation method for second order at $\varepsilon = 1, \gamma = 1$ and $\alpha, \rho_1, \rho_2 = 1, T = 10, t = 3$.

2.6.2 Case Study 2

Taking the case $f_1(t) = \rho_1,\ f_2(t) = \rho_2 \sin\left(\frac{\pi}{T}t\right)$ where ρ_1 & ρ_2 are constants, the following selected results are obtained.

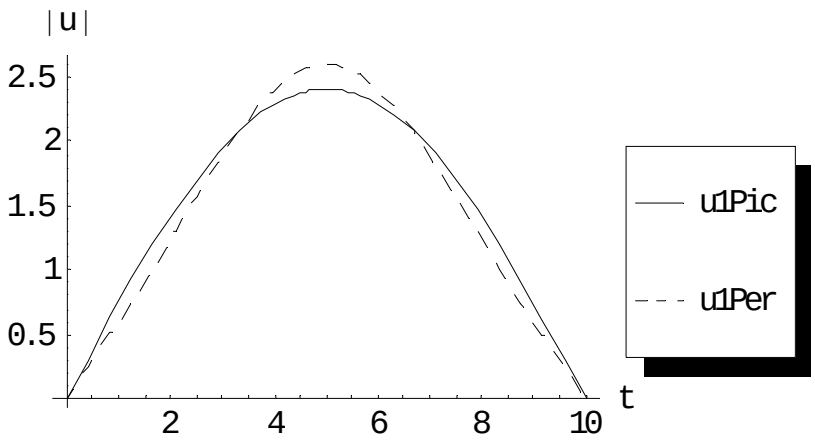

Fig. (2.115) comparison between Picard approximation and Perturbation method for first order at $\varepsilon = 0.2, \gamma = 0$ and $\alpha, \rho_1, \rho_2 = 1, T = 10, z = 5$.

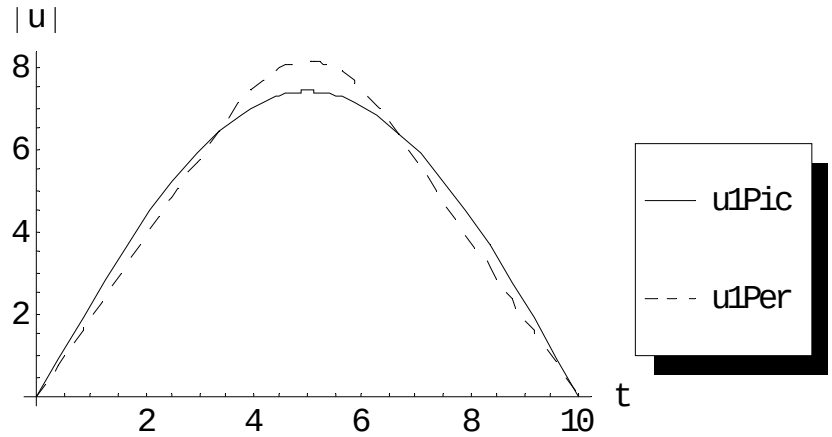

Fig. (2.116) comparison between Picard approximation and Perturbation method for first order at $\varepsilon = 1, \gamma = 0$ and $\alpha, \rho_1, \rho_2 = 1, T = 10, z = 5$.

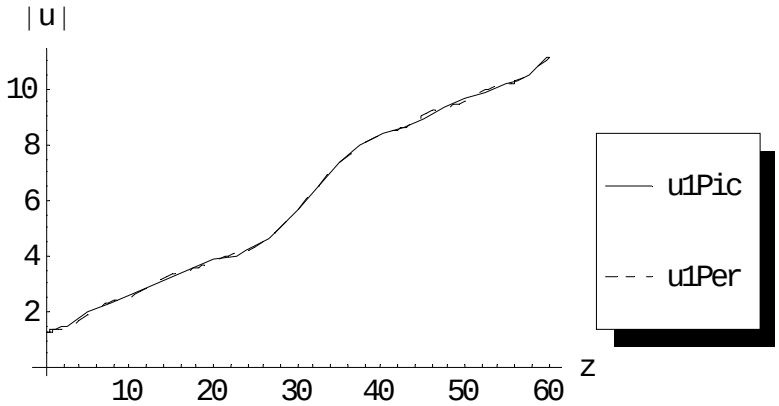

Fig. (2.117) comparison between Picard approximation and Perturbation method for first order at $\varepsilon = 0.2, \gamma = 0$ and $\alpha, \rho_1, \rho_2 = 1, T = 10,\ t = 3$.

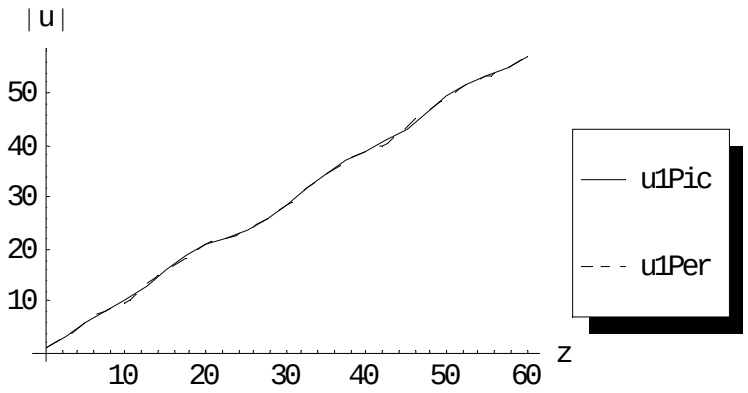

Fig. (2.118) comparison between Picard approximation and Perturbation method for first order at $\varepsilon = 1, \gamma = 0$ and $\alpha, \rho_1, \rho_2 = 1, T = 10,\ t = 3$.

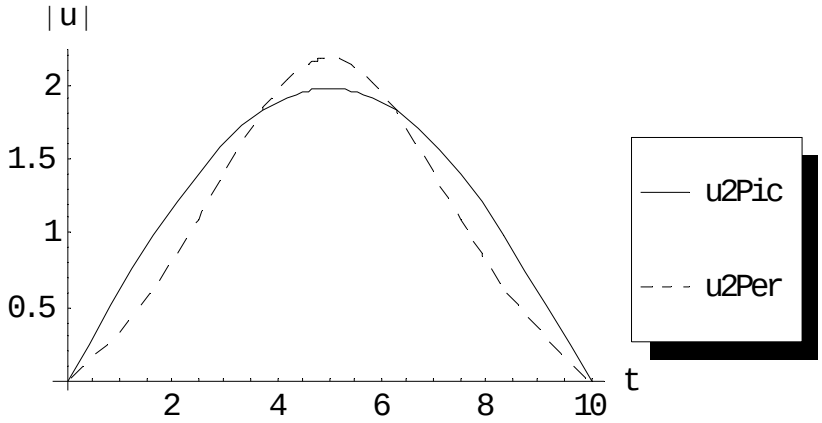

Fig. (2.119) comparison between Picard approximation and Perturbation method for second order at $\varepsilon = 0.1, \gamma = 0$ and $\alpha, \rho_1, \rho_2 = 1, T = 10,\ z = 5$.

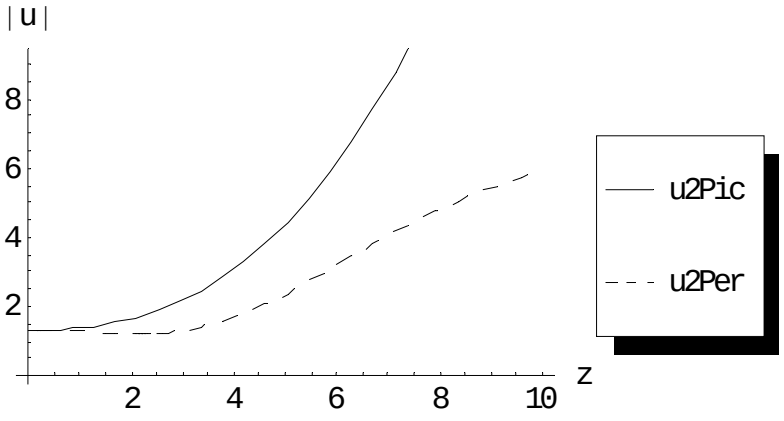

Fig. (2.120) comparison between Picard approximation and Perturbation method for second order at $\varepsilon = 0.2, \gamma = 0$ and $\alpha, \rho_1, \rho_2 = 1, T = 10,\ t = 3$.

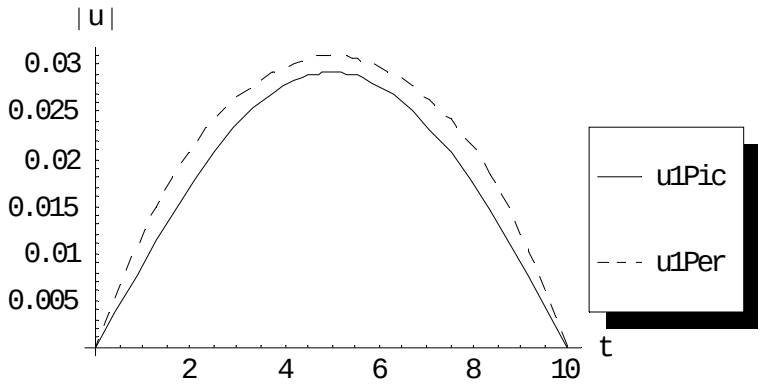

Fig. (2.121) comparison between Picard approximation and Perturbation method for first order at $\varepsilon = 1, \gamma = 1$ and $\alpha, \rho_1, \rho_2 = 1, T = 10,\ z = 4$.

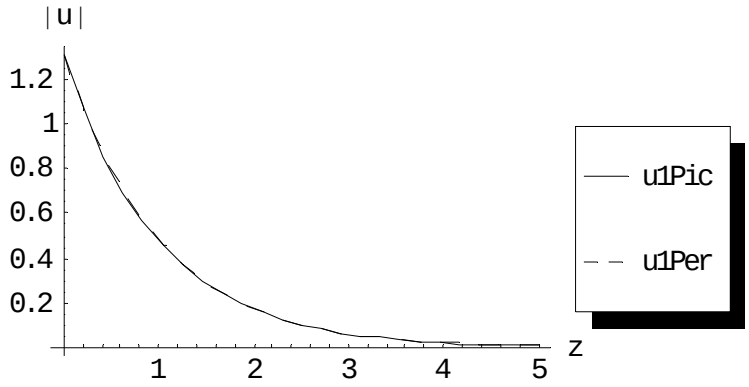

Fig. (2.122) comparison between Picard approximation and Perturbation method for first order at $\varepsilon = 0.2, \gamma = 1$ and $\alpha, \rho_1, \rho_2 = 1, T = 10,\ t = 3$.

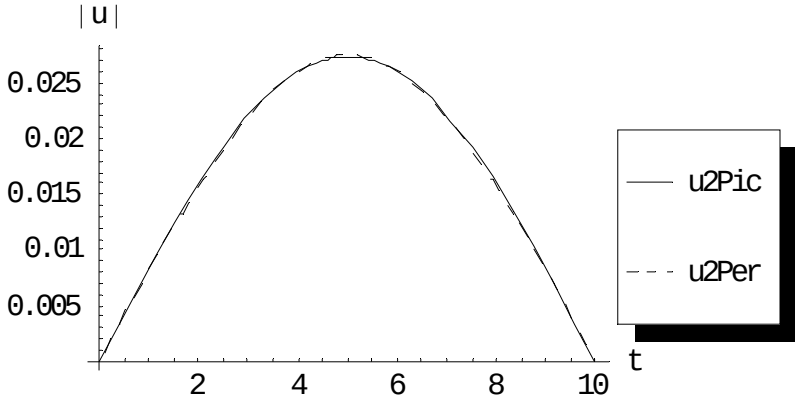

Fig. (2.123) comparison between Picard approximation and Perturbation method for second order at $\varepsilon = 0.2, \gamma = 1$ and $\alpha, \rho_1, \rho_2 = 1, T = 10,\ z = 4$.

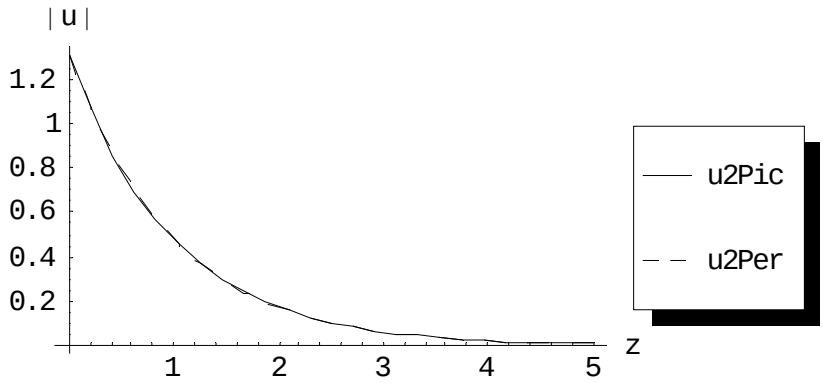

Fig. (2.124) comparison between Picard approximation and Perturbation method for second order at $\varepsilon = 0.2, \gamma = 1$ and $\alpha, \rho_1, \rho_2 = 1, T = 10,\ t = 3.$

2.6.3 Case Study 3

Taking the case $f_1(t) = \rho_1 e^{-t}, f_2(t) = \rho_2 e^{-t}$ where ρ_1 & ρ_2 are constants, the following selected results are obtained.

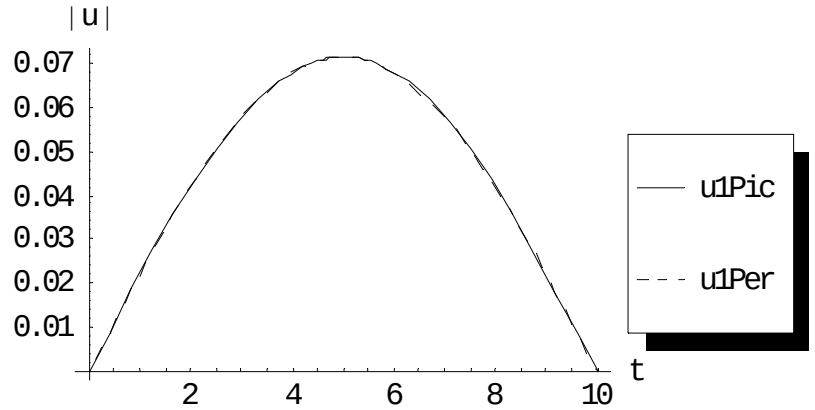

Fig. (2.125) comparison between Picard approximation and Perturbation method for first order at $\varepsilon = 0.1, \gamma = 0$ and $\alpha, \rho_1, \rho_2 = 1, T = 10,\ z = 5.$

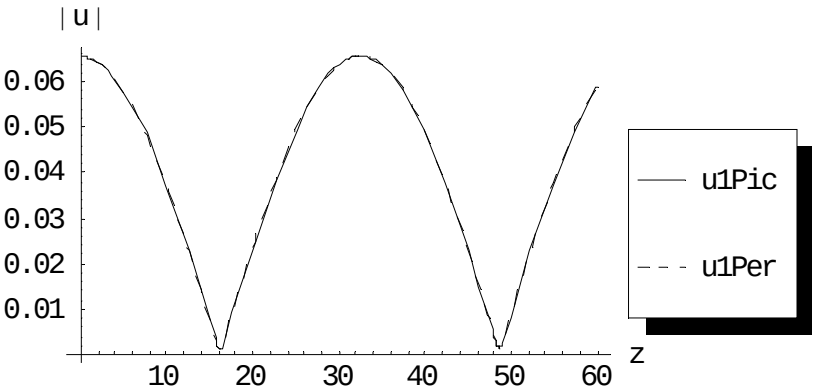

Fig. (2.126) comparison between Picard approximation and Perturbation method for first order at $\varepsilon = 0.2, \gamma = 0$ and $\alpha, \rho_1, \rho_2 = 1, T = 10,\ t = 3.$

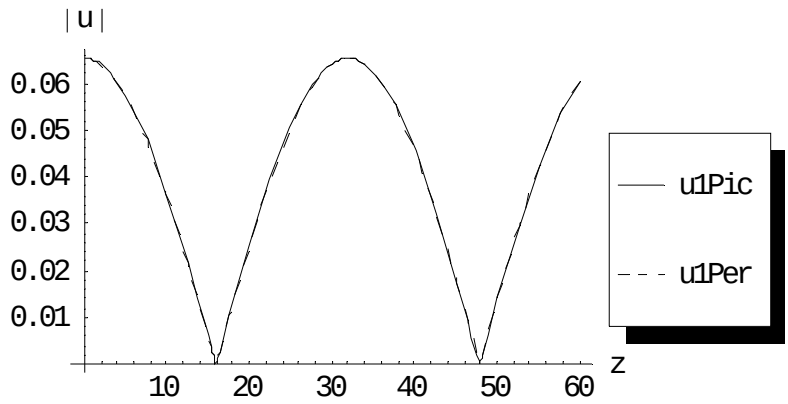

Fig. (2.127) comparison between Picard approximation and Perturbation method for first order at $\varepsilon = 1, \gamma = 0$ and $\alpha, \rho_1, \rho_2 = 1, T = 10,\ t = 3$.

2.7 T – Study

We are here examining the behavior of Perturbation method and Picard Approximation against different values of T through case studies on the same graph.

2.7.1 Case Studies, Perturbation

2.7.1.1 Case study 1

Taking the case $f_1(t) = \rho_1, f_2(t) = \rho_2$ where ρ_1 & ρ_2 are constants and following the algorithm, the following selected results for the first and second order approximations are got:

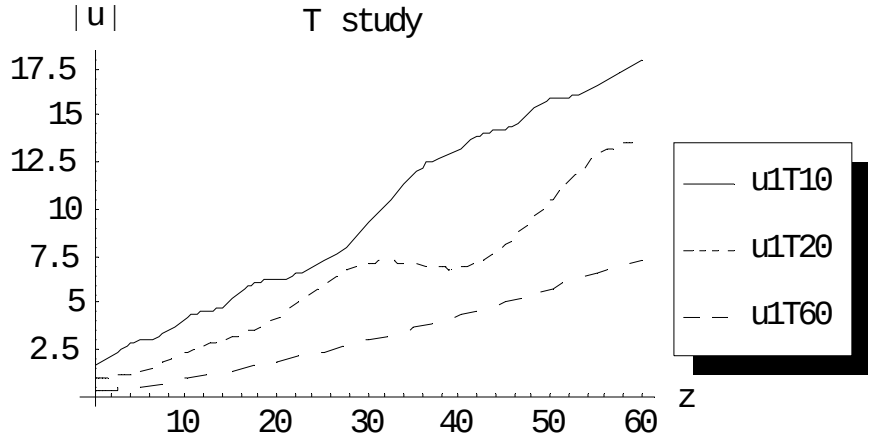

Fig.(2.128) the first order approximation of $\left|u^{(1)}\right|$ at$\varepsilon = 0.2$, $\gamma = 0$ and $\alpha, \rho_1, \rho_2 = 1, M = 10, t = 4$ for different values of T =10, 20 and 60 respectively.

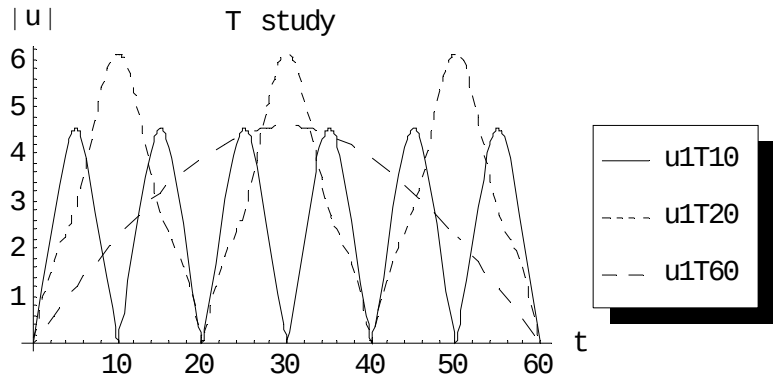

Fig.(2.129) the first order approximation of $\left|u^{(1)}\right|$ at $\varepsilon = 0.2$, $\gamma = 0$ and $\alpha, \rho_1, \rho_2 = 1, M = 10, z = 10$ for different values of T =10, 20 and 60 respectively.

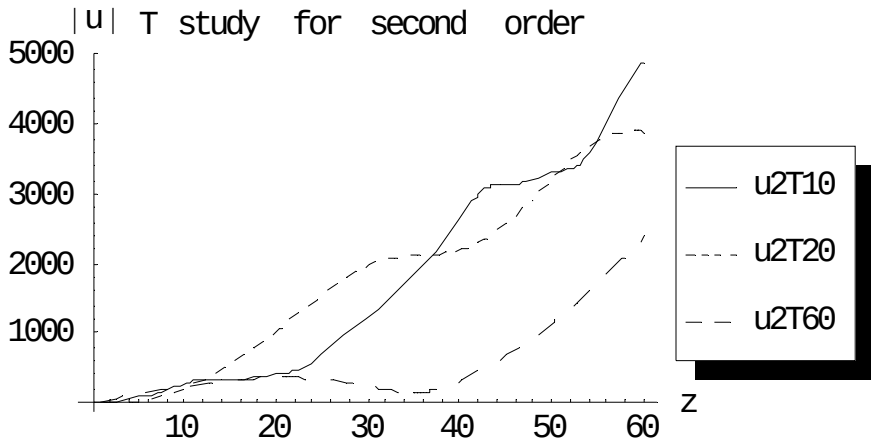

Fig. (2.130) the second order approximation of $\left|u^{(2)}\right|$ at $\varepsilon = 1$, $\gamma = 0$ and $\alpha, \rho_1, \rho_2 = 1, M = 10, t = 4$ for different values of T =10, 20 and 60 respectively.

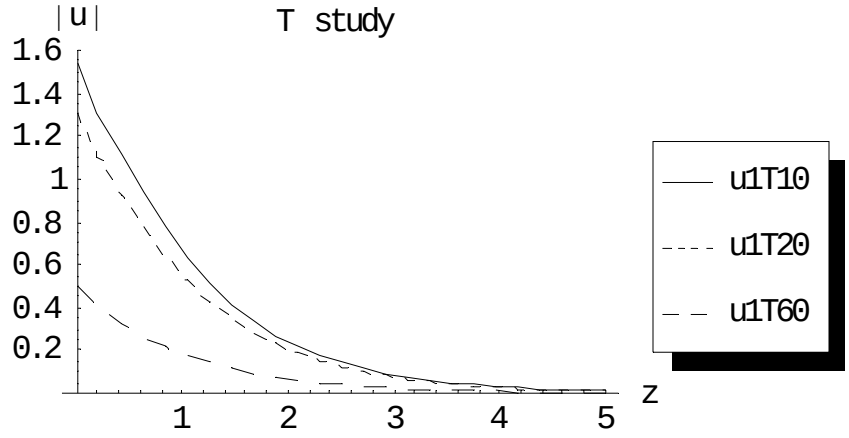

Fig. (2.131) the first order approximation of $\left|u^{(1)}\right|$ at $\varepsilon = 1$, $\gamma = 1$ and $\alpha, \rho_1, \rho_2 = 1, M = 10, t = 6$ for different values of T =10, 20 and 60 respectively.

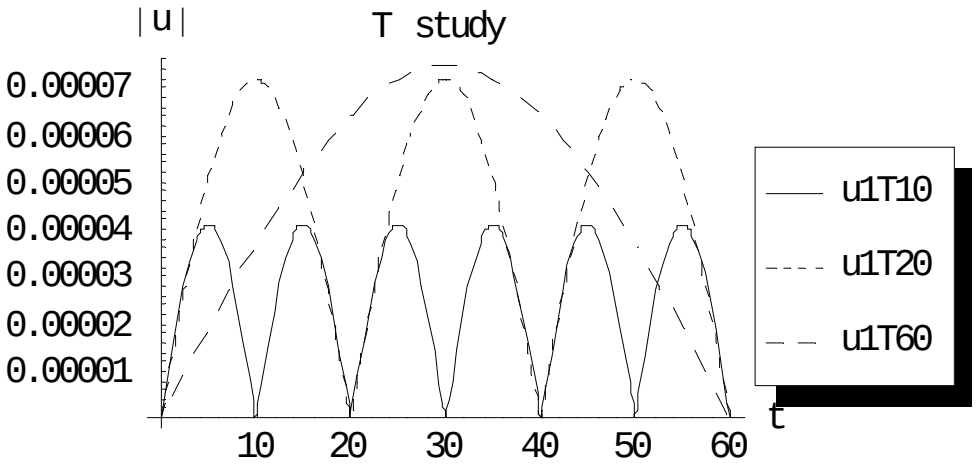

Fig. (2.132) the first order approximation of $\left|u^{(1)}\right|$ at $\varepsilon = 0.2$, $\gamma = 1$ and $\alpha, \rho_1, \rho_2 = 1, M = 10, z = 10$ for different values of T =10, 20 and 60 respectively.

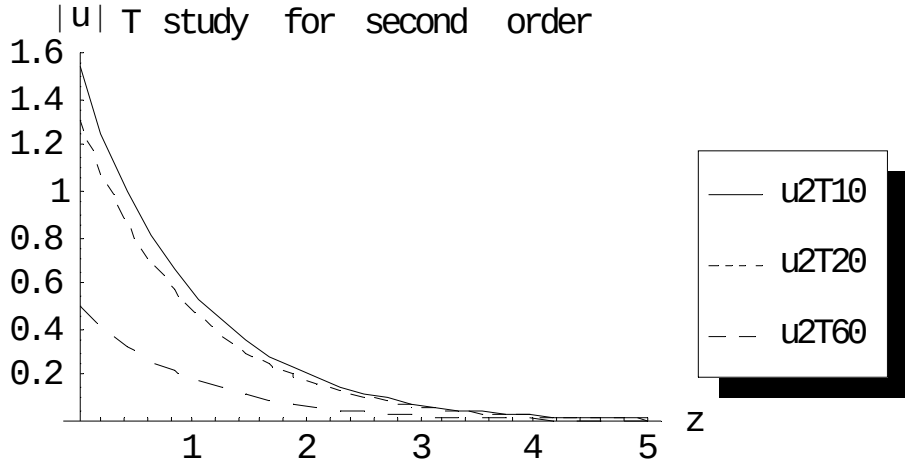

Fig. (2.133) the second order approximation of $\left|u^{(2)}\right|$ at $\varepsilon = 0.2$, $\gamma = 1$ and $\alpha, \rho_1, \rho_2 = 1, M = 10, t = 6$ for different values of T =10, 20 and 60 respectively.

2.7.1.2 Case study 2

Taking the case $f_1(t) = \rho_1 e^{-t}, f_2(t) = \rho_2 e^{-t}$ where ρ_1 & ρ_2 are constants and following the algorithm, the following selected results for the first and second order approximations are got:

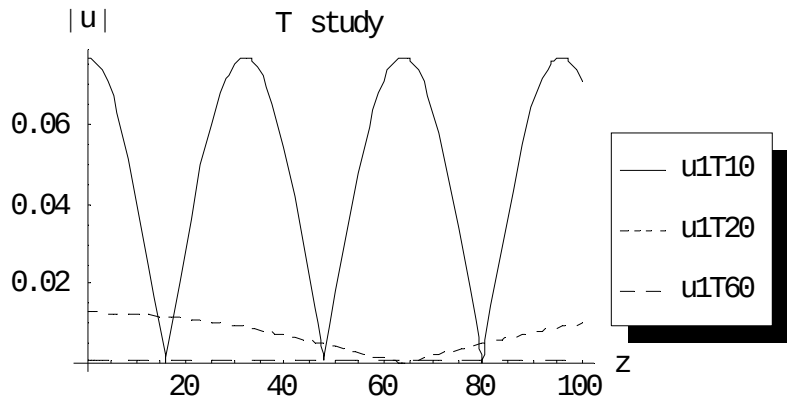

Fig. (2.134) the first order approximation of $\left|u^{(1)}\right|$ at $\varepsilon = 0.2$, $\gamma = 0$ and $\alpha, \rho_1, \rho_2 = 1, M = 10, t = 4$ for different values of T =10, 20 and 60 respectively.

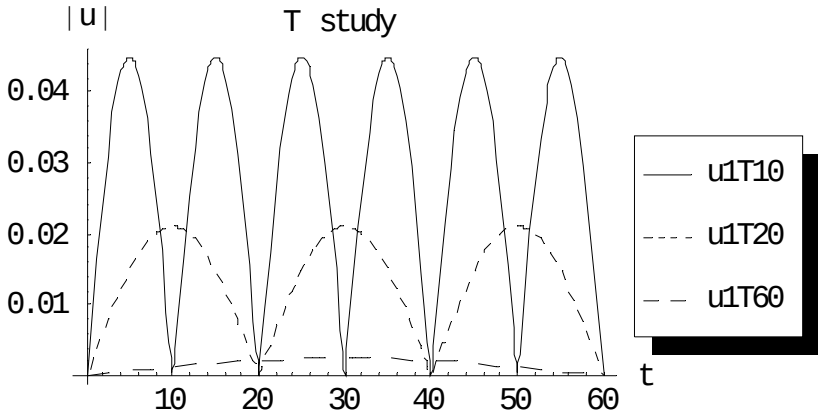

Fig. (2.135) the first order approximation of $\left|u^{(1)}\right|$ at $\varepsilon = 0.2$, $\gamma = 0$ and $\alpha, \rho_1, \rho_2 = 1, M = 10, z = 10$ for different values of T =10, 20 and 60 respectively.

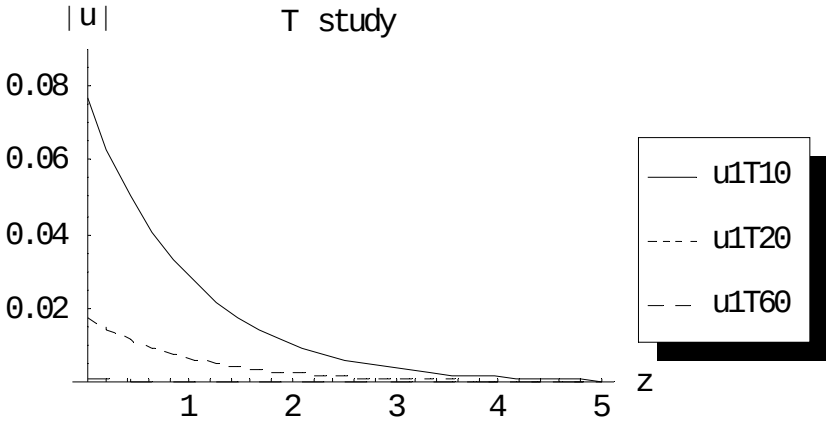

Fig. (2.136) the first order approximation of $\left|u^{(1)}\right|$ at $\varepsilon = 1$, $\gamma = 1$ and $\alpha, \rho_1, \rho_2 = 1, M = 10, t = 6$ for different values of T =10, 20 and 60 respectively.

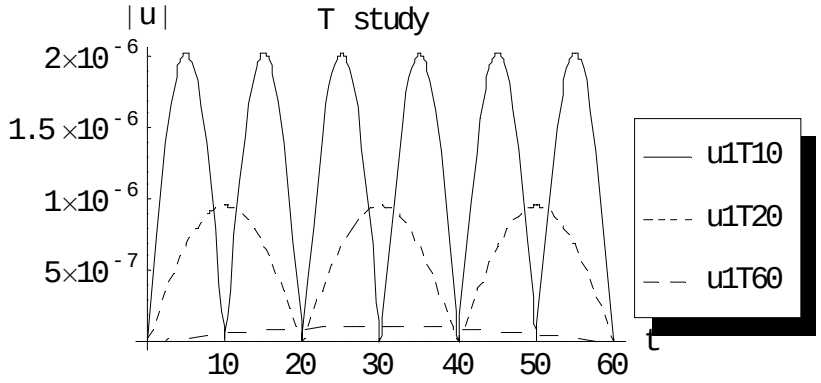

Fig. (2.137) the first order approximation of $\left|u^{(1)}\right|$ at $\varepsilon = 0.2$,$\gamma = 1$ and $\alpha, \rho_1, \rho_2 = 1, M = 10, z = 10$ for different values of T =10, 20 and 60 respectively.

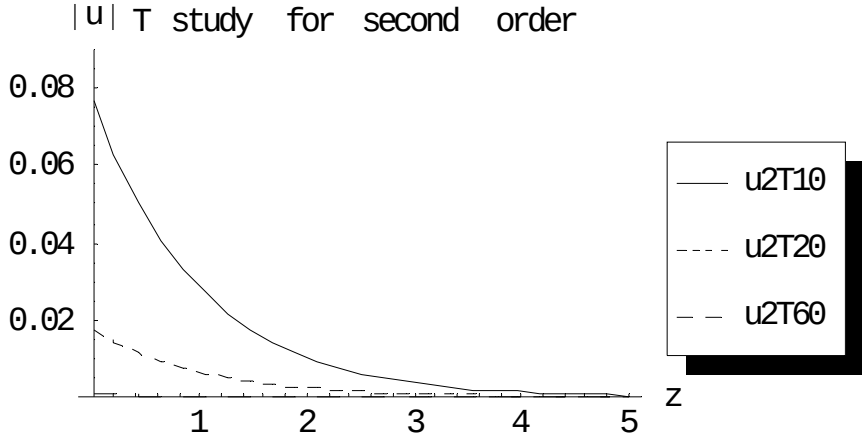

Fig. (2.138) the second order approximation of $\left|u^{(2)}\right|$ at $\varepsilon = 0.2$, $\gamma = 1$ and $\alpha, \rho_1, \rho_2 = 1, M = 10, t = 6$ for different values of T =10, 20 and 60 respectively.

2.7.1.3 Case study 3

Taking the case $f_1(t) = \rho_1,\ f_2(t) = \rho_2 \sin\left(\frac{\pi}{T}t\right)$ where ρ_1 & ρ_2 are constants and following the algorithm, the following selected results for the first, second and order approximations are got:

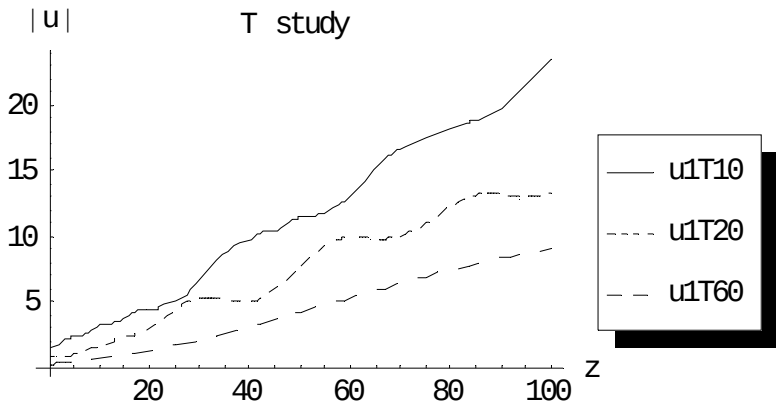

Fig. (2.139) the first order approximation of $\left|u^{(1)}\right|$ at $\varepsilon = 0.2$, $\gamma = 0$ and $\alpha, \rho_1, \rho_2 = 1, M = 10, t = 4$ for different values of T =10, 20 and 60 respectively.

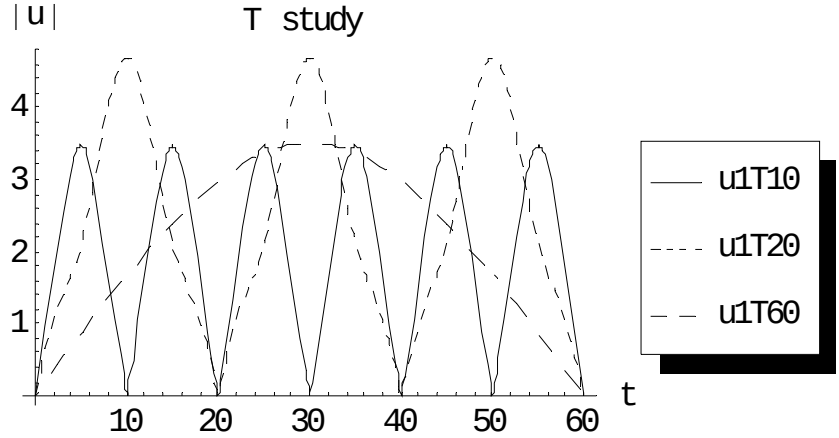

Fig. (2.140) the first order approximation of $\left|u^{(1)}\right|$ at $\varepsilon = 0.2$, $\gamma = 0$ and $\alpha, \rho_1, \rho_2 = 1, M = 10, z = 10$ for different values of T =10, 20 and 60 respectively.

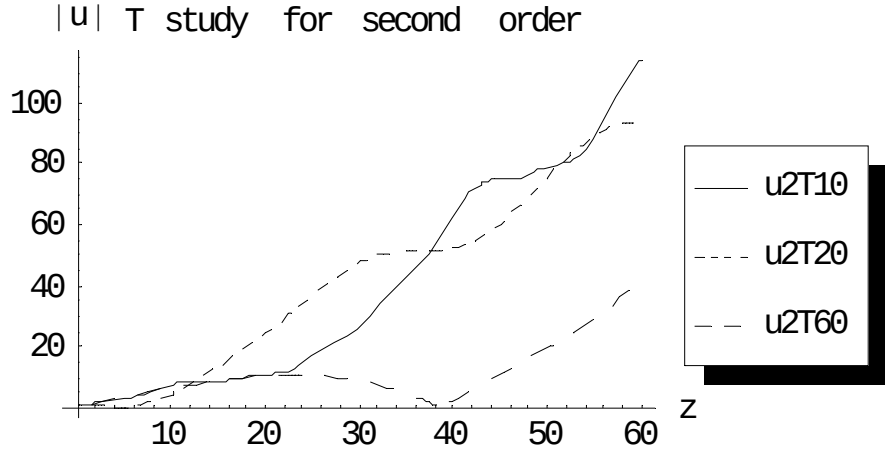

Fig. (2.141) the second order approximation of $\left|u^{(2)}\right|$ at $\varepsilon = 0.2$, $\gamma = 0$ and $\alpha, \rho_1, \rho_2 = 1, M = 10, t = 4$ for different values of T =10, 20 and 60 respectively.

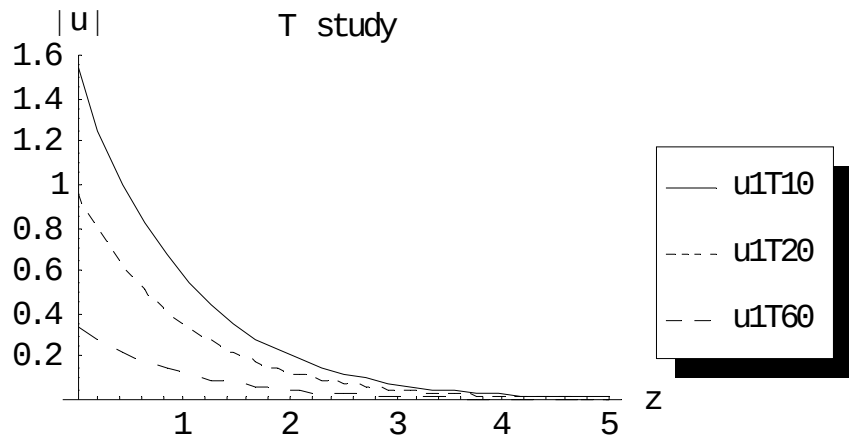

Fig. (2.142) the first order approximation of $\left|u^{(1)}\right|$ at $\varepsilon = 0.2$, $\gamma = 1$ and $\alpha, \rho_1, \rho_2 = 1, M = 10, t = 4$ for different values of T =10, 20 and 60 respectively.

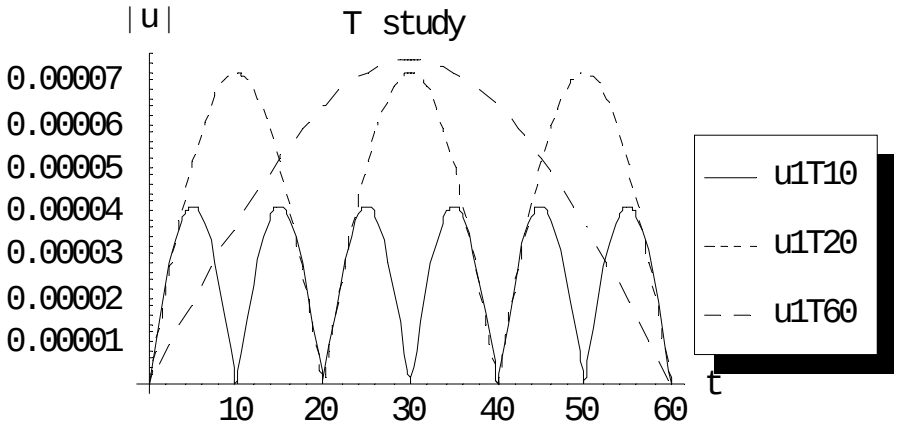

Fig. (2.143) the first order approximation of $\left|u^{(1)}\right|$ at $\varepsilon = 0.2$, $\gamma = 1$ and $\alpha, \rho_1, \rho_2 = 1, M = 10, z = 10$ for different values of T =10, 20 and 60 respectively.

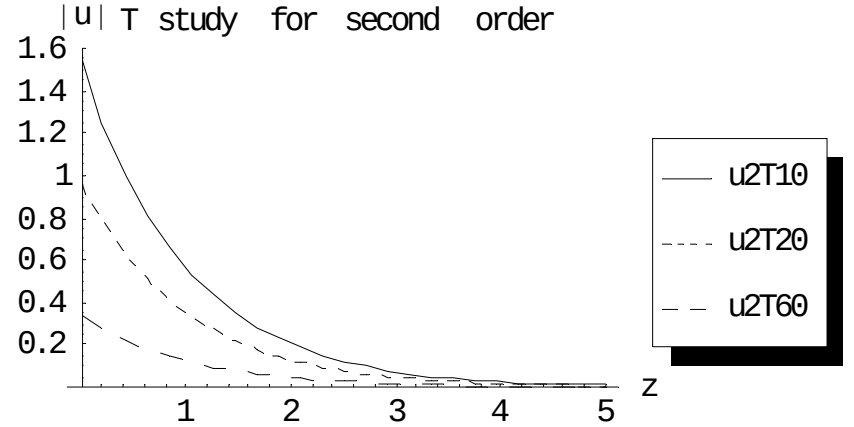

Fig. (2.144) the second order approximation of $\left|u^{(2)}\right|$ at $\varepsilon = 0.2$, $\gamma = 1$ and $\alpha, \rho_1, \rho_2 = 1, M = 10, t = 4$ for different values of T =10, 20 and 60 respectively.

2.7.2 Case Studies, Picard

2.7.2.1 Case study 1

Taking the case $f_1(t) = \rho_1,\ f_2(t) = \rho_2$ where ρ_1 & ρ_2 are constants and following the algorithm, the following selected results for the first and second order approximations are got:

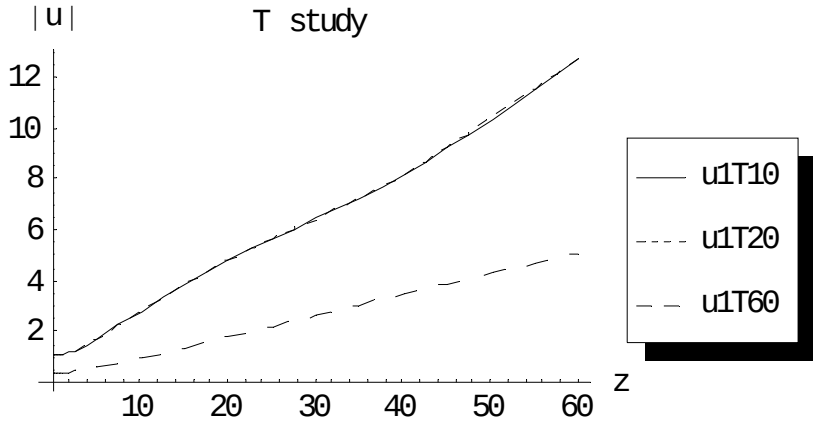

Fig. (2.145) the first order approximation of $\left|u^{(1)}\right|$ at $\varepsilon = 0.2$, $\gamma = 0$ and $\alpha, \rho_1, \rho_2 = 1, M = 1, t = 4$ for different values of T =10, 20 and 60 respectively.

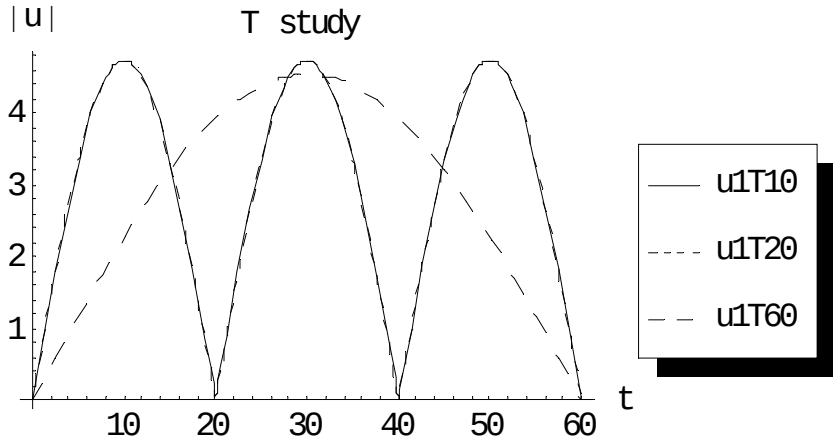

Fig. (2.146) the first order approximation of $\left|u^{(1)}\right|$ at $\varepsilon = 0.2$, $\gamma = 0$ and $\alpha, \rho_1, \rho_2 = 1, M = 1, z = 10$ for different values of T =10, 20 and 60 respectively.

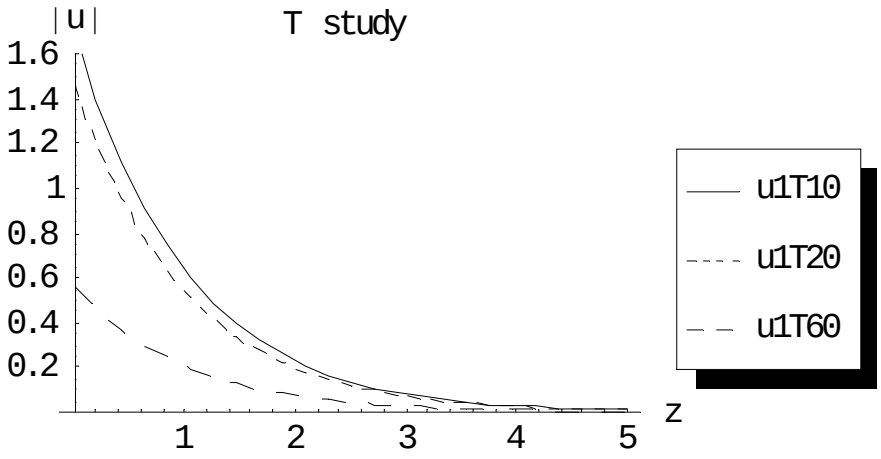

Fig. (2.147) the first order approximation of $\left|u^{(1)}\right|$ at $\varepsilon = 0.2$, $\gamma = 1$ and $\alpha, \rho_1, \rho_2 = 1, M = 1, t = 6$ for different values of T =10, 20 and 60 respectively.

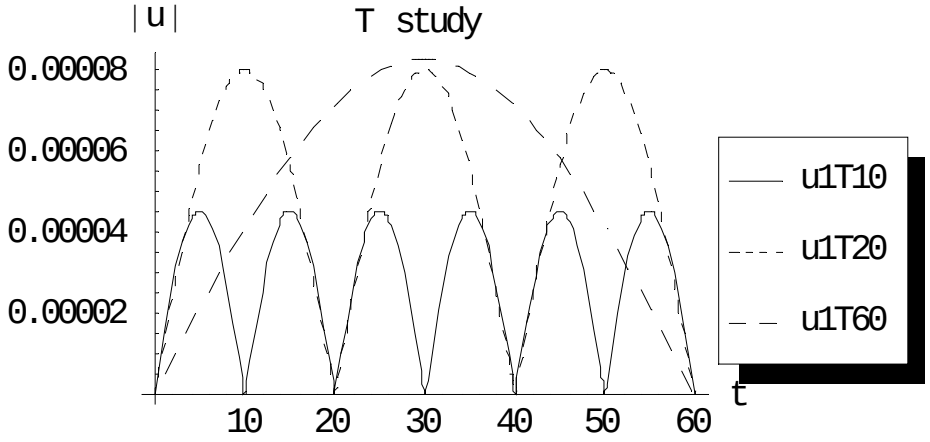

Fig. (2.148) the first order approximation of $\left|u^{(1)}\right|$ at $\varepsilon = 0.2$, $\gamma = 1$ and $\alpha, \rho_1, \rho_2 = 1, M = 1, z = 10$ for different values of T =10, 20 and 60 respectively.

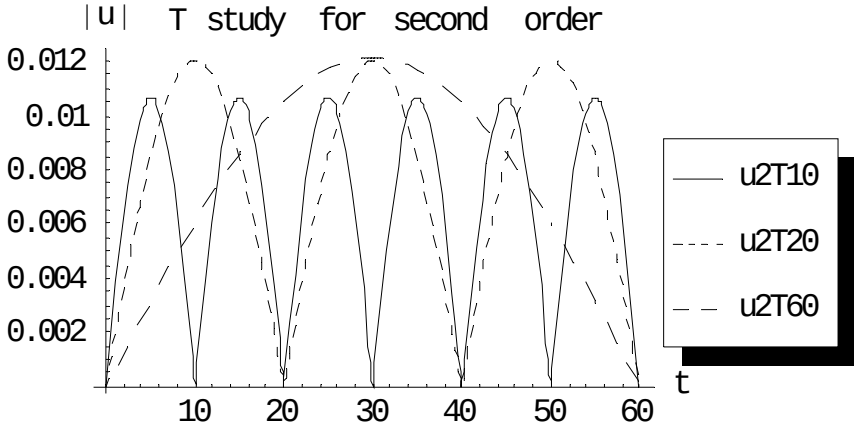

Fig. (2.149) the second order approximation of $\left|u^{(2)}\right|$ at $\varepsilon = 0.2$, $\gamma = 1$ and $\alpha, \rho_1, \rho_2 = 1, M = 1, z = 5$ for different values of T =10, 20 and 60 respectively.

2.7.2.2 Case study 2

Taking the case $f_1(t) = \rho_1,\ f_2(t) = \rho_2 \sin\left(\frac{\pi}{T}t\right)$ where ρ_1 & ρ_2 are constants and following the algorithm, the following selected results for the first and second order approximations are got:

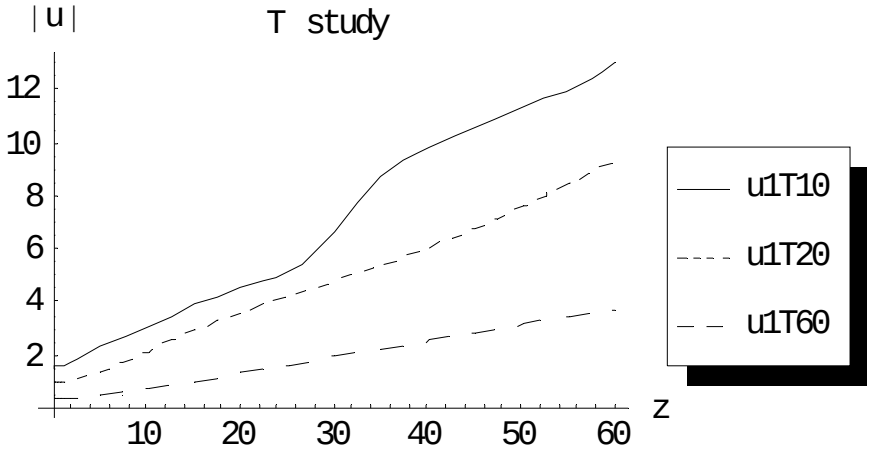

Fig. (2.150) the first order approximation of $\left|u^{(1)}\right|$ at $\varepsilon = 0.2$, $\gamma = 0$ and $\alpha, \rho_1, \rho_2 = 1, M = 1, t = 4$ for different values of T =10, 20 and 60 respectively.

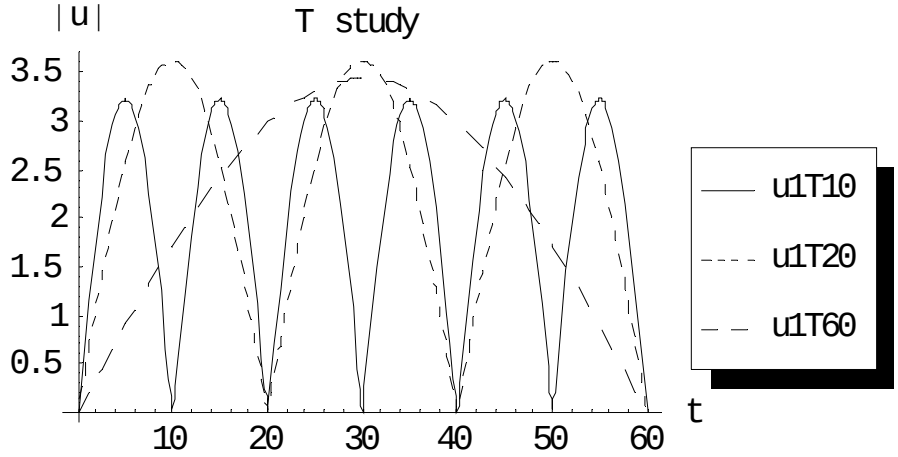

Fig. (2.151) the first order approximation of $\left|u^{(1)}\right|$ at $\varepsilon = 0.2$, $\gamma = 0$ and $\alpha, \rho_1, \rho_2 = 1, M = 1, z = 10$ for different values of T =10, 20 and 60 respectively.

2.7.2.3 Case study 3

Taking the case $f_1(t) = \rho_1 e^{-t}, f_2(t) = \rho_2 e^{-t}$ where ρ_1 & ρ_2 are constants and following the algorithm, the following selected results for the first and second order approximations are got:

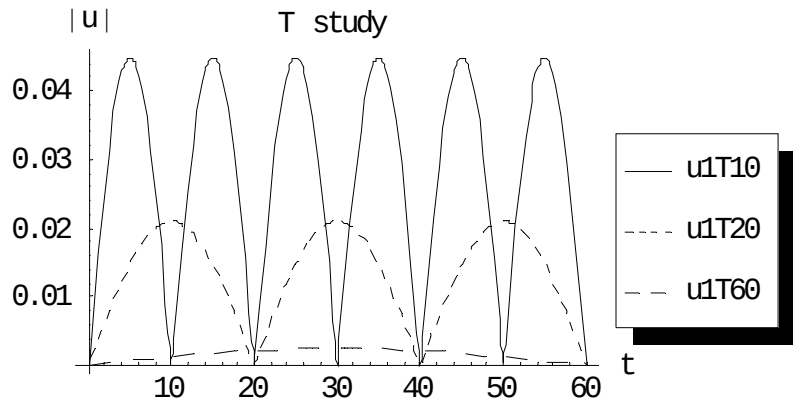

Fig. (2.152) the first order approximation of $\left|u^{(1)}\right|$ at $\varepsilon = 0.2$, $\gamma = 0$ and $\alpha, \rho_1, \rho_2 = 1, M = 1, z = 10$ for different values of T =10, 20 and 60 respectively.

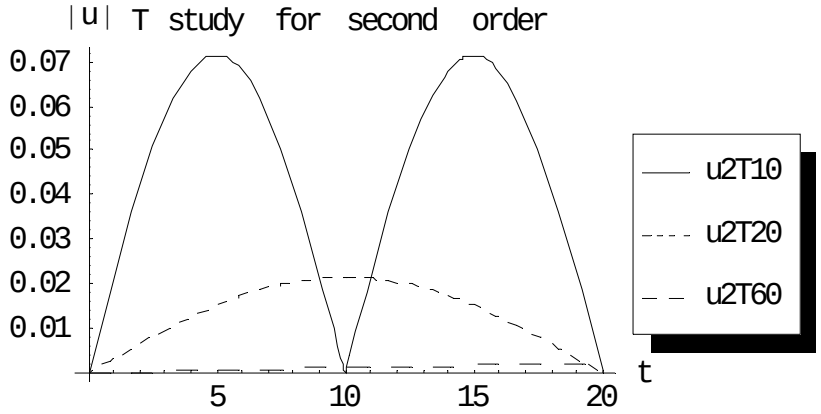

Fig. (2.153) the second order approximation of $\left|u^{(2)}\right|$ at $\varepsilon = 0.2$, $\gamma = 0$ and $\alpha, \rho_1, \rho_2 = 1, M = 1, z = 5$ for different values of T =10, 20 and 60 respectively.

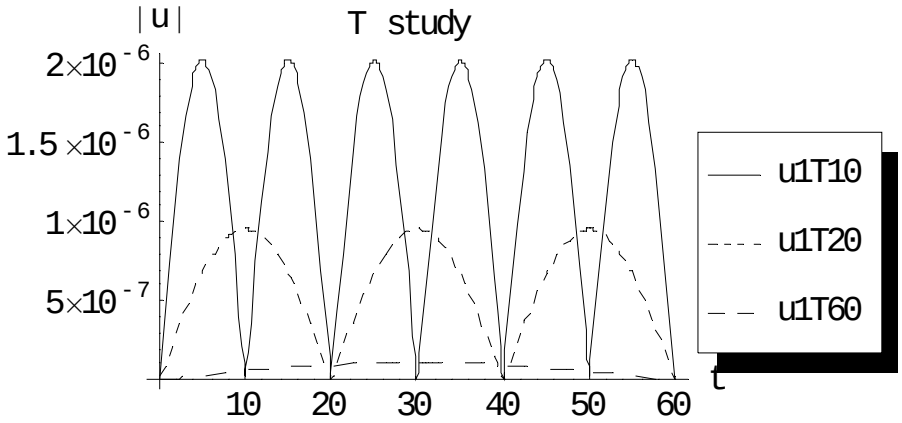

Fig. (2.154) the first order approximation of $\left|u^{(1)}\right|$ at $\varepsilon = 0.2$, $\gamma = 1$ and $\alpha, \rho_1, \rho_2 = 1, M = 1, z = 10$ for different values of T =10, 20 and 60 respectively.

Chapter 3 Non-Homogeneous Nonlinear Cubic Schrodinger Equations

3.0 Introduction

In this chapter, a perturbing nonlinear non-homogeneous Schrodinger equation is studied under limited time interval, complex initial conditions and zero Neumann conditions. The perturbation and Picard approximation methods together with the eigenfunction expansion and variational parameters methods are used to introduce an approximate solution for the perturbative nonlinear case for which a power series solution is proved to exist. Using Mathematica, the solution algorithm is tested through computing the possible orders of approximations. The method of solution is illustrated through case studies and figures.

In this chapter, a straight forward solution algorithm is introduced using the transformation from a complex solution to a coupled equations in two real solutions, eliminating one of the solutions to get separate independent and higher order equations, and finally introducing a perturbative approximate solution to the system.

3.1 The non- linear case

Consider the non-homogeneous non-linear Schrodinger equation:

$$i\,\frac{\partial u(t,z)}{\partial z}+\ \alpha\ \frac{\partial^2 u(t,z)}{\partial t^2}+\ \varepsilon|u(t,z)|^2u(t,z)\ +i\,\gamma u(t,z) = F_1(t,z)+\ i\,F_2(t,z),\ \ (t,z)\in(0,T)\ x\ (0,\infty) \tag{3.1}$$

where $u(t,z)$ is a complex valued function which is subjected to:

$$I.Cs.: u(t,0) = \ f_1(t)+\ i\,f_2(t), \tag{3.2}$$

$$B.Cs.: u(0,z) = \ u(T,z) = 0. \tag{3.3}$$

Lemma (3.1)

The solution of equation (3.1) with the constraints (3.2), (3.3) is a power series in ε if exists.

Proof

At $\varepsilon = 0$ ($u(t,z) = u_0(t,z)$), the following linear non-homogeneous equation is got:

$$i\,\frac{\partial u_0(t,z)}{\partial z} + \alpha\,\frac{\partial^2 u_0(t,z)}{\partial t^2} + i\,\gamma u_0(t,z) = F_1(t,z) + i\,F_2(t,z),$$
$$(t,z) \in (0,T)\,x\,(0,\infty) \tag{3.4}$$

$$u_0(t\,,z) = \psi_0(t\,,z) + i\,\phi_0(t\,,z) \tag{3.5}$$

By following Appendix (A), equation (3.4) has the following solution:

$$\psi_0(t\,,z) = e^{-\gamma z}\sum_{n=0}^{\infty} T_{0n}(z)\sin\left(\frac{n\,\pi}{T}\right)t, \tag{3.6}$$

$$\phi_0(t\,,z) = e^{-\gamma z}\sum_{n=0}^{\infty} \tau_{0n}(z)\sin\left(\frac{n\,\pi}{T}\right)t \tag{3.7}$$

where $T_{0n}(z)$ and $\tau_{0n}(z)$ can be calculated as illustrated in the general linear case, (Appendix (A), equations (A.12), (A.13) respectively).

By following Pickard approximation equation (3.1) can be rewritten as:

$$i\,\frac{\partial u_n(t,z)}{\partial z} + \alpha\,\frac{\partial^2 u_n(t,z)}{\partial t^2} + i\,\gamma u_n(t,z)$$
$$= F_1(t,z) + i\,F_2(t,z) - \varepsilon|u_{n-1}(t,z)|^2 u_{n-1}(t,z), n \geq 1 \tag{3.8}$$

At $n = 1$, the iterative equation takes the form

$$i\,\frac{\partial u_1(t,z)}{\partial z} + \alpha\,\frac{\partial^2 u_1(t,z)}{\partial t^2} + i\,\gamma u_1(t,z)$$
$$= F_1(t,z) + i\,F_2(t,z) - \varepsilon|u_0(t,z)|^2 u_0(t,z) = \varepsilon k_1(t\,,z) \tag{3.9}$$

which can be solved as a linear case with zero initial and boundary conditions. The following general solution can be obtained:

$$\psi_1(t\,,z) = e^{-\gamma z}\sum_{n=0}^{\infty} (T_{0n}(z) + \varepsilon T_{1n}(z))\sin\left(\frac{n\,\pi}{T}\right)t, \tag{3.10}$$

$$\phi_1(t\,,z) = e^{-\gamma z}\sum_{n=0}^{\infty}(\tau_{0n}(z) + \varepsilon\tau_{1n}(z))\sin\left(\frac{n\,\pi}{T}\right)t, \tag{3.11}$$

$$u_1(t\,,z) = \psi_1(t\,,z) + i\,\phi_1(t\,,z), \tag{3.12}$$

$$= {u_1}^{(0)} + \varepsilon\,{u_1}^{(1)}, \tag{3.13}$$

where ${u_1}^{(0)} = u_0$.

at $n = 2$, the following equation is obtained:

$$i\,\frac{\partial u_2(t,z)}{\partial z} + \alpha\,\frac{\partial^2 u_2(t,z)}{\partial t^2} + i\,\gamma u_2(t,z) = F_1(t,z) + i\,F_2(t,z) - \varepsilon|u_1(t,z)|^2 u_1(t,z) = \varepsilon k_2(t\,,z) \tag{3.14}$$

which can be solved as a linear case with zero initial and boundary conditions. The following general solution can be obtained:

$$u_2(t\,,z) = {u_2}^{(0)} + \varepsilon\,{u_2}^{(1)} + \varepsilon^{\,2}{u_2}^{(2)} + \varepsilon^3\,{u_2}^{(3)} + \varepsilon^4\,{u_2}^{(4)}, \tag{3.15}$$

where ${u_1}^{(0)} = u_0$. Continuing like this, one can get:

$$u_n(t\,,z) = {u_n}^{(0)} + \varepsilon\,{u_n}^{(1)} + \varepsilon^{\,2}{u_n}^{(2)} + \varepsilon^3\,{u_n}^{(3)} + .. + \varepsilon^{m(n)}\,{u_n}^{m(n)} \tag{3.16}$$

where $\mathrm{m(n)}$ is an increasing polynomial in n . As $n \to \infty$, the solution (if exists) can be reached as $u(t\,,z) = \lim_{n\to\infty} u_n(t\,,\,z)$. Accordingly the solution is a power series in ε.

According to the previous lemma 3.1, one can assume the solution of equation (3.2) as the following:

$$u(t\,,z) = \sum_{n=0}^{\infty}\varepsilon^n\,u_n(t\,,z) \tag{3.17}$$

Let $u(t\,,z) = \psi(t\,,z) + i\,\phi(t\,,\,z), \psi\,, \phi$: are real valued functions. The following coupled equations are got:

$$\frac{\partial\phi(t,z)}{\partial z} = \alpha\,\frac{\partial^2\psi(t,z)}{\partial t^2} + \varepsilon(\psi^2 + \phi^2)\psi - \gamma\phi - F_1(t\,,z), \tag{3.18}$$

$$\frac{\partial\psi(t,z)}{\partial z} = -\,\alpha\,\frac{\partial^2\phi(t,z)}{\partial t^2} - \varepsilon(\psi^2 + \phi^2)\phi - \gamma\psi + F_2(t\,,z), \tag{3.19}$$

where $\psi(t,0) = f_1(t),\ \phi(t,0) = f_2(t)$, and all corresponding other I.Cs. and B.Cs. are zeros.

As a third order perturbation solution, one can assume that:

$$\psi(t\,,z\,) = \psi_0 + \varepsilon\psi_1 + \varepsilon^2\psi_2 + \varepsilon^3\psi_3\,, \tag{3.20}$$

$$\phi(t\,,z\,) = \phi_0 + \varepsilon\phi_1 + \varepsilon^2\phi_2 + \varepsilon^3\phi_3\,, \tag{3.21}$$

Where $\psi_0(t,0) = f_1(t),\ \phi_0(t,0) = f_2(t)$, and all other corresponding I.Cs. and B.Cs. are zeros.

Substituting from equations (3.20) and (3.21) into equations (3.18) and (3.19) and then equating the equal powers of ε, one can get the following set of coupled equations:

$$\frac{\partial\phi_0(t,z)}{\partial z} = \alpha\,\frac{\partial^2\psi_0(t,z)}{\partial t^2} - \gamma\phi_0 - F_1(t\,,z), \tag{3.22}$$

$$\frac{\partial\psi_0(t,z)}{\partial z} = -\alpha\,\frac{\partial^2\phi_0(t,z)}{\partial t^2} - \gamma\psi_0 + F_2(t\,,z), \tag{3.23}$$

$$\frac{\partial\phi_1(t,z)}{\partial z} = \alpha\,\frac{\partial^2\psi_1(t,z)}{\partial t^2} - \gamma\phi_1 + \left({\psi_0}^3 + \psi_0{\phi_0}^2\right), \tag{3.24}$$

$$\frac{\partial\psi_1(t,z)}{\partial z} = -\alpha\,\frac{\partial^2\phi_1(t,z)}{\partial t^2} - \gamma\psi_1 - \left({\phi_0}^3 + \phi_0{\psi_0}^2\right), \tag{3.25}$$

$$\frac{\partial\phi_2(t,z)}{\partial z} = \alpha\,\frac{\partial^2\psi_2(t,z)}{\partial t^2} - \gamma\phi_2 + \left(3{\psi_0}^2\psi_1 + 2\psi_0\phi_0\phi_1 + \psi_1{\phi_0}^2\right), \tag{3.26}$$

$$\frac{\partial\psi_2(t,z)}{\partial z} = -\alpha\,\frac{\partial^2\phi_2(t,z)}{\partial t^2} - \gamma\psi_2 - \left(3{\phi_0}^2\phi_1 + 2\phi_0\psi_0\psi_1 + \phi_1{\psi_0}^2\right), \tag{3.27}$$

$$\begin{aligned}\frac{\partial\phi_3(t,z)}{\partial z} = {} & \alpha\,\frac{\partial^2\psi_3(t,z)}{\partial t^2} - \gamma\phi_3 \\ & + \left(3{\psi_1}^2\psi_0 + 3{\psi_0}^2\psi_2 + \psi_2{\phi_0}^2 + 2\psi_1\phi_0\phi_1 + \psi_0{\phi_1}^2\right. \\ & \left. + 2\psi_0\phi_0\phi_2\right)\end{aligned} \tag{3.28}$$

$$\begin{aligned}\frac{\partial\psi_3(t,z)}{\partial z} = {} & -\alpha\,\frac{\partial^2\phi_3(t,z)}{\partial t^2} - \gamma\psi_3 \\ & - \left(3{\phi_1}^2\phi_0 + 3{\phi_0}^2\phi_2 + \phi_2{\psi_0}^2 + 2\phi_1\psi_0\psi_1 + \phi_0{\psi_1}^2\right. \\ & \left. + 2\phi_0\psi_0\psi_2\right)\end{aligned} \tag{3.29}$$

and so on. The prototype equations to be solved are:

$$\frac{\partial \phi_i(t,z)}{\partial z} = \alpha \frac{\partial^2 \psi_i(t,z)}{\partial t^2} + G_{1i} \quad , \qquad i \geq 1 \tag{3.30}$$

$$\frac{\partial \psi_i(t,z)}{\partial z} = \alpha \frac{\partial^2 \phi_i(t,z)}{\partial t^2} + G_{2i} \quad , \qquad i \geq 1 \tag{3.31}$$

where $\psi_i(t,0) = \delta_{i,0} f_1(t)$, $\phi_i(t,0) = \delta_{i,0} f_2(t)$, and all other corresponding conditions are zeros. G_{1i}, G_{2i} are functions to be computed from previous steps.

By following the solution algorithm described in Appendix (A) for the linear case, the following final results are obtained.

3.2 The order of approximations

The following final expressions can be used to obtain different order of approximations.

3.2.1 The zero order approximation

The zero order approximation is the linear case illustrated in Appendix (A).

3.2.2 The first order approximation

$$u_1(t,z) = u_0(t,z) + \varepsilon\big(\psi_1(t,z) + i\,\phi_1(t,z)\big) \tag{3.32}$$

Following Appendix (A), for *n=1,* we can find that:

$$\psi_1(t,z) = e^{-\gamma z} \sum_{n=0}^{\infty} T_{1n}(z) \sin\left(\frac{n\pi}{T}\right) t \tag{3.33}$$

$$\phi_1(t,z) = e^{-\gamma z} \sum_{n=0}^{\infty} \tau_{1n}(z) \sin\left(\frac{n\pi}{T}\right) t \tag{3.34}$$

From equations (3.24) and (3.25), we can see that:

$$G_{11} = e^{-2\gamma z}\big({\psi_0}^3 + \psi_0 {\phi_0}^2\big) \tag{3.35}$$

$$G_{21} = e^{-2\gamma z}\big(-{\phi_0}^3 - \phi_0 {\psi_0}^2\big) \tag{3.36}$$

in which

$$T_{1n}(z) = A_{11}(z)\sin\beta_n z + \left(C_{12} + B_{11}(z)\right)\cos\beta_n z, \quad (2.37)$$

$$\tau_{1n}(z) = A_{12}(z)\sin\beta_n z + \left(C_{14} + B_{12}(z)\right)\cos\beta_n z, \quad (2.38)$$

where $C_{12} = -B_{11}(0)$ and $C_{14} = -B_{12}(0)$. The rest constants A_{11} , B_{11} , A_{12} , B_{12} can be calculated in similar manner as illustrated in Appendix (A).

The absolute value of the zero order approximation can be got using

$$|u_1(t\,,z)|^2 = |u_0(t\,,z)|^2 + 2\varepsilon(\psi_0\psi_1 + \phi_0\phi_1) + \varepsilon^2\left({\psi_1}^2 + {\phi_1}^2\right) \quad (3.39)$$

3.2.3 The second order approximation

$$u_2(t\,,z) = u_1(t,z) + \varepsilon^2\left(\psi_2(t,z) + i\,\phi_2(t,z)\right) \quad (3.40)$$

By following Appendix (A), for *n=2,* we can find that:

$$\psi_2(t\,,z) = e^{-\gamma z}\sum_{n=0}^{\infty} T_{2n}(z)\sin\left(\frac{n\,\pi}{T}\right)t \quad (3.41)$$

$$\phi_2(t\,,z) = e^{-\gamma z}\sum_{n=0}^{\infty} \tau_{2n}(z)\sin\left(\frac{n\,\pi}{T}\right)t \quad (3.42)$$

From equations (3.26) and (3.27), we can see that:

$$G_{12} = e^{-2\gamma z}(3{\psi_0}^2\psi_1 + 2\psi_0\phi_0\phi_1 + \psi_1{\phi_0}^2) \quad (3.43)$$

$$G_{22} = e^{-2\gamma z}\left(-3{\phi_0}^2\phi_1 - 2\phi_0\psi_0\psi_1 - \phi_1{\psi_0}^2\right) \quad (3.44)$$

in which

$$T_{2n}(z) = A_{21}(z)\sin\beta_n z + \left(C_{22} + B_{21}(z)\right)\cos\beta_n z, \quad (2.45)$$

$$\tau_{2n}(z) = A_{22}(z)\sin\beta_n z + \left(C_{24} + B_{22}(z)\right)\cos\beta_n z, \quad (2.46)$$

where $C_{22} = -B_{21}(0)$ and $C_{24} = -B_{22}(0)$. The rest constants A_{21} , B_{21} , A_{22} , B_{22} can be calculated in similar manner as illustrated in Appendix (A).

The absolute value of the zero order approximation can be got using

$$|u_2(t\,,z)|^2 = |u_1(t\,,z)|^2 + 2\varepsilon^2(\psi_0\psi_2 + \phi_0\phi_2) + 2\varepsilon^3(\psi_1\psi_2 + \phi_1\phi_2) + \varepsilon^4\left(\psi_2{}^2 + \phi_2{}^2\right) \quad (3.47)$$

3.3 Case Studies

To examine the proposed solution algorithm, some case studies are illustrated.

3.3.1 Case study 1

Taking the case $F_1(t,z) = \rho_1,\ F_2(t,z) = 0$ and $f_1(t) = 0, f_2(t) = 0,\ \rho_1$ is constant and following the algorithm, the following selected results for the first and second order approximations are got:

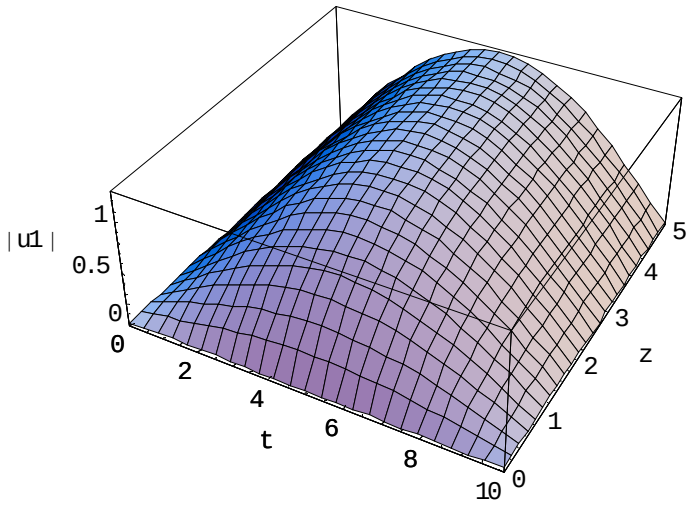

Fig. (3.1) the first order approximation of $\left|u^{(1)}\right|$ at $\varepsilon = 0.2, \gamma = 1$ and $\alpha, \rho_1 = 1, T = 10$ with considering only one term on the series (M=1).

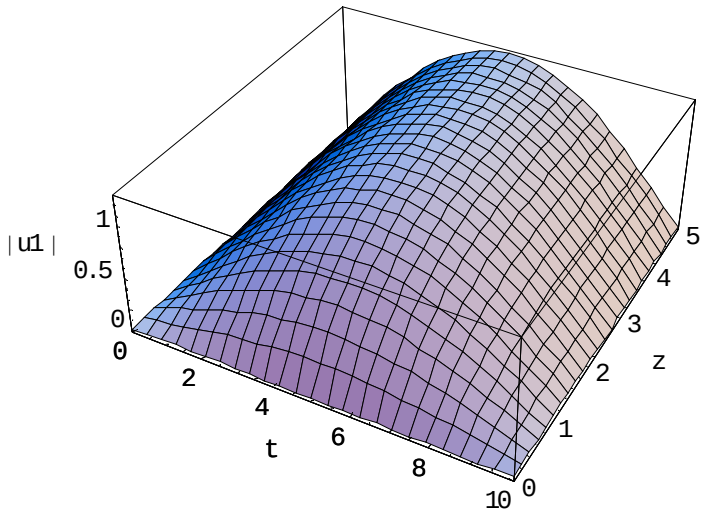

Fig. (3.2) the first order approximation of $\left|u^{(1)}\right|$ at $\varepsilon = 1, \gamma = 1$ and $\alpha, \rho_1 = 1, T = 10$ with considering only one term on the series (M=1).

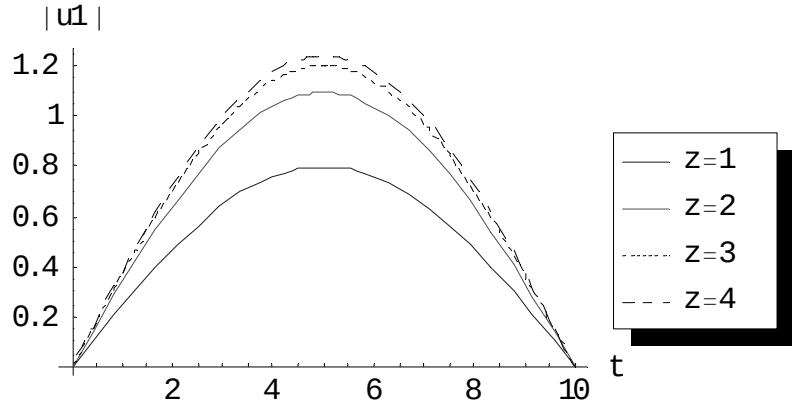

Fig. (3.3) the first order approximation of $\left|u^{(1)}\right|$ at $\varepsilon = 0.2, \gamma = 1$ and $\alpha, \rho_1 = 1, T = 10, M = 1$ for different values of z.

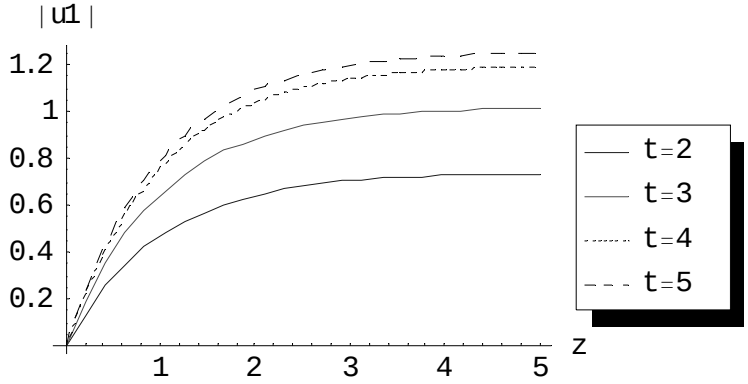

Fig. (3.4) the first order approximation of $\left|u^{(1)}\right|$ at $\varepsilon = 0.2, \gamma = 1$ and $\alpha, \rho_1 = 1, T = 10, M = 1$ for different values of t.

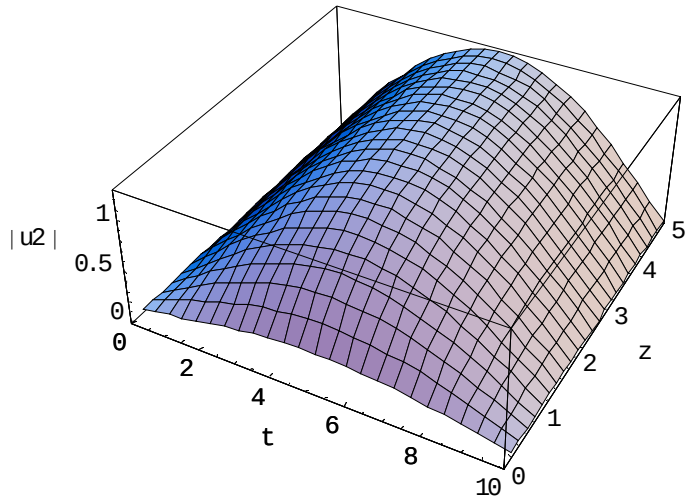

Fig. (3.5) the second order approximation of $\left|u^{(2)}\right|$ at $\varepsilon = 0.2, \gamma = 1$ and $\alpha, \rho_1 = 1, T = 10$ with considering only one term on the series (M=1).

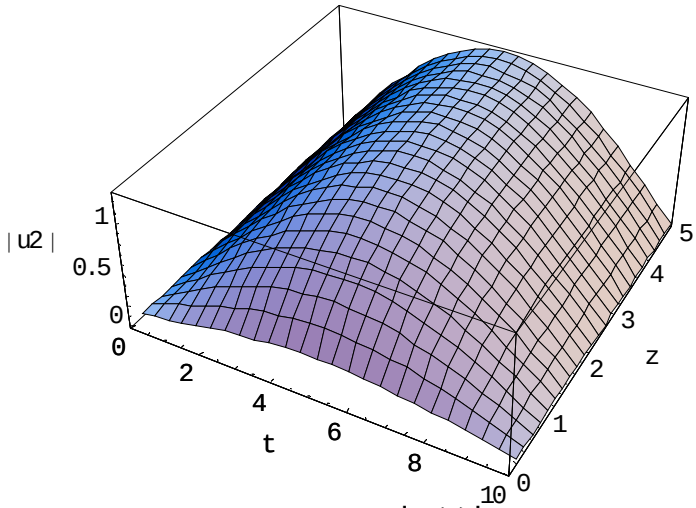

Fig. (3.6) the second order approximation of $\left|u^{(2)}\right|$ at $\varepsilon = 1, \gamma = 1$ and $\alpha, \rho_1 = 1, T = 10$ with considering only one term on the series (M=1).

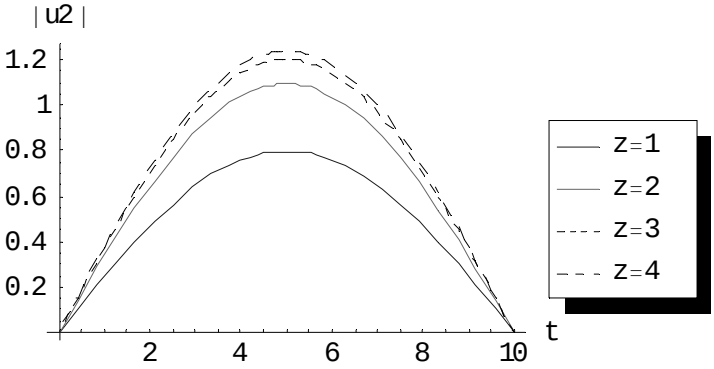

Fig. (3.7) the second order approximation of $\left|u^{(2)}\right|$ at $\varepsilon = 0.2, \gamma = 1$ and $\alpha, \rho_1 = 1, T = 10, M = 1$ for different values of z.

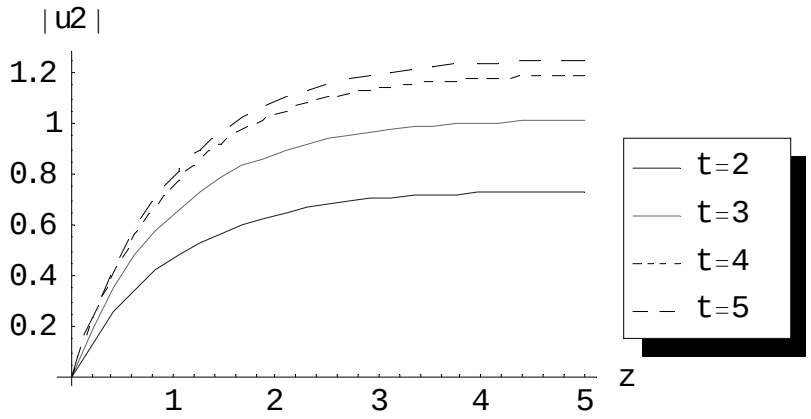

Fig. (3.8) the second order approximation of $\left|u^{(2)}\right|$ at $\varepsilon = 0.2, \gamma = 1$ and $\alpha, \rho_1 = 1, T = 10, M = 1$ for different values of t.

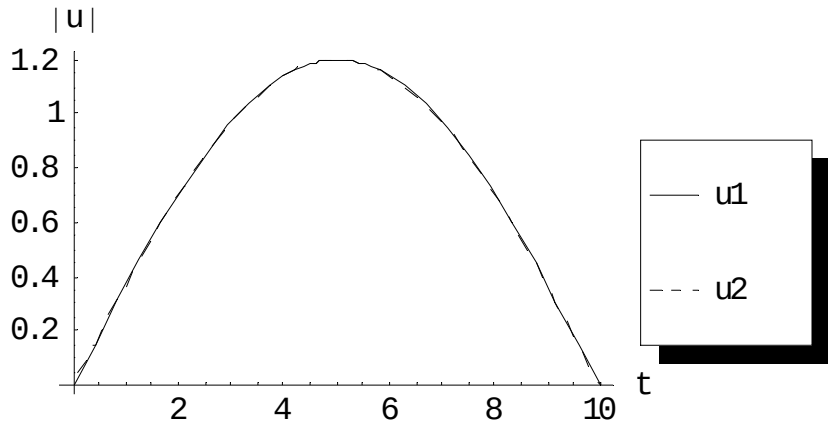

Fig. (3.9) comparison between first and second approximations at $\varepsilon = 0.2, \gamma = 1$ and $\alpha, \rho_1 = 1, T = 10, M = 1, z = 3$.

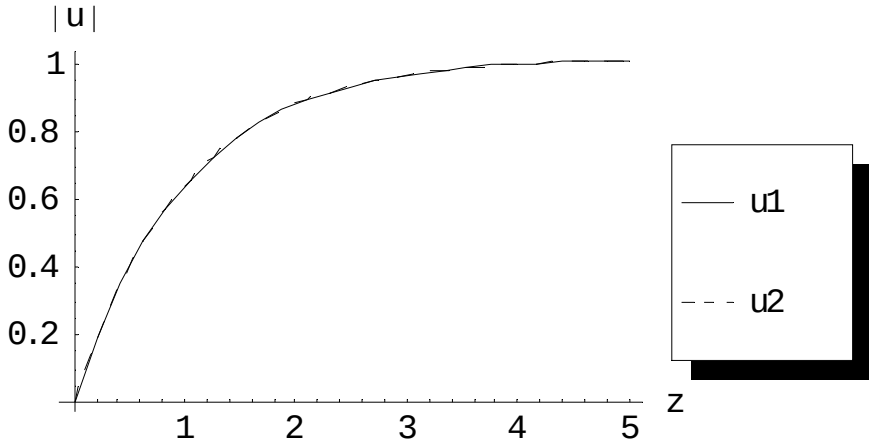

Fig. (3.10) comparison between first and second approximations at $\varepsilon = 0.2, \gamma = 1$ and $\rho_1 = 1, T = 10, M = 1, t = 3$.

Note: we calculated till second order only taking M=1 for both first order and second order and we cannot calculate more since the machine gives "MATHEMATICA KERNEL OUT OF MEMORY".

3.3.2 Case study 2

Taking the case $F_1(t,z) = \rho_1 \sin(\frac{m\pi}{T})t$, $F_2(t,z) = 0$ and $f_1(t) = 0$, $f_2(t) = 0$, ρ_1 is constant and following the algorithm, the following selected results for the first and second order approximations are got:

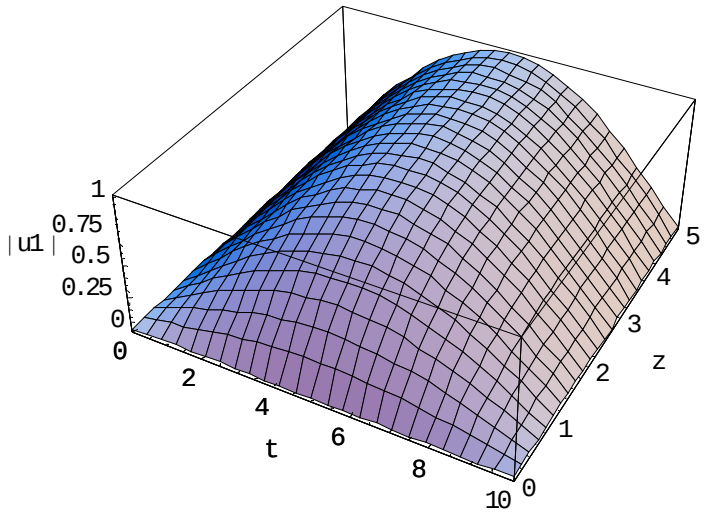

Fig. (3.11) the first order approximation of $\left|u^{(1)}\right|$ at $\varepsilon = 1, \gamma = 1$ and $\alpha, \rho_1 = 1, T = 10$with considering only one term on the series (M=1).

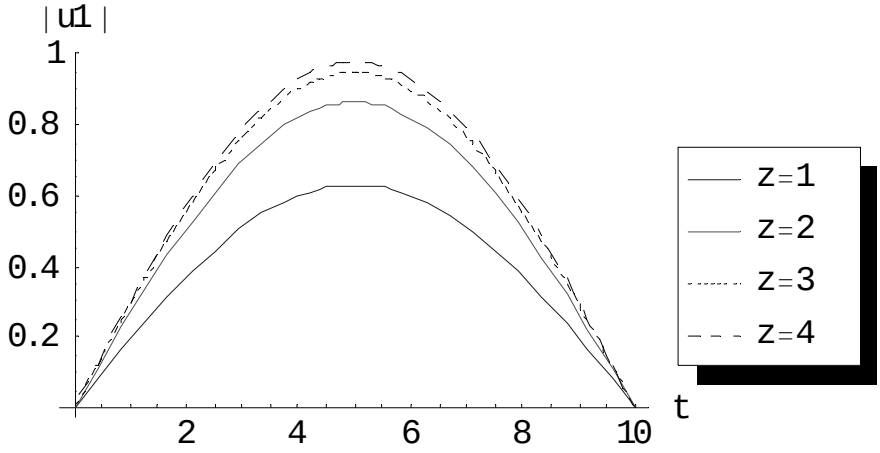

Fig. (3.12) the first order approximation of $\left|u^{(1)}\right|$ at $\varepsilon = 0.2, \gamma = 1$ and $\alpha, \rho_1 = 1, T = 10, M = 1$ for different values of z.

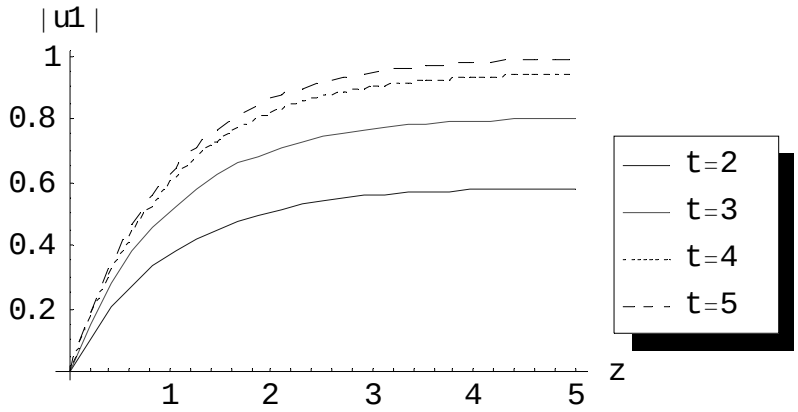

Fig. (3.13) the first order approximation of $\left|u^{(1)}\right|$ at $\varepsilon = 0.2, \gamma = 1$ and $\alpha, \rho_1 = 1, T = 10, M = 1$ for different values of t.

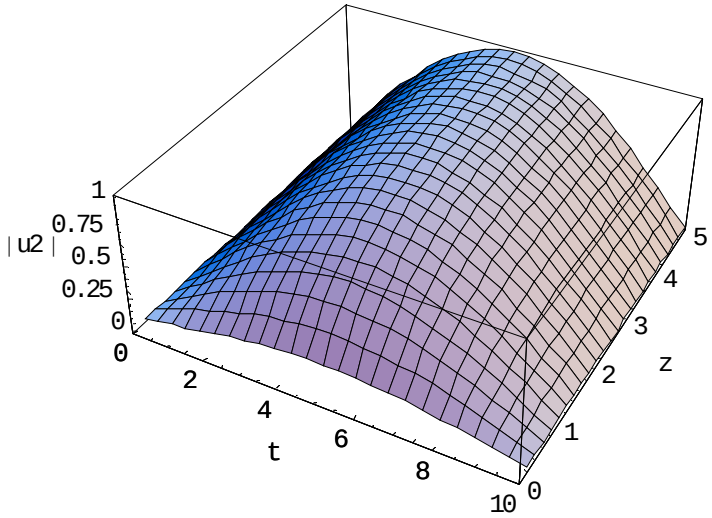

Fig. (3.14) the second order approximation of $\left|u^{(2)}\right|$ at $\varepsilon = 0.2, \gamma = 1$ and $\alpha, \rho_1 = 1, T = 10$ with considering only one term on the series (M=1).

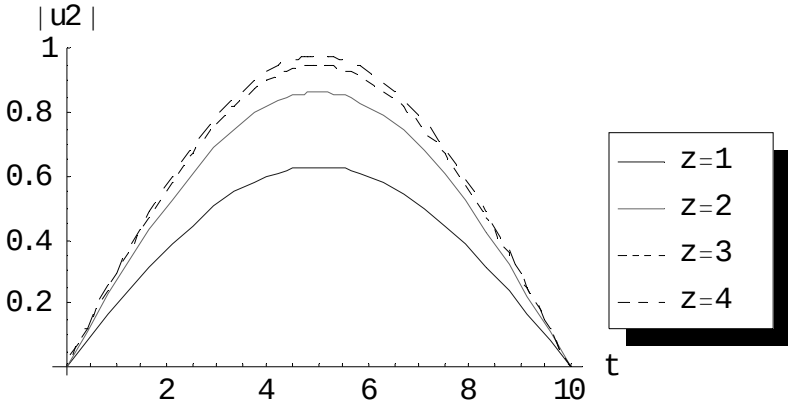

Fig. (3.15) the second order approximation of $\left|u^{(2)}\right|$ at $\varepsilon = 0.2, \gamma = 1$ and $\alpha, \rho_1 = 1, T = 10, M = 1$ for different values of z.

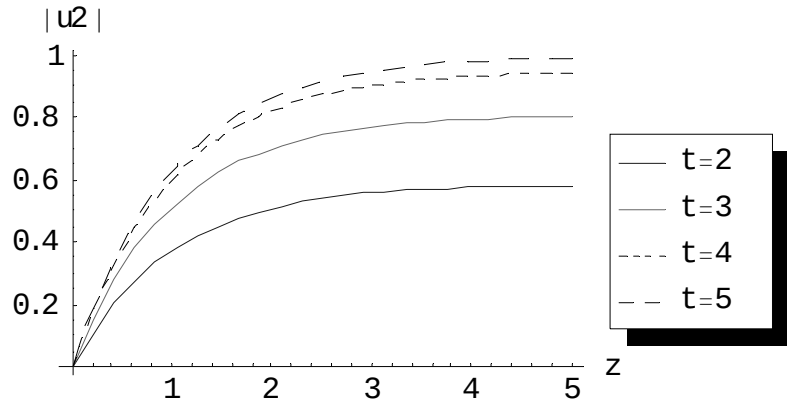

Fig. (3.16) the second order approximation of $\left|u^{(2)}\right|$ at $\varepsilon = 0.2, \gamma = 1$ and $\alpha, \rho_1 = 1, T = 10, M = 1$ for different values of z.

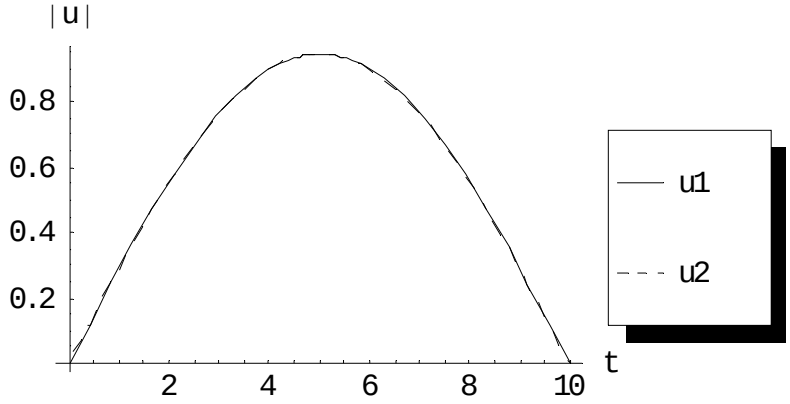

Fig. (3.17) comparison between first and second approximations at $\varepsilon = 0.2, \gamma = 1$ and $\alpha, \rho_1 = 1, T = 10, M = 1, z = 3$.

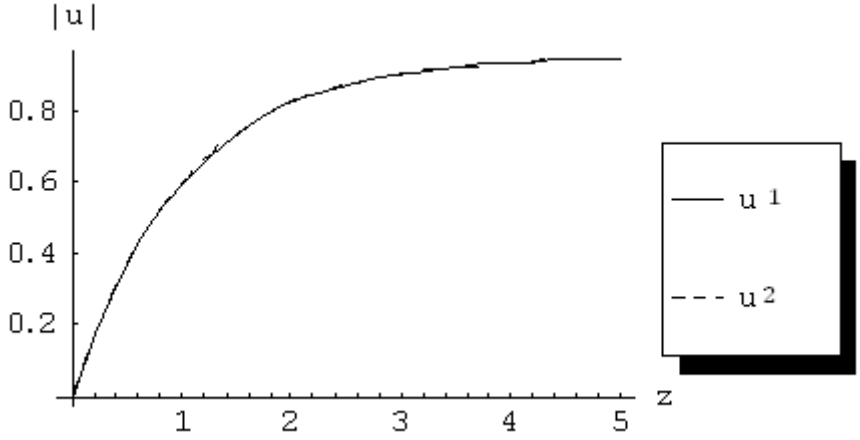

Fig. (3.18) comparison between first and second approximations at $\varepsilon = 0.2, \gamma = 1$ and $\alpha, \rho_1 = 1, T = 10, M = 1, t = 4$.

Note: we calculated till second order only taking M=1 for $\gamma = 0$ and $\gamma = 1$ for both first order and second order respectively and we cannot calculate more since the machine gives "MATHEMATICA KERNEL OUT OF MEMORY".

3.3.3 Case study 3

Taking the case $F_1(t,z) = \rho_1 e^{-t}$, $F_2(t,z) = 0$ and $f_1(t) = 0, f_2(t) = 0$, ρ_1 is constant and following the algorithm, the following selected results for the first and second order approximations are got:

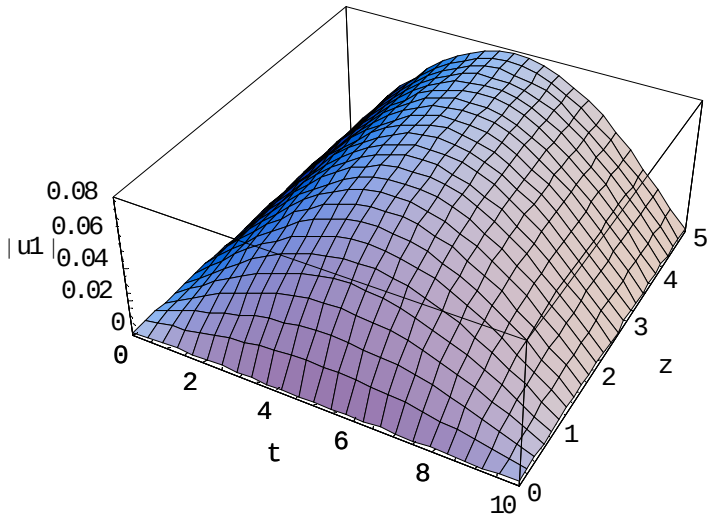

Fig. (3.19) the first order approximation of $\left|u^{(1)}\right|$ at $\varepsilon = 0.2, \gamma = 1$ and $\alpha, \rho_1 = 1, T = 10$ with considering only one term on the series (M=1)

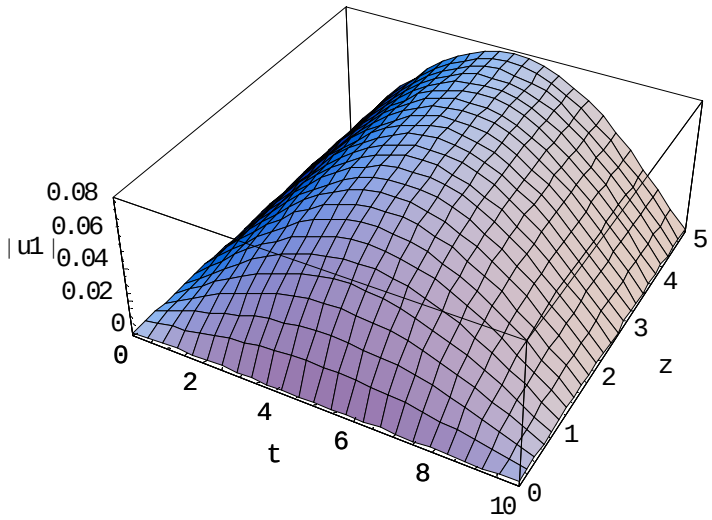

Fig. (3.20) the first order approximation of $\left|u^{(1)}\right|$ at $\varepsilon = 1, \gamma = 1$ and $\alpha, \rho_1 = 1, T = 10$ with considering only one term on the series (M=1)

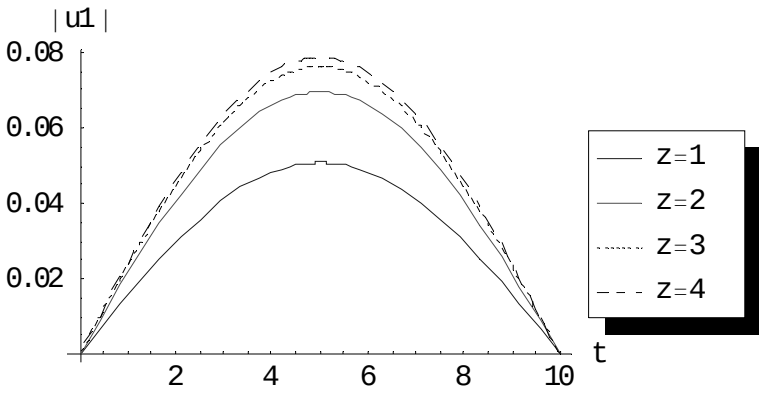

Fig. (3.21) the first order approximation of $\left|u^{(1)}\right|$ at $\varepsilon = 0.2, \gamma = 1$ and $\alpha, \rho_1 = 1, T = 10, M = 1$ for different values of z.

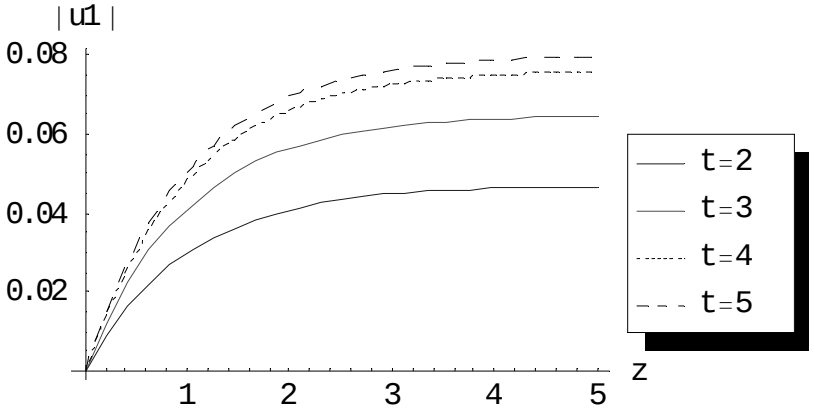

Fig. (3.22) the first order approximation of $\left|u^{(1)}\right|$ at $\varepsilon = 0.2, \gamma = 1$ and $\alpha, \rho_1 = 1, T = 10, M = 1$ for different values of t.

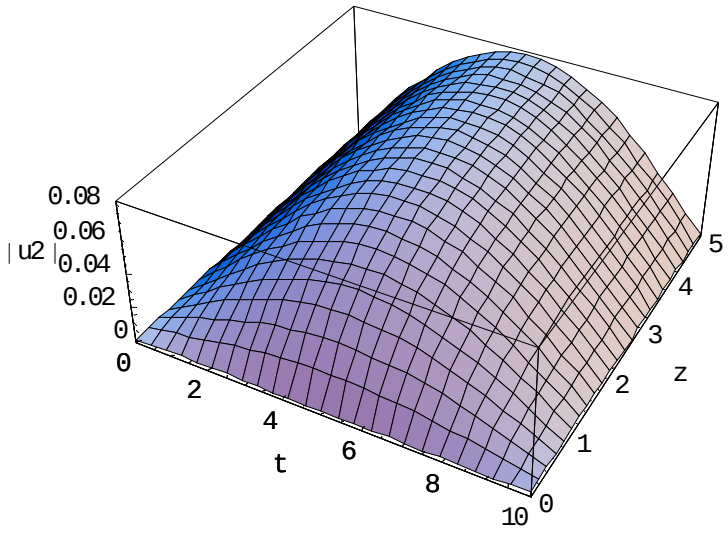

Fig. (3.23) the second order approximation of $\left|u^{(2)}\right|$ at $\varepsilon = 1, \gamma = 1$ and $\alpha, \rho_1 = 1, T = 10$ with considering only one term on the series (M=1)

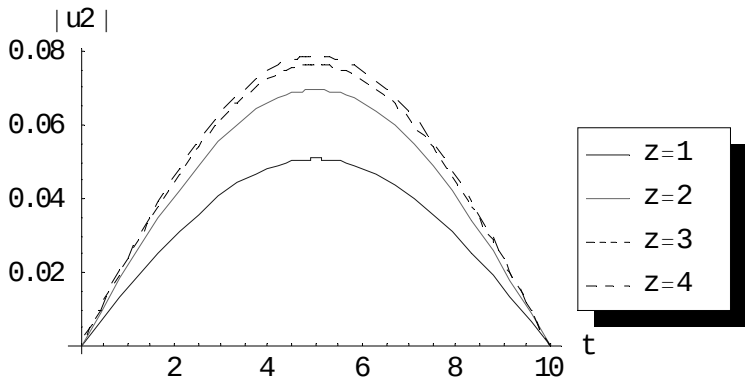

Fig. (3.24) the second order approximation of $\left|u^{(2)}\right|$ at $\varepsilon = 0.2, \gamma = 1$ and $\alpha, \rho_1 = 1, T = 10, M = 1$ for different values of z.

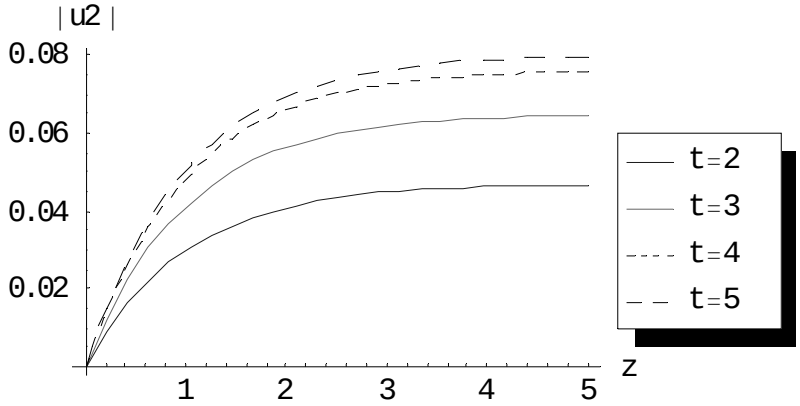

Fig. (3.25) the second order approximation of $\left|u^{(2)}\right|$ at $\varepsilon = 0.2, \gamma = 1$ and $\alpha, \rho_1 = 1, T = 10, M = 1$ for different values of t.

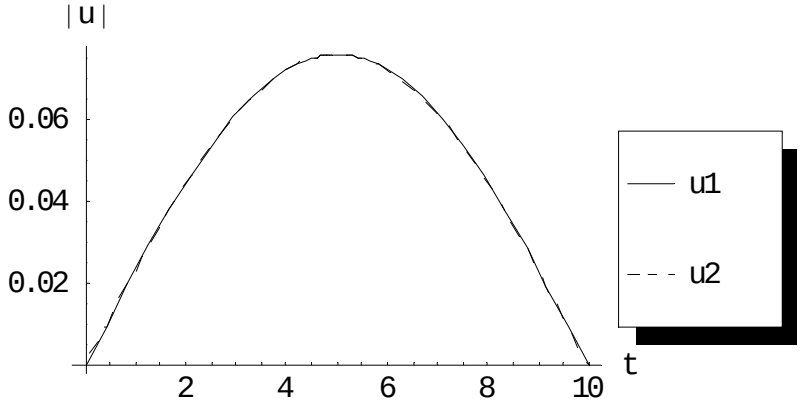

Fig. (3.26) comparison between first and second approximations at $\varepsilon = 0.2, \gamma = 1$ and $\alpha, \rho_1 = 1, T = 10, M = 1, z = 3$.

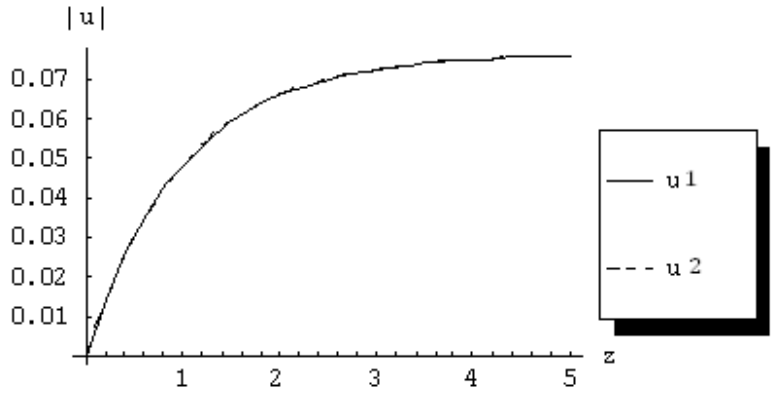

Fig. (3.27) comparison between first and second approximations at $\varepsilon = 0.2, \gamma = 1$ and $\alpha, \rho_1 = 1, T = 10, M = 1, t = 4$.

Note: we calculated till second order only taking M=1 $\gamma = 1$ for both first order and second order respectively and we cannot calculate more since the machine gives "MATHEMATICA KERNEL OUT OF MEMORY".

3.3.4 Case study 4

Taking the case $F_1(t,z) = \rho_1,\ F_2(t,z) = 0$ and $f_1(t) = \rho_2 e^{-t}$, $f_2(t) = 0$ where ρ_1 & ρ_2 are constants and following the algorithm, the following selected results for the first and second order approximations are got:

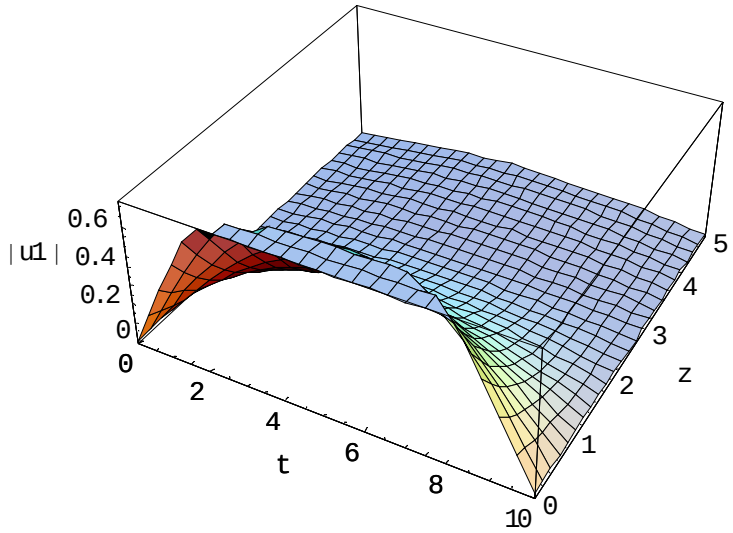

Fig. (3.28) the first order approximation of $\left|u^{(1)}\right|$ at $\varepsilon = 1$, $\gamma = 1$ and $\alpha, \rho_1, \rho_2 = 1, T = 10$ with considering only one term on the series (M=1).

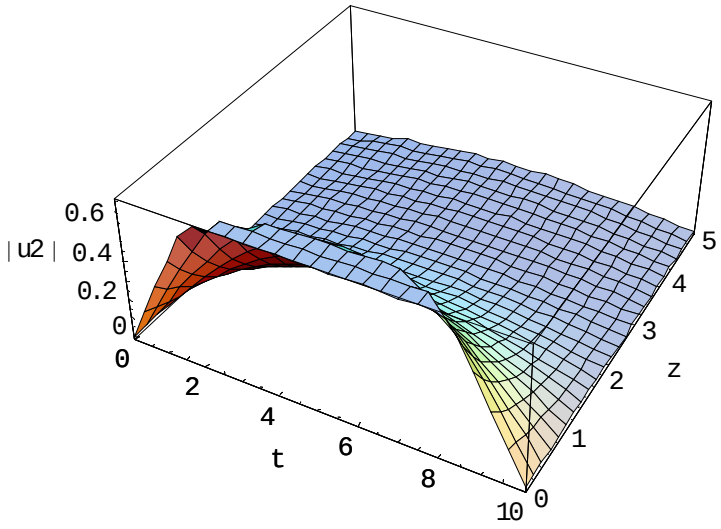

Fig. (3.29) the second order approximation of $\left|u^{(2)}\right|$ at $\varepsilon = 0.2$, $\gamma = 1$ and $\alpha, \rho_1, \rho_2 = 1, T = 10$ with considering only one term on the series (M=1).

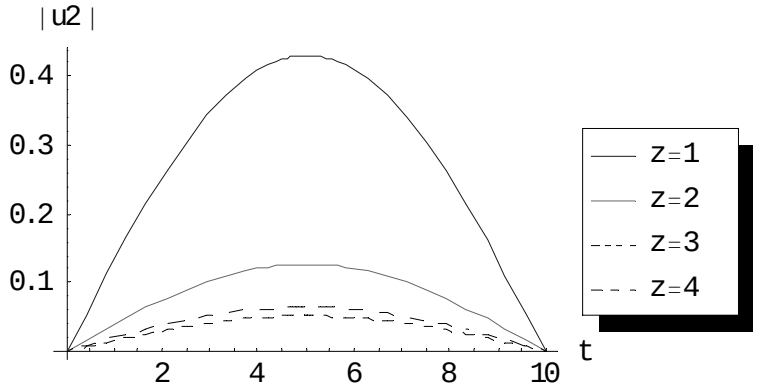

Fig. (3.30) the second order approximation of $\left|u^{(2)}\right|$ at $\varepsilon = 0.2, \gamma = 1$ and $\alpha, \rho_1, \rho_2 = 1, T = 10, M = 1$ for different values of z.

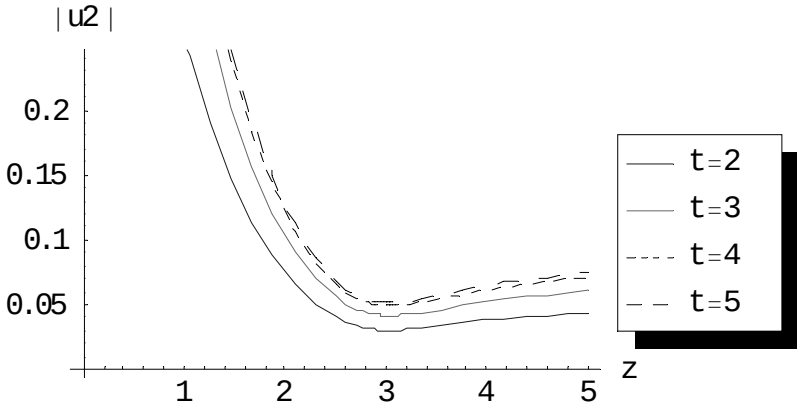

Fig. (3.31) the second order approximation of $\left|u^{(2)}\right|$ at $\varepsilon = 0.2, \gamma = 1$ and $\alpha, \rho_1, \rho_2 = 1, T = 10, M = 1$ for different values of t.

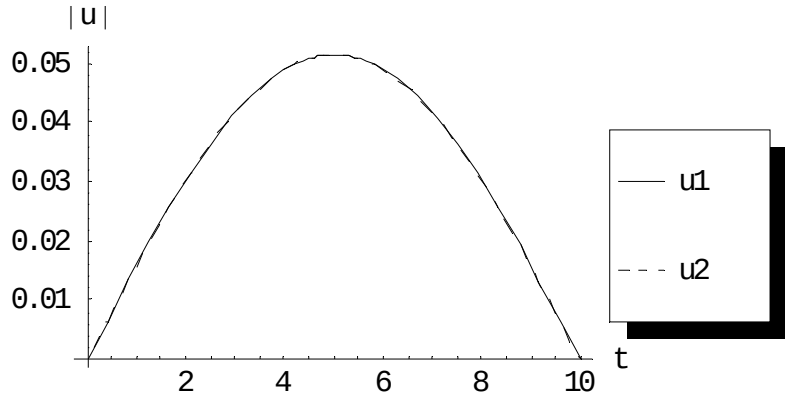

Fig. (3.32) comparison between first and second approximations at $\varepsilon = 0.2, \gamma = 1$ and $\alpha, \rho_1, \rho_2 = 1,\ T = 10,\ M = 1, z = 3.$

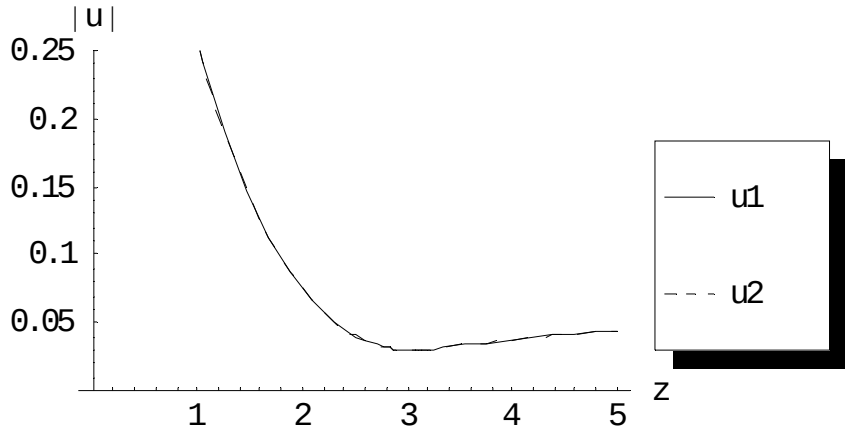

Fig. (3.33) comparison between first and second approximations at $\varepsilon = 0.2, \gamma = 1$ and $\alpha, \rho_1, \rho_2 = 1,\ T = 10, M = 1,\ t = 4.$

Note: we calculated till second order only taking M=1 for $\gamma = 1$ for both first order and second order respectively and we cannot calculate more since the machine gives "MATHEMATICA KERNEL OUT OF MEMORY".

3.3.5 Case study 5

Taking the case $F_1(t,z) = \rho_1 \sin\left(\frac{m\pi}{T}\right) t$, $F_2(t,z) = 0$ and $f_1(t) = \rho_2,\ f_2(t) = 0$ where ρ_1 & ρ_2 are constants and following the algorithm, the following selected result for the first and second order approximations are got:

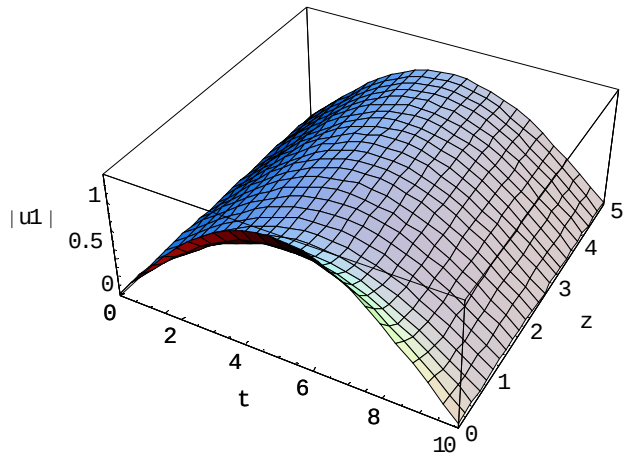

Fig. (3.34) the first order approximation of $\left|u^{(1)}\right|$ at $\varepsilon = 0.2$, $\gamma = 1$ and $\alpha, \rho_1, \rho_2 = 1, T = 10$ with considering only one term on the series (M=1).

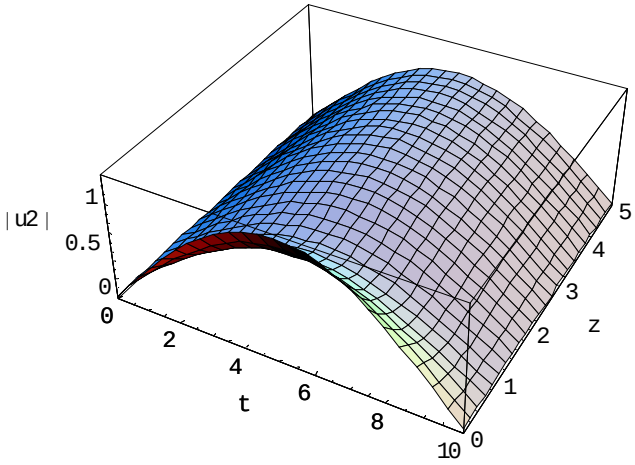

Fig. (3.35) the second order approximation of $\left|u^{(2)}\right|$ at $\varepsilon = 1$, $\gamma = 1$ and $\alpha, \rho_1, \rho_2 = 1, T = 10$ with considering only ten terms on the series (M=10).

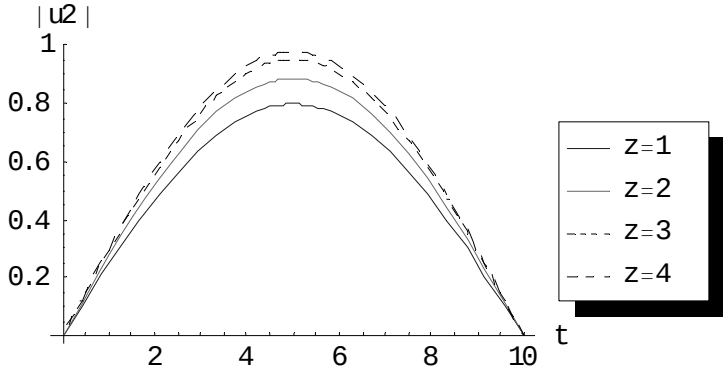

Fig. (3.36) the second order approximation of $\left|u^{(2)}\right|$ at $\varepsilon = 0.2, \gamma = 1$ and $\alpha, \rho_1, \rho_2 = 1, T = 10, M = 10$ for different values of z.

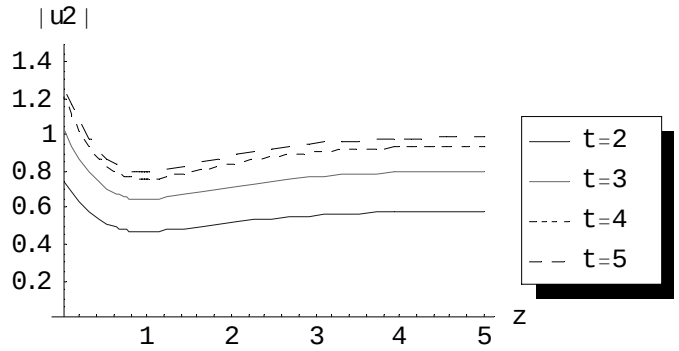

Fig. (3.37) the second order approximation of $\left|u^{(2)}\right|$ at $\varepsilon = 0.2, \gamma = 1$ and $\alpha, \rho_1, \rho_2 = 1, T = 10, M = 10$ for different values of t.

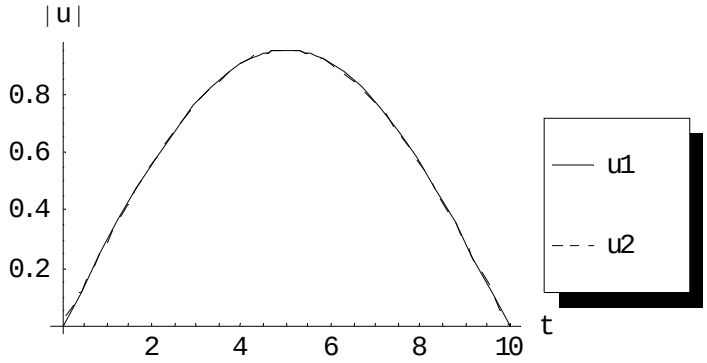

Fig. (3.38) comparison between first and second approximation at $\varepsilon = 0.2, \gamma = 1$ and $\alpha, \rho_1, \rho_2 = 1,\ T = 10,\ z = 3.$

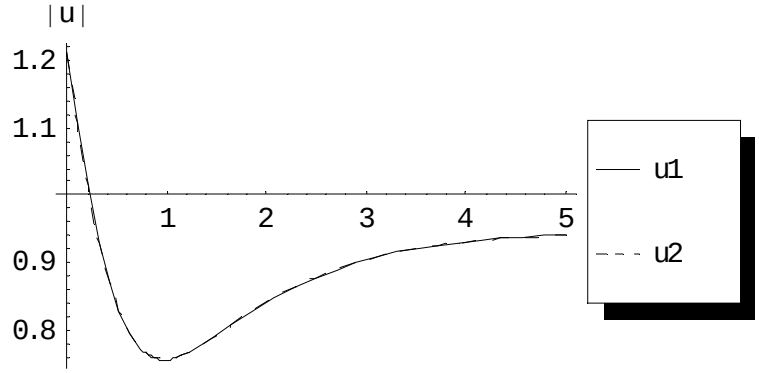

Fig. (3.39) comparison between first and second approximation at $\varepsilon = 0.2, \gamma = 1$ and $\alpha, \rho_1, \rho_2 = 1,\ T = 10,\ t = 4.$

Note: we calculated till second order only taking M=1 for $\gamma = 1$ for both first order and second order respectively and we cannot calculate more since the machine gives "MATHEMATICA KERNEL OUT OF MEMORY".

3.3.6 Case study 6

Taking the case $F_1(t,z) = \rho_1 e^{-t}$, $F_2(t,z) = 0$ and $f_1(t) = \rho_2 e^{-t}$, $f_2(t) = 0$ where ρ_1 & ρ_2 are constants and following the algorithm, the following selected results for the first and second order approximations are got:

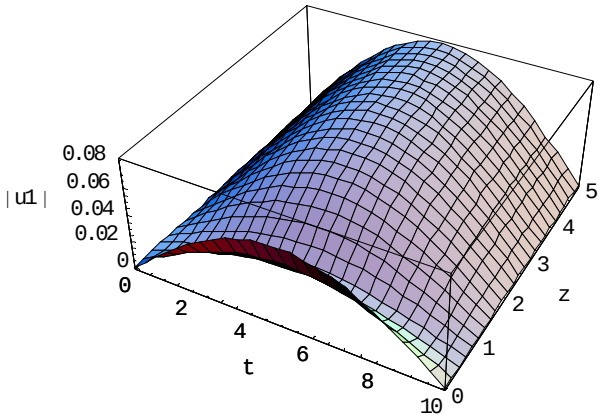

Fig. (3.40) the first order approximation of $\left|u^{(1)}\right|$ at $\varepsilon = 1$, $\gamma = 1$ and $\alpha, \rho_1, \rho_2 = 1, T = 10$ with considering only one term on the series (M=1).

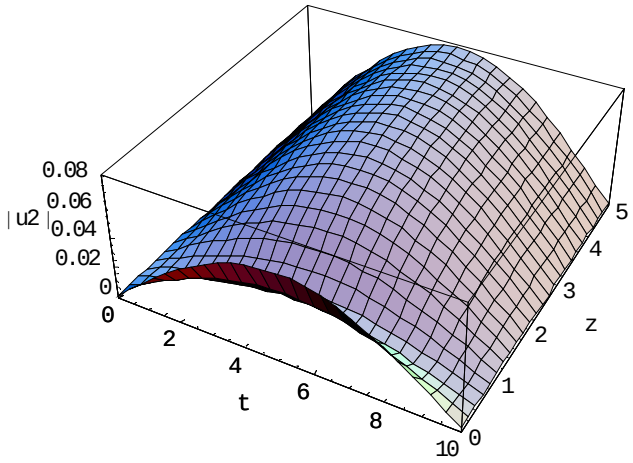

Fig. (3.41) the second order approximation of $\left|u^{(2)}\right|$ at $\varepsilon = 1$, $\gamma = 1$ and $\alpha, \rho_1, \rho_2 = 1, T = 10$ with considering only ten terms on the series (M=10).

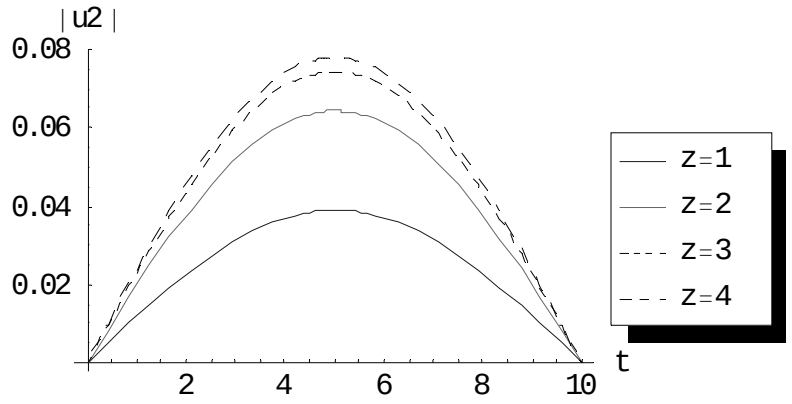

Fig. (3.42) the second order approximation of $\left|u^{(2)}\right|$ at $\varepsilon = 0.2, \gamma = 1$ and $\alpha, \rho_1, \rho_2 = 1, T = 10, M = 10$ for different values of z.

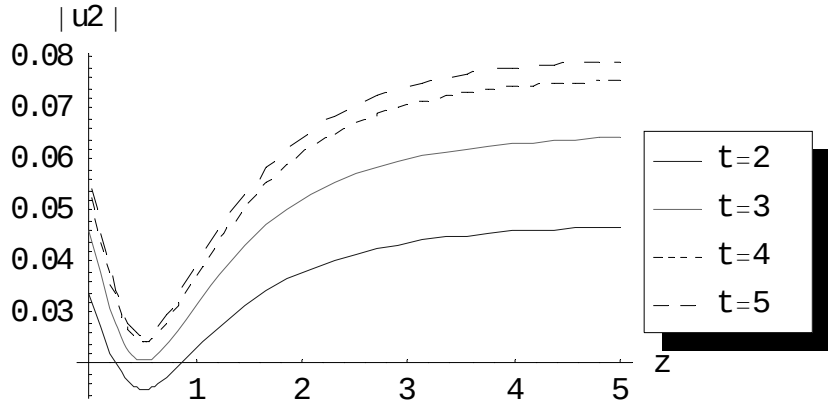

Fig. (3.43) the second order approximation of $\left|u^{(2)}\right|$ at $\varepsilon = 0.2, \gamma = 1$ and $\alpha, \rho_1, \rho_2 = 1, T = 10, M = 10$ for different values of t.

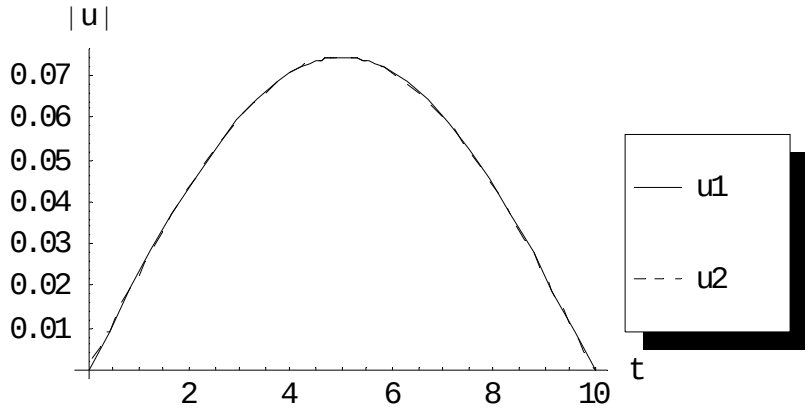

Fig. (3.44) comparison between first and second approximations at $\varepsilon = 0.2, \gamma = 1$ and $\alpha, \rho_1, \rho_2 = 1,\ T = 10,\ z = 3$.

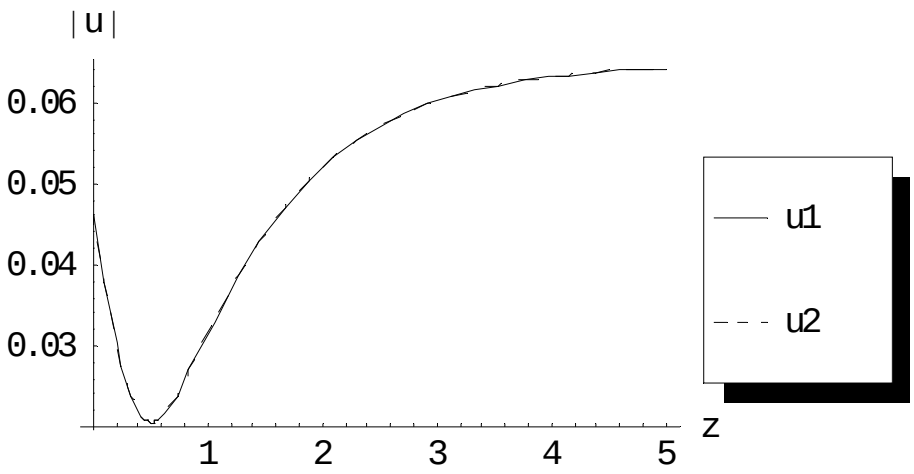

Fig. (3.45) comparison between first and second approximations at $\varepsilon = 0.2, \gamma = 1$ and $\alpha, \rho_1, \rho_2 = 1,\ T = 10,\ t = 4$.

Note: we calculated till second order only taking M=1 for $\gamma = 1$ for both first order and second order respectively and we cannot calculate more since the machine gives "MATHEMATICA KERNEL OUT OF MEMORY".

3.3.7 Case study 7

Taking the case $F_1(t,z) = \rho_1 \sin\left(\frac{m\pi}{T}\right) t$, $F_2(t,z) = 0$ and $f_1(t) = \rho_2 e^{-t}$, $f_2(t) = 0$ where ρ_1 & ρ_2 are constants and following the algorithm, the following selected results for the first and second order approximations are got:

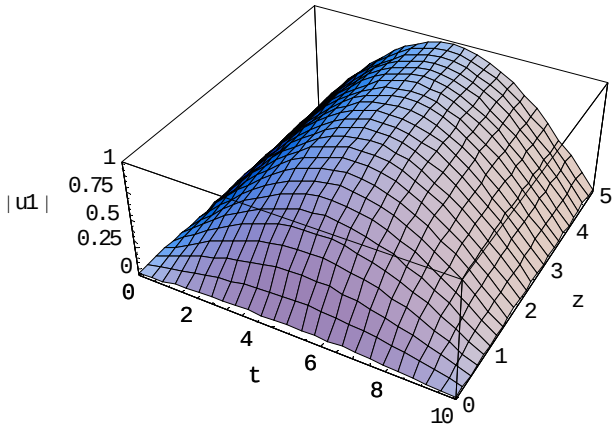

Fig. (3.46) the first order approximation of $\left|u^{(1)}\right|$ at $\varepsilon = 0.2$, $\gamma = 1$ and $\alpha, \rho_1, \rho_2 = 1, T = 10$ with considering only one term on the series (M=1).

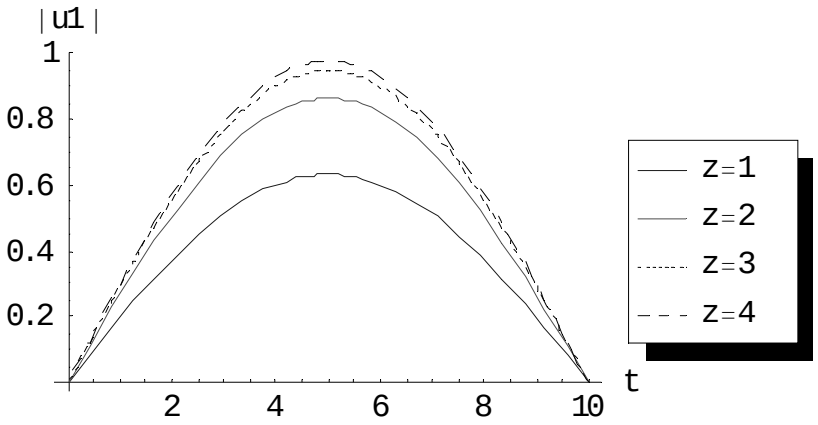

Fig. (3.47) the first order approximation of $\left|u^{(1)}\right|$ at $\varepsilon = 0.2, \gamma = 1$ and $\alpha, \rho_1, \rho_2 = 1, T = 10, M = 1$ for different values of z.

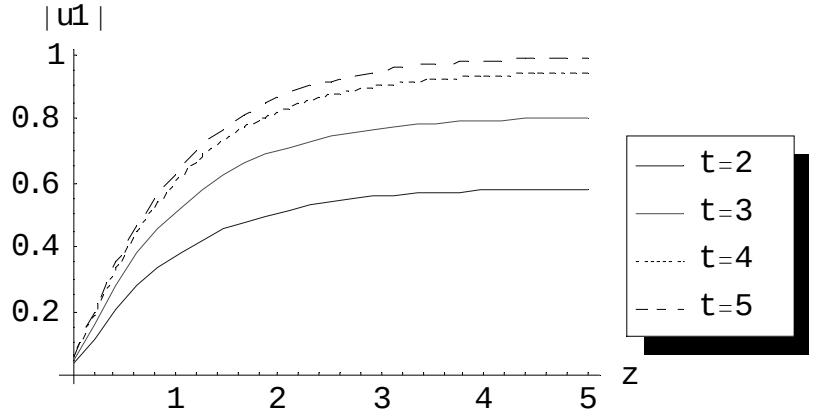

Fig. (3.48) the first order approximation of $\left|u^{(1)}\right|$ at $\varepsilon = 0.2, \gamma = 1$ and $\alpha, \rho_1, \rho_2 = 1, T = 10, M = 1$ for different values of t.

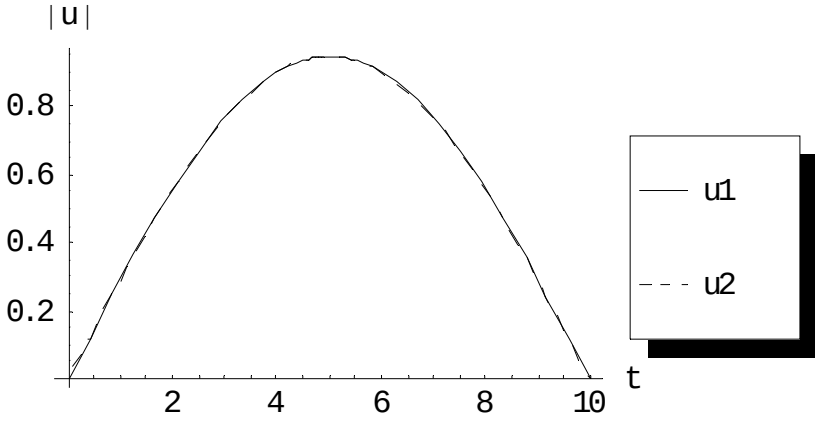

Fig. (3.49) comparison between first and second approximations at $\varepsilon = 0.2, \gamma = 1$ and $\alpha, \rho_1, \rho_2 = 1,\ T = 10,\ z = 3$.

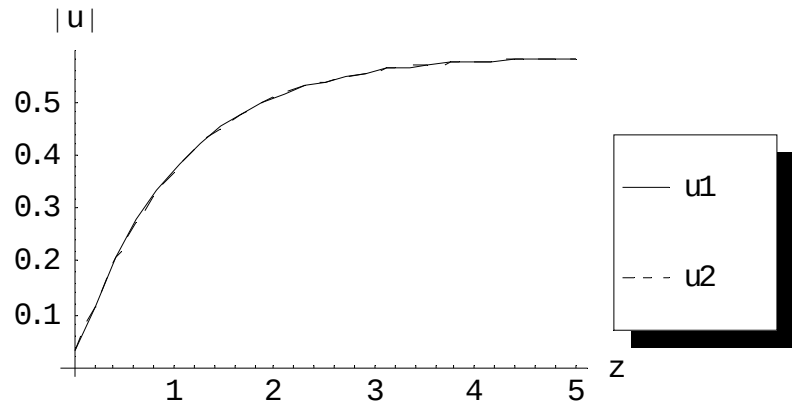

Fig. (3.50) comparison between first and second approximations at $\varepsilon = 0.2, \gamma = 1$ and $\alpha, \rho_1, \rho_2 = 1,\ T = 10,\ t = 3$.

Note: we calculated till second order only taking M=1 for $\gamma = 1$ for both first order and second order respectively and we cannot calculate more since the machine gives "MATHEMATICA KERNEL OUT OF MEMORY".

3.3.8 Case study 8

Taking the case $F_1(t,z) = \rho_1$, $F_2(t,z) = 0$ and $f_1(t) = \rho_2 \sin\left(\frac{m\pi}{T}\right) t$, $f_2(t) = 0$ where ρ_1 & ρ_2 are constants and following the algorithm, the following selected results for the first and second order approximations are got:

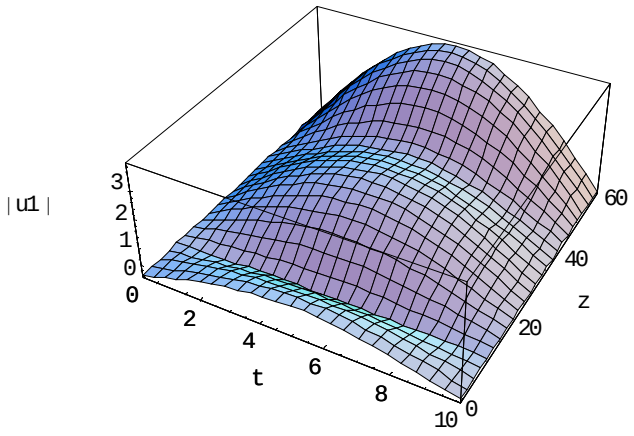

Fig. (3.51) the first order approximation of $\left|u^{(1)}\right|$ at $\varepsilon = 0.2$, $\gamma = 0$ and $\alpha, \rho_1, \rho_2 = 1, T = 10$ with considering only one term on the series (M=1).

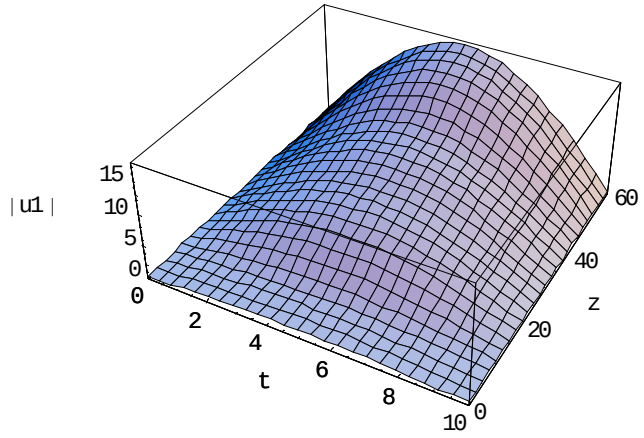

Fig. (3.52) the first order approximation of $\left|u^{(1)}\right|$ at $\varepsilon = 1$, $\gamma = 0$ and $\alpha, \rho_1, \rho_2 = 1, T = 10$ with considering only one term on the series (M=1).

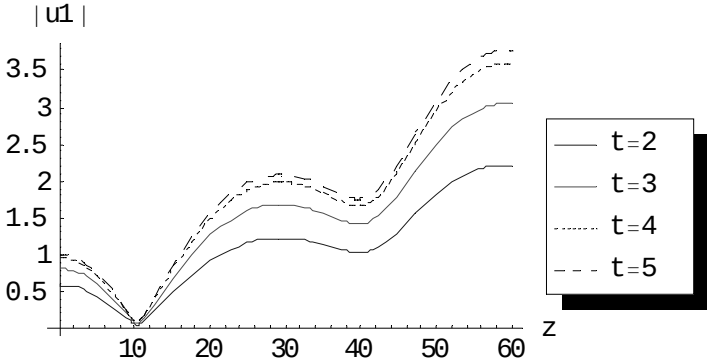

Fig. (3.53) the first order approximation of $\left|u^{(1)}\right|$ at $\varepsilon = 0.2, \gamma = 0$ and $\alpha, \rho_1, \rho_2 = 1, T = 10, M = 1$ for different values of t.

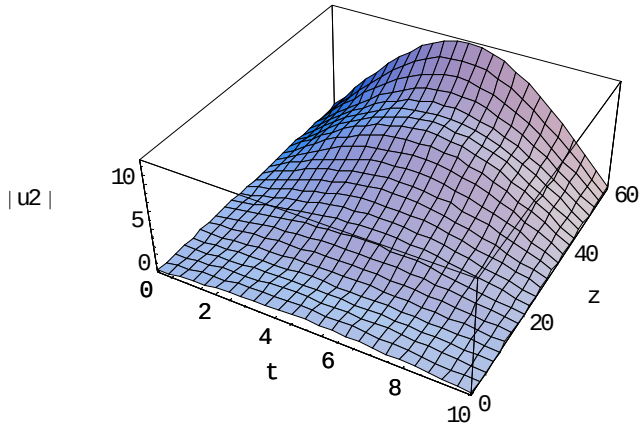

Fig. (3.54) the second order approximation of $\left|u^{(2)}\right|$ at $\varepsilon = 0.2$, $\gamma = 0$ and $\alpha, \rho_1, \rho_2 = 1, T = 10$ with considering only ten terms on the series (M=10).

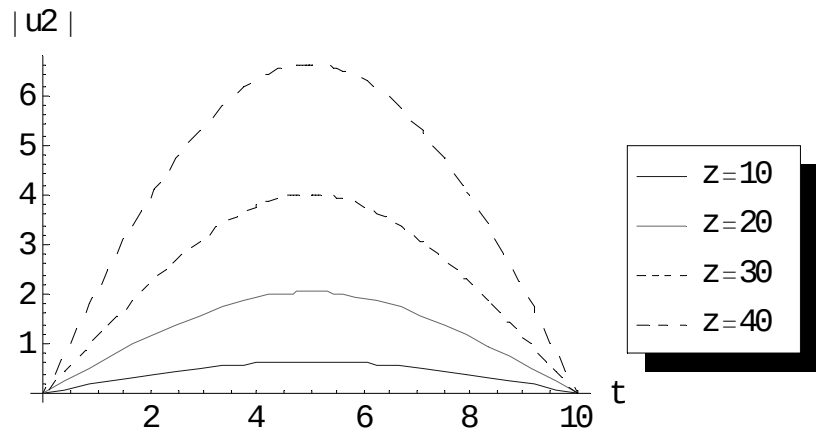

Fig. (3.55) the second order approximation of $\left|u^{(2)}\right|$ at $\varepsilon = 0.2, \gamma = 0$ and $\alpha, \rho_1, \rho_2 = 1, T = 10, M = 10$ for different values of z.

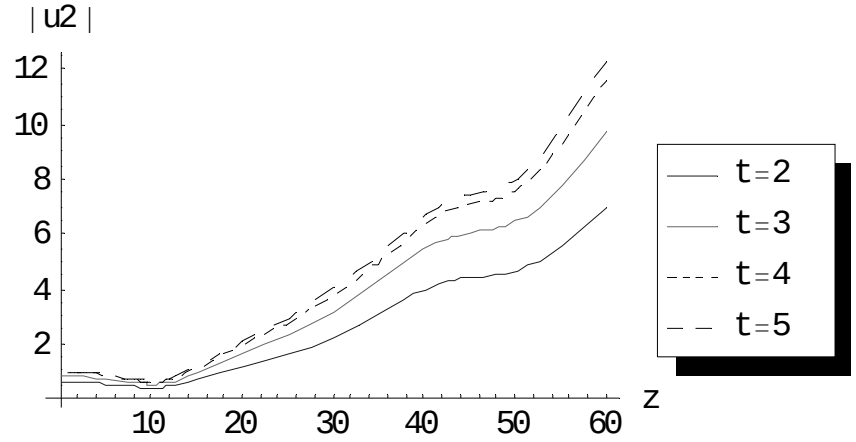

Fig. (3.56) the second order approximation of $\left|u^{(2)}\right|$ at $\varepsilon = 0.2, \gamma = 0$ and $\alpha, \rho_1, \rho_2 = 1, T = 10, M = 10$ for different values of t.

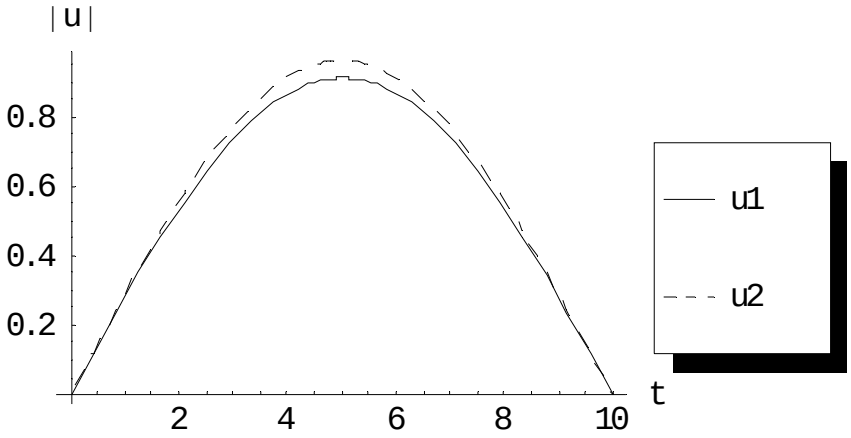

Fig. (3.57) comparison between first and second approximations at $\varepsilon = 0.2, \gamma = 0$ and $\alpha, \rho_1, \rho_2 = 1,\ T = 10,\ z = 3.$

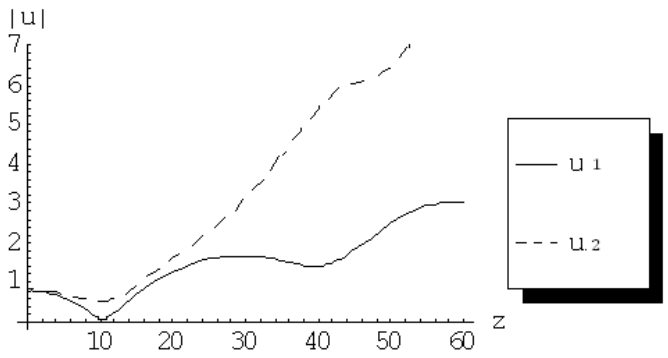

Fig. (3.58) comparison between first and second approximations at $\varepsilon = 0.2, \gamma = 0$ and $\alpha, \rho_1, \rho_2 = 1,\ T = 10,\ t = 3.$

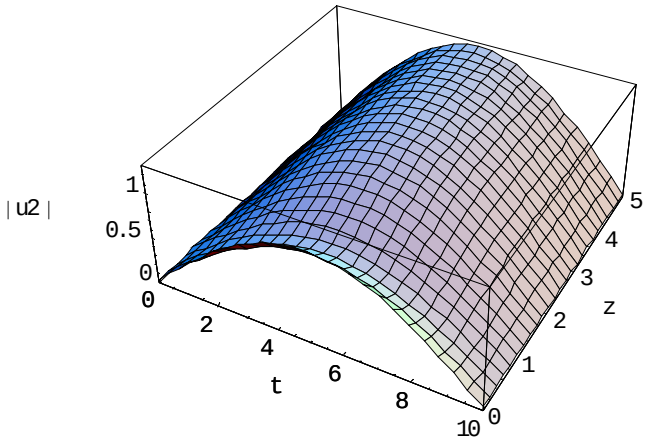

Fig. (3.59) the second order approximation of $\left|u^{(2)}\right|$ at $\varepsilon = 0.2$, $\gamma = 1$ and$\alpha, \rho_1, \rho_2 = 1, T = 10$ with considering only ten terms on the series (M=10).

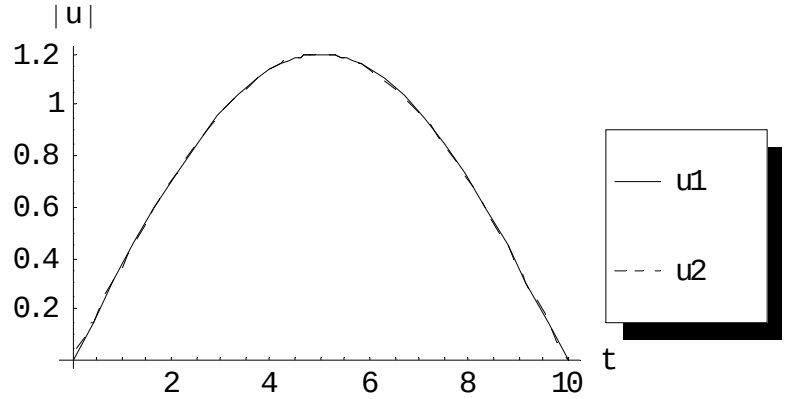

Fig. (3.60) comparison between first and second approximation at $\varepsilon = 0.2, \gamma = 1$ and $\alpha, \rho_1, \rho_2 = 1,\ T = 10,\ z = 3.$

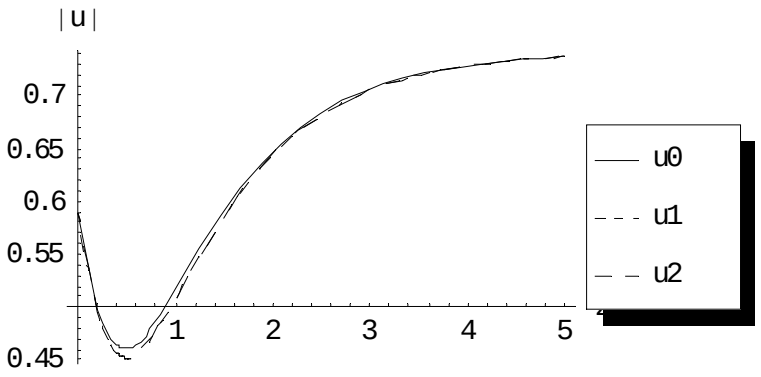

Fig. (3.61) comparison between zero, first and second approximations at $\varepsilon = 0.2, \gamma = 1$ and $\alpha, \rho_1, \rho_2 = 1,\ T = 10,\ t = 3.$

Note: we calculated till second order only taking M=10 and M=1 for $\gamma = 0$ and $\gamma = 1$ for both first order and second order respectively and we cannot calculate more since the machine gives "MATHEMATICA KERNEL OUT OF MEMORY".

3.3.9 Case study 9

Taking the case $F_1(t,z) = \rho_1 e^{-t}$, $F_2(t,z) = 0$ and $f_1(t) = \rho_2 \sin\left(\frac{m\pi}{T}\right) t$, $f_2(t) = 0$ where ρ_1 & ρ_2 are constants and following the algorithm, the following selected results for the first and second order approximations are got:

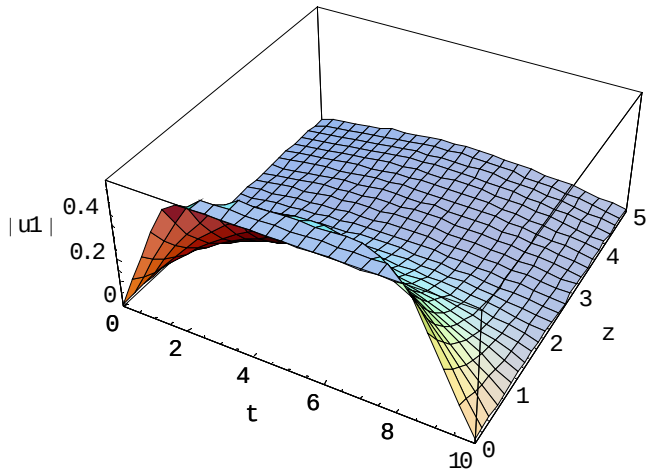

Fig. (3.62) the first order approximation of $\left|u^{(1)}\right|$ at $\varepsilon = 1$, $\gamma = 1$ and $\alpha, \rho_1, \rho_2 = 1, T = 10$ with considering only one term on the series (M=1).

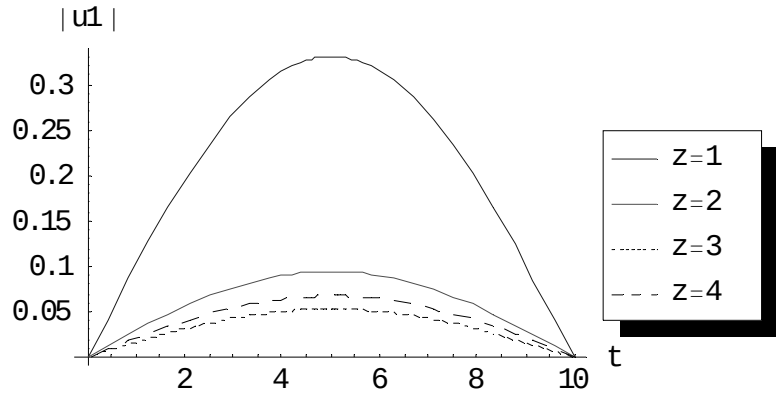

Fig. (3.63) the first order approximation of $\left|u^{(1)}\right|$ at $\varepsilon = 0.2, \gamma = 1$ and $\alpha, \rho_1, \rho_2 = 1, T = 10, M = 1$ for different values of z.

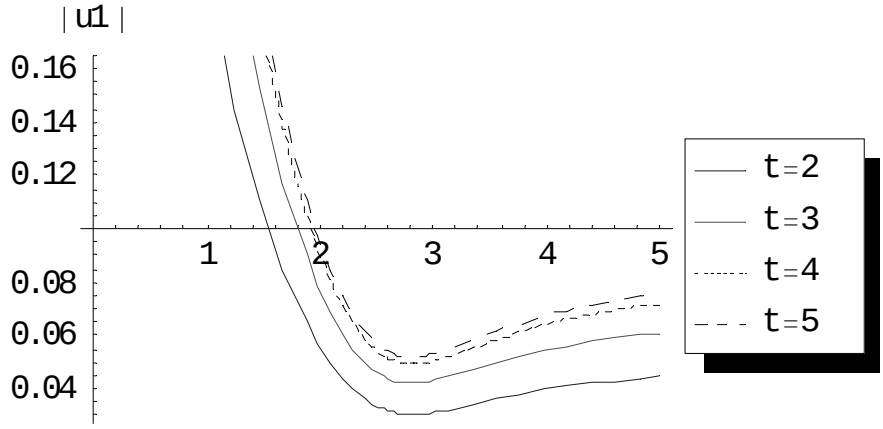

Fig. (3.64) the first order approximation of $\left|u^{(1)}\right|$ at $\varepsilon = 0.2, \gamma = 1$ and $\alpha, \rho_1, \rho_2 = 1, T = 10, M = 1$ for different values of t.

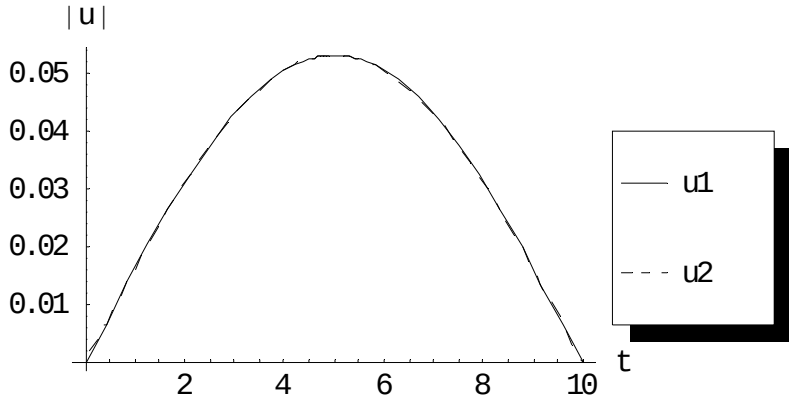

Fig. (3.65) comparison between first and second approximations at $\varepsilon = 0.2, \gamma = 1$ and $\alpha, \rho_1, \rho_2 = 1,\ T = 10,\ z = 3$.

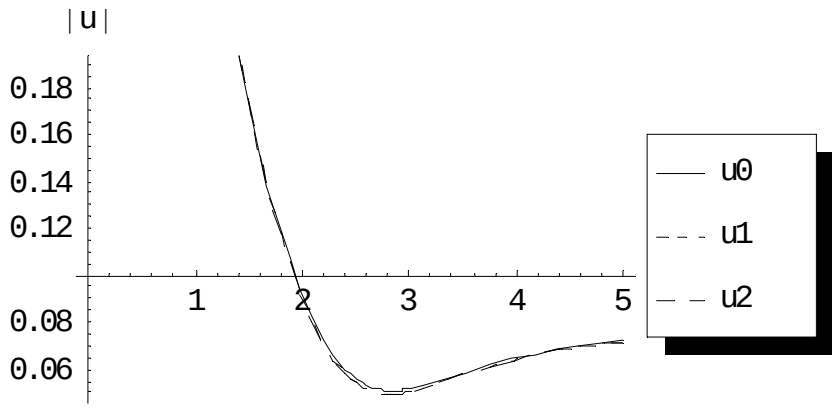

Fig. (3.66) comparison between zero, first and second approximations at $\varepsilon = 0.2, \gamma = 1$ and $\alpha, \rho_1, \rho_2 = 1,\ T = 10,\ t = 4$.

Note: we calculated till second order only taking M=1 for $\gamma = 1$ for both first order and second order respectively and we cannot calculate more since the machine gives "MATHEMATICA KERNEL OUT OF MEMORY".

3.3.10 Case study 10

Taking the case $F_1(t,z) = \rho_1 \sin\left(\frac{m\pi}{T}\right) t$, $F_2(t,z) = 0$ and $f_1(t) = \rho_2 \sin\left(\frac{m\pi}{T}\right) t$, $f_2(t) = 0$ where ρ_1 & ρ_2 are constants and following the algorithm, the following selected results for the first and second order approximations are got:

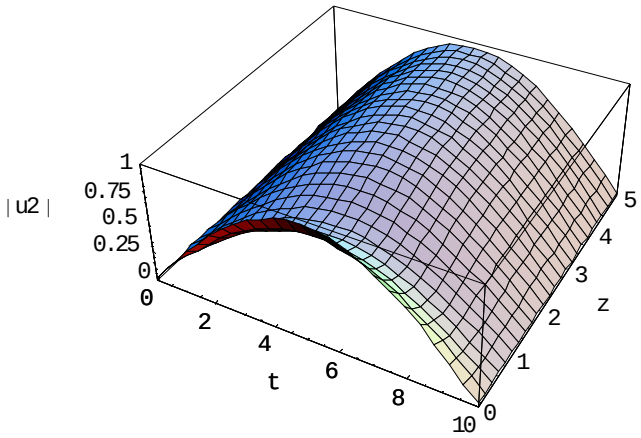

Fig. (3.67) the second order approximation of $\left|u^{(2)}\right|$ at $\varepsilon = 1$, $\gamma = 1$ and $\alpha, \rho_1, \rho_2 = 1, T = 10$ with considering only ten terms on the series (M=10).

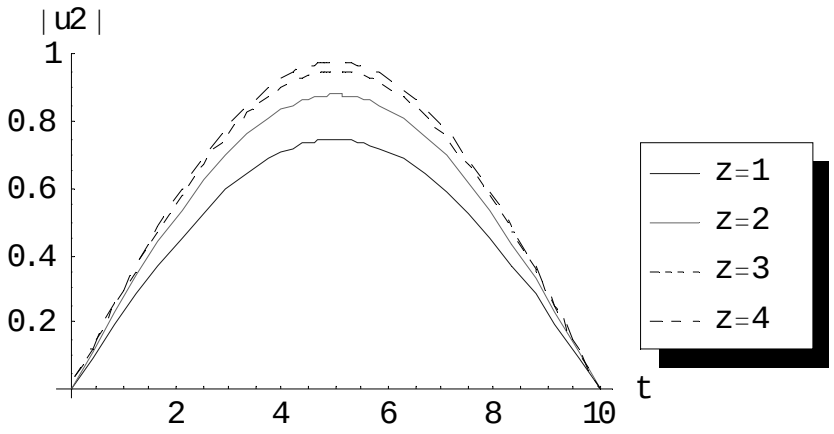

Fig. (3.68) the second order approximation of $\left|u^{(2)}\right|$ at $\varepsilon = 0.2, \gamma = 1$ and $\alpha, \rho_1, \rho_2 = 1, T = 10, M = 10$ for different values of z.

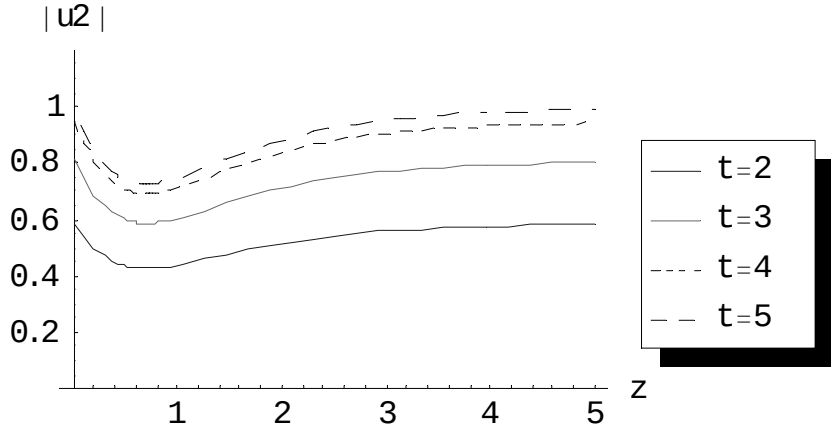

Fig. (3.69) the second order approximation of $\left|u^{(2)}\right|$ at $\varepsilon = 0.2, \gamma = 1$ and $\alpha, \rho_1, \rho_2 = 1, T = 10, M = 10$ for different values of t.

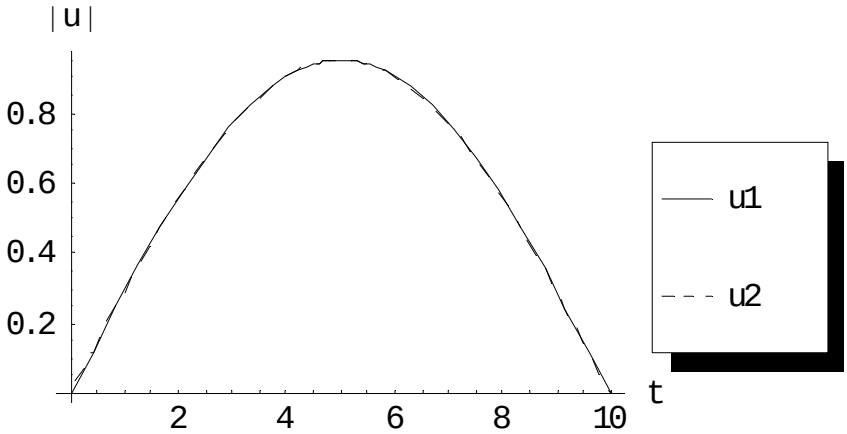

Fig. (3.70) comparison between first and second approximations at $\varepsilon = 0.2, \gamma = 1$ and $\alpha, \rho_1, \rho_2 = 1,\ T = 10,\ z = 3$.

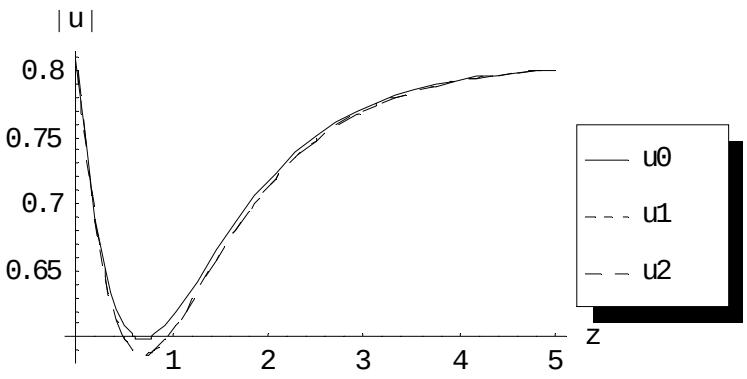

Fig. (3.71) comparison between zero, first and second approximations at $\varepsilon = 0.2, \gamma = 1$ and $\alpha, \rho_1, \rho_2 = 1,\ T = 10,\ t = 4$.

Note: we calculated till second order only taking M=1 for $\gamma = 1$ for both first order and second order respectively and we cannot calculate more since the machine gives "MATHEMATICA KERNEL OUT OF MEMORY".

3.4 Picard Approximation

To validate our previous results, in the absence of the exact solution, let us follow another approximation technique. The Picard approximation is considered in this section.

Solving equation (3.1) with the same conditions (3.2) and (3.3) and following the Picard algorithm which puts the nonlinear terms in the right hand side of the equation evaluated at the previous step, which means that we solve the linear case iteratively.

Let $u(t\,, z) = \psi(t\,, z) + i\,\phi(t\,,\ z), \psi\,, \phi$: are real valued functions. The following coupled equations are got:

$$\frac{\partial \phi(t,z)}{\partial z} = \alpha\,\frac{\partial^2 \psi(t,z)}{\partial t^2} + \varepsilon(\psi^2 + \phi^2)\psi - \gamma\phi - F_1(t\,, z) \qquad (3.48)$$

$$\frac{\partial \psi(t,z)}{\partial z} = -\alpha\,\frac{\partial^2 \phi(t,z)}{\partial t^2} - \varepsilon(\psi^2 + \phi^2)\phi - \gamma\phi + F_2(t\,, z) \qquad (3.49)$$

Where $\psi(t,0) = f_1(t),\ \phi(t,0) = f_2(t)$, and all corresponding other I.C. and B.C. are zeros.

$$\frac{\partial \phi_i(t,z)}{\partial z} = \alpha\,\frac{\partial^2 \psi_i(t,z)}{\partial t^2} + H_{1i}\ ,\qquad i \geq 1 \qquad (3.50)$$

$$\frac{\partial \psi_i(t,z)}{\partial z} = \alpha \frac{\partial^2 \phi_i(t,z)}{\partial t^2} + H_{2i} \quad , \qquad i \geq 1 \tag{3.51}$$

where $\psi_i(t,0) = f_1(t)$, $\phi_i(t,0) = f_2(t)$, and all other all corresponding conditions are zeros. H_{1i} , H_{2i} are functions to be computed from previous steps.

3.4.1 Picard order of approximations

3.4.1.1 Zero order approximation

The zero order approximation is the linear case illustrated in Appendix (A).

3.4.1.2 First order approximation

$$i \frac{\partial u_1(t,z)}{\partial z} + \alpha \frac{\partial^2 u_1(t,z)}{\partial t^2} + \varepsilon |u_0(t,z)|^2 u_0(t,z) + i\,\gamma u_1(t,z) = F_1(t,z) + i\,F_2(t,z), (t,z) \in (0,T)\ x\ (0,\infty) \tag{3.52}$$

With initial conditions $u_1(t,0) = f_1(t) + i\,f_2(t)$ and boundary conditions $u_1(0,z) = u_1(T,z) = 0$. Following Appendix (A), the linear Schrodinger equation (3.52) has the following solution:

$$u_1(t\,,z) = \psi_1 + i\,\phi_1 \tag{3.53}$$

$$\psi_1(t\,,z) = e^{-\gamma z} \sum_{n=0}^{\infty} T_{1n}(z) \sin\left(\frac{n\,\pi}{T}\right) t \tag{3.54}$$

$$\phi_1(t\,,z) = e^{-\gamma z} \sum_{n=0}^{\infty} \tau_{1n}(z) \sin\left(\frac{n\,\pi}{T}\right) t \tag{3.55}$$

$$H_{11} = -e^{\gamma z} F_1(t\,,z) + e^{-2\gamma z} \varepsilon (\psi_0{}^3 + \psi_0 \phi_0{}^2) \tag{3.56}$$

$$H_{21} = e^{\gamma z} F_2(t\,,z) - e^{-2\gamma z} \varepsilon \left(\phi_0{}^3 + \phi_0 \psi_0{}^2\right) \tag{3.57}$$

in which

$$T_{1n}(z) = A_{11}(z) \sin \beta_n z + \left(C_{12} + B_{11}(z)\right) \cos \beta_n z, \tag{2.58}$$

$$\tau_{1n}(z) = A_{12} \sin \beta_n z + \left(C_{14} + B_{12}(z)\right) \cos \beta_n z, \tag{2.59}$$

Where the constants and variables $A_{11}, C_{12}, B_{11}, A_{12}, C_{14}, B_{12}$ can be calculated in similar manner as illustrated in Appendix (A).

The absolute value of the first order approximation is:

$$|u_1(t,z)|^2 = {\psi_1}^2 + {\phi_1}^2 \tag{3.60}$$

3.4.1.3 Second order approximation

$$i\frac{\partial u_2(t,z)}{\partial z} + \alpha\frac{\partial^2 u_2(t,z)}{\partial t^2} + \varepsilon|u_1(t,z)|^2 u_1(t,z) + i\gamma u_2(t,z) = F_1(t,z) + iF_2(t,z), (t,z) \in (0,T)\,x\,(0,\infty) \tag{3.61}$$

with initial conditions $u_2(t,0) = f_1(t) + i f_2(t)$ and boundary conditions $u_2(0,z) = u_2(T,z) = 0$. Following Appendix (A), the linear Schrodinger equation (3.61) has the following solution:

$$u_2(t,z) = \psi_2 + i\phi_2 \tag{3.62}$$

By following Appendix (A), for *n=2,* we can find that:

$$\psi_2(t,z) = e^{-\gamma z}\sum_{n=0}^{\infty} T_{2n}(z)\sin\left(\frac{n\pi}{T}\right)t \tag{3.63}$$

$$\phi_2(t,z) = e^{-\gamma z}\sum_{n=0}^{\infty} \tau_{2n}(z)\sin\left(\frac{n\pi}{T}\right)t \tag{3.64}$$

$$H_{12} = -e^{\gamma z}F_1(t,z) + e^{-2\gamma z}\varepsilon({\psi_1}^3 + \psi_1{\phi_1}^2) \tag{3.65}$$

$$H_{22} = e^{\gamma z}F_2(t,z) - e^{-2\gamma z}\varepsilon\left({\phi_1}^3 + \phi_1{\psi_1}^2\right) \tag{3.66}$$

in which

$$T_{2n}(z) = A_{21}(z)\sin\beta_n z + \left(C_{22} + B_{21}(z)\right)\cos\beta_n z, \tag{2.67}$$

$$\tau_{2n}(z) = A_{22}\sin\beta_n z + \left(C_{24} + B_{22}(z)\right)\cos\beta_n z, \tag{2.68}$$

where the constants and variables $A_{21}, C_{22}, B_{21}, A_{22}, C_{24}, B_{22}$ can be calculated in similar manner as illustrated in Appendix A.

The absolute value of the second order approximation is:

$$|u_2(t\,,z)|^2 = \ {\psi_2}^2 + \ \ {\phi_2}^2 \qquad (3.69)$$

3.5 Case Studies, Picard

To examine the proposed solution algorithm, some case studies are illustrated.

3.5.1 Case study 1

Taking the case $F_1(t,z) = \rho_1 e^{-t}$, $F_2(t,z) = 0$ and $f_1(t) = 0$, $f_2(t) = 0$, ρ_1 is constant and following the algorithm of Picard Approximation, the following selected results for the first and second order approximations are got:

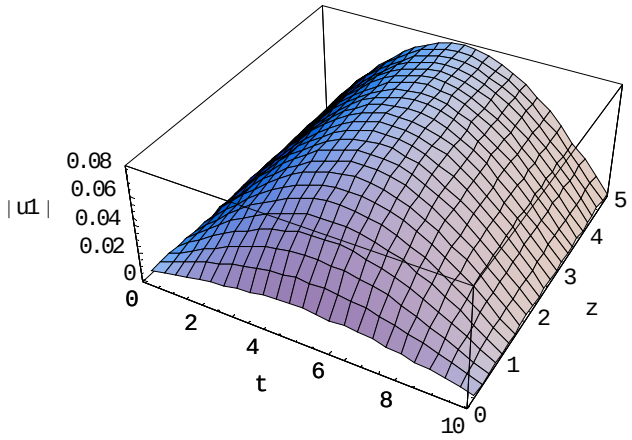

Fig. (3.72) the first order approximation of $\left|u^{(1)}\right|$ at $\varepsilon = 0.2$, $\gamma = 1$ and $\alpha, \rho_1 = 1, T = 10$ with considering only one term on the series (M=1).

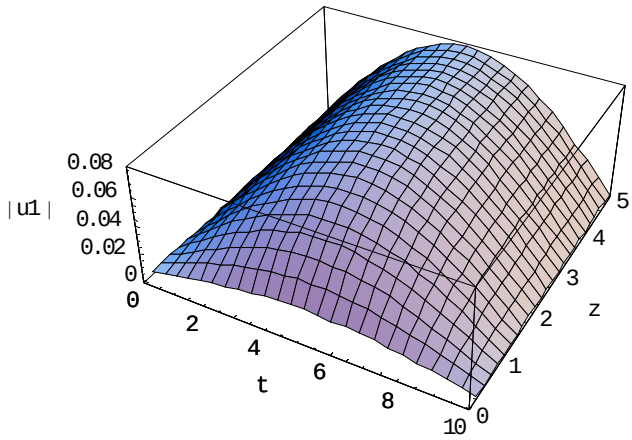

Fig. (3.73) the first order approximation of $\left|u^{(1)}\right|$ at $\varepsilon = 1$, $\gamma = 1$ and $\alpha, \rho_1 = 1, T = 10$ with considering only one term on the series (M=1).

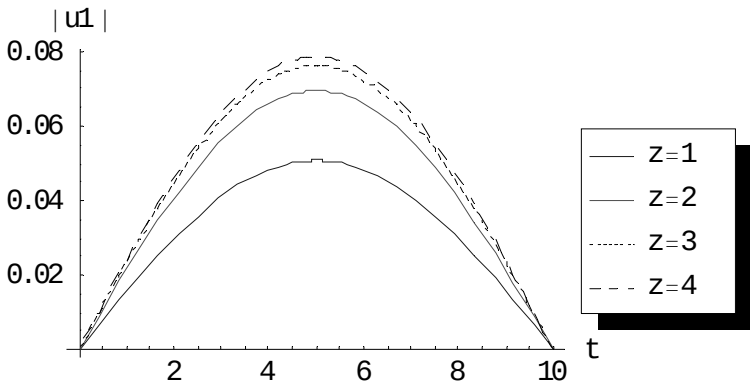

Fig. (3.74) the first order approximation of $\left|u^{(1)}\right|$ at $\varepsilon = 0.2, \gamma = 1$ and $\alpha, \rho_1 = 1, T = 10, M = 1$ for different values of z.

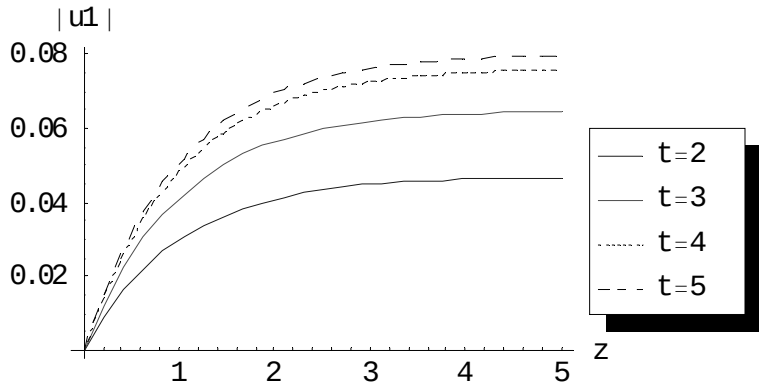

Fig. (3.75) the first order approximation of $\left|u^{(1)}\right|$ at $\varepsilon = 0.2, \gamma = 1$ and $\alpha, \rho_1 = 1, T = 10, M = 1$ for different values of t.

Note: we calculated till first order at $\gamma = 1$ and we cannot calculate more since the machine gives "MATHEMATICA KERNEL OUT OF MEMORY".

3.5.2 Case study 2

Taking the case $F_1(t,z) = \rho_1 \sin\left(\frac{m\pi}{T}\right) t$, $F_2(t,z) = 0$ and $f_1(t) = 0$, $f_2(t) = 0$, ρ_1 is constants and following the algorithm of Picard Approximation, the following selected results for the first and second order approximations are got:

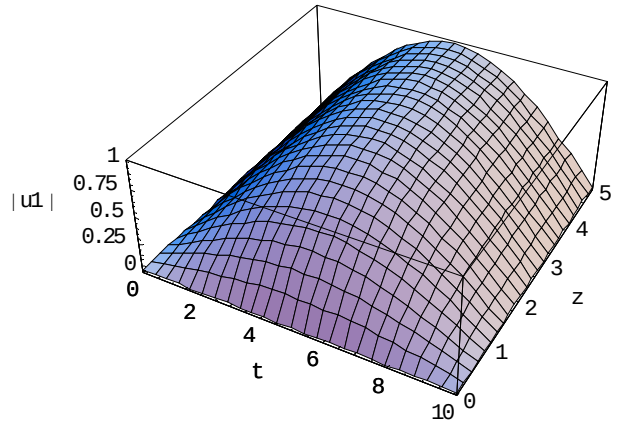

Fig. (3.76) the first order approximation of $\left|u^{(1)}\right|$ at $\varepsilon = 0.2$, $\gamma = 1$ and $\alpha, \rho_1 = 1, T = 10$ with considering only one term on the series (M=1).

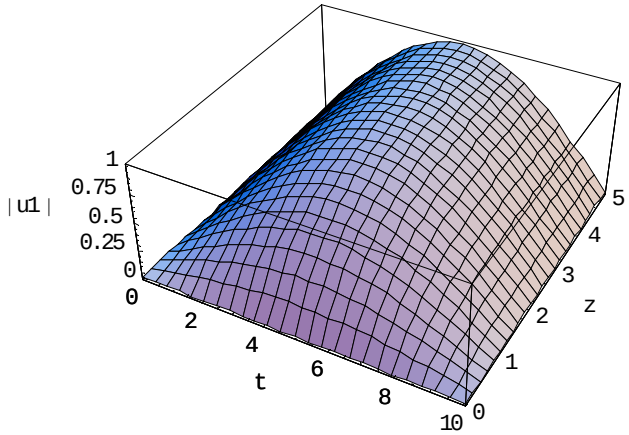

Fig. (3.77) the first order approximation of $\left|u^{(1)}\right|$ at $\varepsilon = 1$, $\gamma = 1$ and $\alpha, \rho_1 = 1, T = 10$ with considering only one term on the series (M=1).

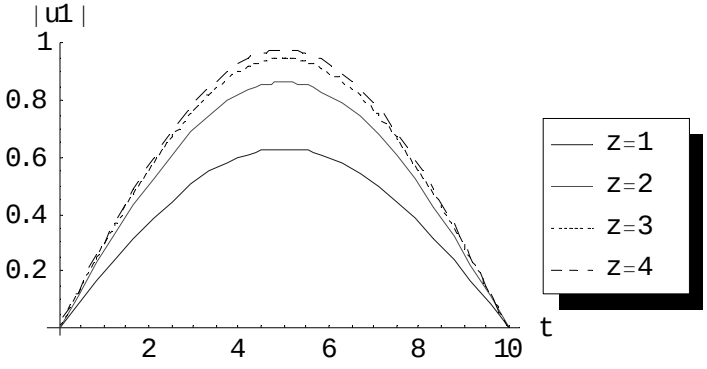

Fig. (3.78) the first order approximation of $\left|u^{(1)}\right|$ at $\varepsilon = 0.2, \gamma = 1$ and $\alpha, \rho_1 = 1, T = 10, M = 1$ for different values of z.

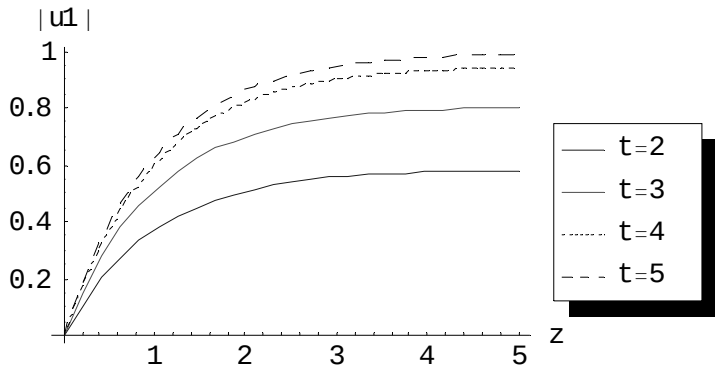

Fig. (3.79) the first order approximation of $\left|u^{(1)}\right|$ at $\varepsilon = 0.2, \gamma = 1$ and $\alpha, \rho_1 = 1, T = 10, M = 1$ for different values of t.

Note: we calculated till first order at $\gamma = 1$ and we cannot calculate more since the machine gives "MATHEMATICA KERNEL OUT OF MEMORY".

3.5.3 Case study 3

Taking the case $F_1(t,z) = \rho_1$, $F_2(t,z) = 0$ and $f_1(t) = \rho_2$, $f_2(t) = 0$ where ρ_1 & ρ_2 are constants and following the algorithm of Picard Approximation, the following selected results for the first and second order approximations are got:

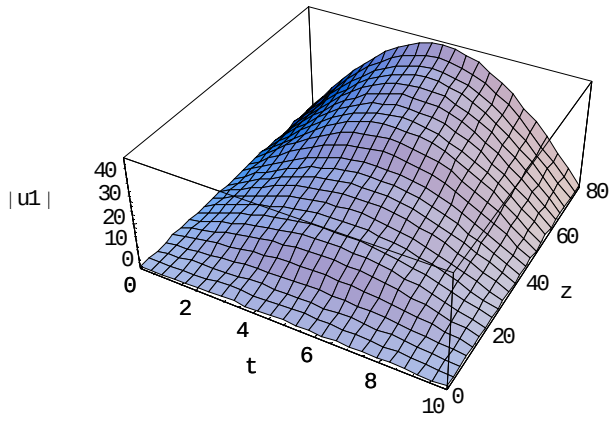

Fig. (3.80) the first order approximation of $\left|u^{(1)}\right|$ at $\varepsilon = 1$, $\gamma = 0$ and $\alpha, \rho_1, \rho_2 = 1, T = 10$ with considering only one term on the series (M=1).

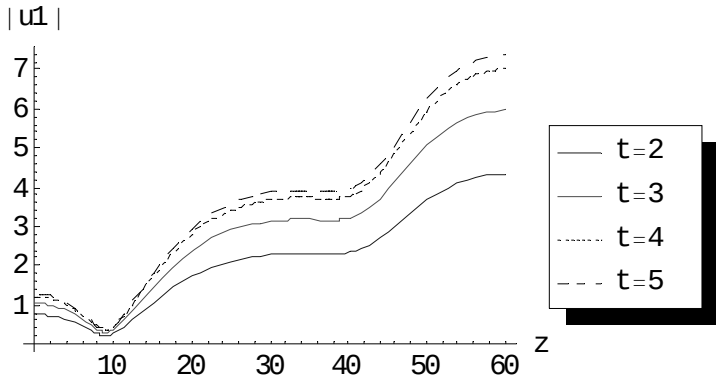

Fig. (3.81) the first order approximation of $\left|u^{(1)}\right|$ at $\varepsilon = 0.2, \gamma = 0$ and $\alpha, \rho_1, \rho_2 = 1, T = 10, M = 1$ for different values of t.

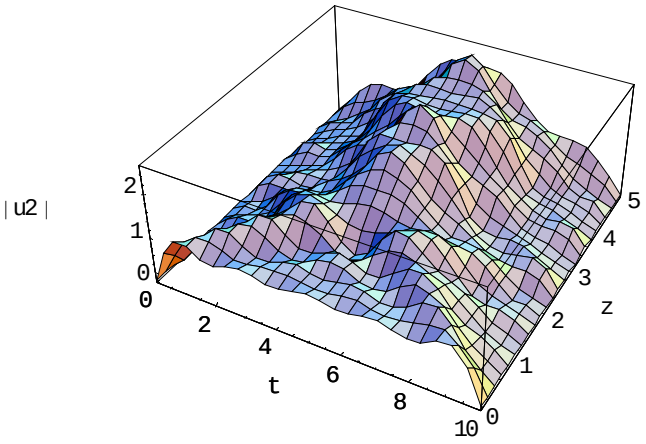

Fig. (3.82) the second order approximation of $\left|u^{(2)}\right|$ at $\varepsilon = 0.2$, $\gamma = 0$ and $\alpha, \rho_1, \rho_2 = 1, T = 10$ with considering only one term on the series (M=10).

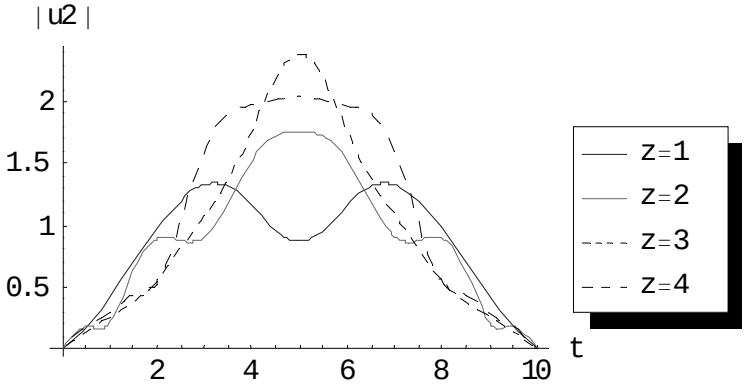

Fig. (3.83) the second order approximation of $\left|u^{(2)}\right|$ at $\varepsilon = 0.2, \gamma = 0$ and $\alpha, \rho_1, \rho_2 = 1, T = 10, M = 10$ for different values of z.

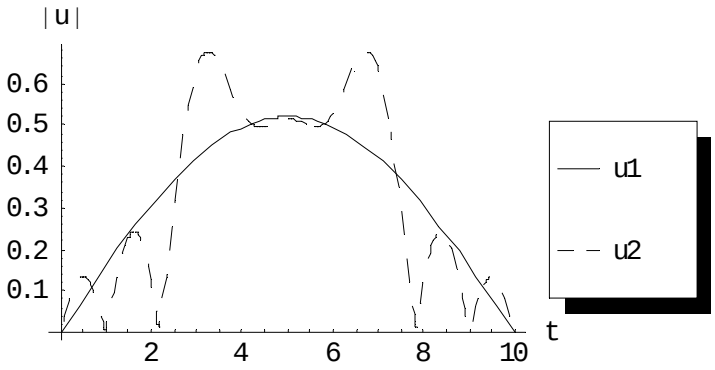

Fig. (3.84) comparison between first and second approximations at $\varepsilon = 0.002, \gamma = 0$ and $\alpha, \rho_1, \rho_2 = 1,\ T = 10,\ z = 20.$

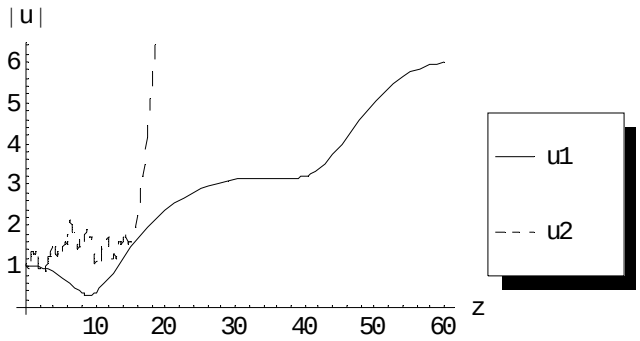

Fig. (3.85) comparison between first and second approximations at $\varepsilon = 0.2, \gamma = 0$ and $\alpha, \rho_1, \rho_2 = 1,\ T = 10,\ t = 4.$

3.5.4 Case study 4

Taking the case $F_1(t,z) = \rho_1 e^{-t},\ F_2(t,z) = 0$ and $f_1(t) = \rho_2\, e^{-t}\ ,\ f_2(t) = 0$ where ρ_1 & ρ_2 are constants and following the algorithm of Picard Approximation, the following selected results for the first and second order approximations are got:

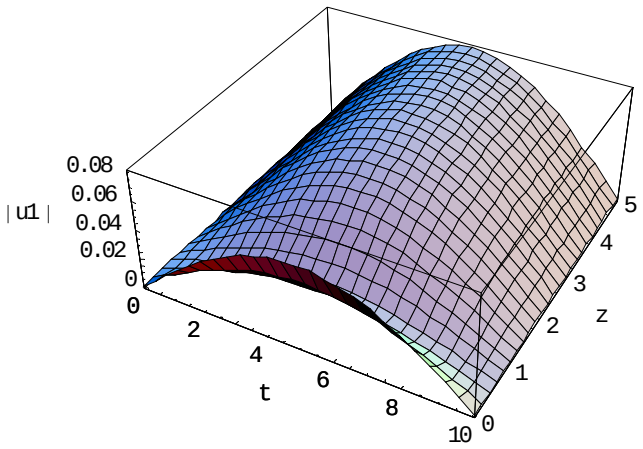

Fig. (3.86) the first order approximation of $\left|u^{(1)}\right|$ at $\varepsilon = 1,\ \gamma = 1$ and $\alpha, \rho_1, \rho_2 = 1, T = 10$ with considering only one term on the series (M=1).

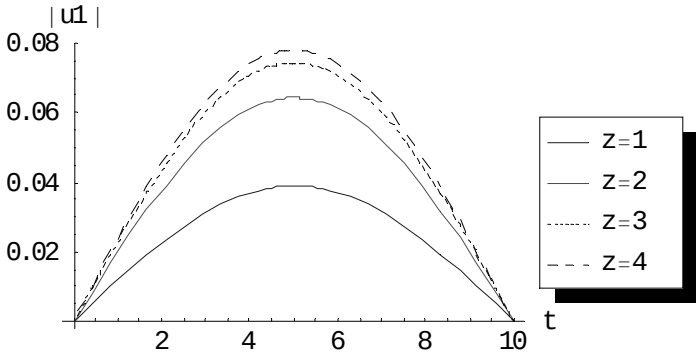

Fig. (3.87) the first order approximation of $\left|u^{(1)}\right|$ at $\varepsilon = 0.2, \gamma = 1$ and $\alpha, \rho_1, \rho_2 = 1, T = 1, M = 1$ for different values of z.

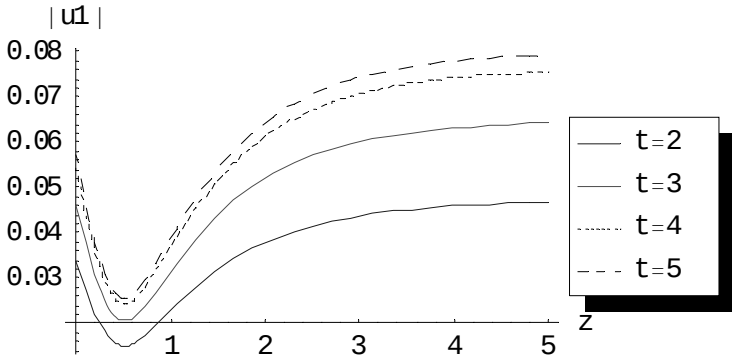

Fig. (3.88) the first order approximation of $\left|u^{(1)}\right|$ at $\varepsilon = 0.2, \gamma = 1$ and $\alpha, \rho_1, \rho_2 = 1, T = 1, M = 1$ for different values of t.

Note: we calculated till first order at $\gamma = 1$ and we cannot calculate more since the machine gives "MATHEMATICA KERNEL OUT OF MEMORY".

3.5.5 Case study 5

Taking the case $F_1(t,z) = \rho_1 \sin\left(\frac{m\pi}{T}\right) t$, $F_2(t,z) = 0$ and $f_1(t) = \rho_2 e^{-t}$, $f_2(t) = 0$ where ρ_1 & ρ_2 are constants and following the algorithm of Picard Approximation, the following selected results for the first and second order approximations are got:

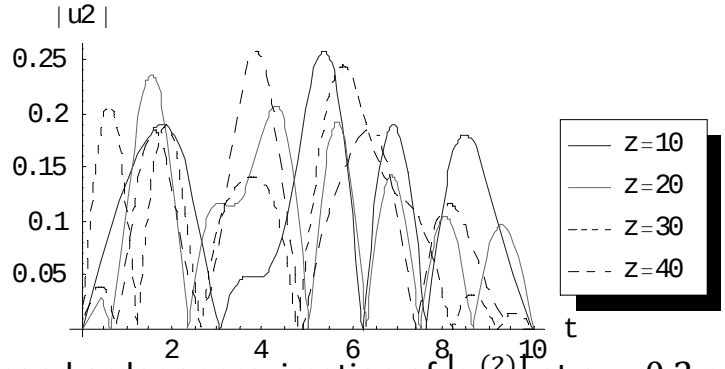

Fig. (3.89) the second order approximation of $\left|u^{(2)}\right|$ at $\varepsilon = 0.2, \gamma = 0$ and $\alpha, \rho_1, \rho_2 = 1, T = 1, M = 10$ for different values of t.

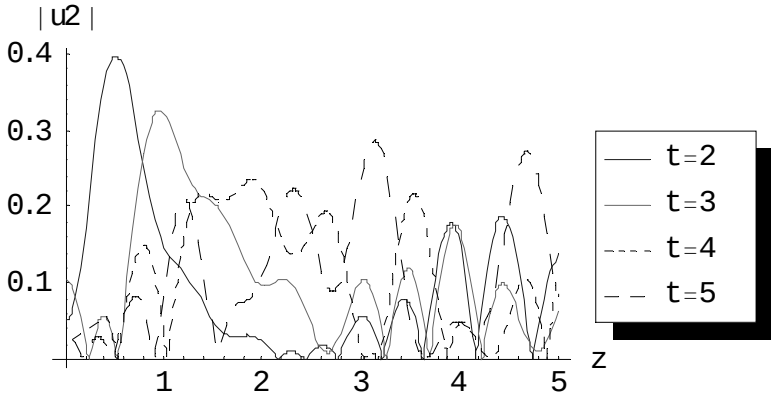

Fig. (3.90) the second order approximation of $\left|u^{(2)}\right|$ at $\varepsilon = 0.2, \gamma = 0$ and $\alpha, \rho_1, \rho_2 = 1, T = 1, M = 10$ for different values of t.

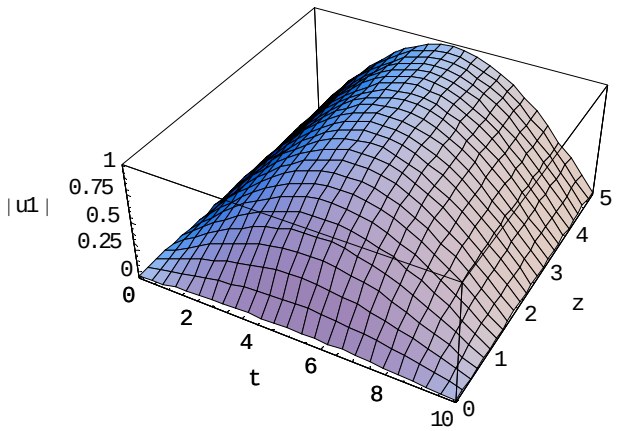

Fig. (3.91) the first order approximation of $\left|u^{(1)}\right|$ at $\varepsilon = 1$, $\gamma = 1$ and $\alpha, \rho_1, \rho_2 = 1, T = 10$ with considering only one term on the series (M=1).

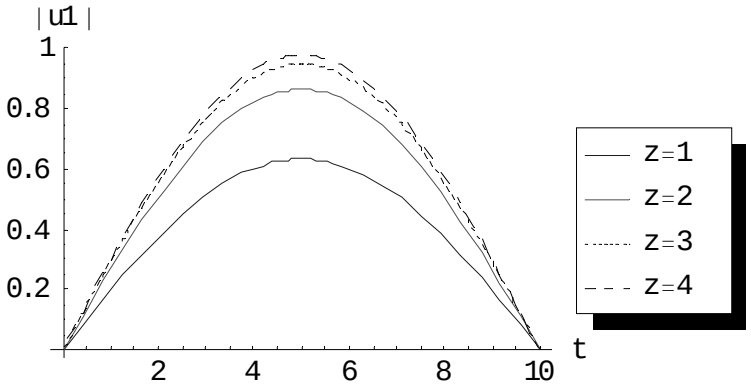

Fig. (3.92) the first order approximation of $\left|u^{(1)}\right|$ at $\varepsilon = 0.2, \gamma = 1$ and $\alpha, \rho_1, \rho_2 = 1, T = 1, M = 1$ for different values of z.

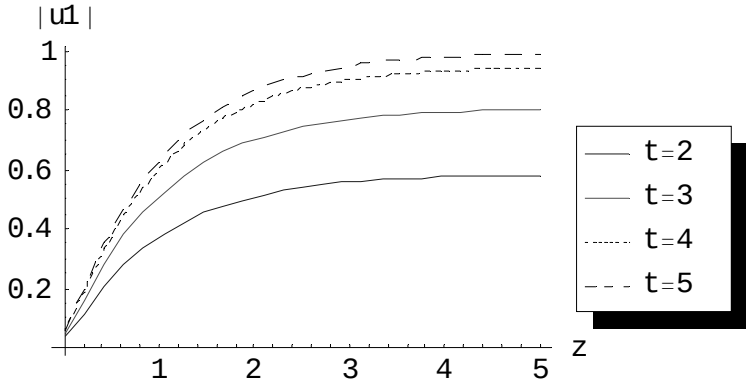

Fig. (3.93) the first order approximation of $\left|u^{(1)}\right|$ at $\varepsilon = 0.2, \gamma = 1$ and $\alpha, \rho_1, \rho_2 = 1, T = 1, M = 1$ for different values of t.

3.5.6 Case study 6

Taking the case $F_1(t,z) = \rho_1, F_2(t,z) = 0$ and $f_1(t) = \rho_2 \sin\left(\frac{m\pi}{T}\right) t$, $f_2(t) = 0$ where ρ_1 & ρ_2 are constants and following the algorithm of Picard Approximation, the following selected results for the first and second order approximations are got:

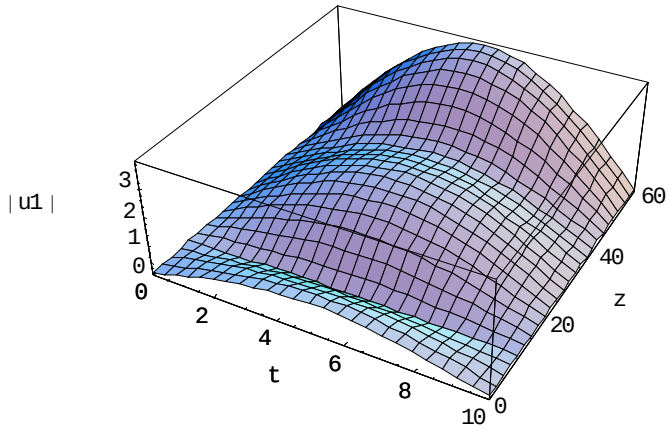

Fig. (3.94) the first order approximation of $\left|u^{(1)}\right|$ at $\varepsilon = 0.2,\ \gamma = 0$ and $\alpha, \rho_1, \rho_2 = 1, T = 10$ with considering only one term on the series (M=1).

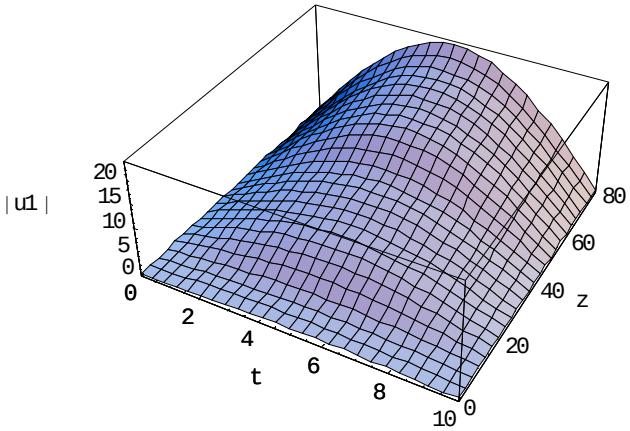

Fig.(3.95) the first order approximation of $\left|u^{(1)}\right|$ at $\varepsilon = 1,\ \gamma = 0$ and $\alpha, \rho_1, \rho_2 = 1, T = 10$ with considering only one term on the series (M=1).

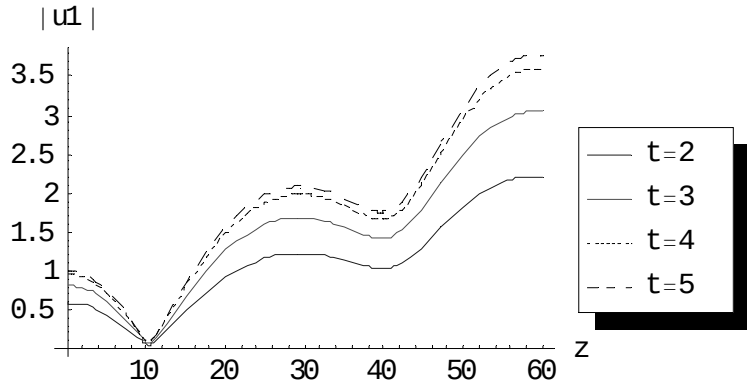

Fig.(3.96) the first order approximation of $\left|u^{(1)}\right|$ at $\varepsilon = 0.2, \gamma = 0$ and $\alpha, \rho_1, \rho_2 = 1, T = 1, M = 1$ for different values of t.

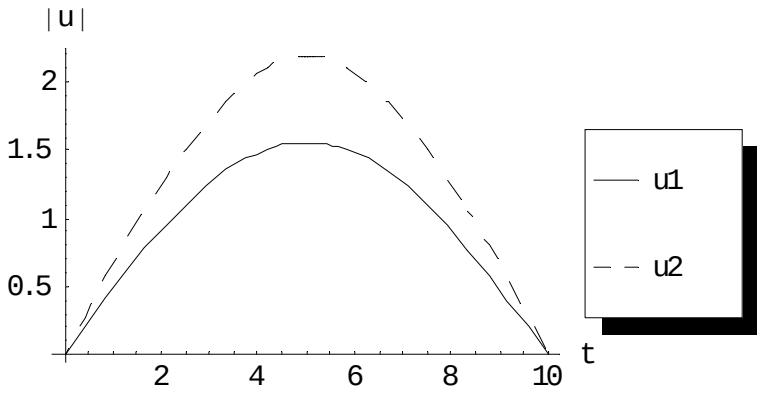

Fig.(3.97) comparison between first and second approximations at $\varepsilon = 0.2, \gamma = 0$ and $\alpha, \rho_1, \rho_2 = 1,\ T = 10,\ z = 20.$

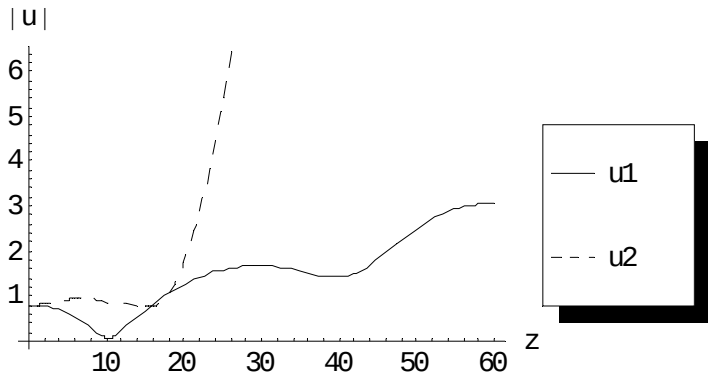

Fig.(3.98) comparison between first and second approximations at $\varepsilon = 0.2, \gamma = 0$ and $\alpha, \rho_1, \rho_2 = 1,\ T = 10,\ t = 4.$

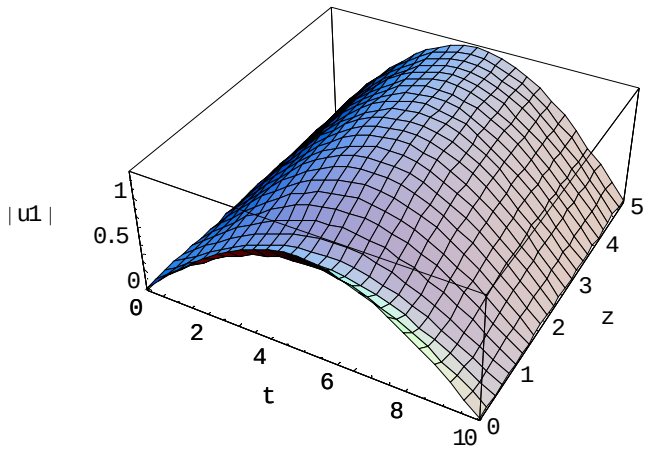

Fig.(3.99) the first order approximation of $\left|u^{(1)}\right|$ at $\varepsilon = 1,\ \gamma = 1$ and $\alpha, \rho_1, \rho_2 = 1, T = 10$ with considering only one term on the series (M=1).

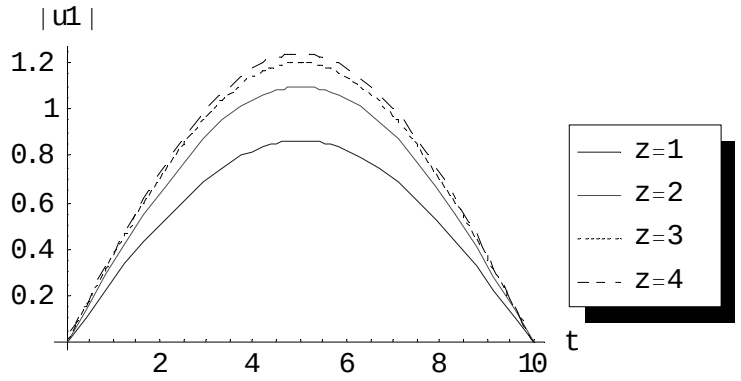

Fig. (3.100) the first order approximation of $\left|u^{(1)}\right|$ at $\varepsilon = 0.2, \gamma = 1$ and $\alpha, \rho_1, \rho_2 = 1, T = 1, M = 1$ for different values of z.

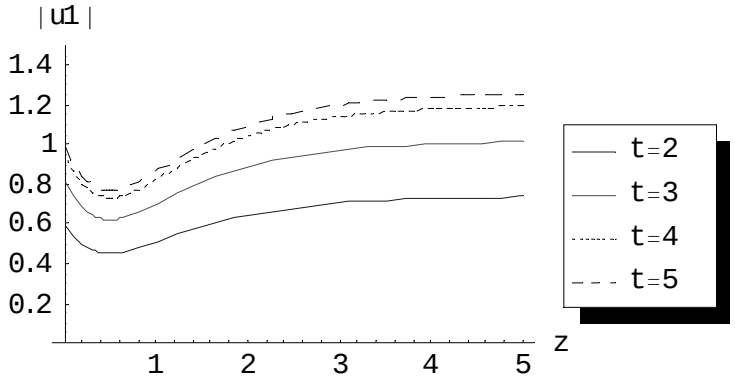

Fig.(3.101) the first order approximation of $\left|u^{(1)}\right|$ at $\varepsilon = 0.2, \gamma = 1$ and $\alpha, \rho_1, \rho_2 = 1, T = 1, M = 1$ for different values of t.

3.5.7 Case study 7

Taking the case $F_1(t,z) = \rho_1 e^{-t}$, $F_2(t,z) = 0$ and $f_1(t) = \rho_2 \sin\left(\frac{m\pi}{T}\right)t$, $f_2(t) = 0$ where ρ_1 & ρ_2 are constants and following the algorithm of Picard Approximation, the following selected results for the first and second order approximations are got:

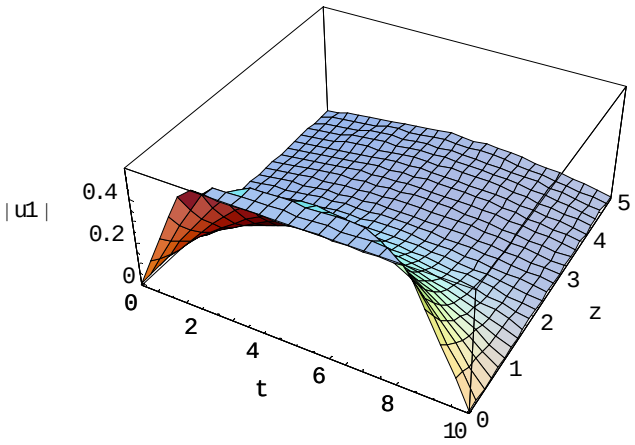

Fig.(3.102) the first order approximation of $\left|u^{(1)}\right|$ at $\varepsilon = 0.2,\ \gamma = 1$ and $\alpha, \rho_1, \rho_2 = 1, T = 10$ with considering only one term on the series (M=1).

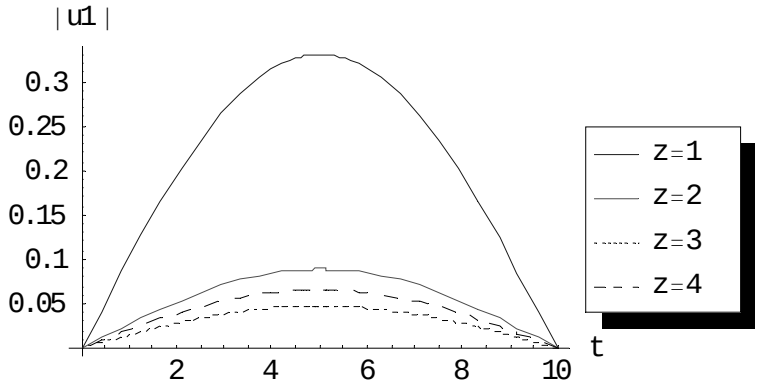

Fig.(3.103) the first order approximation of $\left|u^{(1)}\right|$ at $\varepsilon = 0.2, \gamma = 1$ and $\alpha, \rho_1, \rho_2 = 1, T = 1, M = 1$ for different values of z.

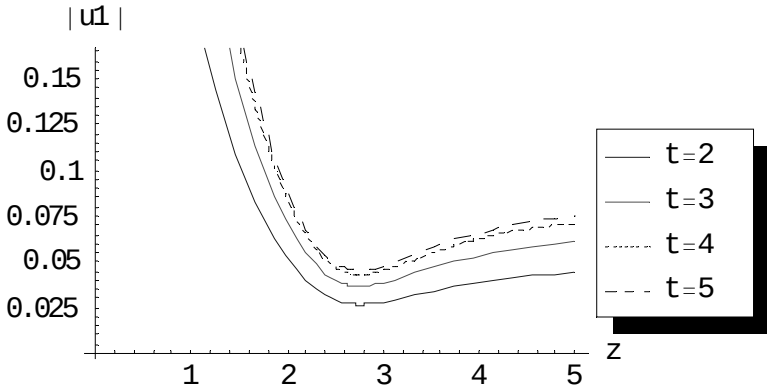

Fig.(3.104) the first order approximation of $\left|u^{(1)}\right|$ at $\varepsilon = 0.2, \gamma = 1$ and $\alpha, \rho_1, \rho_2 = 1, T = 1, M = 1$ for different values of t.

3.6 Comparison between Perturbation & Picard Approximation

We are here giving both perturbation method and Picard approximation results in the same graph for some selected cases to compare between the two methods.

3.6.1 Case study 1

Taking the case $F_1(t,z) = \rho_1,\ F_2(t,z) = 0$ and $f_1(t) = \rho_2, f_2(t) = 0$, the following results are obtained.

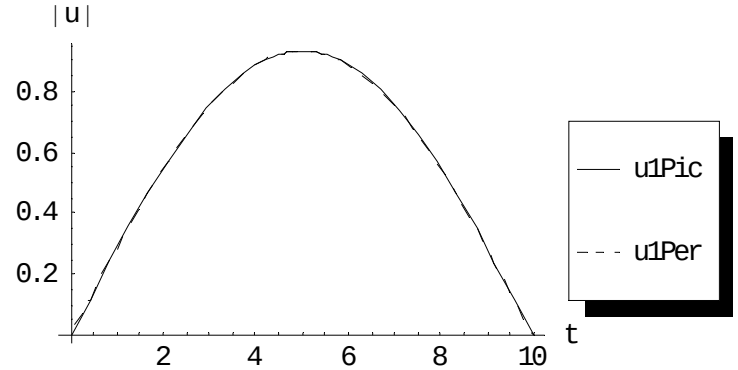

Fig.(3.105) comparison between Picard approximation and Perturbation method for first order at $\varepsilon = 0.2, \gamma = 0$ and $\alpha, \rho_1, \rho_2 = 1, T = 10, z = 5$.

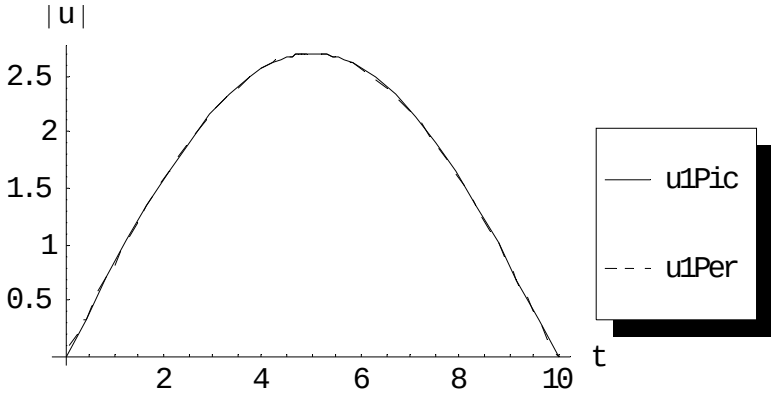

Fig. (3.106) comparison between Picard approximation and Perturbation method for first order at $\varepsilon = 1, \gamma = 0$ and $\alpha, \rho_1, \rho_2 = 1, T = 10, z = 5$.

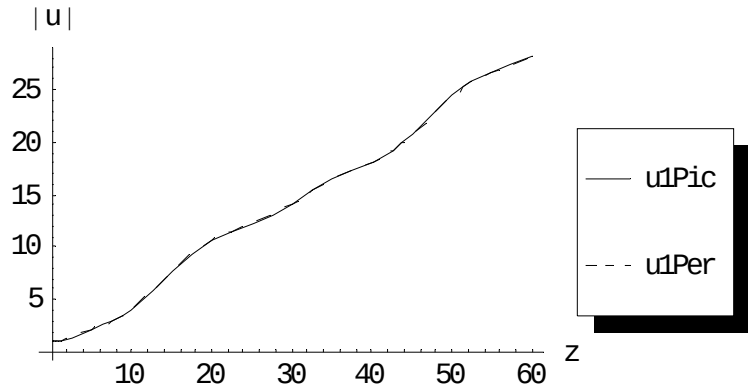

Fig. (3.107) comparison between Picard approximation and Perturbation method for first order at $\varepsilon = 1, \gamma = 0$ and $\alpha, \rho_1, \rho_2 = 1, T = 10, t = 3$.

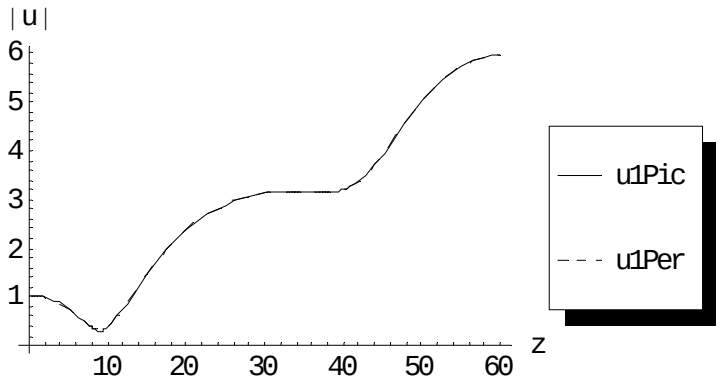

Fig. (3.108) comparison between Picard approximation and Perturbation method for first order at $\varepsilon = 0.2, \gamma = 0$ and $\alpha, \rho_1, \rho_2 = 1, T = 10, t = 3$.

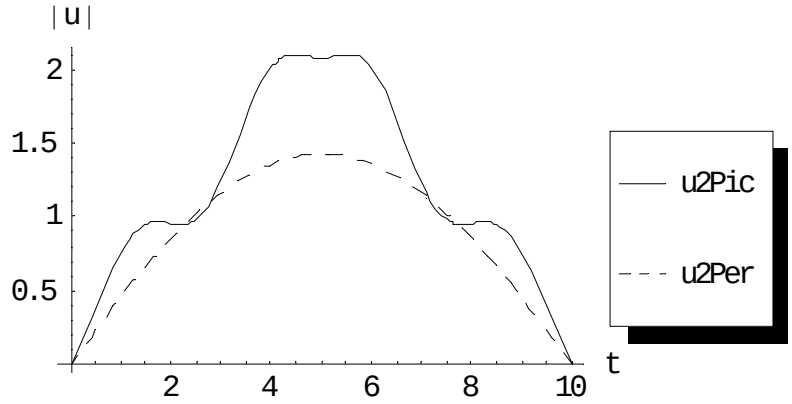

Fig. (3.109) comparison between Picard approximation and Perturbation method for second order at $\varepsilon = 0.2, \gamma = 0$ and $\alpha, \rho_1, \rho_2 = 1, T = 10, z = 5$.

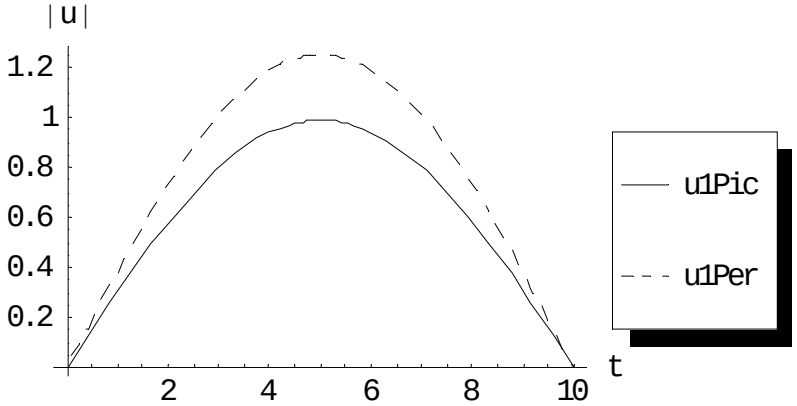

Fig. (3.110) comparison between Picard approximation and Perturbation method for first order at $\varepsilon = 0.2, \gamma = 1$ and $\alpha, \rho_1, \rho_2 = 1, T = 10, z = 5$.

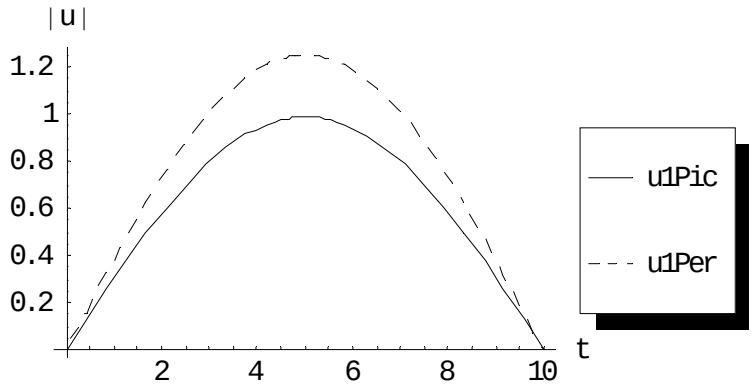

Fig. (3.111) comparison between Picard approximation and Perturbation method for first order at $\varepsilon = 1, \gamma = 1$ and $\alpha, \rho_1, \rho_2 = 1, T = 10, z = 5$.

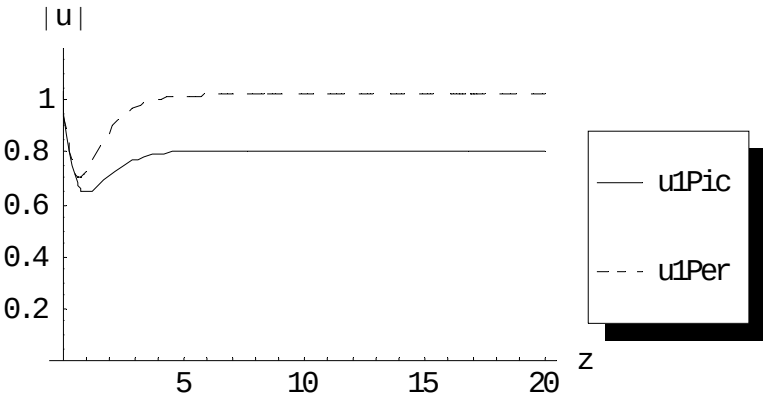

Fig. (3.112) comparison between Picard approximation and Perturbation method for first order at $\varepsilon = 0.2, \gamma = 1$ and $\alpha, \rho_1, \rho_2 = 1, T = 10, t = 3$.

3.6.2 Case study 2

Taking the case $F_1(t,z) = \rho_1 e^{-t}$, $F_2(t,z) = 0$ and $f_1(t) = \rho_2, f_2(t) = 0$, the following results are obtained.

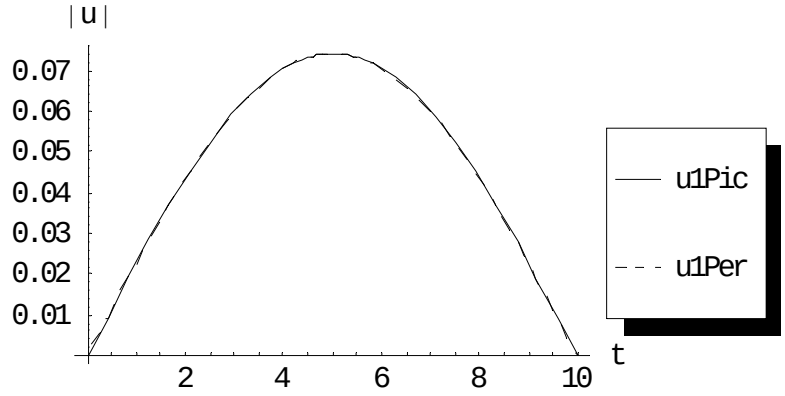

Fig. (3.113) comparison between Picard approximation and Perturbation method for first order at $\varepsilon = 0.2, \gamma = 1$ and $\alpha, \rho_1, \rho_2 = 1, T = 10, z = 5$.

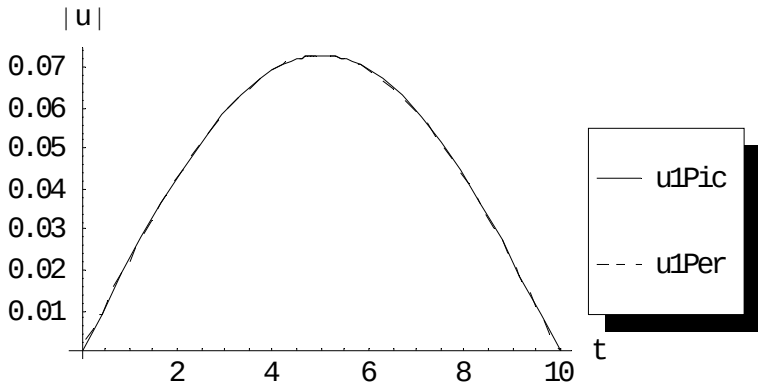

Fig. (3.114) comparison between Picard approximation and Perturbation method for first order at $\varepsilon = 1, \gamma = 1$ and $\alpha, \rho_1, \rho_2 = 1, T = 10, z = 5$.

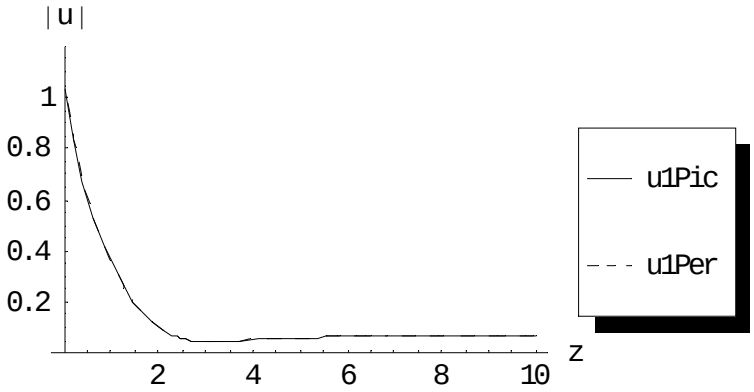

Fig. (3.115) comparison between Picard approximation and Perturbation method for first order at $\varepsilon = 0.2, \gamma = 1$ and $\alpha, \rho_1, \rho_2 = 1, T = 10, t = 3$.

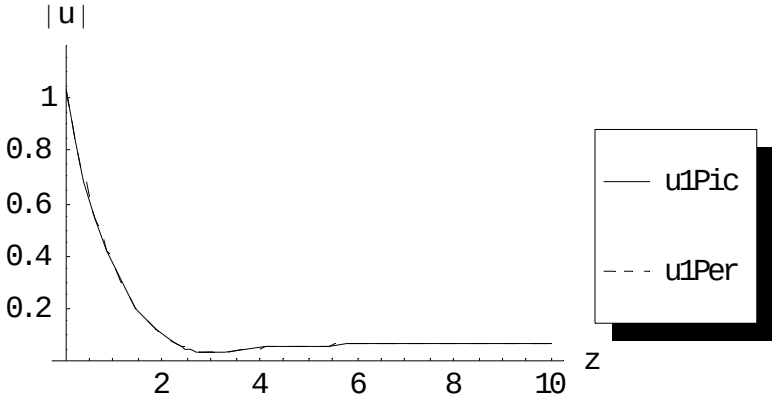

Fig. (3.116) comparison between Picard approximation and Perturbation method for first order at $\varepsilon = 1, \gamma = 1$ and $\alpha, \rho_1, \rho_2 = 1, T = 10, t = 3$.

3.6.3 Case study 3

Taking the case $F_1(t,z) = \rho_1 \sin\left(\frac{m\pi}{T}\right) t$, $F_2(t,z) = 0$ and $f_1(t) = \rho_2, f_2(t) = 0$, the following results are obtained.

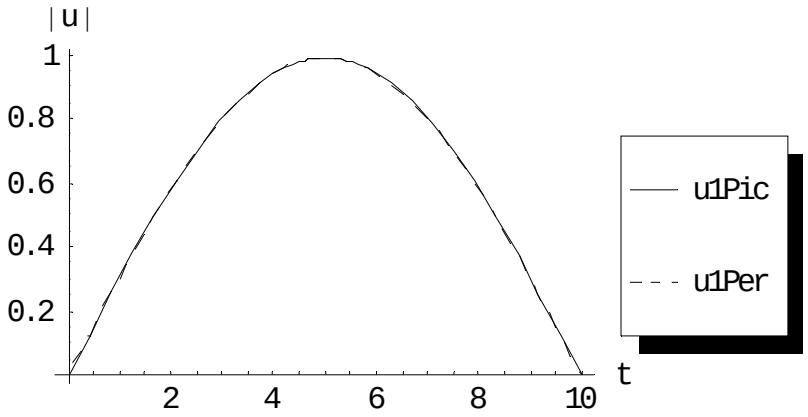

Fig .(3.117) comparison between Picard approximation and Perturbation method for first order at $\varepsilon = 0.2, \gamma = 1$ and $\alpha, \rho_1, \rho_2 = 1, T = 10,\ z = 5.$

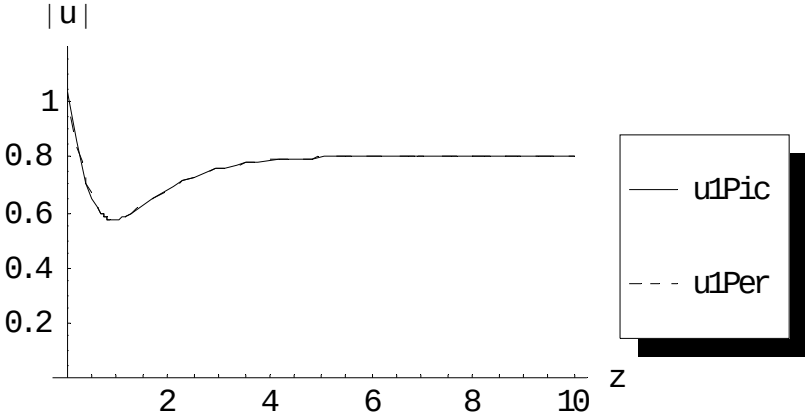

Fig. (3.118) comparison between Picard approximation and Perturbation method for first order at $\varepsilon = 1, \gamma = 1$ and $\alpha, \rho_1, \rho_2 = 1, T = 10,\ t = 3.$

3.6.4 Case study 4

Taking the case $F_1(t,z) = \rho_1 e^{-t},\ F_2(t,z) = 0$ and $f_1(t) = \rho_2 e^{-t}, f_2(t) = 0$, the following results are obtained.

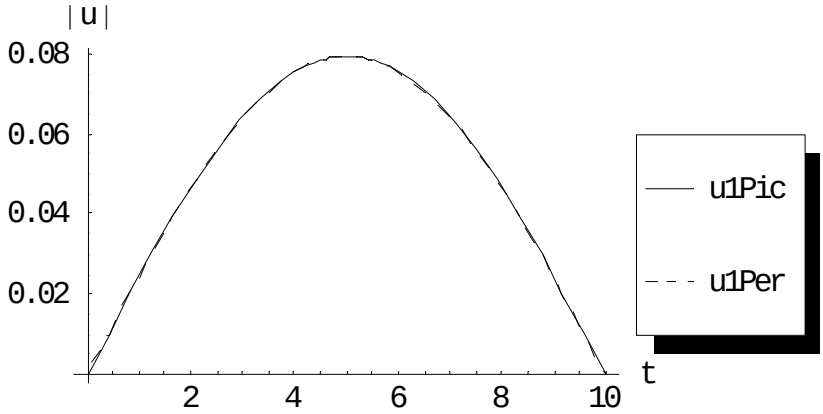

Fig. (3.119) comparison between Picard approximation and Perturbation method for first order at $\varepsilon = 0.2, \gamma = 1$ and $\alpha, \rho_1, \rho_2 = 1, T = 10,\ z = 5.$

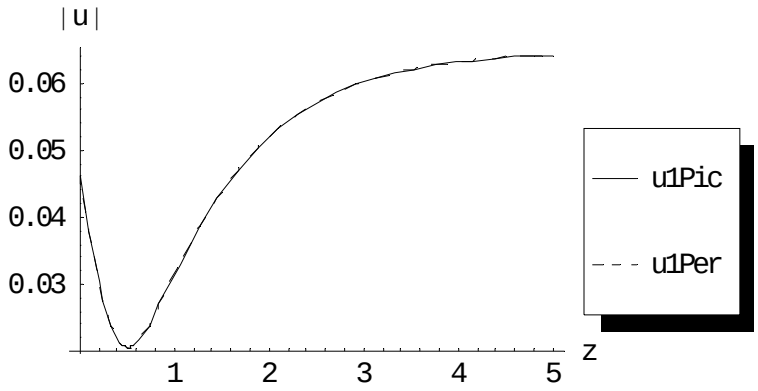

Fig. (3.120) comparison between Picard approximation and Perturbation method for first order at $\varepsilon = 0.2, \gamma = 1$ and $\alpha, \rho_1, \rho_2 = 1, T = 10,\ t = 3.$

3.6.5 Case study 5

Taking the case $F_1(t,z) = \rho_1 \sin\left(\frac{m\,\pi}{T}\right) t,\ F_2(t,z) = 0$ and $f_1(t) = \rho_2 e^{-t}, f_2(t) = 0$, the following results are obtained.

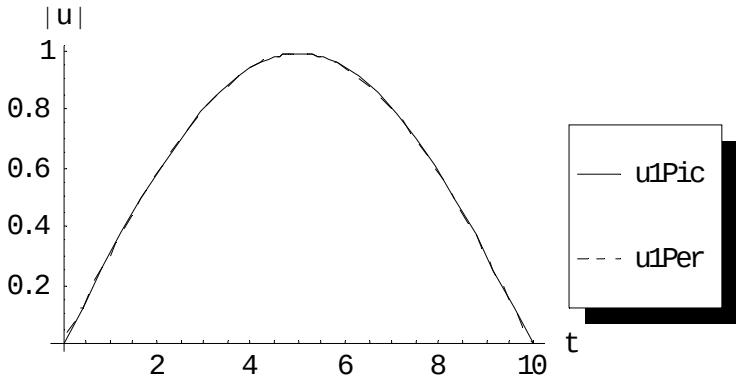

Fig. (3.121) comparison between Picard approximation and Perturbation method for first order at $\varepsilon = 0.2, \gamma = 1$ and $\alpha, \rho_1, \rho_2 = 1, T = 10,\ z = 5.$

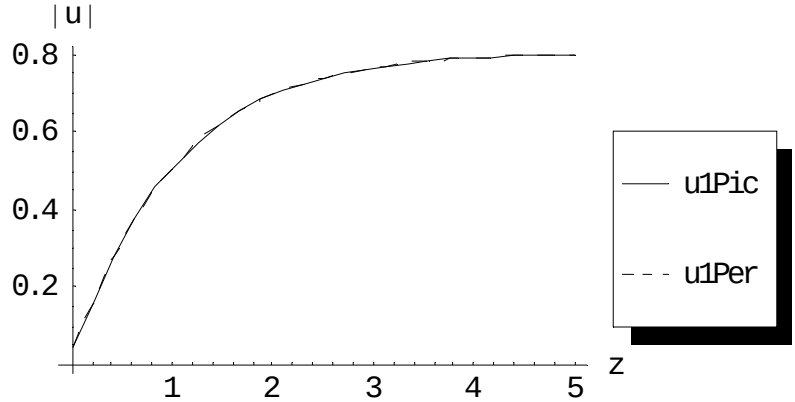

Fig. (3.122) comparison between Picard approximation and Perturbation method for first order at $\varepsilon = 1, \gamma = 1$ and $\alpha, \rho_1, \rho_2 = 1, T = 10,\ t = 3.$

3.6.6 Case study 6

Taking the case $F_1(t,z) = \rho_1 e^{-t}$, $F_2(t,z) = 0$ and $f_1(t) = \rho_2 \sin\left(\frac{m\pi}{T}\right) t, f_2(t) = 0$, the following results are obtained.

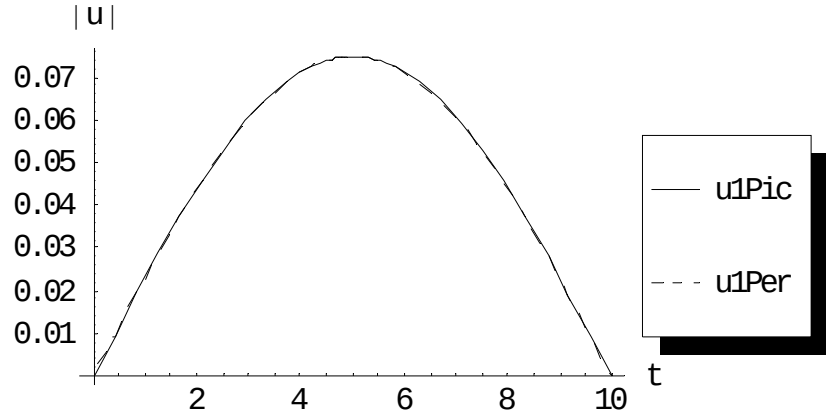

Fig. (3.123) comparison between Picard approximation and Perturbation method for first order at $\varepsilon = 1, \gamma = 1$ and $\alpha, \rho_1, \rho_2 = 1, T = 10,\ z = 5$.

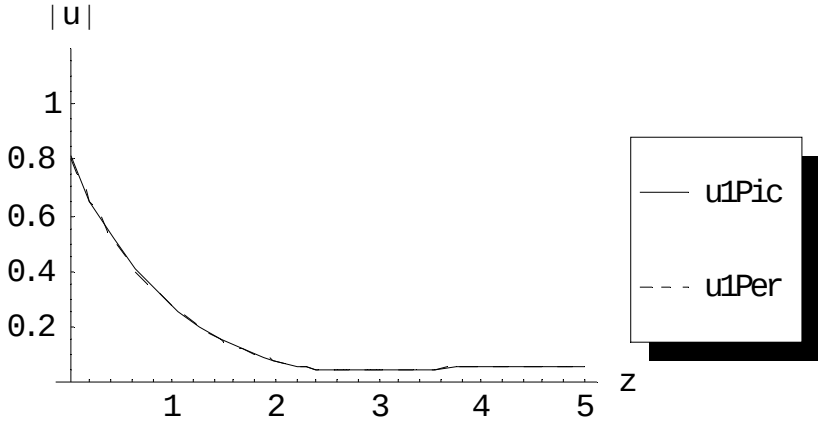

Fig. (3.124) comparison between Picard approximation and Perturbation method for first order at $\varepsilon = 0.2, \gamma = 1$ and $\alpha, \rho_1, \rho_2 = 1, T = 10,\ t = 3$.

3.6.7 Case study 7

Taking the case $F_1(t,z) = \rho_1 \sin\left(\frac{m\pi}{T}\right)$, $F_2(t,z) = 0$ and $f_1(t) = \rho_2 \sin\left(\frac{m\pi}{T}\right) t$, $f_2(t) = 0$, the following results are obtained.

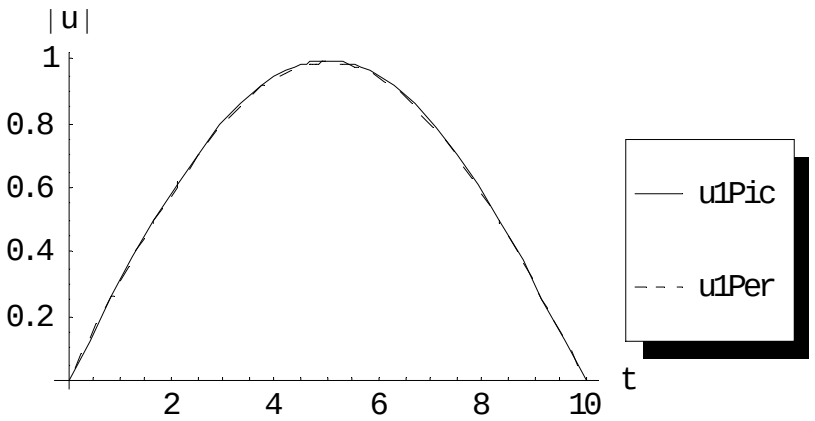

Fig. (3.125) comparison between Picard approximation and Perturbation method for first order at $\varepsilon = 0.2, \gamma = 1$ and $\alpha, \rho_1, \rho_2 = 1, T = 10,\ z = 5.$

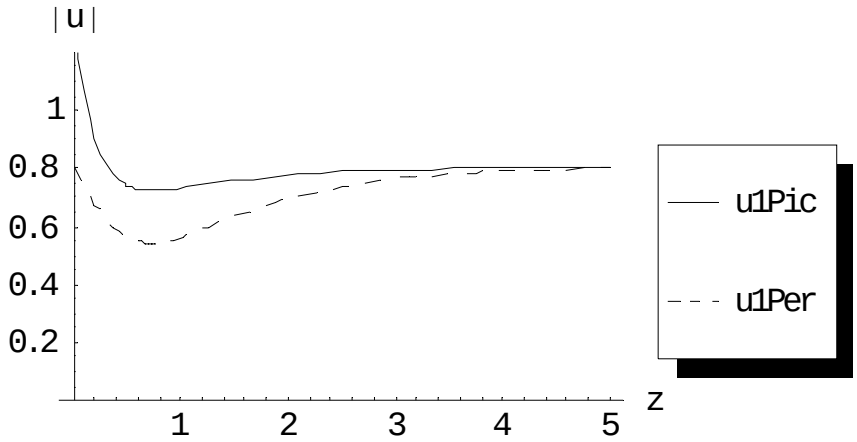

Fig. (3.126) comparison between Picard approximation and Perturbation method for first order at $\varepsilon = 1, \gamma = 1$ and $\alpha, \rho_1, \rho_2 = 1, T = 10,\ t = 3.$

3.7 T – Study

We are here examining the behavior of Perturbation method and Picard Approximation against different values of T through case studies on the same graph.

3.7.1 Case Studies, Perturbation

3.7.1.1 Case study 1

Taking the case $F_1(t,z) = \rho_1, F_2(t,z) = 0,\ f_1(t) = \rho_2, f_2(t) = 0$ and following the algorithm, the following selected results for the first and second order approximations are got:

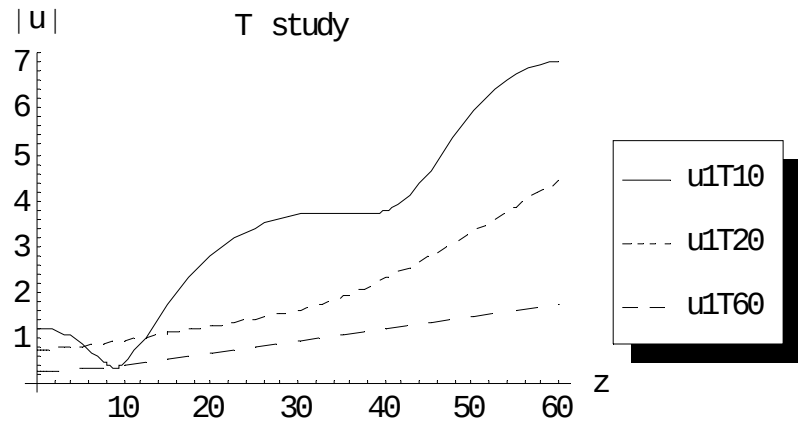

Fig.(3.127) the first order approximation of $\left|u^{(1)}\right|$ at $\varepsilon = 0.2$, $\gamma = 0$ and $\alpha, \rho_1, \rho_2 = 1, M = 10, t = 4$ for different values of T =10, 20 and 60 respectively.

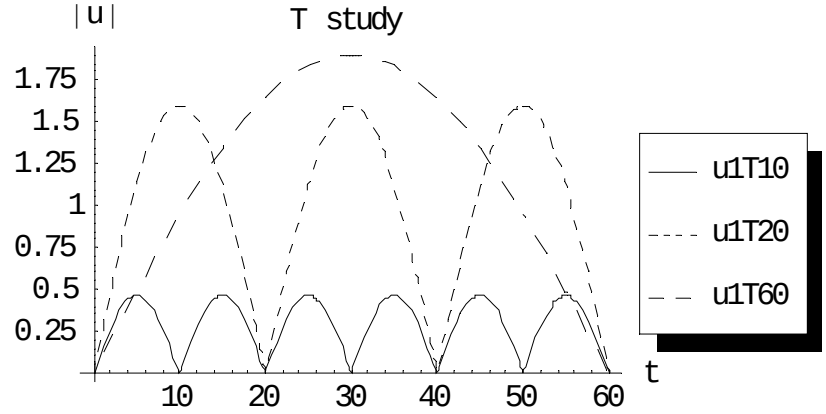

Fig. (3.128) the first order approximation of $\left|u^{(1)}\right|$ at $\varepsilon = 0.2$, $\gamma = 0$ and $\alpha, \rho_1, \rho_2 = 1, M = 10, z = 10$ for different values of T =10, 20and 60 respectively.

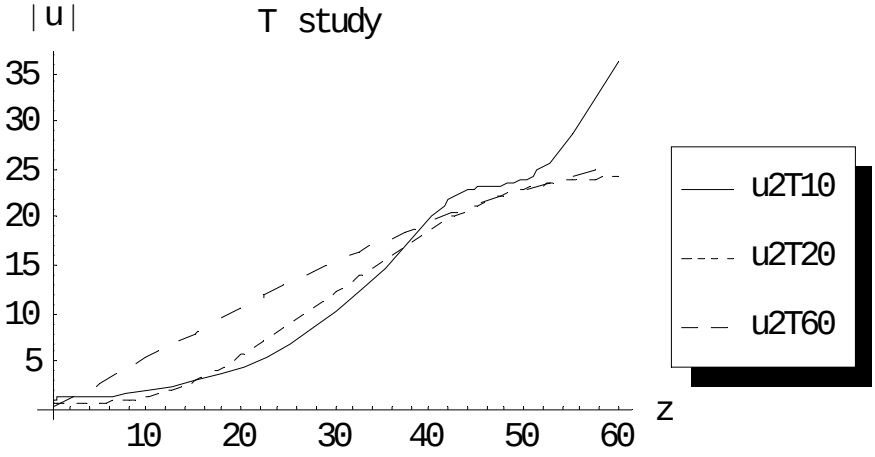

Fig. (3.129) the second order approximation of $\left|u^{(2)}\right|$ at $\varepsilon = 0.2$, $\gamma = 0$ and $\alpha, \rho_1, \rho_2 = 1, M = 10, t = 4$ for different values of T =10, 20 and 60 respectively.

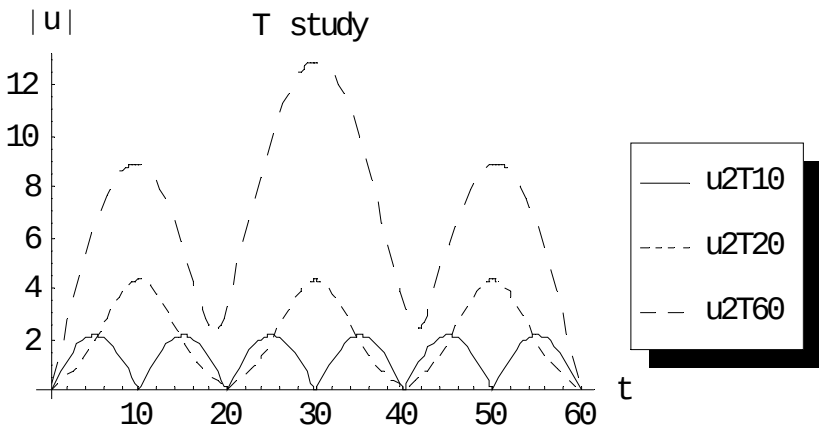

Fig.(3.130) the second order approximation of $\left|u^{(2)}\right|$ at $\varepsilon = 0.2$, $\gamma = 0$ and $\alpha, \rho_1, \rho_2 = 1, M = 10, z = 10$ for different values of T =10,20 and 60 respectively.

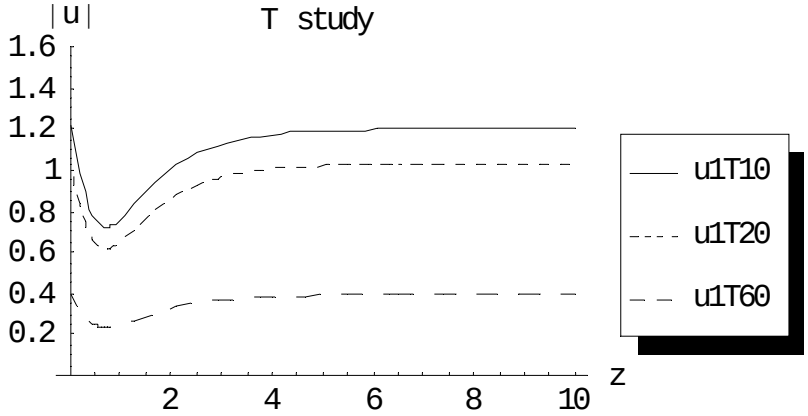

Fig. (3.131) the first order approximation of $\left|u^{(1)}\right|$ at $\varepsilon = 1$, $\gamma = 1$ and $\alpha, \rho_1, \rho_2 = 1, M = 10, t = 6$ for different values of T =10, 20 and 60 respectively.

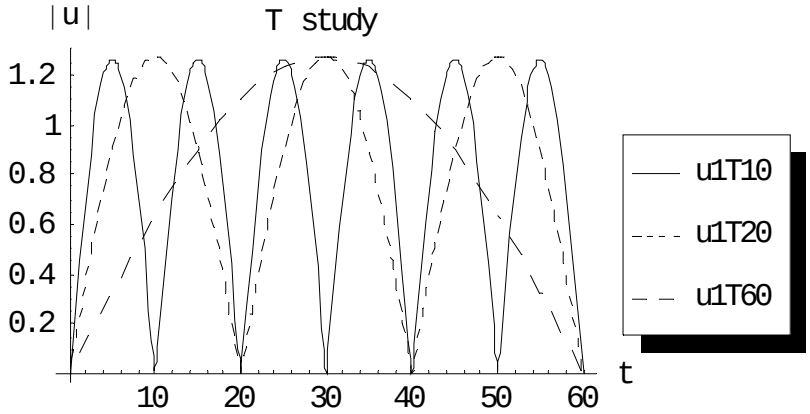

Fig.(3.132) the first order approximation of $\left|u^{(1)}\right|$ at $\varepsilon = 0.2$, $\gamma = 1$ and $\alpha, \rho_1, \rho_2 = 1, M = 10, z = 10$ for different values of T =10,20 and 60 respectively.

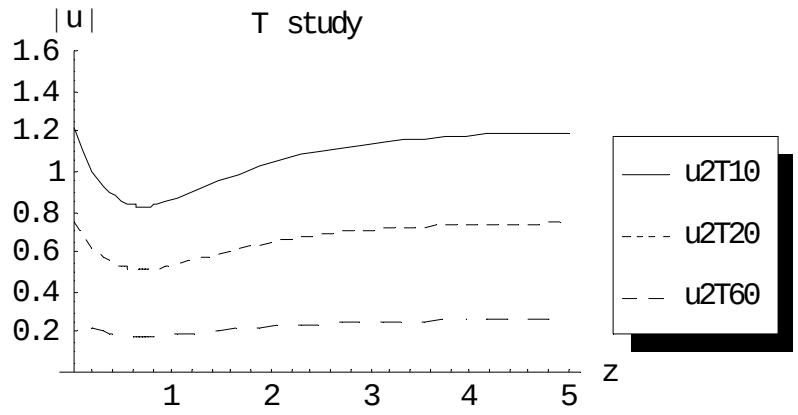

Fig. (3.133) the second order approximation of $\left|u^{(2)}\right|$ at $\varepsilon = 0.2$, $\gamma = 1$ and $\alpha, \rho_1, \rho_2 = 1, M = 10, t = 4$ for different values of T =10, 20 and 60 respectively.

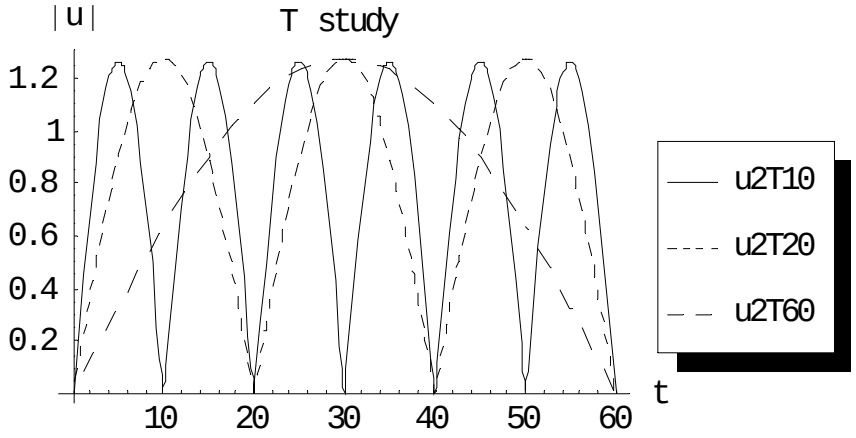

Fig. (3.134) the second order approximation of $\left|u^{(2)}\right|$ at $\varepsilon = 1$, $\gamma = 1$ and $\alpha, \rho_1, \rho_2 = 1, M = 10, z = 10$ for different values of T =10, 20 and 60 respectively.

3.7.1.2 Case study 2

Taking the case $F_1(t,z) = Sin\left(\frac{m\,\pi}{T}t\right), F_2(t,z) = 0$, $f_1(t) = \rho_2, f_2(t) = 0$ and following the algorithm, the following selected results for the first and second order approximations are got:

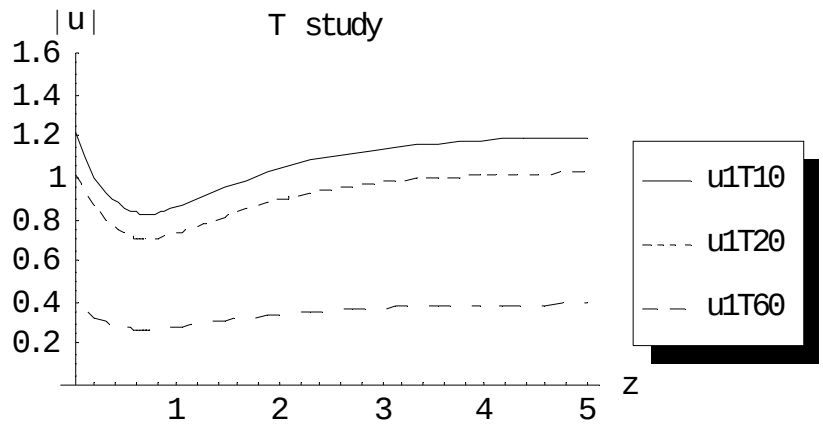

Fig. (3.135) the first order approximation of $\left|u^{(1)}\right|$ at $\varepsilon = 0.2$, $\gamma = 1$ and $\alpha, \rho_1, \rho_2 = 1, M = 10, t = 6$ for different values of T =10, 20 and 60 respectively.

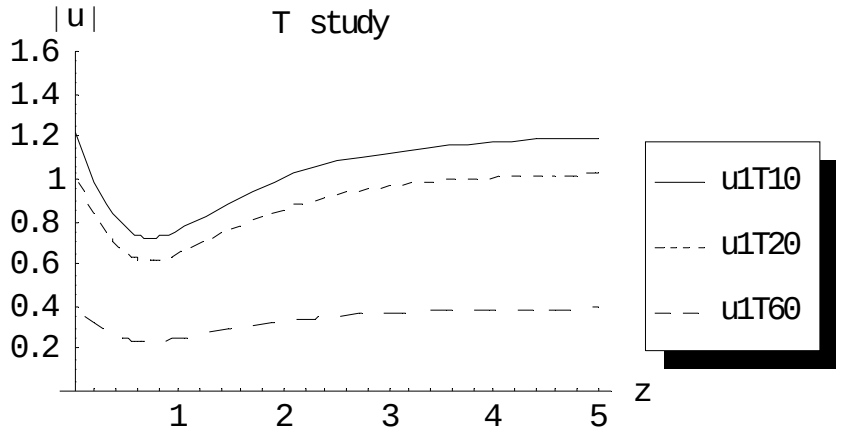

Fig. (3.136) the first order approximation of $\left|u^{(1)}\right|$ at $\varepsilon = 1$, $\gamma = 1$ and $\alpha, \rho_1, \rho_2 = 1, M = 10, t = 6$ for different values of T =10, 20 and 60 respectively.

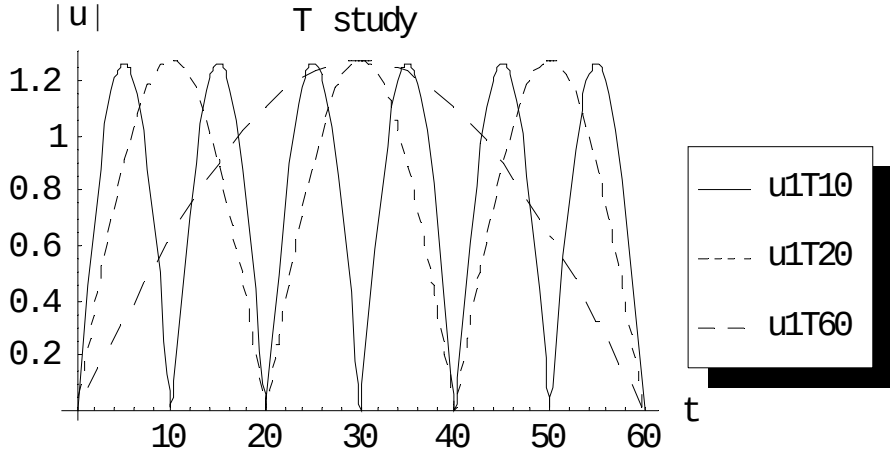

Fig. (3.137) the first order approximation of $\left|u^{(1)}\right|$ at $\varepsilon = 0.2$, $\gamma = 1$ and $\alpha, \rho_1, \rho_2 = 1, M = 10, z = 10$ for different values of T =10, 20and 60 respectively.

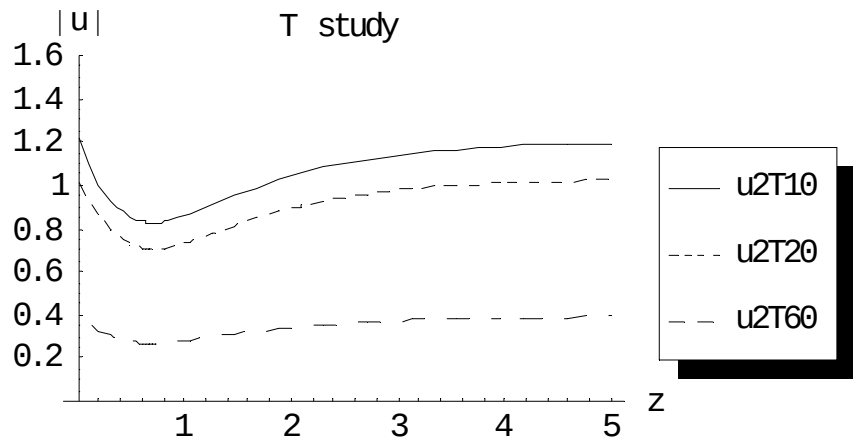

Fig. (3.138) the second order approximation of $\left|u^{(2)}\right|$ at $\varepsilon = 0.2$, $\gamma = 1$ and $\alpha, \rho_1, \rho_2 = 1, M = 10, t = 6$ for different values of T =10, 20 and 60 respectively.

3.7.1.3 Case study 3

Taking the case $F_1(t,z) = \rho_1 e^{-t}$, $F_2(t,z) = 0$, $f_1(t) = \rho_2\, e^{-t}, f_2(t) = 0$ and following the algorithm, the following selected results for the first and second order approximations are got:

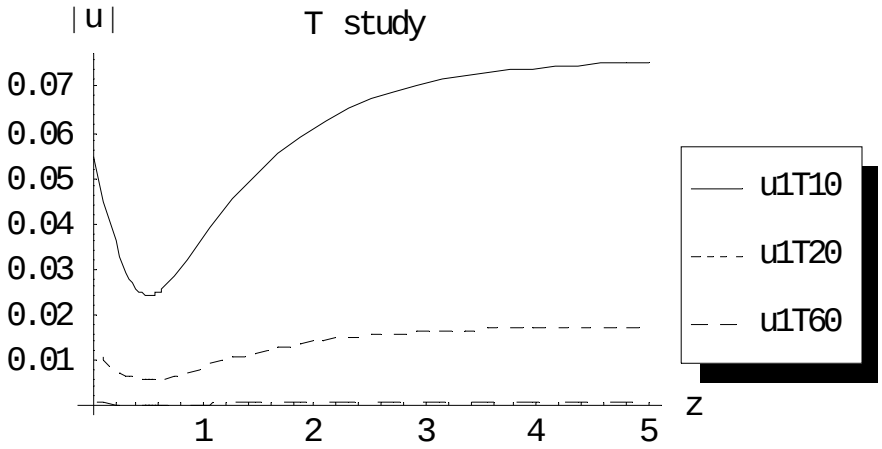

Fig. (3.139) the first order approximation of $\left|u^{(1)}\right|$ at $\varepsilon = 0.2$, $\gamma = 1$ and $\alpha, \rho_1, \rho_2 = 1, M = 10, t = 6$ for different values of T =10, 20 and 60 respectively.

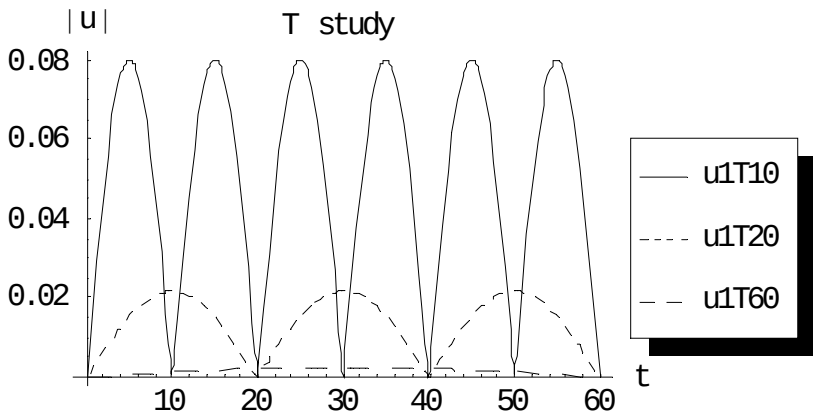

Fig. (3.140) the first order approximation of $\left|u^{(1)}\right|$ at $\varepsilon = 0.2$, $\gamma = 1$ and $\alpha, \rho_1, \rho_2 = 1, M = 10, z = 10$ for different values of T =10, 20and 60 respectively.

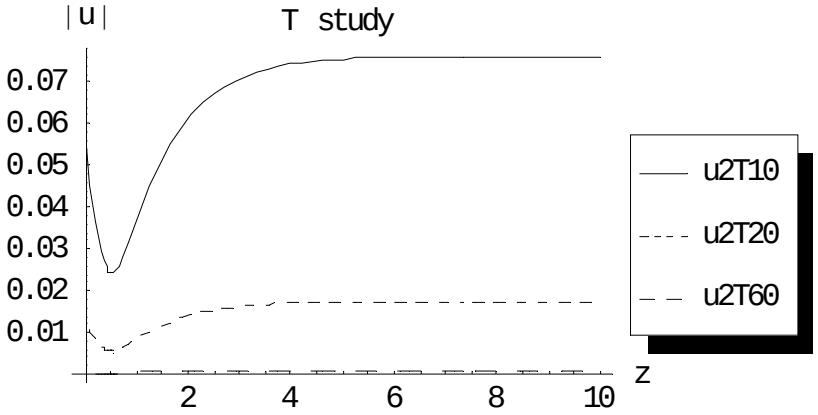

Fig. (3.141) the second order approximation of $\left|u^{(2)}\right|$ at $\varepsilon = 1$, $\gamma = 1$ and $\alpha, \rho_1, \rho_2 = 1, M = 10, t = 6$ for different values of T =10, 20 and 60 respectively.

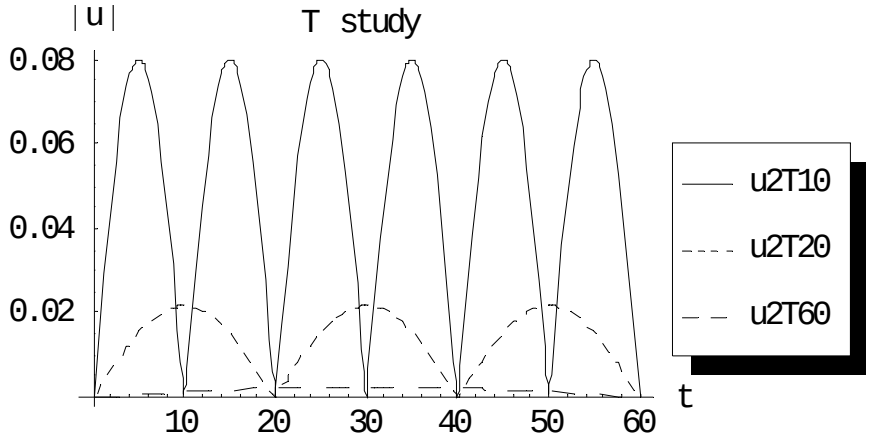

Fig. (3.142) the second order approximation of $\left|u^{(2)}\right|$ at $\varepsilon = 0.2$, $\gamma = 1$ and $\alpha, \rho_1, \rho_2 = 1, M = 10, z = 10$ for different values of T =10,20 and 60 respectively.

3.7.1.4 Case study 4

Taking the case $F_1(t,z) = \rho_1 \sin\left(\frac{m\pi}{T}t\right), F_2(t,z) = 0, f_1(t) = \rho_2 e^{-t}, f_2(t) = 0$ and following the algorithm, the following selected results for the first and second order approximations are got:

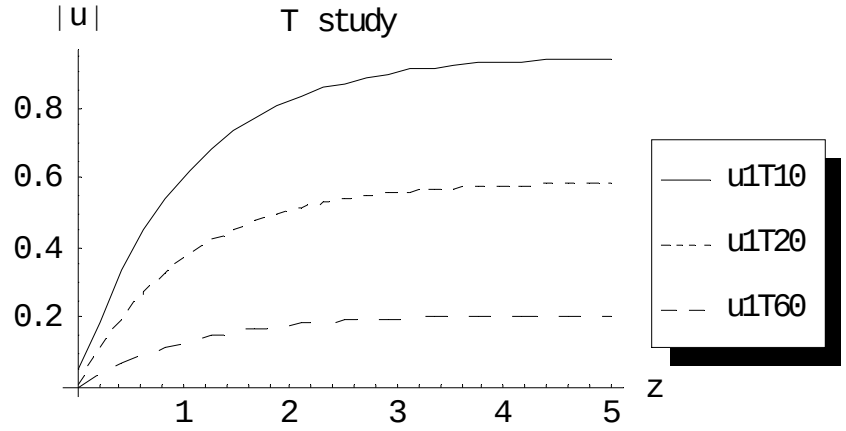

Fig. (3.143) the first order approximation of $\left|u^{(1)}\right|$ at $\varepsilon = 0.2$, $\gamma = 1$ and $\alpha, \rho_1, \rho_2 = 1, M = 10, t = 4$ for different values of T =10, 20 and 60 respectively.

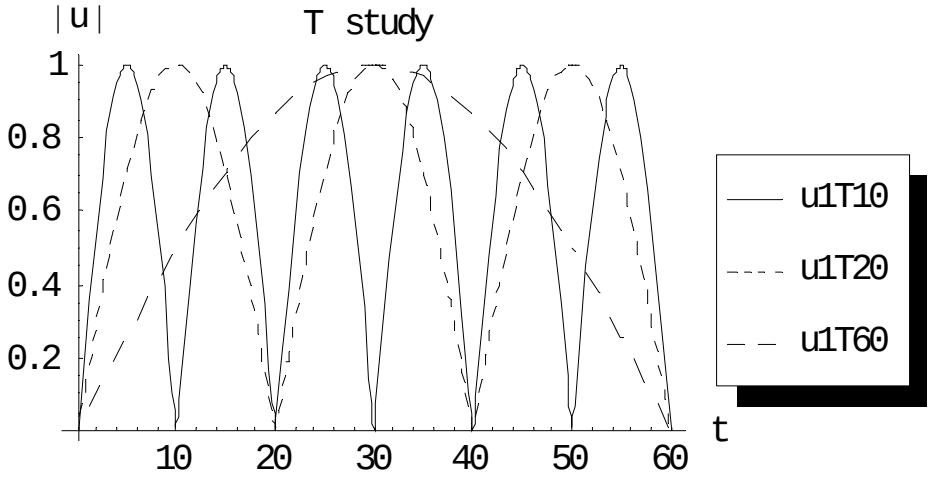

Fig. (3.144) the first order approximation of $\left|u^{(1)}\right|$ at $\varepsilon = 0.2$, $\gamma = 1$ and $\alpha, \rho_1, \rho_2 = 1, M = 10, z = 10$ for different values of T =10, 20 and 60 respectively.

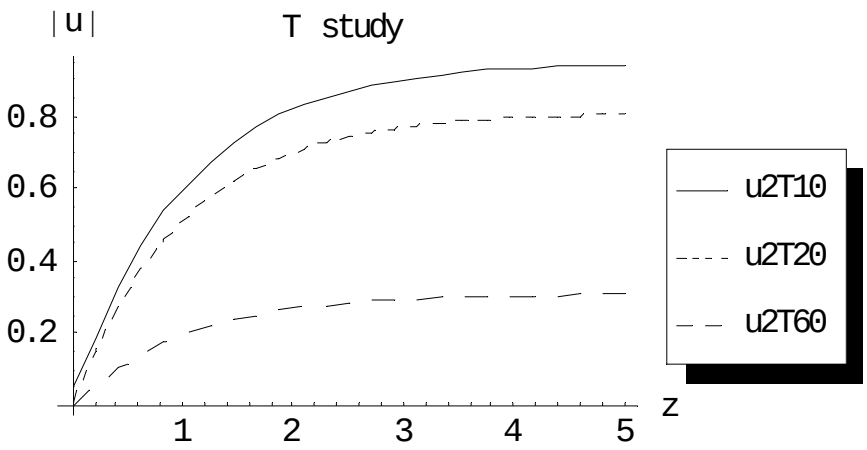

Fig. (3.145) the second order approximation of $\left|u^{(2)}\right|$ at $\varepsilon = 1$, $\gamma = 1$ and $\alpha, \rho_1, \rho_2 = 1, M = 10, t = 6$ for different values of T =10, 20 and 60 respectively.

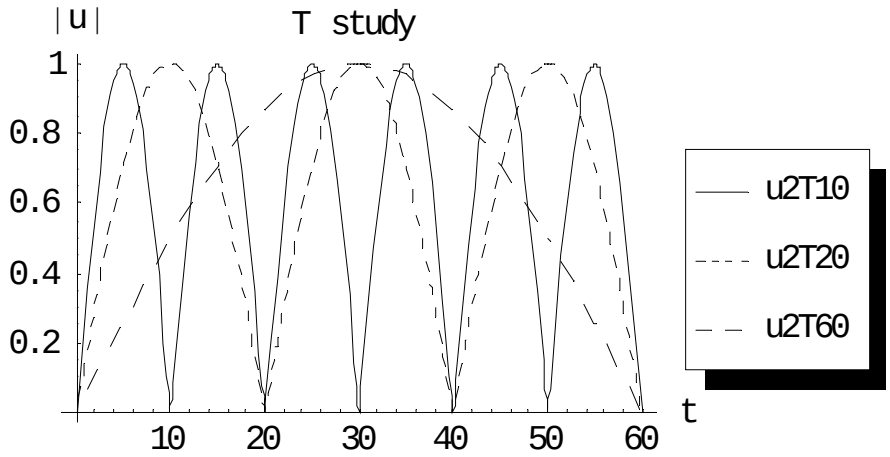

Fig. (3.146) the second order approximation of $\left|u^{(2)}\right|$ at $\varepsilon = 0.2$, $\gamma = 1$ and $\alpha, \rho_1, \rho_2 = 1, M = 10, z = 10$ for different values of T =10, 20 and 60 respectively.

3.7.1.5 Case study 5

Taking the case $F_1(t,z) = \rho_1 e^{-t}, F_2(t,z) = 0$, $f_1(t) = \rho_2 \sin\left(\frac{m\pi}{T}t\right), f_2(t) = 0$ and following the algorithm, the following selected results for the first and approximation are got:

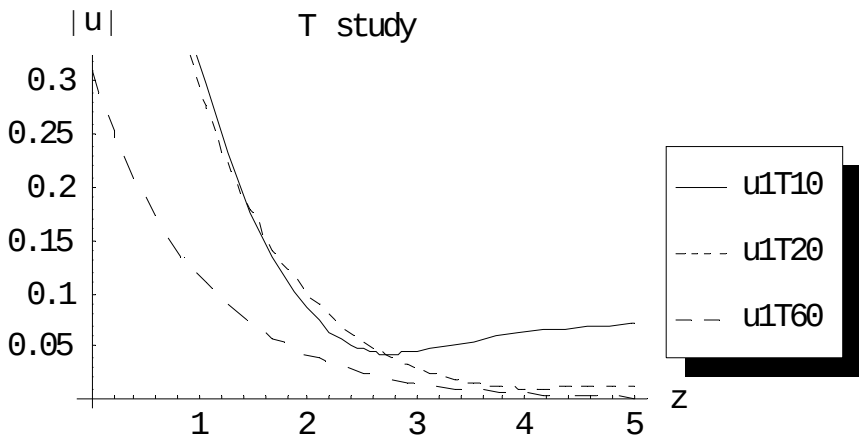

Fig. (3.147) the first order approximation of $\left|u^{(1)}\right|$ at $\varepsilon = 0.2$, $\gamma = 1$ and $\alpha, \rho_1, \rho_2 = 1, M = 1, t = 6$ for different values of T =10, 20 and 60 respectively.

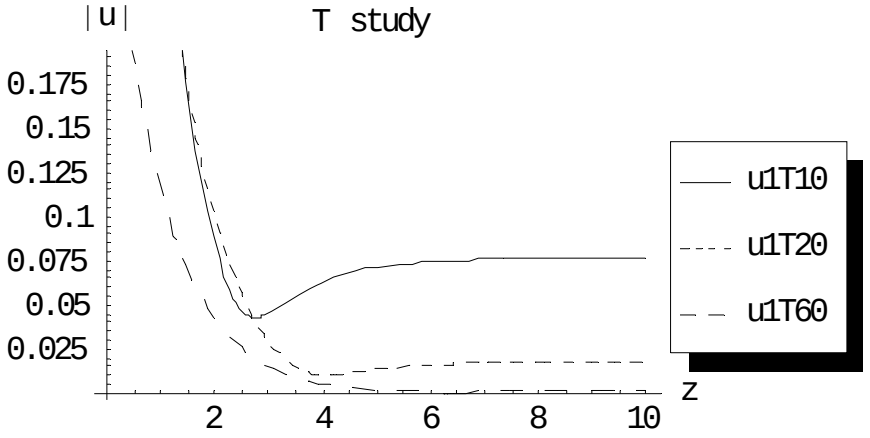

Fig. (3.148) the first order approximation of $\left|u^{(1)}\right|$ at $\varepsilon = 1$, $\gamma = 1$ and $\alpha, \rho_1, \rho_2 = 1, M = 1, t = 6$ for different values of T =10, 20 and 60 respectively.

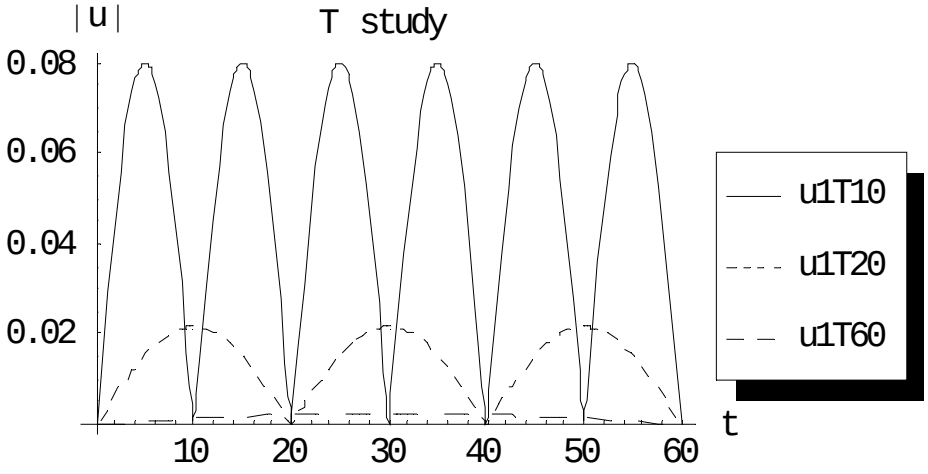

Fig. (3.149) the first order approximation of $\left|u^{(1)}\right|$ at $\varepsilon = 0.2$, $\gamma = 1$ and $\alpha, \rho_1, \rho_2 = 1, M = 1, z = 10$ for different values of T =10, 20 and 60 respectively.

3.7.1.6 Case study 6

Taking the case $F_1(t,z) = \rho_1 \sin\left(\frac{m\pi}{T}t\right), F_2(t,z) = 0$, $f_1(t) = \rho_2 \sin\left(\frac{m\pi}{T}t\right)$, $f_2(t) = 0$ and following the algorithm, the following selected results for the first approximation are got:

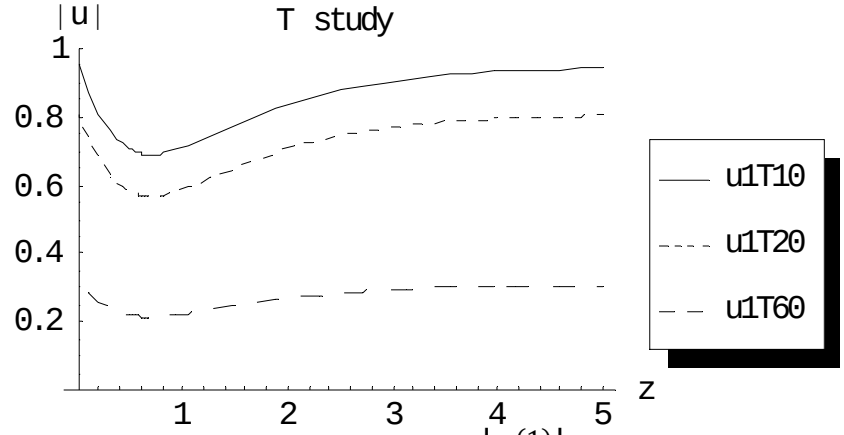

Fig. (3.150) the first order approximation of $\left|u^{(1)}\right|$ at $\varepsilon = 0.2$, $\gamma = 1$ and $\alpha, \rho_1, \rho_2 = 1, M = 1, t = 6$ for different values of T =10, 20 and 60 respectively.

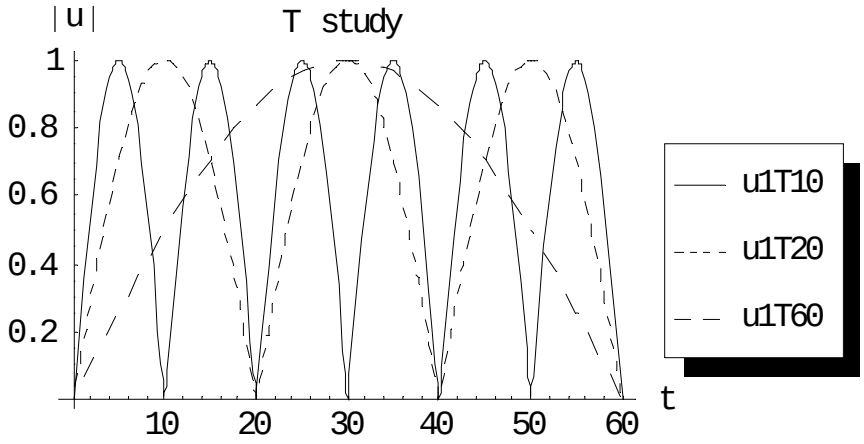

Fig. (3.151) the first order approximation of $\left|u^{(1)}\right|$ at $\varepsilon = 0.2$, $\gamma = 1$ and $\alpha, \rho_1, \rho_2 = 1, M = 1, z = 10$ for different values of T =10, 20 and 60 respectively.

3.7.1.7 Case study 7

Taking the case $F_1(t,z) = \rho_1, F_2(t,z) = 0$, $f_1(t) = 0, f_2(t) = 0$ and following the algorithm, the following selected results for the first and second order approximations are got:

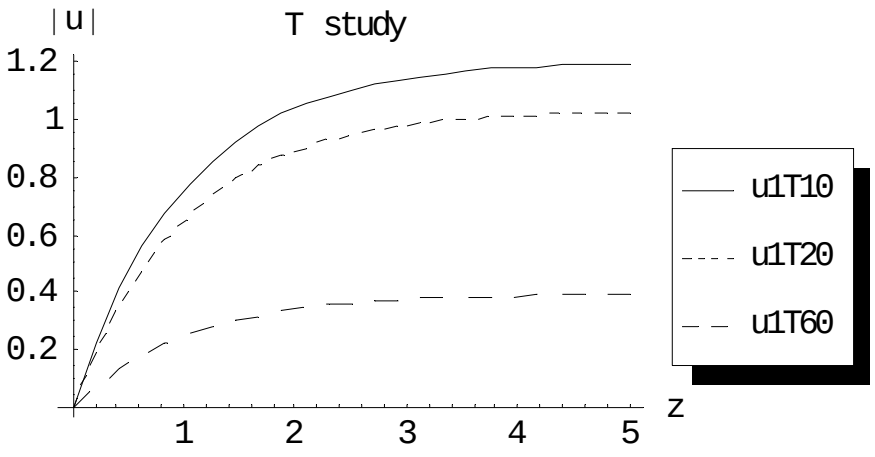

Fig. (3.152) the first order approximation of $\left|u^{(1)}\right|$ at $\varepsilon = 1$, $\gamma = 1$ and $\alpha, \rho_1 = 1, M = 1, t = 6$ for different values of T =10, 20 and 60 respectively.

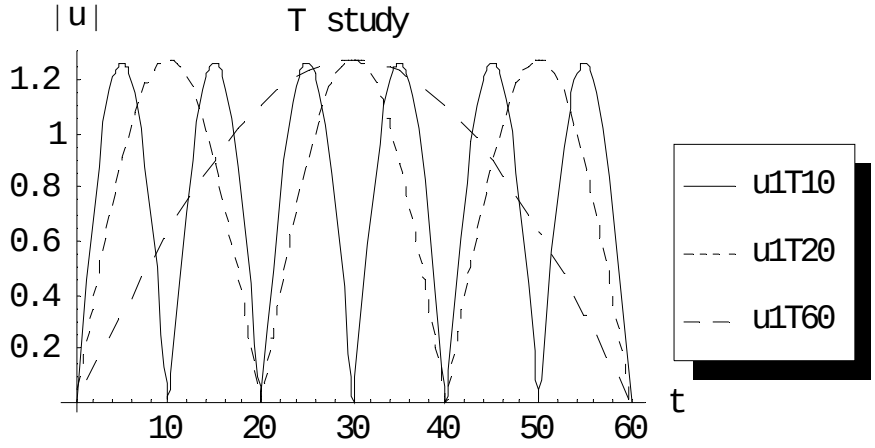

Fig. (3.153) the first order approximation of $\left|u^{(1)}\right|$ at $\varepsilon = 0.2$, $\gamma = 1$ and $\alpha, \rho_1 = 1, M = 1, z = 10$ for different values of T =10, 20 and 60 respectively.

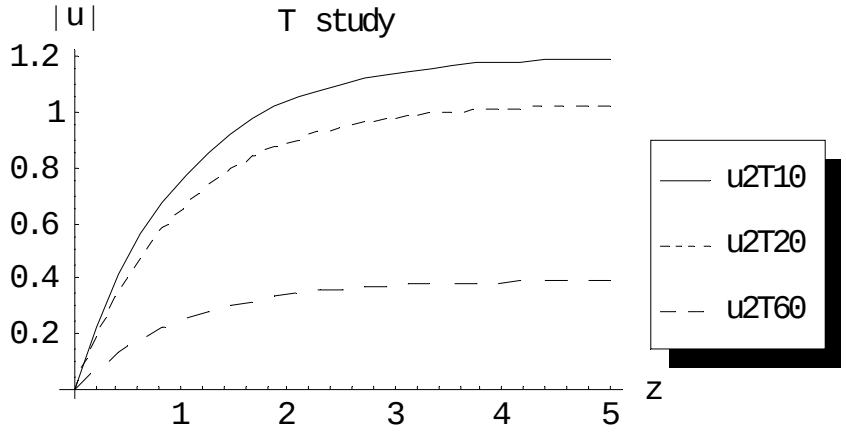

Fig. (3.154) the second order approximation of $\left|u^{(2)}\right|$ at $\varepsilon = 1$, $\gamma = 1$ and $\alpha, \rho_1 = 1, M = 1, t = 6$ for different values of T =10, 20 and 60 respectively.

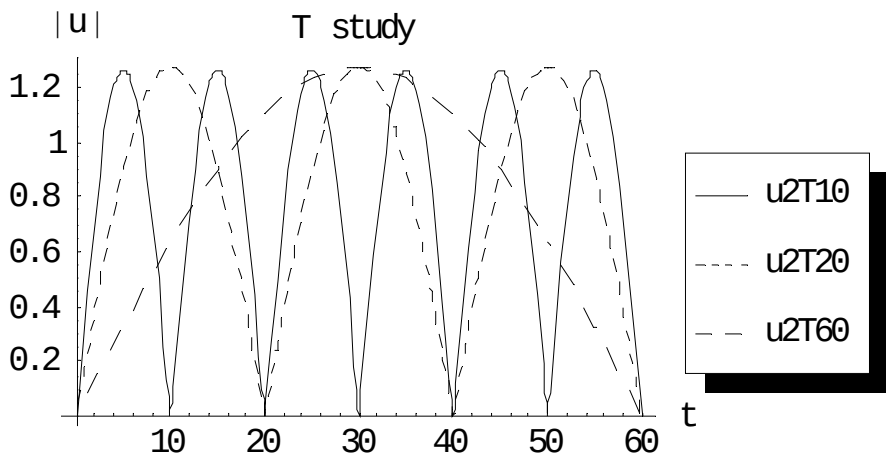

Fig. (3.155) the second order approximation of $\left|u^{(2)}\right|$ at $\varepsilon = 0.2$, $\gamma = 1$ and $\alpha, \rho_1 = 1, M = 1, z = 10$ for different values of T =10, 20 and 60 respectively.

3.7.2 Case Studies, Picard

3.7.2.1 Case study 1

Taking the case $F_1(t,z) = \rho_1, F_2(t,z) = 0$, $f_1(t) = \rho_2$, $f_2(t) = 0$ and following the algorithm, the following selected result for the first and second order approximations are got:

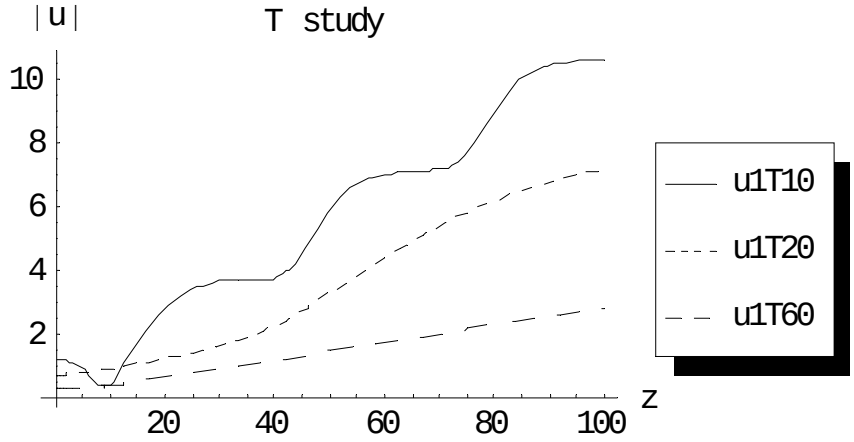

Fig. (3.156) the first order approximation of $\left|u^{(1)}\right|$ at $\varepsilon = 0.2$, $\gamma = 0$ and $\alpha, \rho_1, \rho_2 = 1, M = 1, t = 4$ for different values of T =10, 20 and 60 respectively.

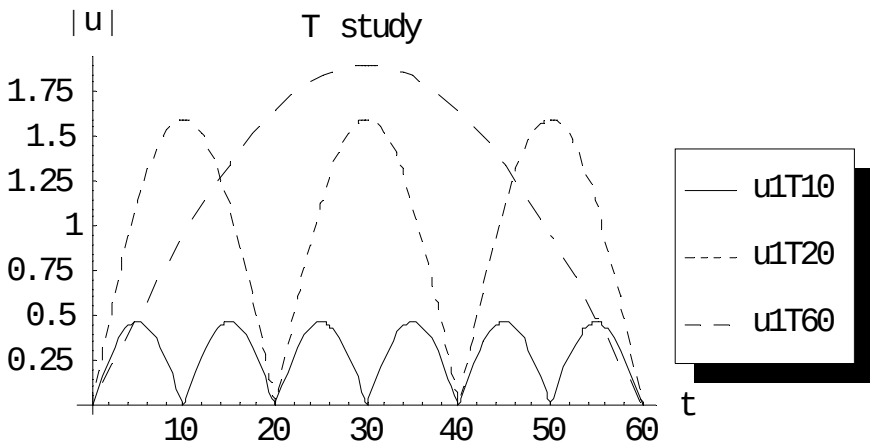

Fig. (3.157) the first order approximation of $\left|u^{(1)}\right|$ at $\varepsilon = 0.2$, $\gamma = 0$ and $\alpha, \rho_1, \rho_2 = 1, M = 1, z = 10$ for different values of T =10, 20 and 60 respectively.

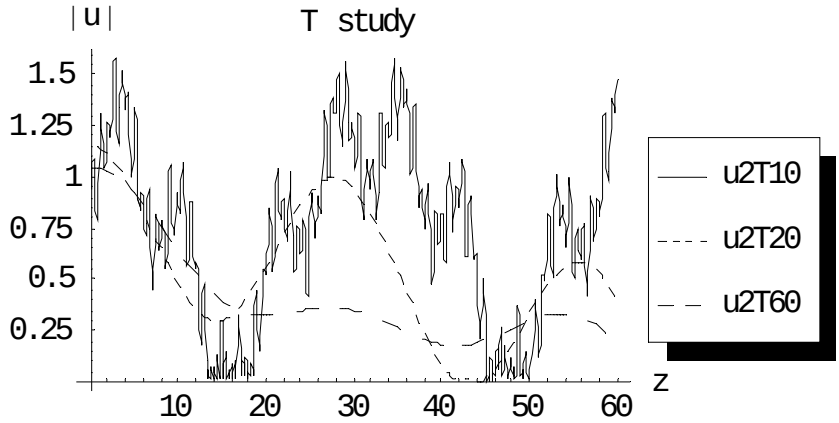

Fig. (3.158) the second order approximation of $\left|u^{(2)}\right|$ at $\varepsilon = 0.002$, $\gamma = 0$ and $\alpha, \rho_1, \rho_2 = 1, M = 10, t = 4$ for different values of T =10, 20 and 60 respectively.

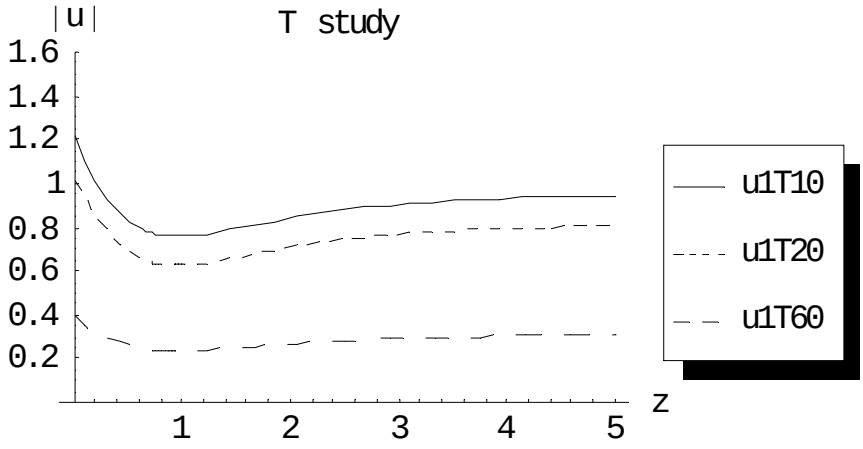

Fig. (3.159) the first order approximation of $\left|u^{(1)}\right|$ at $\varepsilon = 0.2$, $\gamma = 1$ and $\alpha, \rho_1, \rho_2 = 1, M = 1, t = 6$ for different values of T =10, 20 and 60 respectively.

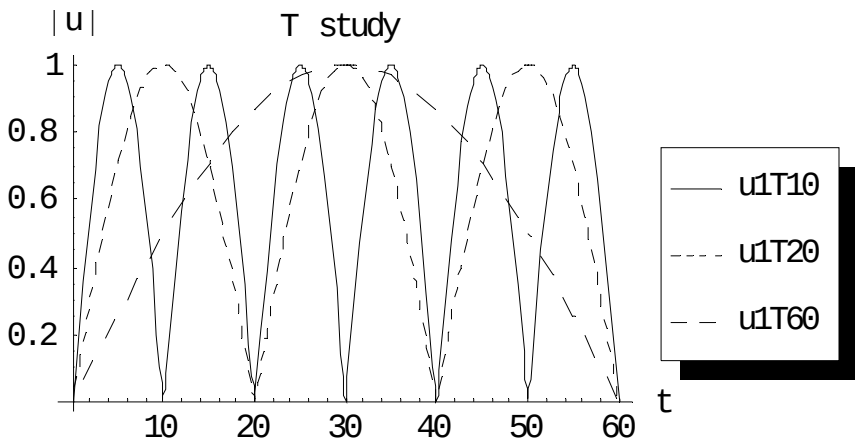

Fig. (3.160) the first order approximation of $\left|u^{(1)}\right|$ at $\varepsilon = 0.2$, $\gamma = 1$ and $\alpha, \rho_1, \rho_2 = 1, M = 1, z = 10$ for different values of T =10, 20 and 60 respectively.

3.7.2.2 Case study 2

Taking the case $F_1(t,z) = \rho_1 e^{-t}, F_2(t,z) = 0$, $f_1(t) = \rho_2$, $f_2(t) = 0$ and following the algorithm, the following selected results for the first approximation are got:

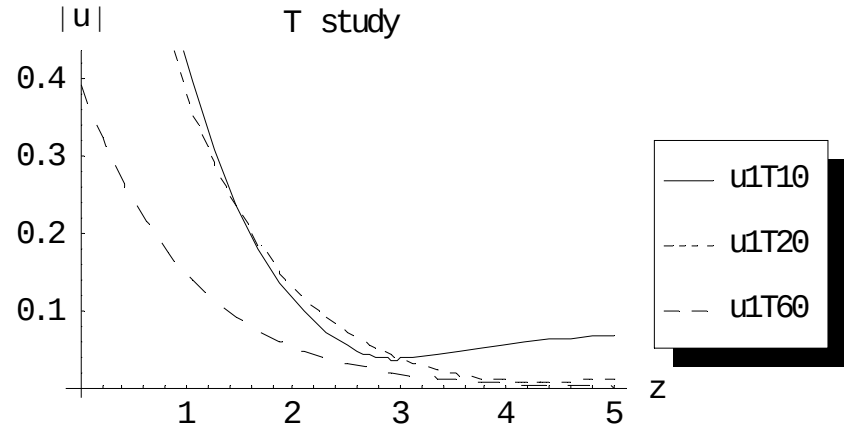

Fig. (3.161) the first order approximation of $\left|u^{(1)}\right|$ at $\varepsilon = 1$, $\gamma = 1$ and $\alpha, \rho_1, \rho_2 = 1, M = 1, t = 6$ for different values of T =10, 20 and 60 respectively.

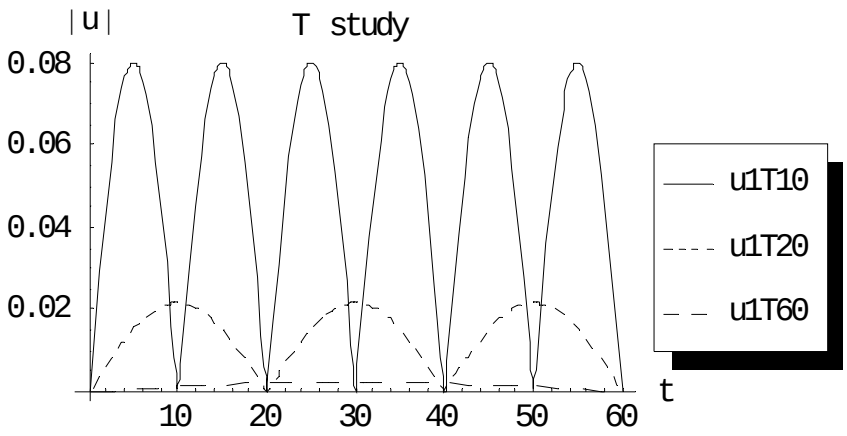

Fig. (3.162) the first order approximation of $\left|u^{(1)}\right|$ at $\varepsilon = 0.2$, $\gamma = 1$ and $\alpha, \rho_1, \rho_2 = 1, M = 1, z = 10$ for different values of T =10, 20 and 60 respectively.

3.7.2.3 Case study 3

Taking the case $F_1(t,z) = \rho_1 \sin\left(\frac{m\,\pi}{T}\,t\right)$, $F_2(t,z) = 0$, $f_1(t) = \rho_2$, $f_2(t) = 0$ and following the algorithm, the following selected results for the first approximation are got:

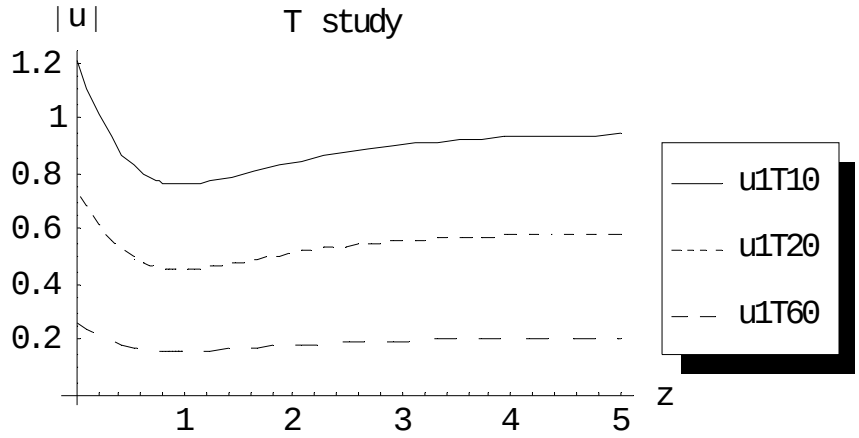

Fig. (3.163) the first order approximation of $\left|u^{(1)}\right|$ at $\varepsilon = 0.2$, $\gamma = 1$ and $\alpha, \rho_1, \rho_2 = 1, M = 1, t = 4$ for different values of T =10, 20 and 60 respectively.

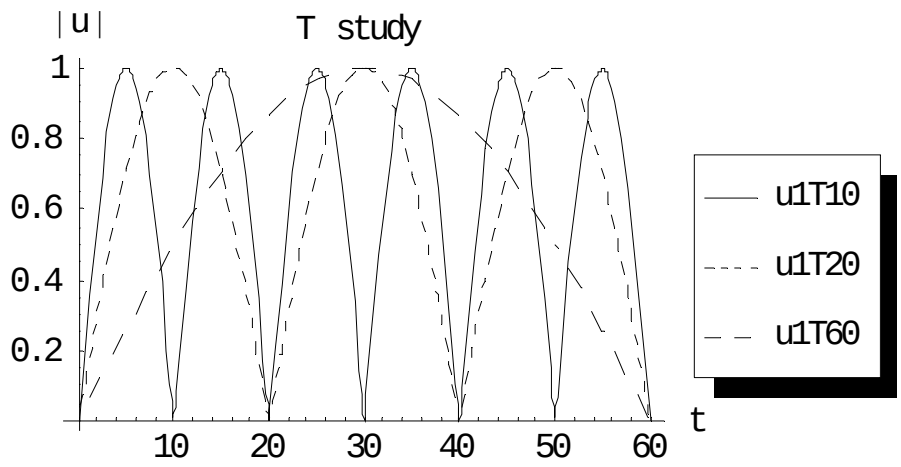

Fig. (3.164) the first order approximation of $\left|u^{(1)}\right|$ at $\varepsilon = 0.2$, $\gamma = 1$ and $\alpha, \rho_1, \rho_2 = 1, M = 1, z = 10$ for different values of T =10, 20 and 60 respectively.

3.7.2.4 Case study 4

Taking the case $F_1(t,z) = \rho_1 \sin\left(\frac{m\,\pi}{T}t\right), F_2(t,z) = 0$, $f_1(t) = \rho_2 e^{-t}, f_2(t) = 0$ and following the algorithm, the following selected results for the first approximation are got:

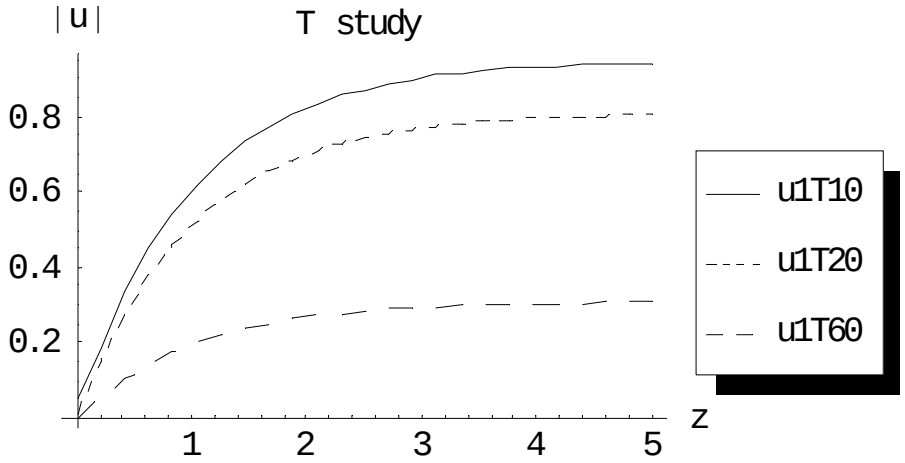

Fig. (3.165) the first order approximation of $\left|u^{(1)}\right|$ at $\varepsilon = 0.2$, $\gamma = 1$ and $\alpha, \rho_1, \rho_2 = 1, M = 1, t = 6$ for different values of T =10, 20 and 60 respectively.

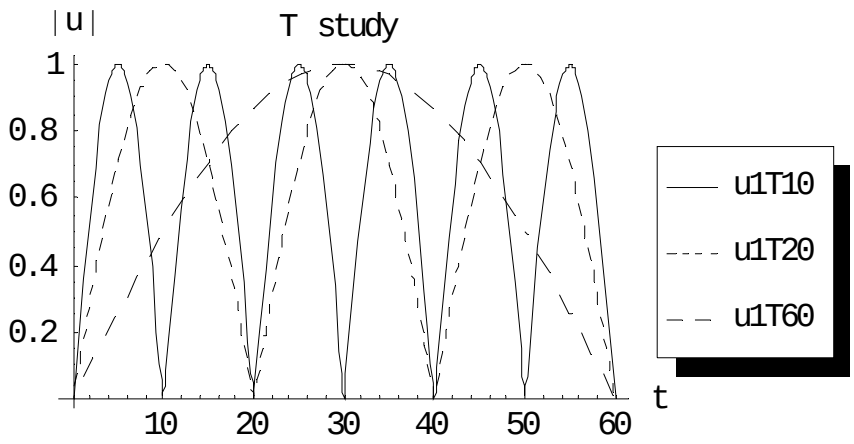

Fig. (3.166) the first order approximation of $\left|u^{(1)}\right|$ at $\varepsilon = 0.2$, $\gamma = 1$ and $\alpha, \rho_1, \rho_2 = 1, M = 1, z = 10$ for different values of T =10, 20 and 60 respectively.

3.7.2.5 Case study 5

Taking the case $F_1(t,z) = \rho_1 e^{-t}$, $F_2(t,z) = 0$, $f_1(t) = \rho_2 \sin\left(\frac{m\pi}{T}t\right), f_2(t) = 0$ and following the algorithm, the following selected results for the first approximation are got:

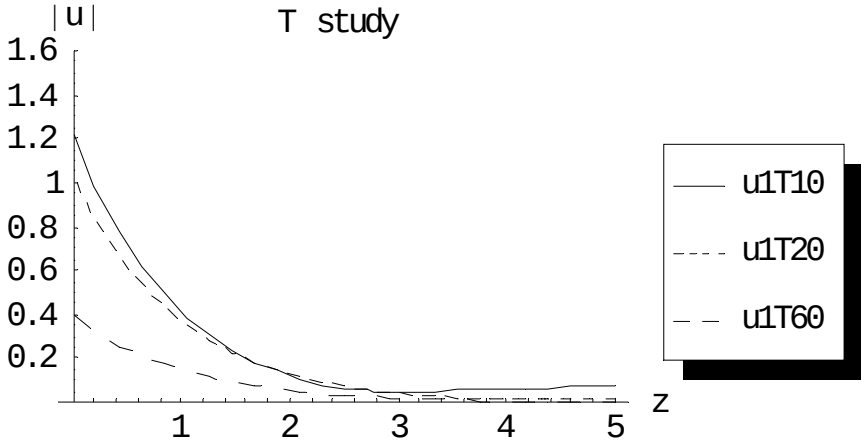

Fig. (3.167) the first order approximation of $\left|u^{(1)}\right|$ at $\varepsilon = 0.2$, $\gamma = 1$ and $\alpha, \rho_1, \rho_2 = 1, M = 1, t = 6$ for different values of T =10, 20 and 60 respectively.

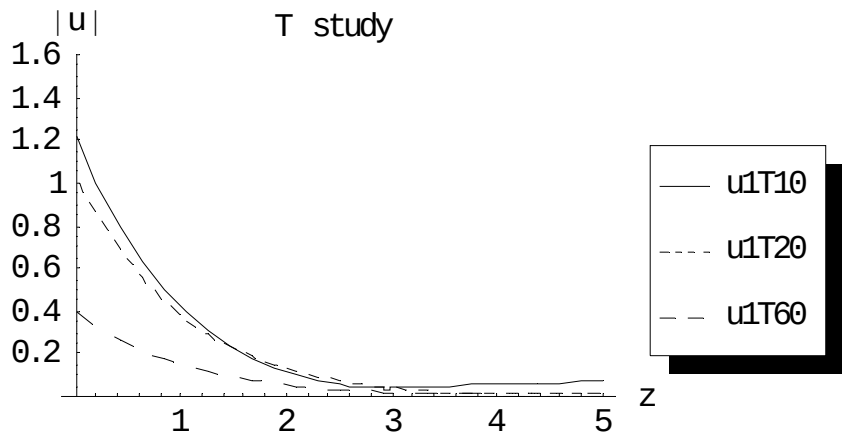

Fig. (3.168) the first order approximation of $\left|u^{(1)}\right|$ at $\varepsilon = 1$, $\gamma = 1$ and $\alpha, \rho_1, \rho_2 = 1, M = 1, t = 6$ for different values of T =10, 20 and 60 respectively.

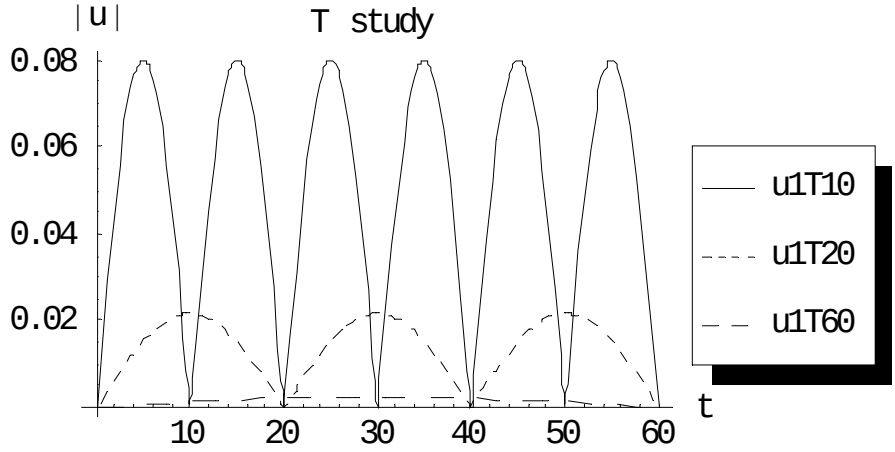

Fig. (3.169) the first order approximation of $\left|u^{(1)}\right|$ at $\varepsilon = 0.2$, $\gamma = 1$ and $\alpha, \rho_1, \rho_2 = 1, M = 1, z = 10$ for different values of T =10, 20 and 60 respectively.

3.7.2.6 Case study 6

Taking the case $F_1(t,z) = \rho_1 \sin\left(\frac{m\pi}{T}t\right), F_2(t,z) = \rho_1$, $f_1(t) = \rho_2 \sin\left(\frac{m\,\pi}{T}t\right)$, $f_2(t) = 0$ and following the algorithm, the following selected results for the first approximation are got:

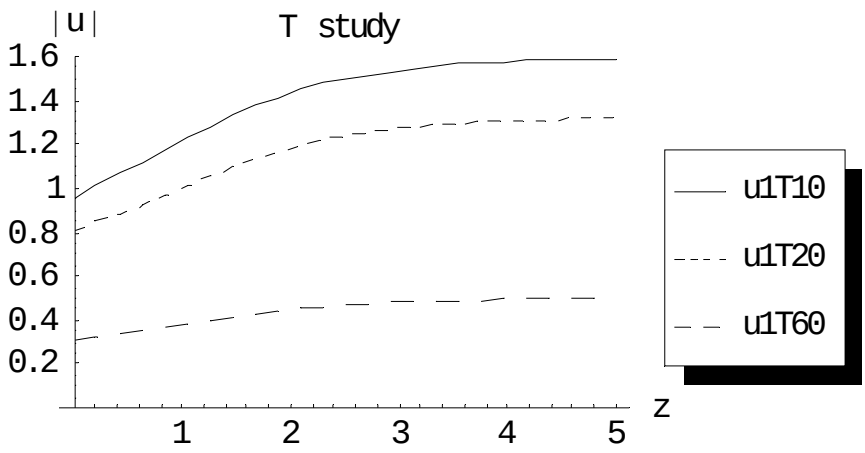

Fig. (3.170) the first order approximation of $\left|u^{(1)}\right|$ at $\varepsilon = 1$, $\gamma = 1$ and $\alpha, \rho_1, \rho_2 = 1, M = 1, t = 6$ for different values of T =10, 20 and 60 respectively.

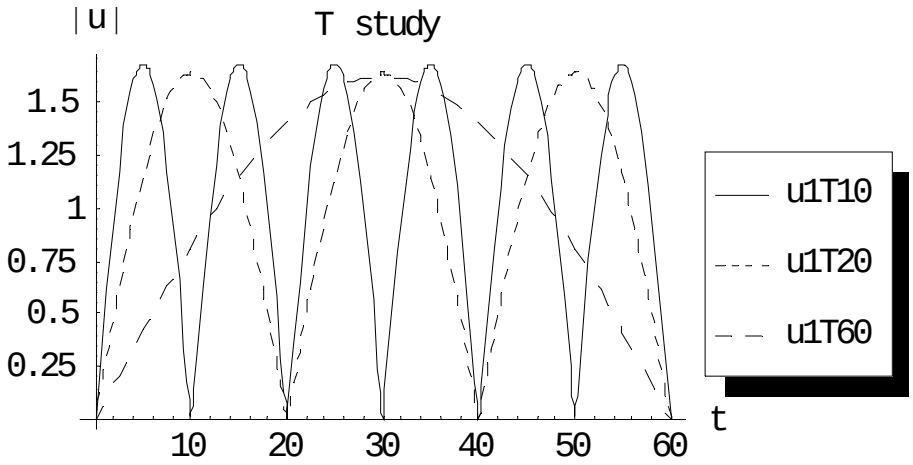

Fig. (3.171) the first order approximation of $\left|u^{(1)}\right|$ at $\varepsilon = 0.2$, $\gamma = 1$ and $\alpha, \rho_1, \rho_2 = 1, M = 1, z = 10$ for different values of T =10, 20 and 60 respectively.

Chapter 4 Homogeneous Nonlinear Quintic Schrodinger Equations

4.0 Introduction

In this chapter, a perturbing nonlinear quintic homogeneous Schrodinger equation is studied under limited time interval, complex initial conditions and zero Neumann conditions. The perturbation and Picard approximation methods together with the eigenfunction expansion and variational parameters methods are used to introduce an approximate solution for the perturbative nonlinear case for which a power series solution is proved to exist. Using Mathematica, the solution algorithm is tested through computing the possible orders of approximations. The method of solution is illustrated through case studies and figures.

4.1 The non- linear case

Consider the homogeneous non-linear Schrodinger equation:

$$i\,\frac{\partial u(t,z)}{\partial z}+\ \alpha\,\frac{\partial^2 u(t,z)}{\partial t^2}+\ \varepsilon|u(t,z)|^4u(t,z)\ +i\,\gamma u(t,z)=0,$$
$$(t,z)\in(0,T)\ x\ (0,\infty) \qquad (4.1)$$

where $u(t\ ,z)$ is a complex valued function which is subjected to:

$$I.Cs.: u(t,0)=\ f_1(t)+\ i\,f_2(t), \qquad (4.2)$$

$$B.Cs.: u(0,z)=\ u(T,z)=0. \qquad (4.3)$$

Lemma 4.1

the solution of equation (4.1) with the constraints (4.2), (4.3) is a power series in ε if exists.

Proof

At $\varepsilon=0\ (u(t,z)=u_0(t,z))$, the following linear homogeneous equation is got:

$$i\,\frac{\partial u_0(t,z)}{\partial z}+\ \alpha\,\frac{\partial^2 u_0(t,z)}{\partial t^2}+i\,\gamma u_0(t,z)=0,(\ t,z)\in(0,T)\ x\ (0,\infty) \qquad (4.4)$$

$$u_0(t\,,z) = \psi_0(t\,,z) + i\,\phi_0(t\,,z) \tag{4.5}$$

By following Appendix (A), the linear Schrodinger equation (4.4) has the following solution:

$$\psi_0(t\,,z) = e^{-\gamma z}\sum_{n=0}^{\infty} T_{0n}(z)\sin\left(\frac{n\,\pi}{T}\right)t, \tag{4.6}$$

$$\phi_0(t\,,z) = e^{-\gamma z}\sum_{n=0}^{\infty} \tau_{0n}(z)\sin\left(\frac{n\,\pi}{T}\right)t \tag{4.7}$$

Where $T_{0n}(z)$ and $\tau_{0n}(z)$ can be calculated as illustrated in the general linear case, (Appendix (A), equations (A.12), (A.13) respectively).

By following Pickard approximation equation (4.1) can be rewritten as:

$$i\frac{\partial u_n(t,z)}{\partial z} + \alpha\,\frac{\partial^2 u_n(t,z)}{\partial t^2} + i\,\gamma u_n(t,z) = -\varepsilon|u_{n-1}(t,z)|^4 u_{n-1}(t,z), n \geq 1 \tag{4.8}$$

at $n = 1$, the iterative equation takes the form

$$i\,\frac{\partial u_1(t,z)}{\partial z} + \alpha\,\frac{\partial^2 u_1(t,z)}{\partial t^2} + i\,\gamma u_1(t,z) = -\varepsilon|u_0(t,z)|^4 u_0(t,z) = \varepsilon k_1(t\,,z) \tag{4.9}$$

which can be solved as a linear case with zero initial and boundary conditions. The following general solution can be obtained:

$$\psi_1(t\,,z) = e^{-\gamma z}\sum_{n=0}^{\infty}\big(T_{0n}(z) + \varepsilon T_{1n}(z)\big)\sin\left(\frac{n\,\pi}{T}\right)t, \tag{4.10}$$

$$\phi_1(t\,,z) = e^{-\gamma z}\sum_{n=0}^{\infty}\big(\tau_{0n}(z) + \varepsilon \tau_{1n}(z)\big)\sin\left(\frac{n\,\pi}{T}\right)t, \tag{4.11}$$

$$u_1(t\,,z) = \psi_1(t\,,z) + i\,\phi_1(t\,,z), \tag{4.12}$$

$$= {u_1}^{(0)} + \varepsilon\,{u_1}^{(1)}, \tag{4.13}$$

where ${u_1}^{(0)} = u_0$.

At $n = 2$, the following equation is obtained:

$$i\,\frac{\partial u_2(t,z)}{\partial z} + \alpha\,\frac{\partial^2 u_2(t,z)}{\partial t^2} + i\,\gamma u_2(t,z) = -\varepsilon|u_1(t,z)|^4 u_1(t,z) = \varepsilon k_2(t\,,z) \tag{4.14}$$

which can be solved as a linear case with zero initial and boundary conditions. The following general solution can be obtained:

$$u_2(t\,,z) = {u_2}^{(0)} + \varepsilon\,{u_2}^{(1)} + \varepsilon^2 {u_2}^{(2)} + \varepsilon^3\,{u_2}^{(3)} + \varepsilon^4\,{u_2}^{(4)}, \tag{4.15}$$

where ${u_2}^{(0)} = u_0$. Continuing like this, one can get:

$$u_n(t\,,z) = {u_n}^{(0)} + \varepsilon\,{u_n}^{(1)} + \varepsilon^2 {u_n}^{(2)} + \varepsilon^3\,{u_n}^{(3)} + \cdots + \varepsilon^{m(n)}\,{u_n}^{m(n)}. \tag{4.16}$$

where $\mathrm{m(n)}$ is an increasing polynomial in n . As $n \to \infty$, the solution (if exists) can be reached as $u(t\,,z) = \lim_{n\to\infty} u_n(t\,,\,z)$. Accordingly the solution is a power series in ε .

According to the previous lemma (4.1), one can assume the solution of equation (4.1) as the following:

$$u(t\,,z) = \sum_{n=0}^{\infty} \varepsilon^n\,u_n(t\,,z) \tag{4.17}$$

Let $u(t\,,z) = \psi(t\,,z) + i\,\phi(t\,,\,z), \psi\,, \phi$: are real valued functions. The following coupled equations are got:

$$\frac{\partial \phi(t,z)}{\partial z} = \alpha\,\frac{\partial^2 \psi(t,z)}{\partial t^2} + \varepsilon(\psi^2 + \phi^2)^2\psi - \gamma\phi, \tag{4.18}$$

$$\frac{\partial \psi(t,z)}{\partial z} = -\alpha\,\frac{\partial^2 \phi(t,z)}{\partial t^2} - \varepsilon(\psi^2 + \phi^2)^2\phi - \gamma\psi, \tag{4.19}$$

Where $\psi(t,0) = f_1(t),\ \phi(t,0) = f_2(t)$, and all other corresponding I.Cs. and B.Cs. are zeros.

As a third order perturbation solution, one can assume that:

$$\psi(t\,,z\,) = \psi_0 + \varepsilon\psi_1 + \varepsilon^2\psi_2 + \varepsilon^3\psi_3\,, \tag{4.20}$$

$$\phi(t\,,z\,) = \phi_0 + \varepsilon\phi_1 + \varepsilon^2\phi_2 + \varepsilon^3\phi_3\,, \tag{4.21}$$

Where $\psi_0(t,0) = f_1(t),\ \phi_0(t,0) = f_2(t)$, and all other corresponding I.Cs. and B.Cs. are zeros.

Substituting from equations (4.20) and (4.21) into equations (4.18) and (4.19) and then equating the equal powers of ε, one can get the following set of coupled equations:

$$\frac{\partial \phi_0(t,z)}{\partial z} = \alpha \frac{\partial^2 \psi_0(t,z)}{\partial t^2} - \gamma \phi_0, \tag{4.22}$$

$$\frac{\partial \psi_0(t,z)}{\partial z} = -\alpha \frac{\partial^2 \phi_0(t,z)}{\partial t^2} - \gamma \psi_0 \tag{4.23}$$

$$\frac{\partial \phi_1(t,z)}{\partial z} = \alpha \frac{\partial^2 \psi_1(t,z)}{\partial t^2} - \gamma \phi_1 + \left({\psi_0}^2 + {\phi_0}^2\right)^2 \psi_0, \tag{4.24}$$

$$\frac{\partial \psi_1(t,z)}{\partial z} = -\alpha \frac{\partial^2 \phi_1(t,z)}{\partial t^2} - \gamma \psi_1 - \left({\phi_0}^2 + {\psi_0}^2\right)^2 \phi_0, \tag{4.25}$$

$$\begin{aligned}\frac{\partial \phi_2(t,z)}{\partial z} = {} & \alpha \frac{\partial^2 \psi_2(t,z)}{\partial t^2} - \gamma \phi_2 + \left({\phi_0}^2 + {\psi_0}^2\right)^2 \psi_1 \\ & + \left(4\,{\psi_0}^3 \psi_1 + 4\,{\phi_0}^3 \phi_1 + 4\psi_0 \psi_1 {\phi_0}^2 + 4{\psi_0}^2 \phi_0 \phi_1\right)\psi_0,\end{aligned} \tag{4.26}$$

$$\begin{aligned}\frac{\partial \psi_2(t,z)}{\partial z} = {} & -\alpha \frac{\partial^2 \phi_2(t,z)}{\partial t^2} - \gamma \psi_2 - \left({\phi_0}^2 + {\psi_0}^2\right)^2 \phi_1 \\ & - \left(4\,{\psi_0}^3 \psi_1 + 4\,{\phi_0}^3 \phi_1 + 4\psi_0 \psi_1 {\phi_0}^2 + 4{\psi_0}^2 \phi_0 \phi_1\right)\phi_0,\end{aligned} \tag{4.27}$$

and so on. The prototype equations to be solved are:

$$\frac{\partial \phi_i(t,z)}{\partial z} = \alpha \frac{\partial^2 \psi_i(t,z)}{\partial t^2} + G_{1i} \quad , \qquad i \geq 1 \tag{4.28}$$

$$\frac{\partial \psi_i(t,z)}{\partial z} = \alpha \frac{\partial^2 \phi_i(t,z)}{\partial t^2} + G_{2i} \quad , \qquad i \geq 1 \tag{4.29}$$

Where $\psi_i(t,0) = \delta_{i,0} f_1(t),\ \phi_i(t,0) = \delta_{i,0} f_2(t)$, and all other all corresponding conditions are zeros. G_{1i}, G_{2i} are functions to be computed from previous steps.

Following the solution algorithm described in Appendix (A) for the linear case, the following final results are obtained.

4.2 The order of approximations

The following final expressions can be used to obtain different order of approximations.

4.2.1 The zero order approximation

The zero order approximation is the linear case illustrated in Appendix (A).

4.2.2 The first order approximation

$$u_1(t\,,z) = u_0(t,z) + \varepsilon\big(\,\psi_1(t,z) + \,i\,\phi_1(t,z)\big) \tag{4.30}$$

By following Appendix (A), for *n=1,* we can find that:

$$\psi_1(t\,,z) = e^{-\gamma z}\sum_{n=0}^{\infty} T_{1n}(z)\sin\,(\frac{n\,\pi}{T})t, \tag{4.31}$$

$$\phi_1(t\,,z) = e^{-\gamma z}\sum_{n=0}^{\infty} \tau_{1n}(z)\sin\,(\frac{n\,\pi}{T})t\,, \tag{4.32}$$

From equations (4.24) and (4.25), we can see that:

$$G_{11} = \,e^{-4\gamma z}({\psi_0}^2 + \,{\phi_0}^2)^2\,\psi_0 \tag{4.33}$$

$$G_{21} = \,-e^{-4\gamma z}({\phi_0}^2 + {\psi_0}^2)^2\,\phi_0 \tag{4.34}$$

in which

$$T_{1n}(z) = A_{11}(z)\sin\beta_n z + \,\big(C_{12} + \,B_{11}(z)\big)\cos\beta_n z, \tag{4.35}$$

$$\tau_{1n}(z) = A_{12}(z)\sin\beta_n z + \,\big(C_{14} + \,B_{12}(z)\big)\cos\beta_n z, \tag{4.36}$$

where $C_{12} = -B_{11}(0)$ and $C_{14} = -B_{12}(0)$. The rest constants A_{11}, B_{11}, A_{12}, B_{12} can be calculated in similar manner as illustrated in Appendix (A).

The absolute value of the first order approximation can be got using

$$|u_1(t\,,z)|^2 = |u_0(t\,,z)|^2 + 2\varepsilon(\psi_0\psi_1 + \phi_0\phi_1) + \,\varepsilon^2\big({\psi_1}^2 + \,\,{\phi_1}^2\big) \tag{4.37}$$

4.2.3 The second order approximation

$$u_2(t\,,z) = u_1(t,z) + \varepsilon^2\big(\,\psi_2(t,z) + \,i\,\phi_2(t,z)\big) \tag{4.38}$$

By following Appendix (A), for *n=2,* we can find that

$$\psi_2(t\,,z) = e^{-\gamma z}\sum_{n=0}^{\infty} T_{2n}(z)\sin\left(\frac{n\,\pi}{T}\right)t, \tag{4.39}$$

$$\phi_2(t\,,z) = e^{-\gamma z}\sum_{n=0}^{\infty} \tau_{2n}(z)\sin\left(\frac{n\,\pi}{T}\right)t\,, \tag{4.40}$$

From equations (4.26) and (4.27), we can see that:

$$G_{12} = e^{-4\gamma z}\left(\left({\phi_0}^2 + {\psi_0}^2\right)^2\psi_1 + \left(4\,{\psi_0}^3\psi_1 + 4\,{\phi_0}^3\phi_1 + 4\psi_0\psi_1{\phi_0}^2 + 4{\psi_0}^2\phi_0\phi_1\right)\psi_0\right) \tag{4.41}$$

$$G_{22} = -e^{-4\gamma z}\left(\left({\phi_0}^2 + {\psi_0}^2\right)^2\phi_1 + \left(4\,{\psi_0}^3\psi_1 + 4\,{\phi_0}^3\phi_1 + 4\psi_0\psi_1{\phi_0}^2 + 4{\psi_0}^2\phi_0\phi_1\right)\phi_0\right) \tag{4.42}$$

in which

$$T_{2n}(z) = A_{21}(z)\sin\beta_n z + \left(C_{22} + B_{21}(z)\right)\cos\beta_n z, \tag{4.43}$$

$$\tau_{2n}(z) = A_{22}(z)\sin\beta_n z + \left(C_{24} + B_{22}(z)\right)\cos\beta_n z, \tag{4.44}$$

Where $C_{22} = -B_{21}(0)$ and $C_{24} = -B_{22}(0)$. The rest constants A_{11}, B_{11}, A_{12}, B_{12} can be calculated in similar manner as illustrated in Appendix A.

The absolute value of the second order approximation can be got using

$$|u_2(t\,,z)|^2 = |u_1(t\,,z)|^2 + 2\varepsilon^2(\psi_0\psi_2 + \phi_0\phi_2) + 2\varepsilon^3(\psi_1\psi_2 + \phi_1\phi_2) + \varepsilon^4\left({\psi_2}^2 + {\phi_2}^2\right) \tag{4.45}$$

4.3 Case studies

To examine the proposed solution algorithm, some case studies are illustrated.

4.3.1 Case study 1

Taking the case and $f_1(t) = \rho_1$, $f_2(t) = \rho_2$ where ρ_1 & ρ_2 are constants and following the algorithm, the following selected results for the first and second order approximations are got:

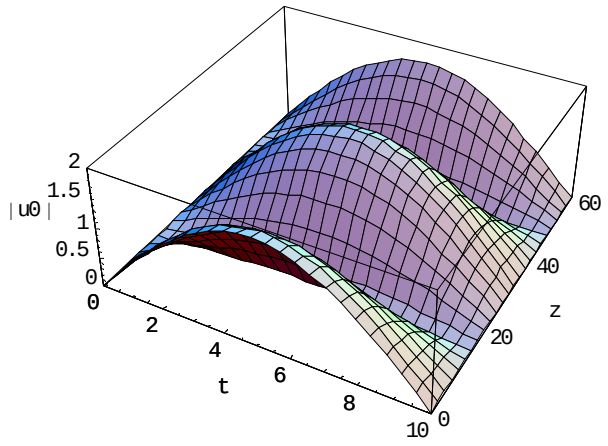

Fig. (4.1) the zero order approximation of $\left|u^{(0)}\right|$ at $\varepsilon = 0, \gamma = 0$ and $\alpha, \rho_1, \rho_2 = 1, T = 10$ with considering only one term on the series (M=1)

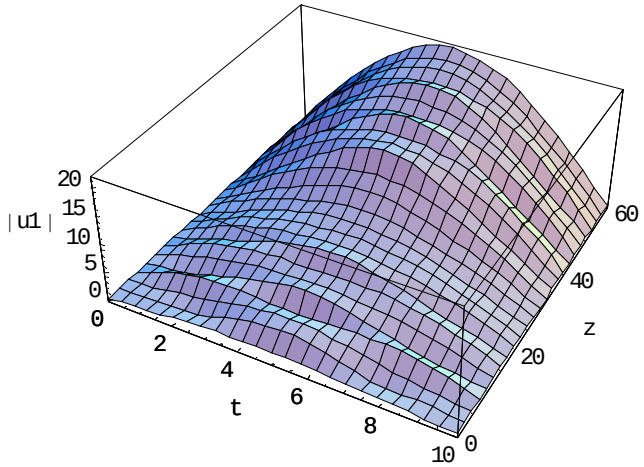

Fig. (4.2) the first order approximation of $\left|u^{(1)}\right|$ at $\varepsilon = 0.1, \gamma = 0$ and $\alpha, \rho_1, \rho_2 = 1, T = 10$ with considering only ten terms on the series (M=10).

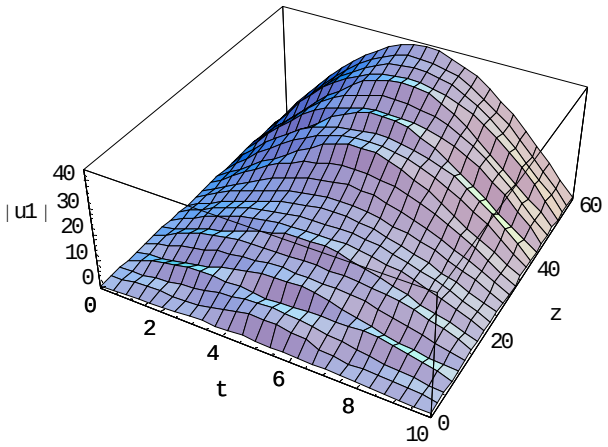

Fig. (4.3) the first order approximation of $\left|u^{(1)}\right|$ at $\varepsilon = 0.2$, $\gamma = 0$ and $\alpha, \rho_1, \rho_2 = 1, T = 10$ with considering only ten terms on the series (M=10).

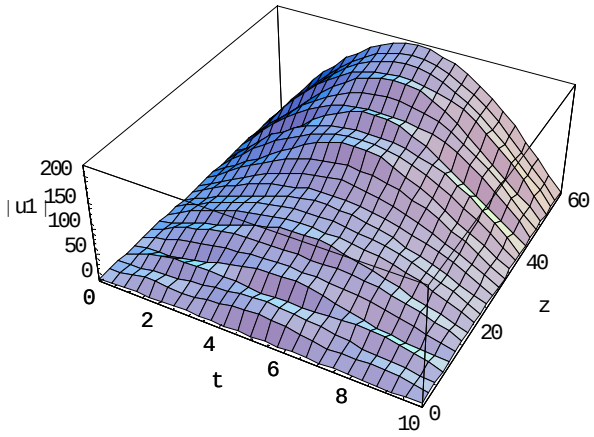

Fig. (4.4) the first order approximation of $\left|u^{(1)}\right|$ at $\varepsilon = 1$, $\gamma = 0$ and $\alpha, \rho_1, \rho_2 = 1, T = 10$ with considering only ten terms on the series (M=10).

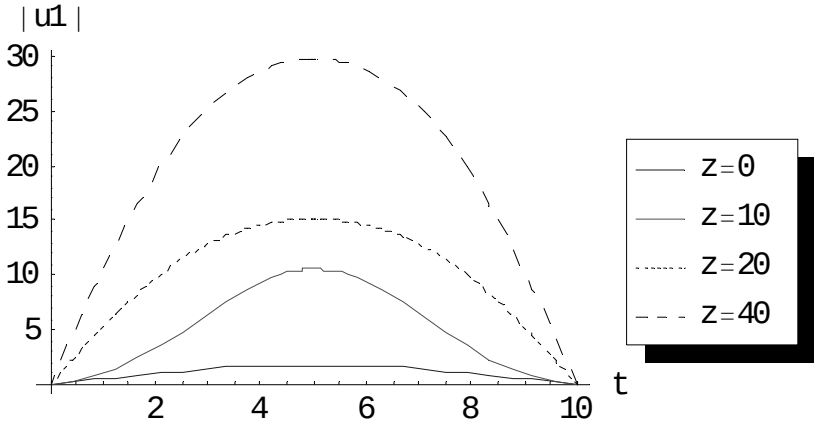

Fig. (4.5) the first order approximation of $\left|u^{(1)}\right|$ at $\varepsilon = 0.2, \gamma = 0$ and $\alpha, \rho_1, \rho_2 = 1, T = 10, M = 10$ for different values of z.

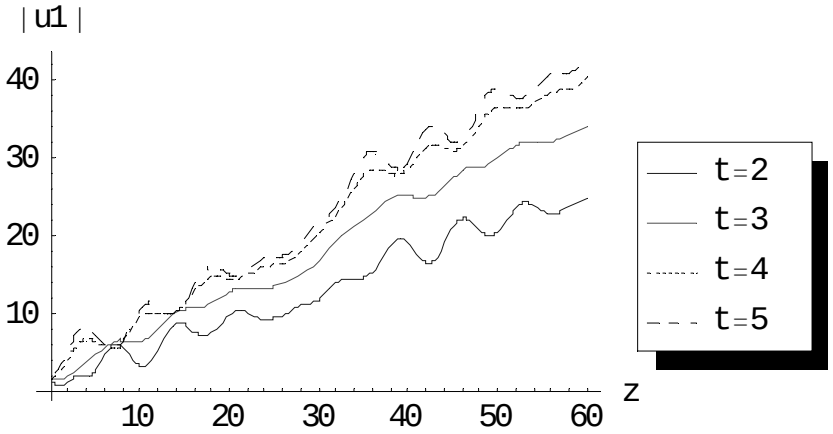

Fig. (4.6) the first order approximation of $\left|u^{(1)}\right|$ at $\varepsilon = 0.2, \gamma = 0$ and $\alpha, \rho_1, \rho_2 = 1, T = 10, M = 10$ for different values of t.

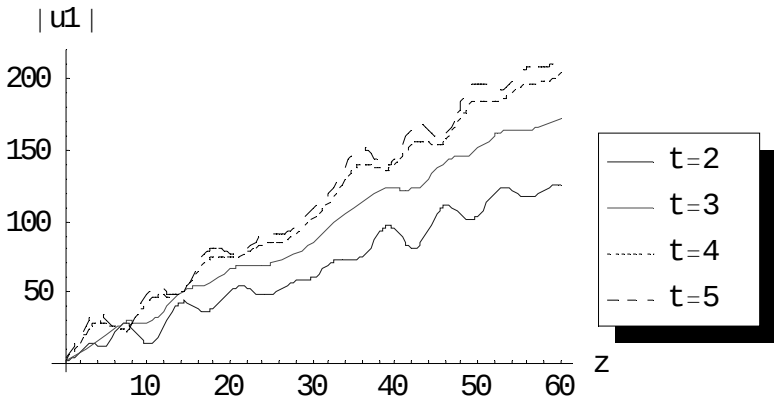

Fig. (4.7) the first order approximation of $\left|u^{(1)}\right|$ at $\varepsilon = 1, \gamma = 0$ and $\alpha, \rho_1, \rho_2 = 1, T = 10, M = 10$ for different values of t.

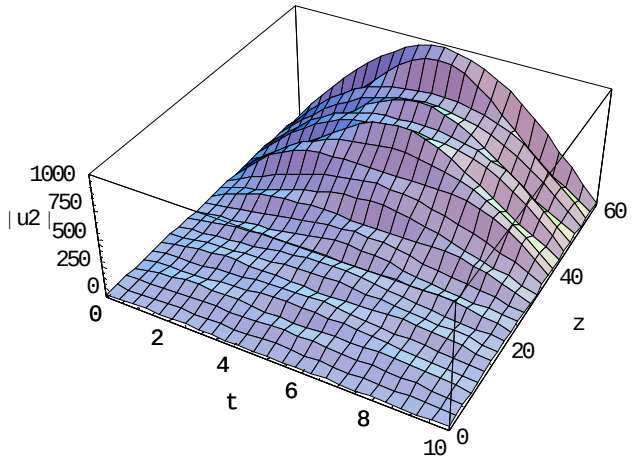

Fig. (4.8) the second order approximation of $\left|u^{(2)}\right|$ at $\varepsilon = 0.2$, $\gamma = 0$ and $\alpha, \rho_1, \rho_2 = 1, T = 10$ with considering only ten terms on the series (M=10).

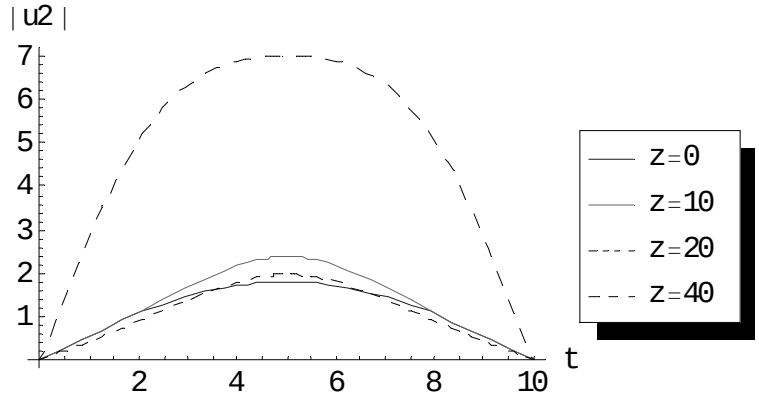

Fig. (4.9) the second order approximation of $\left|u^{(2)}\right|$ at $\varepsilon = 0.02, \gamma = 0$ and $\alpha, \rho_1, \rho_2 = 1, T = 10, M = 10$ for different values of z.

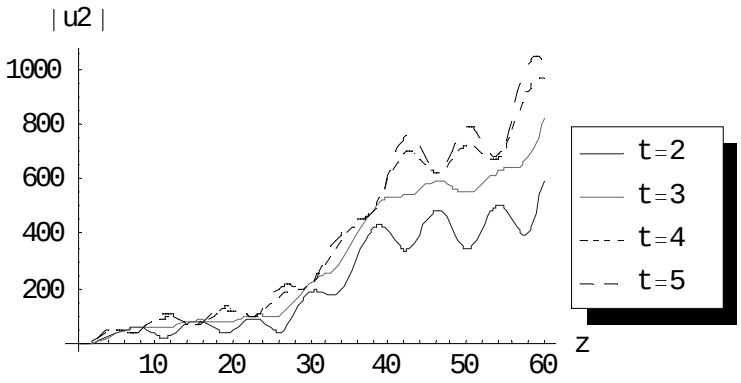

Fig. (4.10) the second order approximation of $\left|u^{(2)}\right|$ at $\varepsilon = 0.2, \gamma = 0$ and $\alpha, \rho_1, \rho_2 = 1, T = 10, M = 10$ for different values of t.

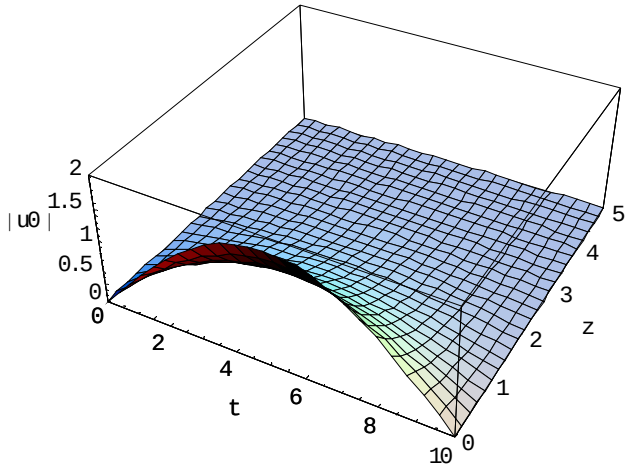

Fig.(4.11) the zero order approximation of $\left|u^{(0)}\right|$ at $\varepsilon = 0$, $\gamma = 1$ and $\alpha, \rho_1, \rho_2 = 1, T = 10$ with considering only ten terms on the series (M=10).

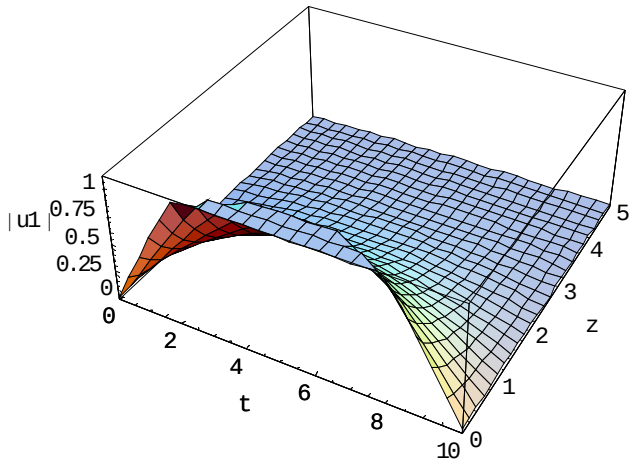

Fig.(4.12) the first order approximation of $\left|u^{(1)}\right|$ at $\varepsilon = 0.2$, $\gamma = 1$ and $\alpha, \rho_1, \rho_2 = 1, T = 10$ with considering only ten terms on the series (M=10).

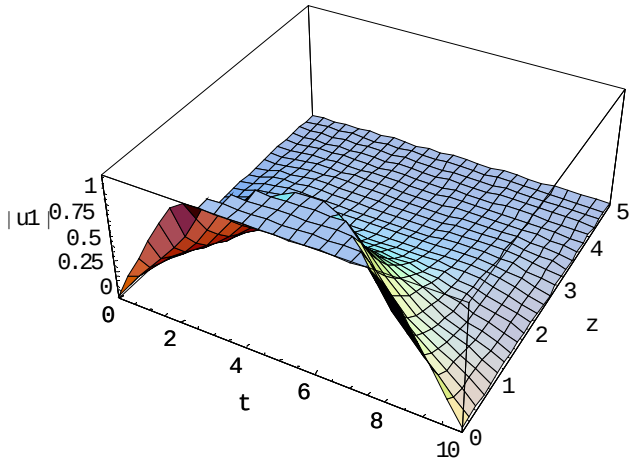

Fig.(4.13) the first order approximation of $\left|u^{(1)}\right|$ at $\varepsilon = 1$, $\gamma = 1$ and $\alpha, \rho_1, \rho_2 = 1, T = 10$ with considering only ten terms on the series (M=10).

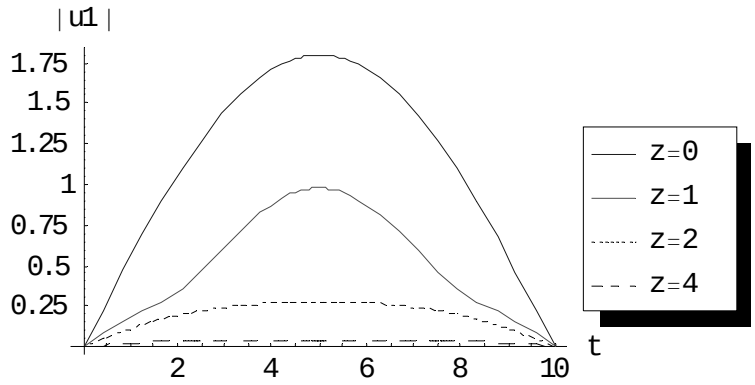

Fig.(4.14) the first order approximation of $\left|u^{(1)}\right|$ at $\varepsilon = 0.2, \gamma = 1$ and $\alpha, \rho_1, \rho_2 = 1, T = 10, M = 10$ for different values of z.

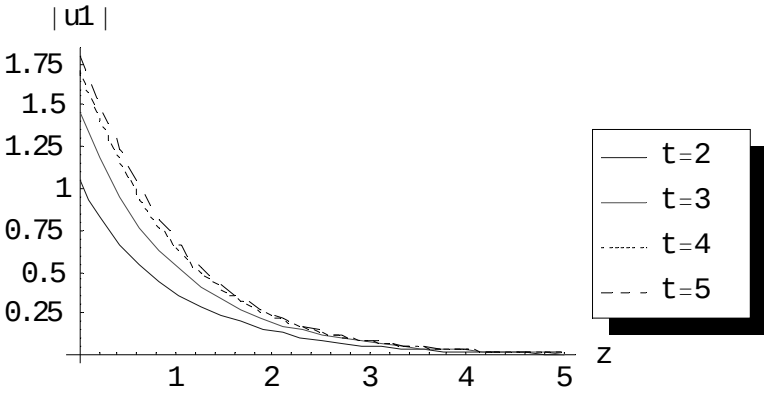

Fig.(4.15) the first order approximation of $\left|u^{(1)}\right|$ at $\varepsilon = 0.2, \gamma = 1$ and $\alpha, \rho_1, \rho_2 = 1, T = 10, M = 10$ for different values of t.

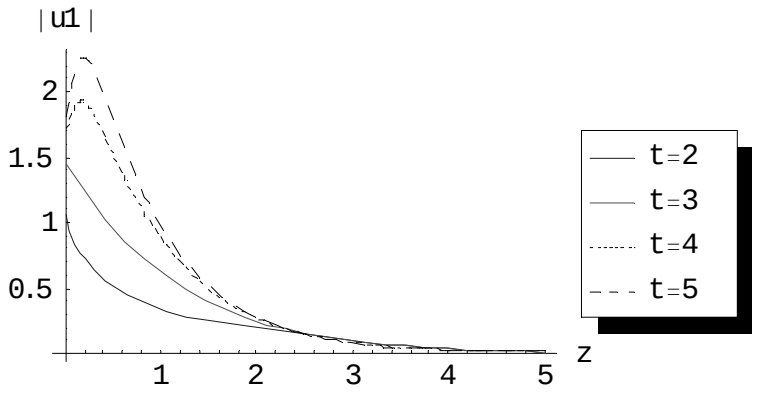

Fig. (4.16) the first order approximation of $\left|u^{(1)}\right|$ at $\varepsilon = 1, \gamma = 1$ and $\alpha, \rho_1, \rho_2 = 1, T = 10, M = 10$ for different values of t.

Note: we calculated till second order only taking M=10 for $\gamma = 0$, while we calculated till first order taking M=10 for $\gamma = 1$ and we cannot calculate more since the machine gives "MATHEMATICA KERNEL OUT OF MEMORY".

4.3.2 Case study 2

Taking the case $f_1(t) = \rho_1$, $f_2(t) = \rho_2 \sin\left(\frac{m\pi}{T}\right) t$, where ρ_1 & ρ_2 are constants and following the algorithm, the following selected results for the first and second order approximations are got:

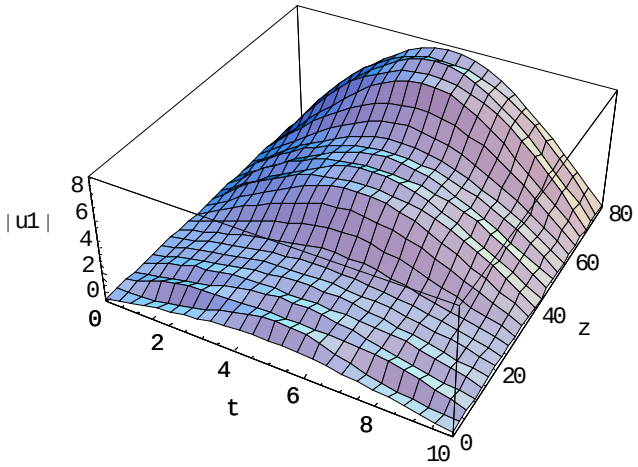

Fig. (4.17) the first order approximation of $\left|u^{(1)}\right|$ at $\varepsilon = 0.05$, $\gamma = 0$ and $\alpha, \rho_1, \rho_2 = 1, T = 10$ with considering only ten terms on the series (M=10).

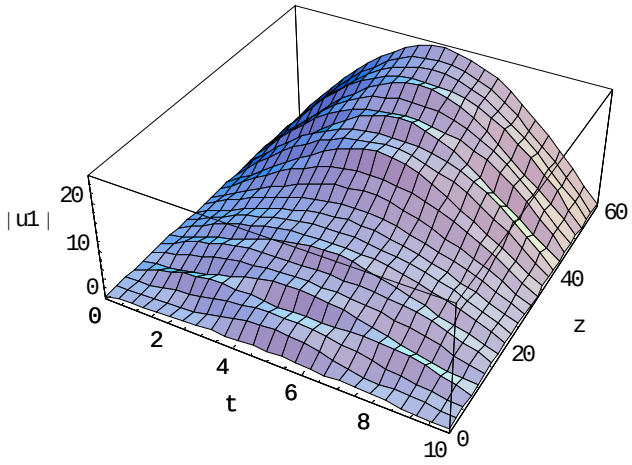

Fig. (4.18) the first order approximation of $\left|u^{(1)}\right|$ at $\varepsilon = 0.2$, $\gamma = 0$ and $\alpha, \rho_1, \rho_2 = 1, T = 10$ with considering only ten terms on the series (M=10).

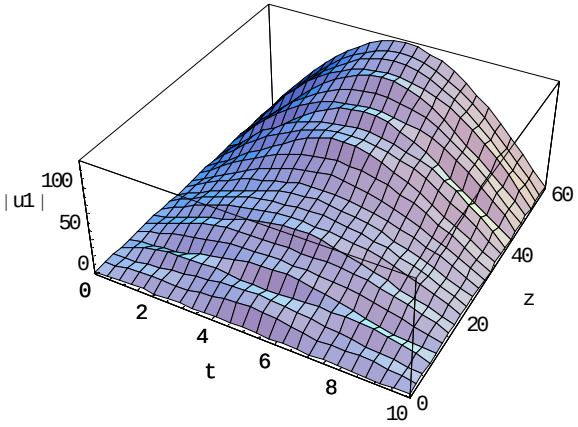

Fig. (4.19) the first order approximation of $\left|u^{(1)}\right|$ at $\varepsilon = 1$, $\gamma = 0$ and $\alpha, \rho_1, \rho_2 = 1, T = 10$ with considering only ten terms on the series (M=10).

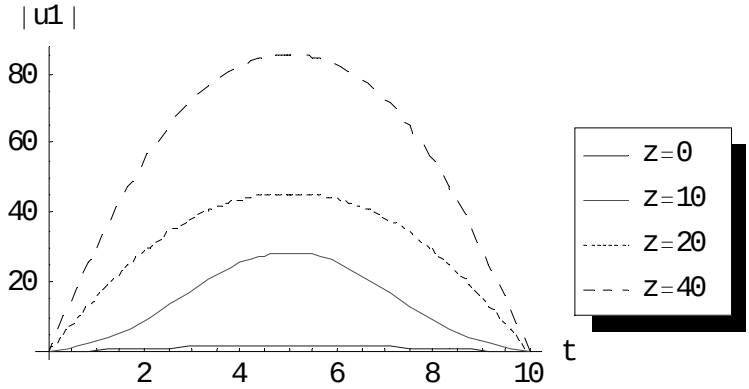

Fig. (4.20) the first order approximation of $\left|u^{(1)}\right|$ at $\varepsilon = 0.2, \gamma = 0$ and $\alpha, \rho_1, \rho_2 = 1, T = 10, M = 10$ for different values of z.

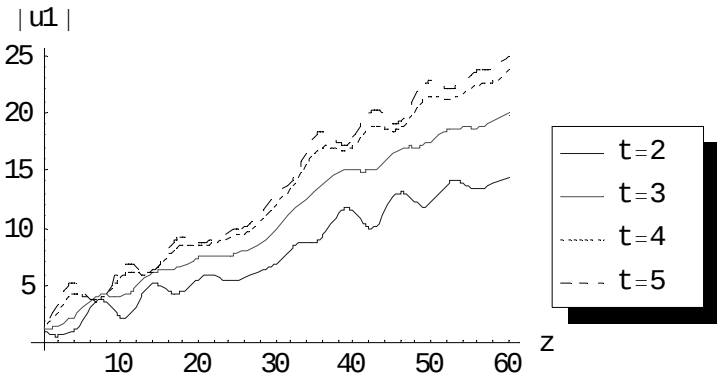

Fig. (4.21) the first order approximation of $\left|u^{(1)}\right|$ at $\varepsilon = 0.2, \gamma = 0$ and $\alpha, \rho_1, \rho_2 = 1, T = 10, M = 10$ for different values of t.

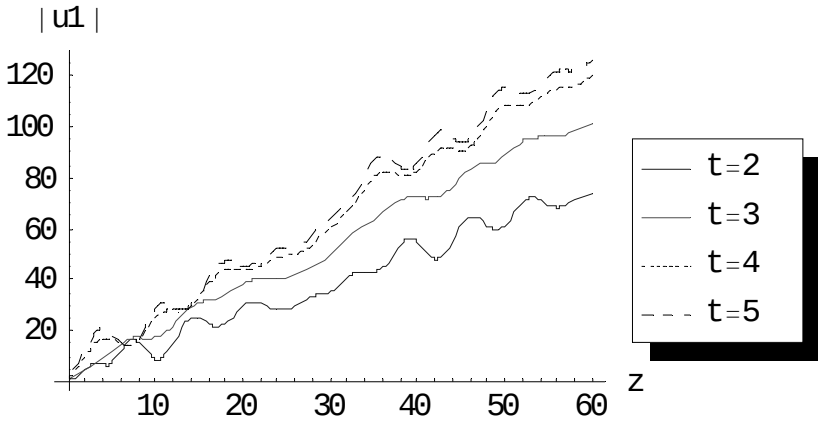

Fig. (4.22) the first order approximation of $\left|u^{(1)}\right|$ at $\varepsilon = 1, \gamma = 0$ and $\alpha, \rho_1, \rho_2 = 1, T = 10, M = 10$ for different values of t.

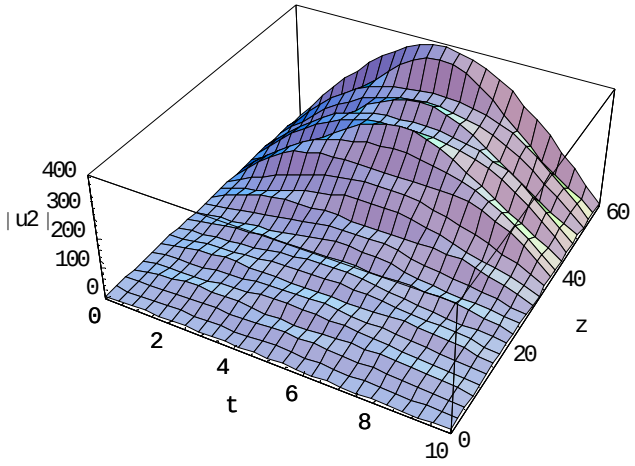

Fig. (4.23) the second order approximation of $\left|u^{(2)}\right|$ at $\varepsilon = 0.2$, $\gamma = 0$ and $\alpha, \rho_1, \rho_2 = 1, T = 10$ with considering only ten terms on the series (M=10).

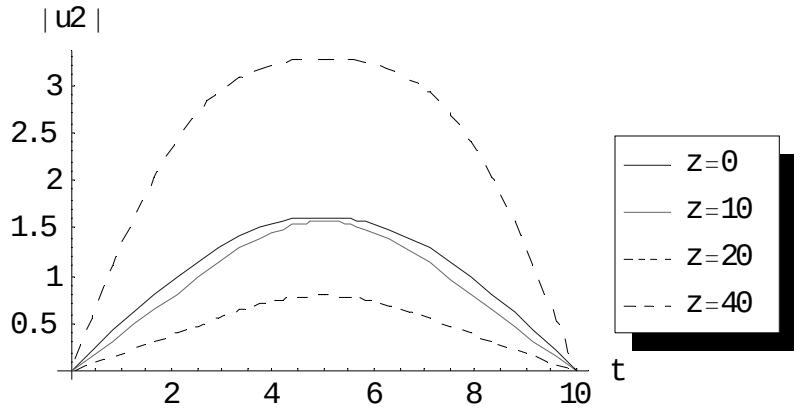

Fig. (4.24) the second order approximation of $\left|u^{(2)}\right|$ at $\varepsilon = 0.05, \gamma = 0$ and $\alpha, \rho_1, \rho_2 = 1, T = 10, M = 10$ for different values of z.

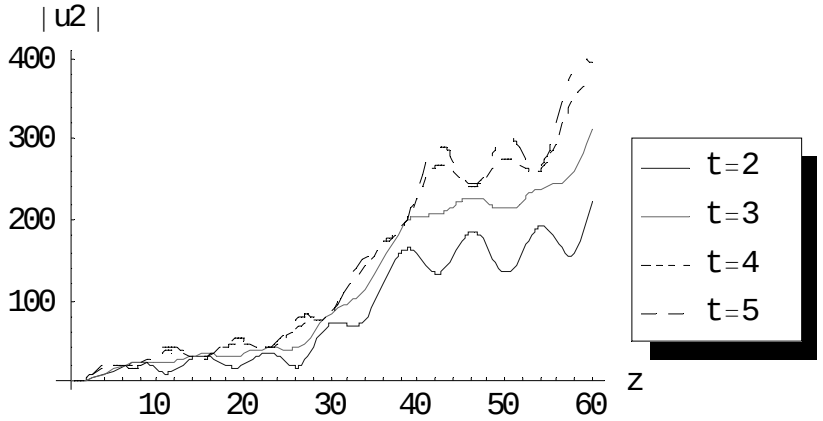

Fig. (4.25) the second order approximation of $\left|u^{(2)}\right|$ at $\varepsilon = 0.2, \gamma = 0$ and $\alpha, \rho_1, \rho_2 = 1, T = 10, M = 10$ for different values of t.

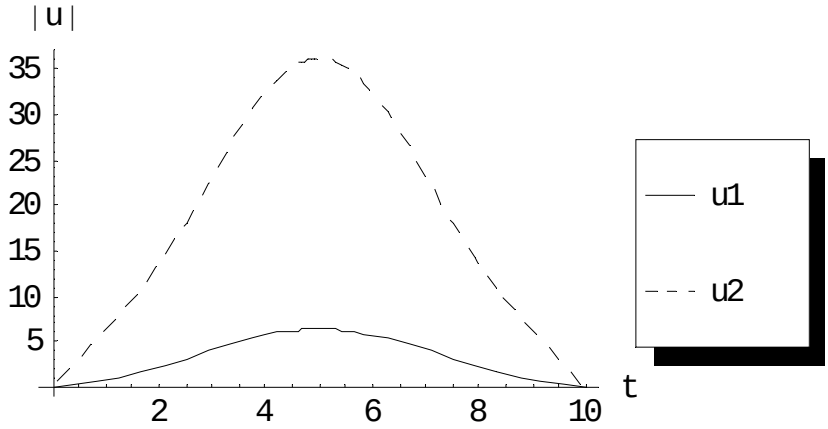

Fig.(4.26) comparison between first and second approximations at $\varepsilon = 0.2, \gamma = 0$ and $\alpha, \rho_1, \rho_2 = 1,\ T = 10,\ z = 10.$

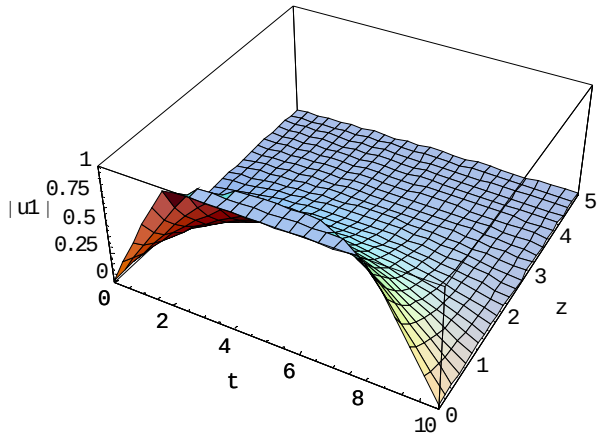

Fig. (4.27) the first order approximation of $\left|u^{(1)}\right|$ at $\varepsilon = 0.2$, $\gamma = 1$ and $\alpha, \rho_1, \rho_2 = 1, T = 10$ with considering only ten terms on the series (M=10).

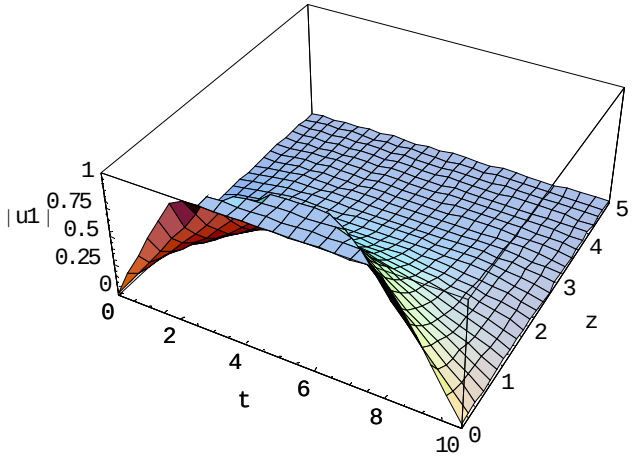

Fig. (4.28) the first order approximation of $\left|u^{(1)}\right|$ at $\varepsilon = 1$, $\gamma = 1$ and $\alpha, \rho_1, \rho_2 = 1, T = 10$ with considering only ten terms on the series (M=10).

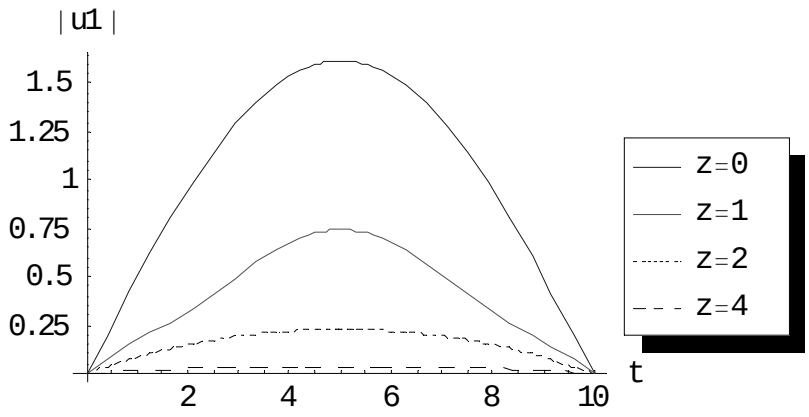

Fig. (4.29) the first order approximation of $\left|u^{(1)}\right|$ at $\varepsilon = 1, \gamma = 1$ and $\alpha, \rho_1, \rho_2 = 1, T = 10, M = 10$ for different values of z.

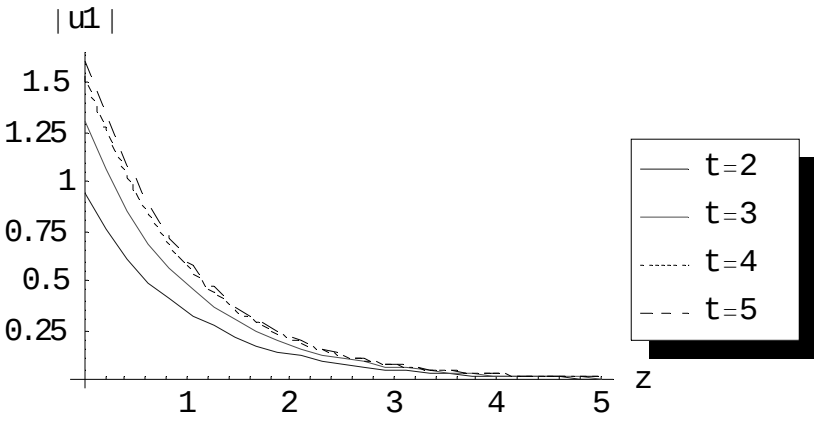

Fig. (4.30) the first order approximation of $\left|u^{(1)}\right|$ at $\varepsilon = 0.2, \gamma = 1$ and $\alpha, \rho_1, \rho_2 = 1, T = 10, M = 10$ for different values of z.

Note: we calculated till second order only taking M=10 for $\gamma = 0$, while we calculated till first order taking M=10 for $\gamma = 1$ and we cannot calculate more since the machine gives "MATHEMATICA KERNEL OUT OF MEMORY".

4.3.3 Case study 3

Taking the case $f_1(t) = \rho_1 e^{-t}$, $f_2(t) = \rho_2 e^{-t}$ where ρ_1 & ρ_2 are constants and following the algorithm, the following selected results for the first and second order approximations are got:

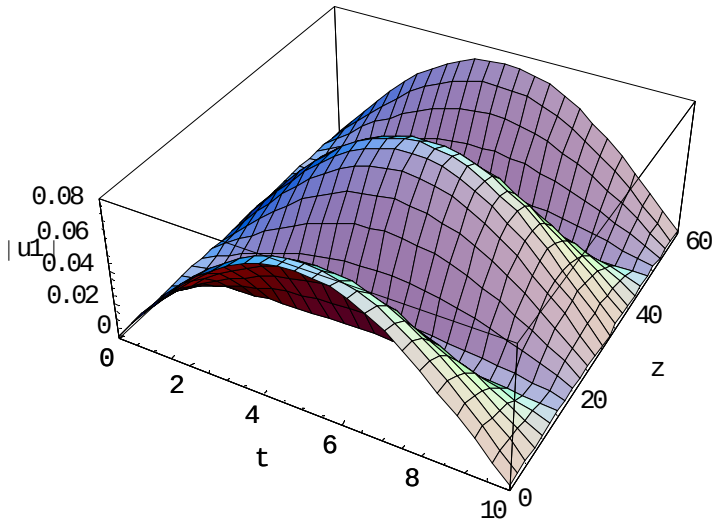

Fig. (4.31) the first order approximation of $\left|u^{(1)}\right|$ at $\varepsilon = 1$, $\gamma = 0$ and $\alpha, \rho_1, \rho_2 = 1, T = 10$ with considering only ten terms on the series (M=10).

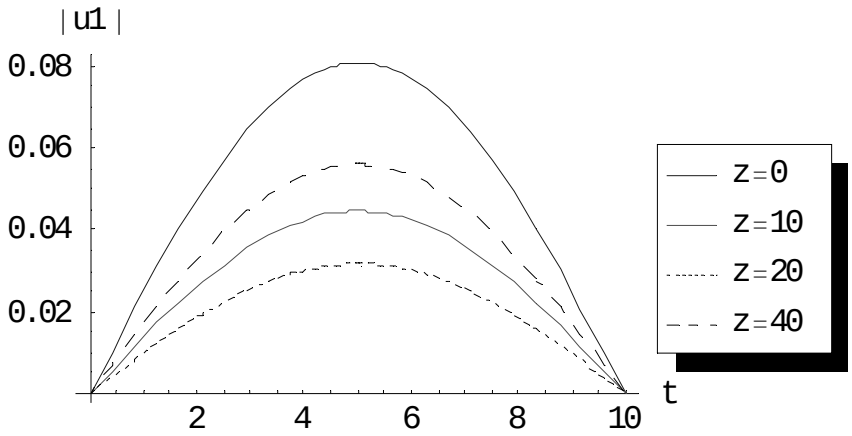

Fig. (4.32) the first order approximation of $\left|u^{(1)}\right|$ at $\varepsilon = 0.2, \gamma = 0$ and $\alpha, \rho_1, \rho_2 = 1, T = 10, M = 10$ for different values of z.

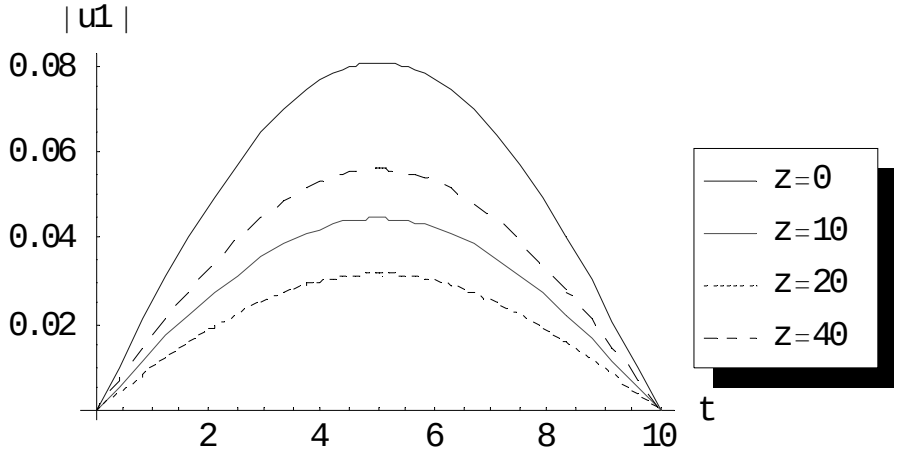

Fig. (4.33) the first order approximation of $\left|u^{(1)}\right|$ at $\varepsilon = 1, \gamma = 0$ and $\alpha, \rho_1, \rho_2 = 1, T = 10, M = 10$ for different values of z.

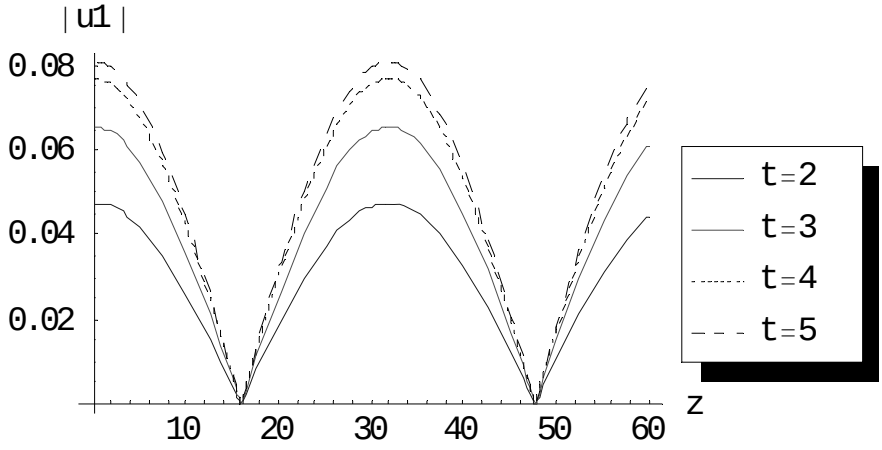

Fig. (4.34) the first order approximation of $\left|u^{(1)}\right|$ at $\varepsilon = 1, \gamma = 0$ and $\alpha, \rho_1, \rho_2 = 1, T = 10, M = 10$ for different values of t.

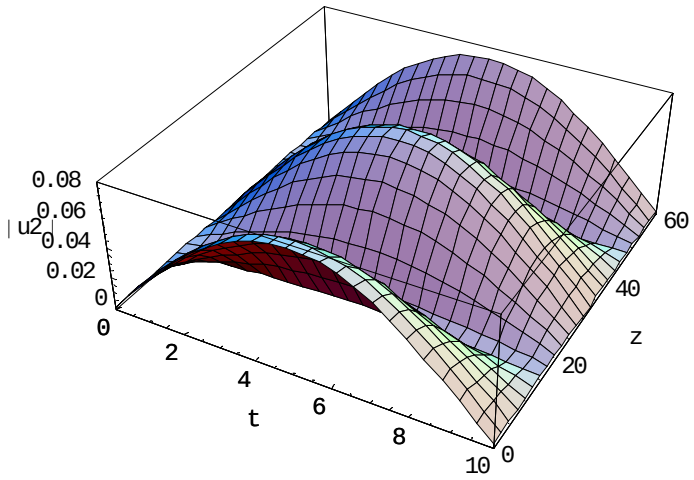

Fig. (4.35) the second order approximation of $\left|u^{(2)}\right|$ at $\varepsilon = 0.2$, $\gamma = 0$ and $\alpha, \rho_1, \rho_2 = 1, T = 10$ with considering only ten terms on the series (M=10).

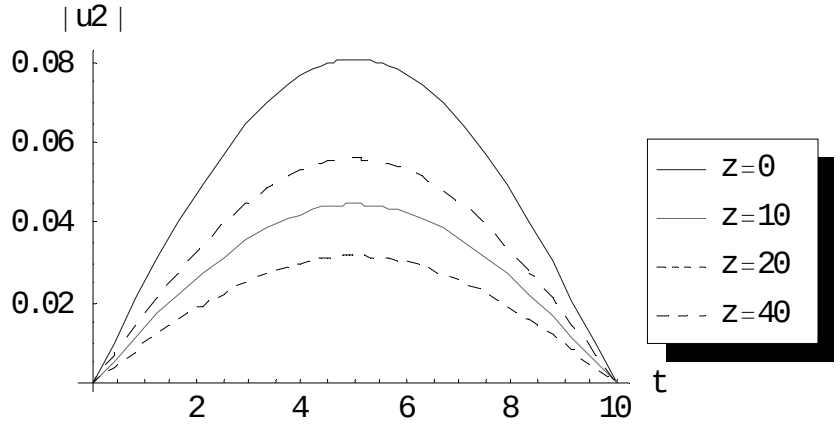

Fig. (4.36) the second order approximation of $\left|u^{(2)}\right|$ at $\varepsilon = 0.2, \gamma = 0$ and $\alpha, \rho_1, \rho_2 = 1, T = 10, M = 10$ for different values of z.

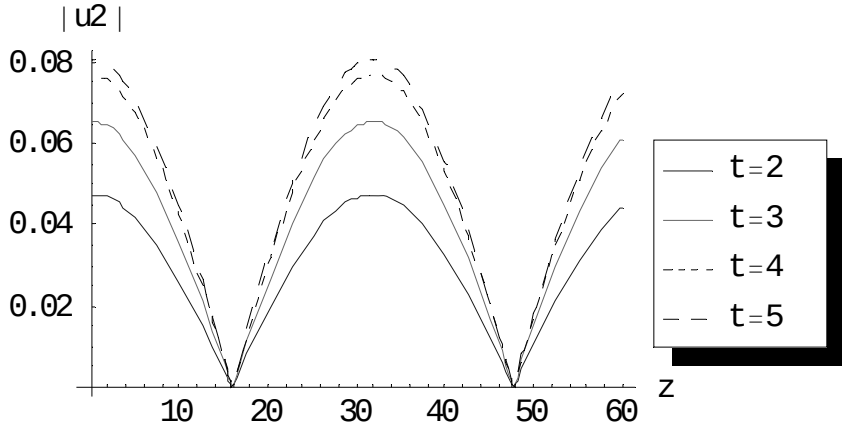

Fig. (4.37) the second order approximation of $\left|u^{(2)}\right|$ at $\varepsilon = 0.2, \gamma = 0$ and $\alpha, \rho_1, \rho_2 = 1, T = 10, M = 10$ for different values of t.

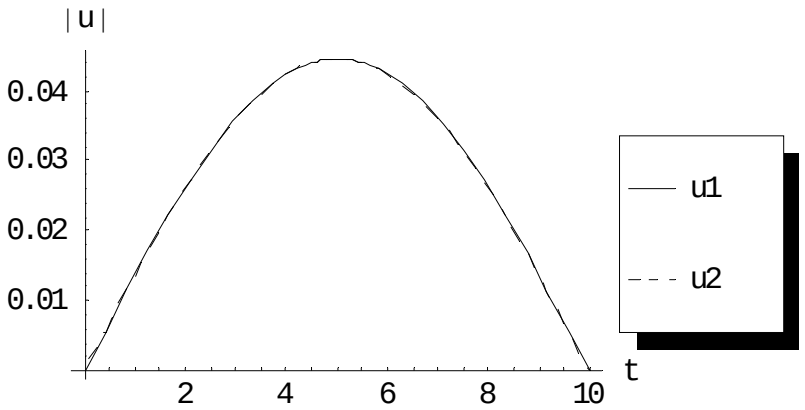

Fig. (4.38) comparison between first and second approximations at $\varepsilon = 0.2, \gamma = 0$ and $\alpha, \rho_1, \rho_2 = 1,\ T = 10,\ z = 10.$

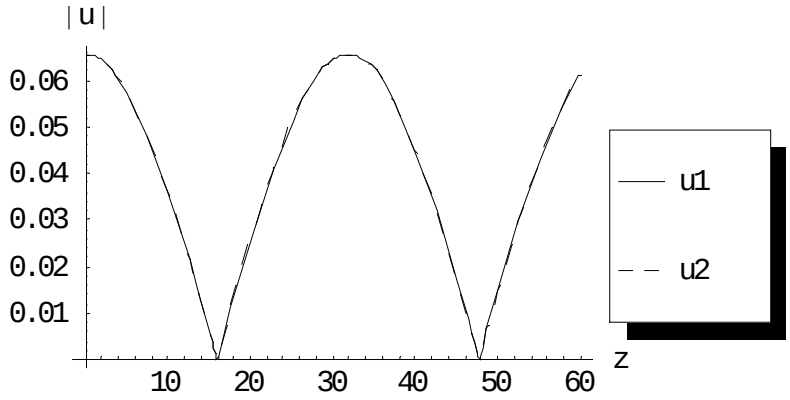

Fig. (4.39) comparison between first and second approximations at $\varepsilon = 0.2, \gamma = 0$ and $\alpha, \rho_1, \rho_2 = 1,\ T = 10,\ t = 4.$

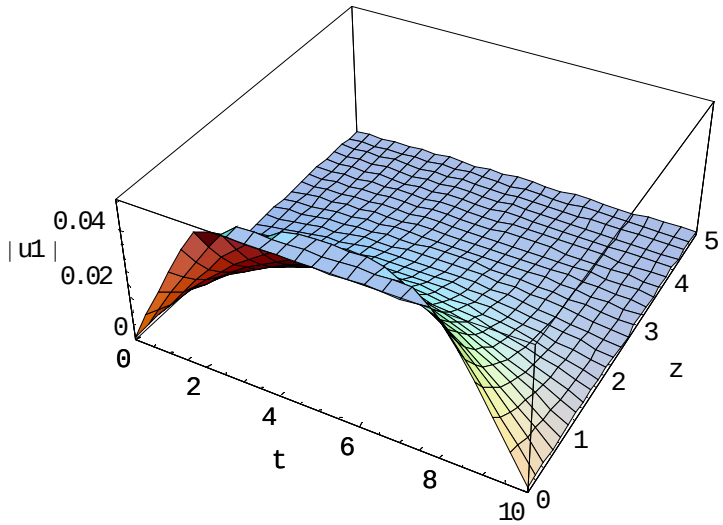

Fig. (4.40) the first order approximation of $\left|u^{(1)}\right|$ at $\varepsilon = 0.2$, $\gamma = 1$ and $\alpha, \rho_1, \rho_2 = 1, T = 10$ with considering only ten terms on the series (M=10).

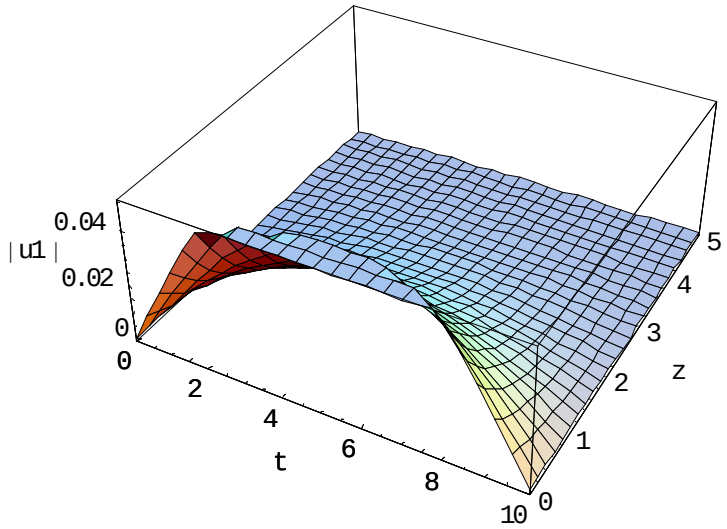

Fig. (4.41) the first order approximation of $\left|u^{(1)}\right|$ at $\varepsilon = 1$, $\gamma = 1$ and $\alpha, \rho_1, \rho_2 = 1, T = 10$ with considering only ten terms on the series (M=10).

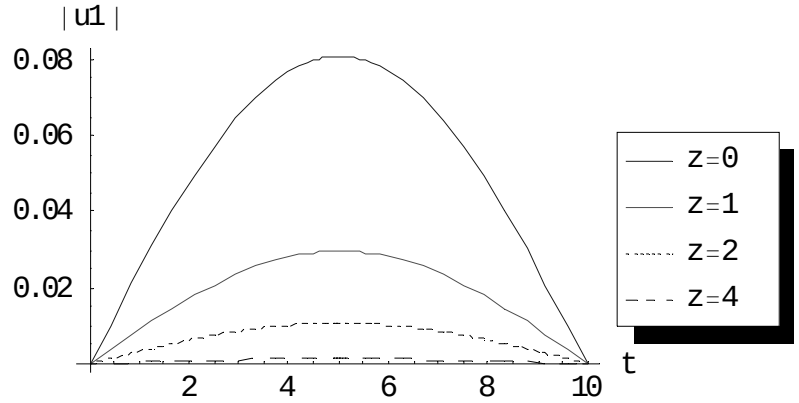

Fig. (4.42) the first order approximation of $\left|u^{(1)}\right|$ at $\varepsilon = 0.2, \gamma = 1$ and $\alpha, \rho_1, \rho_2 = 1, T = 10, M = 10$ for different values of z.

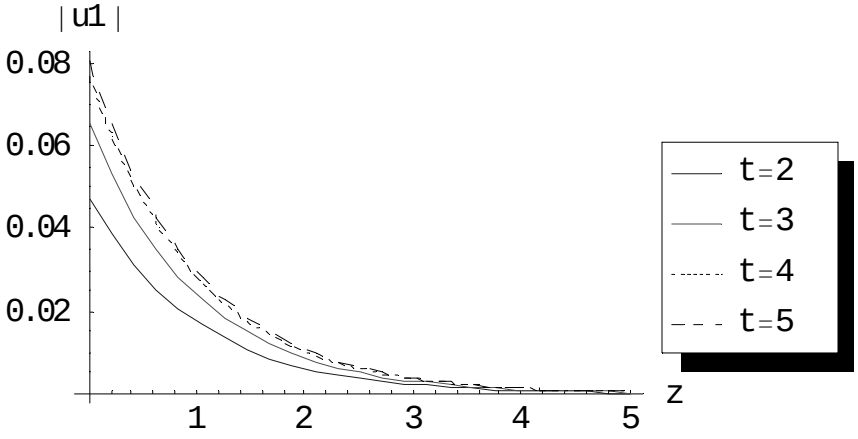

Fig. (4.43) the first order approximation of $\left|u^{(1)}\right|$ at $\varepsilon = 0.2, \gamma = 1$ and $\alpha, \rho_1, \rho_2 = 1, T = 10, M = 10$ for different values of t.

Note: we calculated till second order only taking M=10 for $\gamma = 0$, while we calculated till first order taking M=10 for $\gamma = 1$ and we cannot calculate more since the machine gives "MATHEMATICA KERNEL OUT OF MEMORY".

4.4 Picard Approximation

Consider the homogeneous nonlinear Schrodinger equation:

$$i\,\frac{\partial u(t,z)}{\partial z} + \alpha\,\frac{\partial^2 u(t,z)}{\partial t^2} + \varepsilon|u(t,z)|^4 u(t,z) + i\,\gamma u(t,z) = 0,$$

$$(t,z) \in (0,T)\ x\ (0,\infty) \tag{4.46}$$

where $u(t,z)$ is a complex valued function which is subjected to the initial and boundary conditions mentioned before in equations (4.2), (4.3) respectively.

Let $u(t\,,z) = \psi(t\,,z) + i\,\phi(t\,,\ z), \psi\,, \phi$: are real valued functions. The following coupled equations are got:

$$\frac{\partial \phi(t,z)}{\partial z} = \alpha\,\frac{\partial^2 \psi(t,z)}{\partial t^2} + \varepsilon(\psi^2 + \phi^2)^2\psi - \gamma\phi, \tag{4.47}$$

$$\frac{\partial \psi(t,z)}{\partial z} = -\alpha\,\frac{\partial^2 \phi(t,z)}{\partial t^2} - \varepsilon(\psi^2 + \phi^2)^2\phi - \gamma\phi, \tag{4.48}$$

Where $\psi(t,0) = f_1(t),\ \phi(t,0) = f_2(t)$, and all other corresponding I.Cs. and B.Cs. are zeros.

$$\frac{\partial \phi_i(t,z)}{\partial z} = \alpha\,\frac{\partial^2 \psi_i(t,z)}{\partial t^2} + H_{1i}\ ,\qquad i \geq 1 \tag{4.49}$$

$$\frac{\partial \psi_i(t,z)}{\partial z} = \alpha\,\frac{\partial^2 \phi_i(t,z)}{\partial t^2} + H_{2i}\ ,\qquad i \geq 1 \tag{4.50}$$

Where $\psi_i(t,0) = f_1(t),\ \phi_i(t,0) = f_2(t)$, and all other all corresponding conditions are zeros. H_{1i}, H_{2i} are functions to be computed from previous steps.

4.4.1 Picard order of approximations

4.4.1.1 Zero order approximation

The zero order approximation is similar as illustrated in Appendix (A).

4.4.1.2 First order approximation

$$i\,\frac{\partial u_1(t,z)}{\partial z} + \alpha\,\frac{\partial^2 u_1(t,z)}{\partial t^2} + \varepsilon|u_0(t,z)|^4 u_0(t,z) + i\,\gamma u_1(t,z) = 0\,,(t,z) \in (0,T)\,x\,(0,\infty) \tag{4.51}$$

With initial conditions $u_1(t,0) = f_1(t) + i\,f_2(t)$ and boundary conditions $u_1(0,z) = u_1(T,z) = 0$. Following Appendix (A), the linear Schrodinger equation (4.51) has the following solution:

$$u_1(t\,,z) = \psi_1 + i\,\phi_1\,, \tag{4.52}$$

$$\psi_1(t\,,z) = e^{-\gamma z}\sum_{n=0}^{\infty} T_{1n}(z)\sin\left(\frac{n\,\pi}{T}\right)t, \tag{4.53}$$

$$\phi_1(t\,,z) = e^{-\gamma z}\sum_{n=0}^{\infty} \tau_{1n}(z)\sin\left(\frac{n\,\pi}{T}\right)t \tag{4.54}$$

Following Appendix (A), for *n=1,* we can find that:

$$H_{11} = \varepsilon e^{-4\gamma z}\,({\psi_0}^2 + {\phi_0}^2)^2\psi_0 \tag{4.55}$$

$$H_{21} = -\,\varepsilon e^{-4\gamma z}({\phi_0}^2 + {\psi_0}^2)^2\phi_0 \tag{4.56}$$

where

$$T_{1n}(z) = A_{11}(z)\sin\beta_n z + \left(\left(C_{12} + B_{11}(z)\right)\cos\beta_n z, \tag{4.57}$$

$$\tau_{1n}(z) = A_{12}\,(\mathrm{z})\sin\beta_n z + \left(\left(C_{14} + B_{12}(z)\right)\cos\beta_n z, \tag{4.58}$$

Where the constants and variables $A_{11}\,, C_{12}\,,\ B_{11}\,,\ A_{12}\,, C_{14}\,, B_{12}$ can be calculated in similar manner calculated in similar manner as illustrated in Appendix (A).

The absolute value of the first order approximation is:

$$|u_1(t\,,z)|^2 = \psi_1{}^2 + \phi_1{}^2 \tag{4.59}$$

4.4.1.3 Second order approximation

$$i\,\frac{\partial u_2(t,z)}{\partial z} + \alpha\,\frac{\partial^2 u_2(t,z)}{\partial t^2} + \varepsilon|u_1(t,z)|^4 u_1(t,z) + i\,\gamma u_2(t,z) = 0,$$

$$(t,z) \in (0,T)\;x\;(0,\infty) \tag{4.60}$$

with initial conditions $u_2(t,0) = f_1(t) + i\,f_2(t)$ and boundary conditions $u_2(0,z) = u_2(T,z) = 0$. Following Appendix (A), the linear Schrodinger equation (4.60) has the following solution:

$$u_2(t\,,z) = \psi_2 + i\,\phi_2\,, \tag{4.61}$$

$$\psi_2(t\,,z) = e^{-\gamma z}\sum_{n=0}^{\infty} T_{2n}(z)\sin\left(\frac{n\,\pi}{T}\right)t, \tag{4.62}$$

$$\phi_2(t\,,z) = e^{-\gamma z}\sum_{n=0}^{\infty} \tau_{2n}(z)\sin\left(\frac{n\,\pi}{T}\right)t \tag{4.63}$$

Following Appendix (A), for *n=2,* we can find that:

$$H_{12} = \varepsilon\,e^{-4\gamma z}(\psi_1{}^2 + \phi_1{}^2)^2\,\psi_1 \tag{4.64}$$

$$H_{22} = -\varepsilon\,e^{-4\gamma z}(\,\phi_1{}^2 + \psi_1{}^2)^2\phi_1 \tag{4.65}$$

where

$$T_{2n}(z) = A_{21}(z)\sin\beta_n z + \left(\left(C_{22} + B_{21}(z)\right)\cos\beta_n z, \right. \tag{4.66}$$

$$\tau_{2n}(z) = A_{22}(z)\sin\beta_n z + \left(\left(C_{24} + B_{22}(z)\right)\cos\beta_n z, \right. \tag{4.67}$$

where the constants and variables $A_{21}\,, C_{22}\,,\ B_{21}\,,\ A_{22}\,, C_{24}\,, B_{22}$ can be calculated in similar manner as illustrated in Appendix A.

The absolute value of the second order approximation is:

$$|u_2(t\,,z)|^2 = \psi_2{}^2 + \phi_2{}^2 \tag{4.76}$$

4.5 Case Studies, Picard

To examine the proposed solution algorithm, some case studies are illustrated.

4.5.1 Case study 1

Taking the case and $f_1(t) = \rho_1$, $f_2(t) = \rho_2$ where ρ_1 & ρ_2 are constants and following the algorithm of Picard Approximation, the following selected results for the first and second order approximations are got:

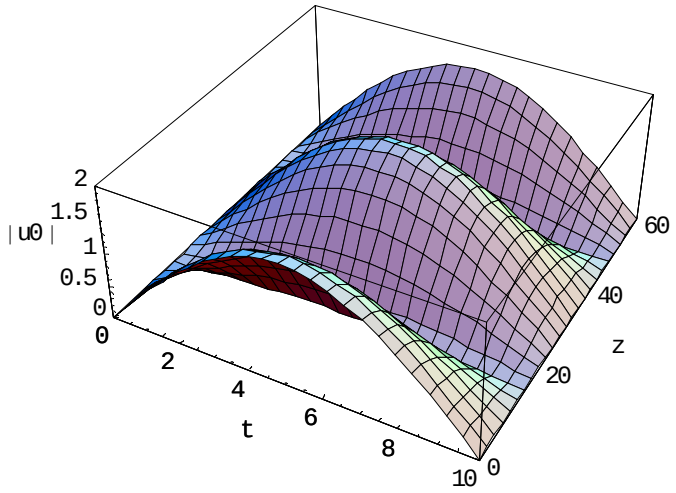

Fig. (4.44) the zero order approximation of $\left|u^{(0)}\right|$ at $\varepsilon = 0$, $\gamma = 0$ and $\alpha, \rho_1, \rho_2 = 1, T = 10$ with considering only one term on the series (M=1).

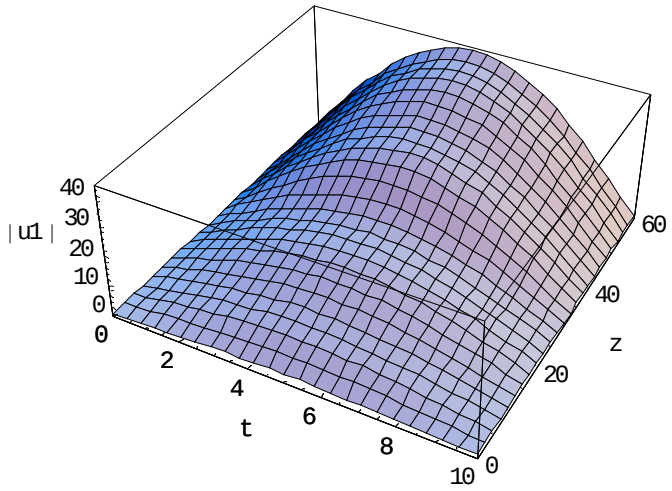

Fig. (4.45) the first order approximation of $\left|u^{(1)}\right|$ at $\varepsilon = 0.2$, $\gamma = 0$ and $\alpha, \rho_1, \rho_2 = 1, T = 10$ with considering only one term on the series (M=1).

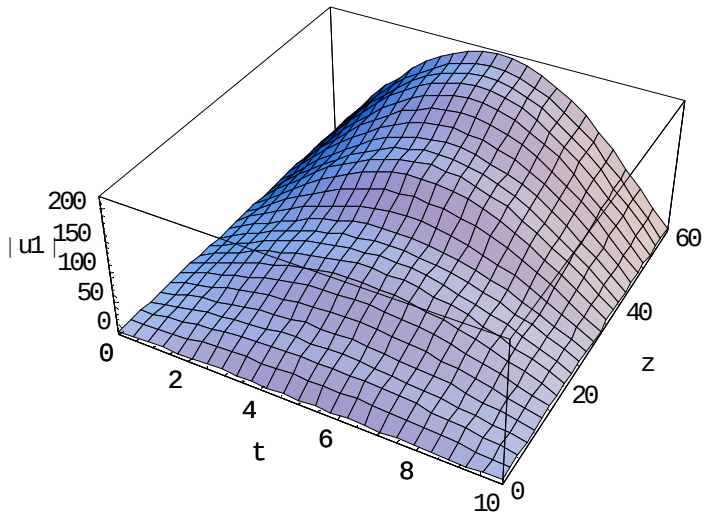

Fig. (4.46) the first order approximation of $\left|u^{(1)}\right|$ at $\varepsilon = 1$, $\gamma = 0$ and $\alpha, \rho_1, \rho_2 = 1, T = 10$ with considering only one term on the series (M=1).

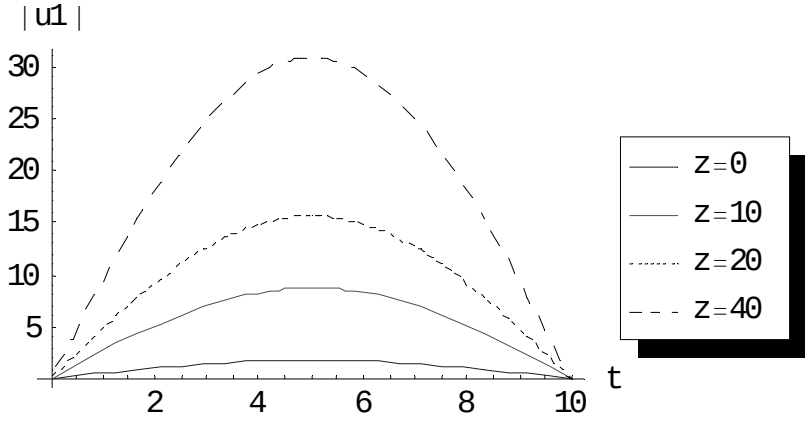

Fig. (4.47) the first order approximation of $\left|u^{(1)}\right|$ at $\varepsilon = 0.2, \gamma = 0$ and $\alpha, \rho_1, \rho_2 = 1, T = 10, M = 1$ for different values of z.

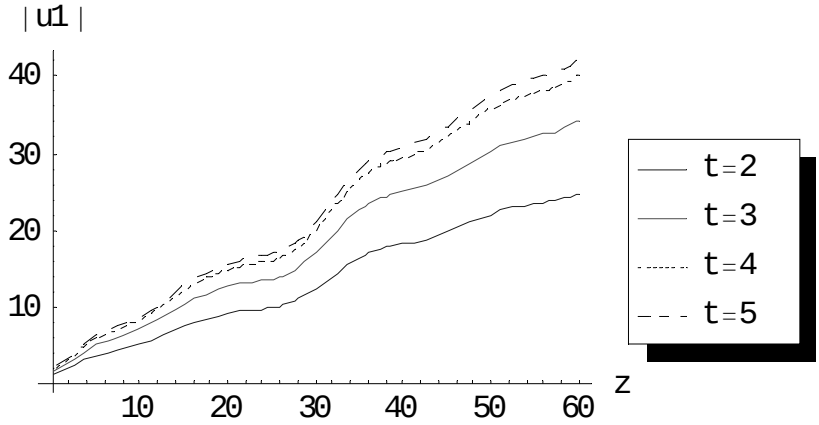

Fig. (4.48) the first order approximation of $\left|u^{(1)}\right|$ at $\varepsilon = 0.2, \gamma = 0$ and $\alpha, \rho_1, \rho_2 = 1, T = 10, M = 1$ for different values of t.

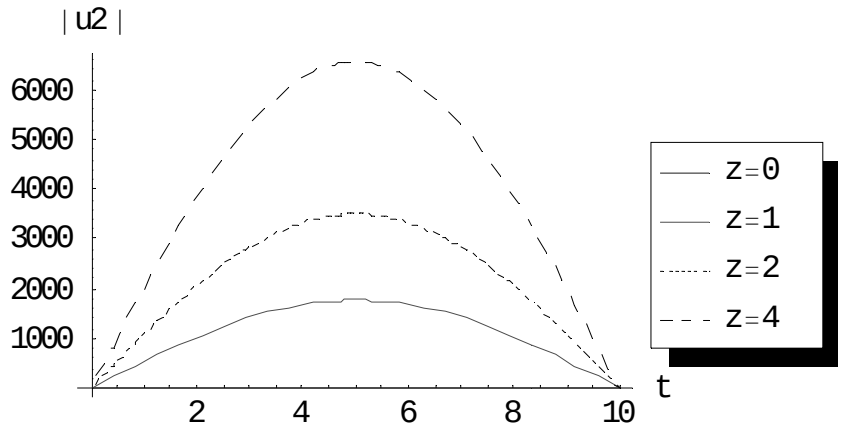

Fig.(4.49) the second order approximation of $\left|u^{(2)}\right|$ at $\varepsilon = 0.2, \gamma = 0$ and $\alpha, \rho_1, \rho_2 = 1, T = 10, M = 1$ for different values of z.

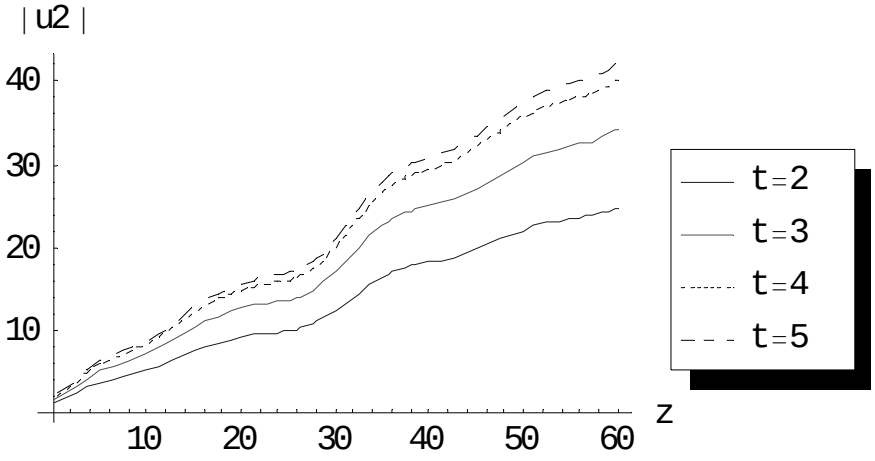

Fig. (4.50) the second order approximation of $\left|u^{(2)}\right|$ at $\varepsilon = 0.2, \gamma = 0$ and $\alpha, \rho_1, \rho_2 = 1, T = 10, M = 1$ for different values of t.

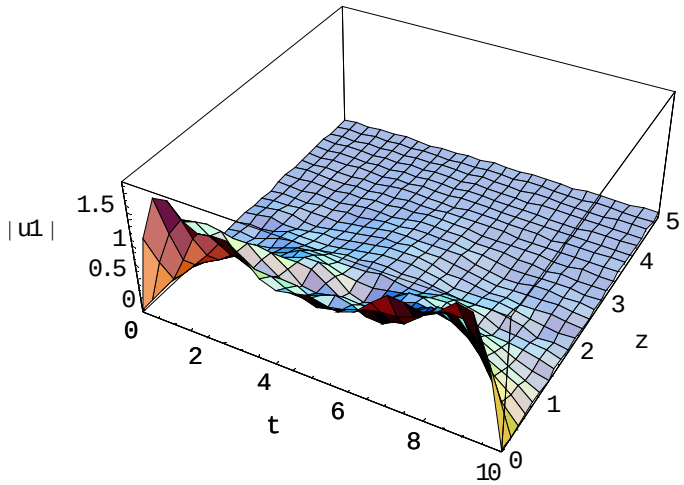

Fig. (4.51) the first order approximation of $\left|u^{(1)}\right|$ at $\varepsilon = 0.2$, $\gamma = 1$ and $\alpha, \rho_1, \rho_2 = 1, T = 10$ with considering only ten terms on the series (M=10).

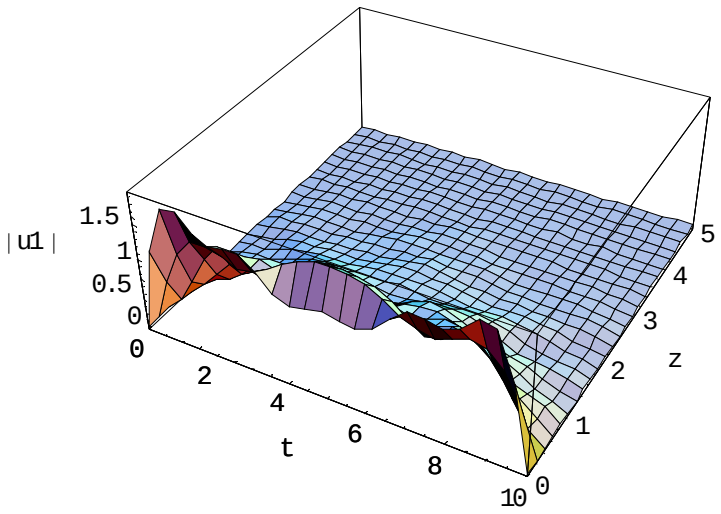

Fig.(4.52) the first order approximation of $\left|u^{(1)}\right|$ at $\varepsilon = 1$, $\gamma = 1$ and $\alpha, \rho_1, \rho_2 = 1, T = 10$ with considering only ten terms on the series (M=10).

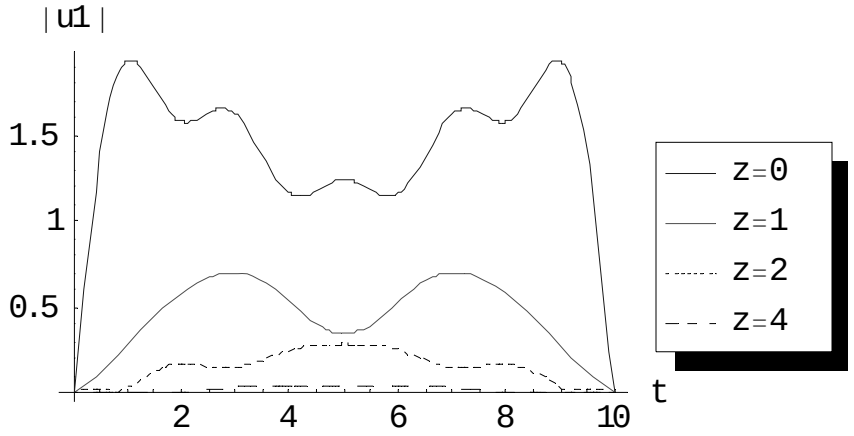

Fig. (4.53) the first order approximation of $\left|u^{(1)}\right|$ at $\varepsilon = 0.2, \gamma = 1$ and $\alpha, \rho_1, \rho_2 = 1, T = 10, M = 10$ for different values of z.

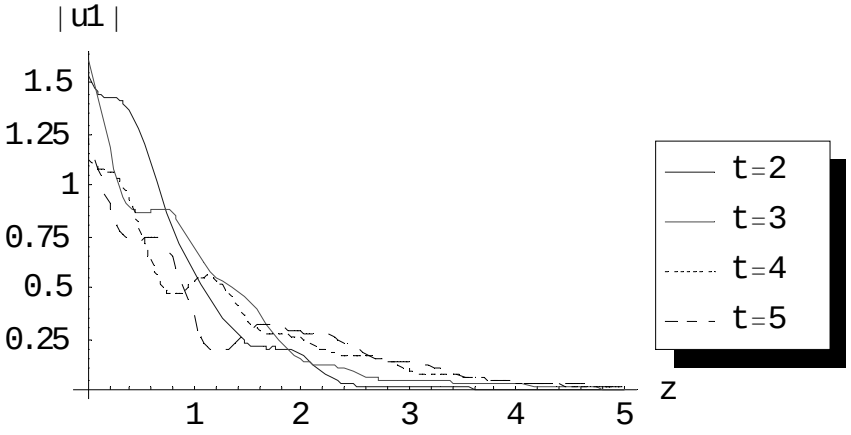

Fig. (4.54) the first order approximation of $\left|u^{(1)}\right|$ at $\varepsilon = 0.2, \gamma = 1$ and $\alpha, \rho_1, \rho_2 = 1, T = 10, M = 10$ for different values of t.

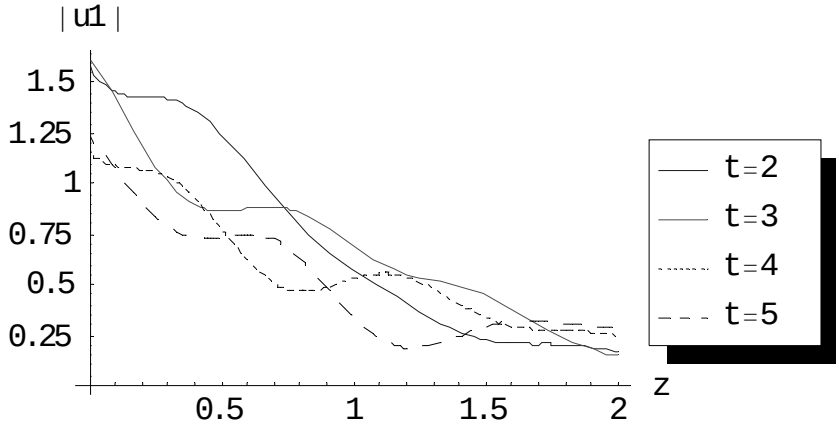

Fig. (4.55) the first order approximation of $\left|u^{(1)}\right|$ at $\varepsilon = 0.2, \gamma = 1$ and $\alpha, \rho_1, \rho_2 = 1, T = 10, M = 10$ for different values of t.

Note: we calculated till second order only taking M=1 for $\gamma = 0$ for both first order and second order respectively , while we calculated only till first order at $\gamma = 1$ taking M=10 and we cannot calculate more since the machine gives "MATHEMATICA KERNEL OUT OF MEMORY".

4.5.2 Case study 2

Taking the case $f_1(t) = \rho_1$, $f_2(t) = \rho_2 \sin\left(\frac{m\pi}{T}\right) t$ where ρ_1 & ρ_2 are constants and following the algorithm of Picard Approximation, the following selected results for the first and second order approximations are got:

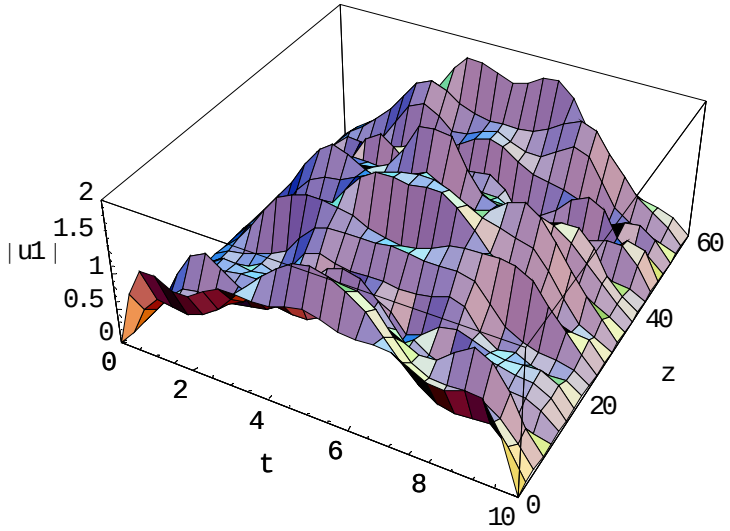

Fig. (4.56) the first order approximation of $\left|u^{(1)}\right|$ at $\varepsilon = 0$, $\gamma = 0$ and $\alpha, \rho_1, \rho_2 = 1, T = 10$ with considering only ten terms on the series (M=10).

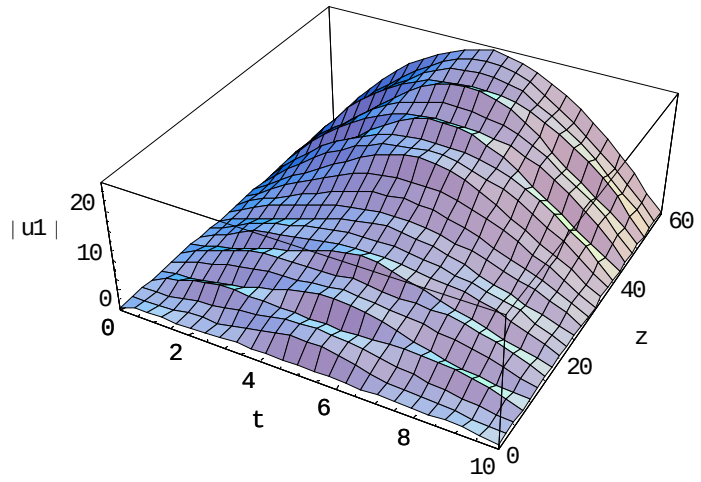

Fig. (4.57) the first order approximation of $\left|u^{(1)}\right|$ at $\varepsilon = 0.2$, $\gamma = 0$ and $\alpha, \rho_1, \rho_2 = 1, T = 10$ with considering only ten terms on the series (M=10).

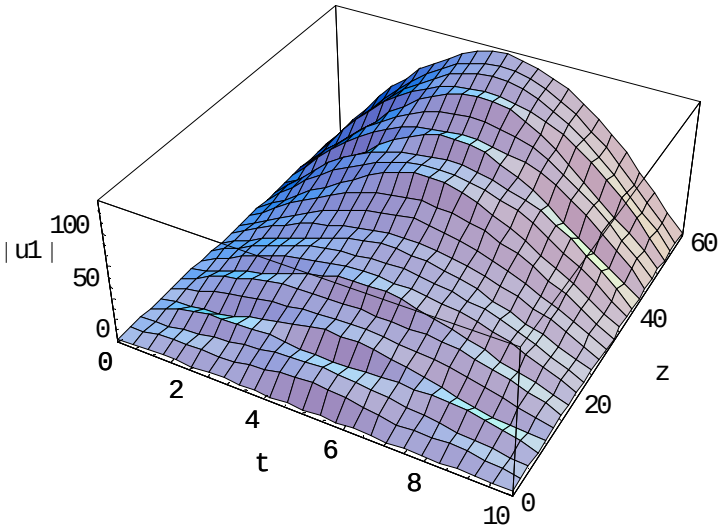

Fig. (4.58) the first order approximation of $\left|u^{(1)}\right|$ at $\varepsilon = 1$, $\gamma = 0$ and $\alpha, \rho_1, \rho_2 = 1, T = 10$ with considering only ten terms on the series (M=10).

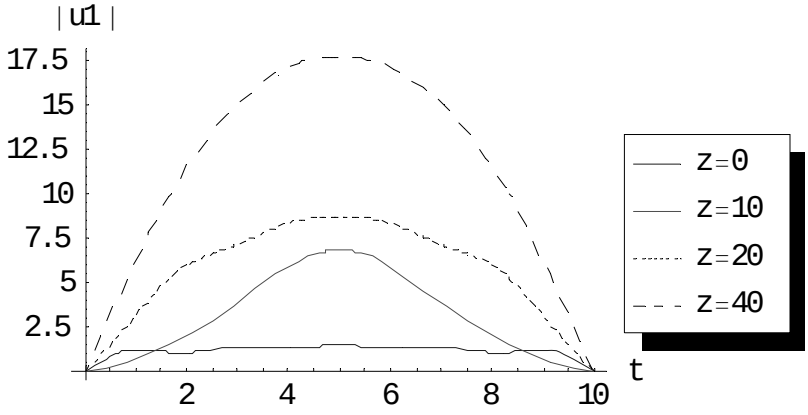

Fig. (4.59) the first order approximation of $\left|u^{(1)}\right|$ at $\varepsilon = 0.2, \gamma = 0$ and $\alpha, \rho_1, \rho_2 = 1, T = 10, M = 10$ for different values of z.

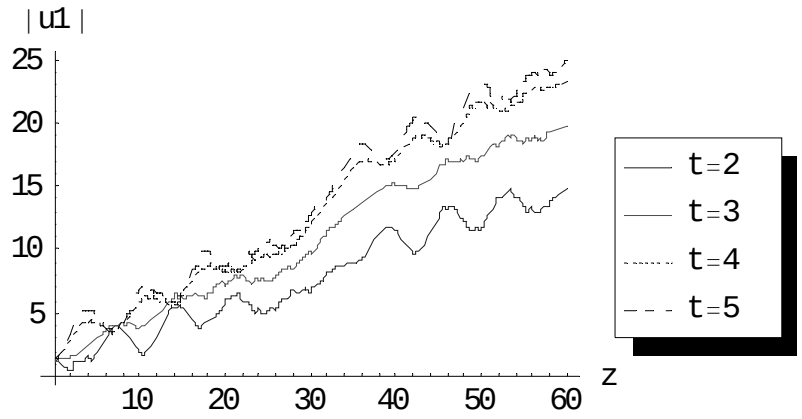

Fig. (4.60) the first order approximation of $\left|u^{(1)}\right|$ at $\varepsilon = 0.2, \gamma = 0$ and $\alpha, \rho_1, \rho_2 = 1, T = 10, M = 10$ for different values of t.

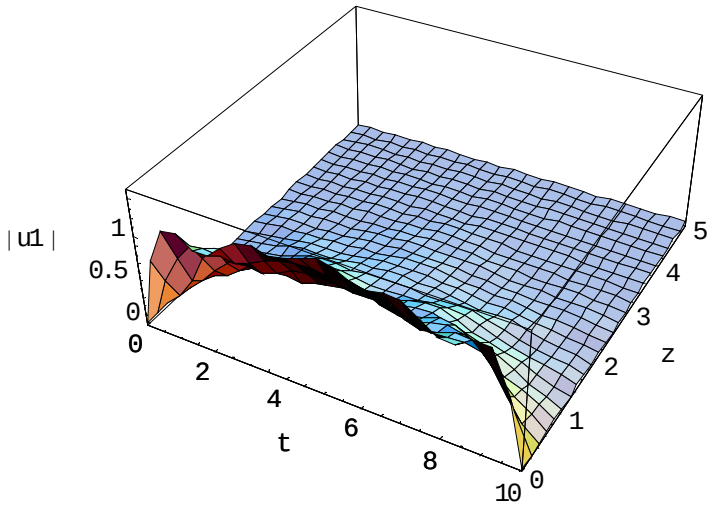

Fig. (4.61) the first order approximation of $\left|u^{(1)}\right|$ at $\varepsilon = 0.2$, $\gamma = 1$ and $\alpha, \rho_1, \rho_2 = 1, T = 10$ with considering only ten terms on the series (M=10).

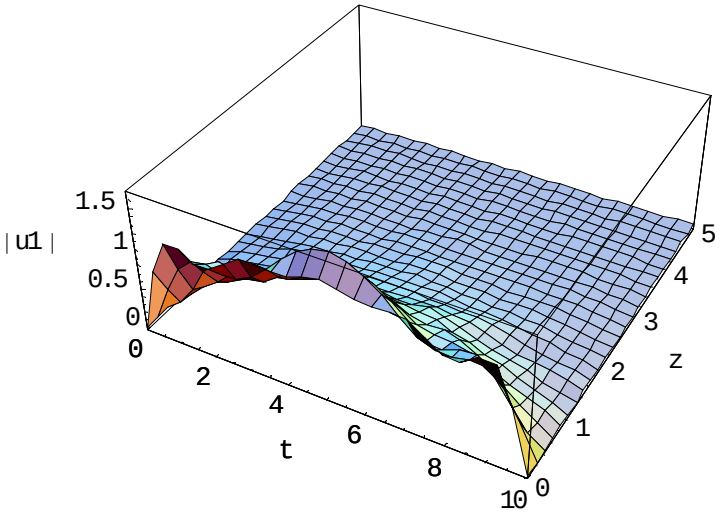

Fig. (4.62) the first order approximation of $\left|u^{(1)}\right|$ at $\varepsilon = 1$, $\gamma = 1$ and $\alpha, \rho_1, \rho_2 = 1, T = 10$ with considering only ten terms on the series (M=10).

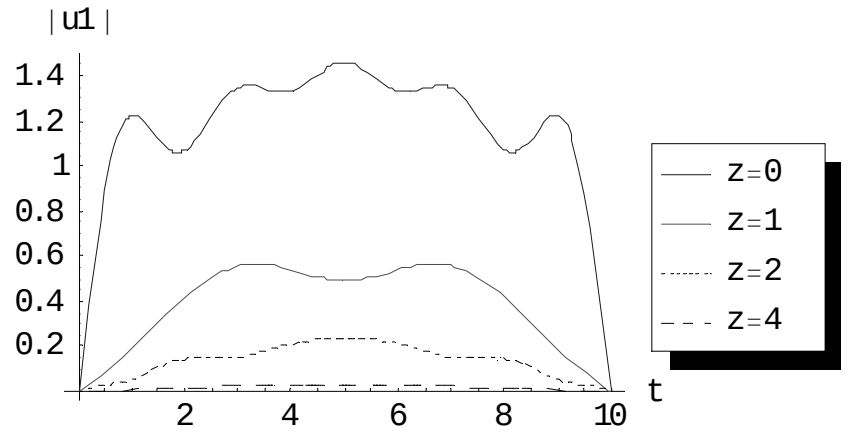

Fig. (4.63) the first order approximation of $\left|u^{(1)}\right|$ at $\varepsilon = 0.2, \gamma = 1$ and $\alpha, \rho_1, \rho_2 = 1, T = 10, M = 10$ for different values of z.

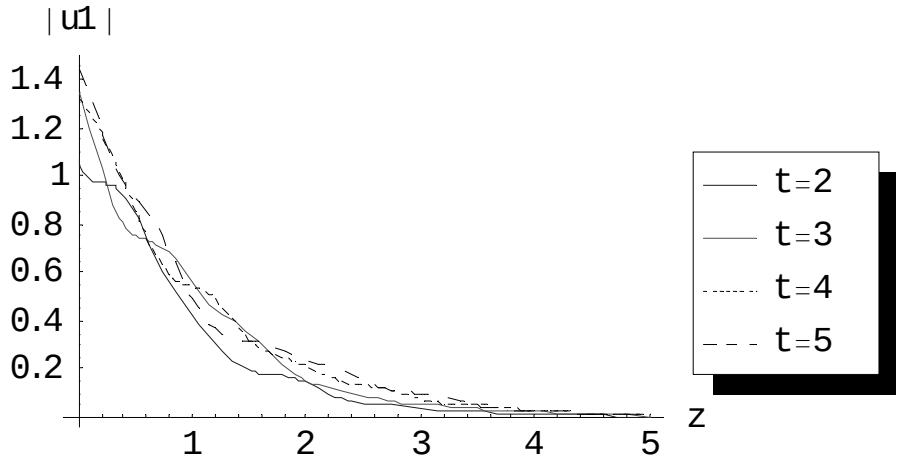

Fig. (4.64) the first order approximation of $\left|u^{(1)}\right|$ at $\varepsilon = 0.2, \gamma = 1$ and $\alpha, \rho_1, \rho_2 = 1, T = 10, M = 10$ for different values of t.

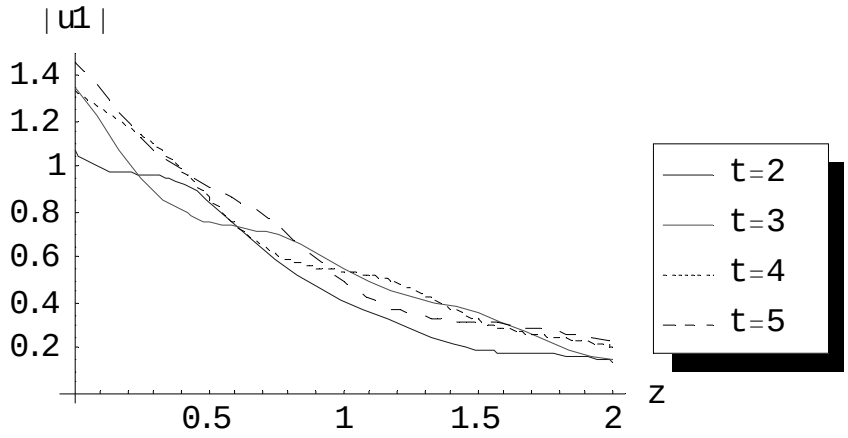

Fig. (4.65) the first order approximation of $\left|u^{(1)}\right|$ at $\varepsilon = 0.2, \gamma = 1$ and $\alpha, \rho_1, \rho_2 = 1, T = 10, M = 10$ for different values of t.

Note: we calculated till first order only taking M=10 for both $\gamma = 0$ and $\gamma = 1$ and we cannot calculate more since the machine gives "MATHEMATICA KERNEL OUT OF MEMORY".

4.5.3 Case study 3

Taking the case $f_1(t) = \rho_1 e^{-t}$, $f_2(t) = \rho_2 e^{-t}$ where ρ_1 & ρ_2 are constants and following the algorithm of Picard Approximation, the following selected results for the first and second order approximations are got:

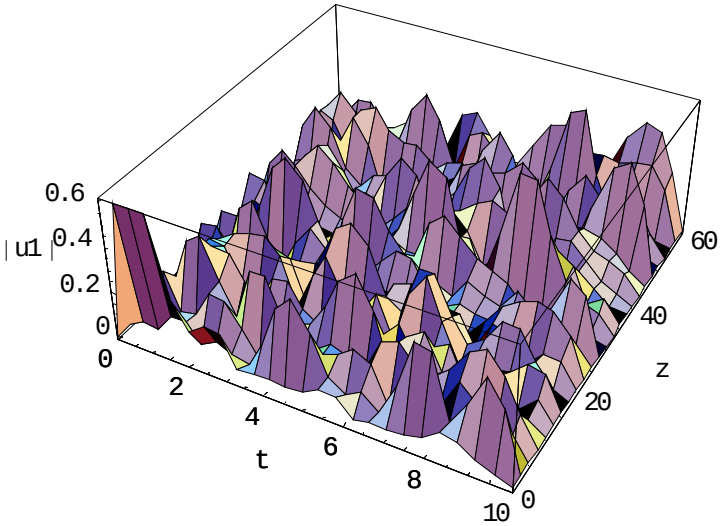

Fig. (4.66) the first order approximation of $\left|u^{(1)}\right|$ at $\varepsilon = 0.2$, $\gamma = 0$ and $\alpha, \rho_1, \rho_2 = 1, T = 10$ with considering only ten terms on the series (M=10).

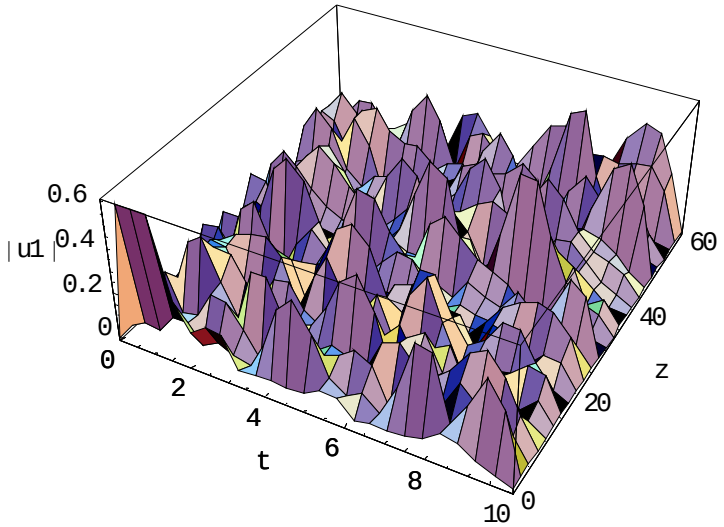

Fig. (4.67) the first order approximation of $\left|u^{(1)}\right|$ at $\varepsilon = 1$, $\gamma = 0$ and $\alpha, \rho_1, \rho_2 = 1, T = 10$ with considering only ten terms on the series (M=10).

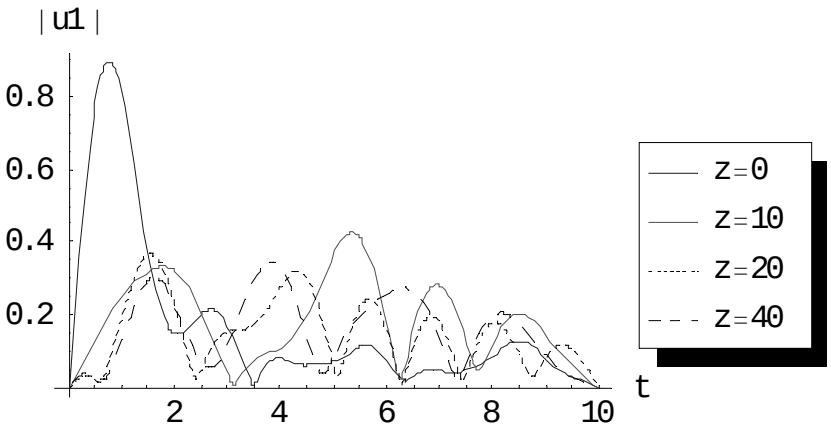

Fig. (4.68) the first order approximation of $\left|u^{(1)}\right|$ at $\varepsilon = 0.2, \gamma = 0$ and $\alpha, \rho_1, \rho_2 = 1, T = 10, M = 10$ for different values of z.

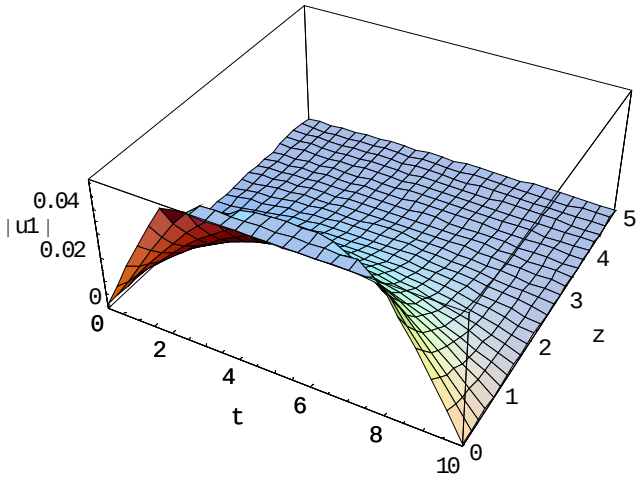

Fig. (4.69) the first order approximation of $\left|u^{(1)}\right|$ at $\varepsilon = 0.2$, $\gamma = 1$ and $\alpha, \rho_1, \rho_2 = 1, T = 10$ with considering only one term on the series (M=1).

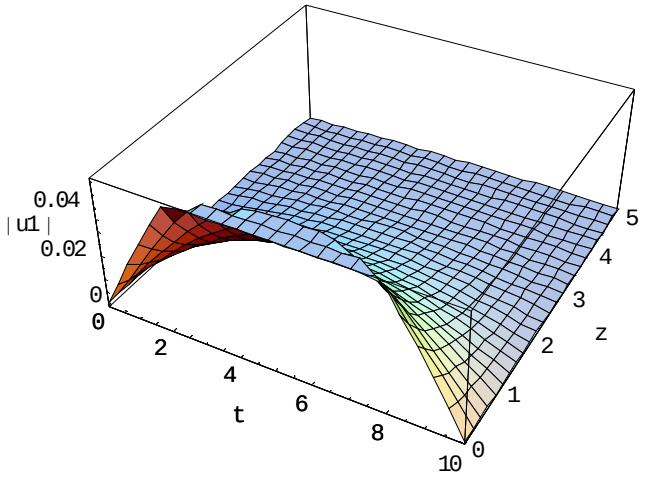

Fig. (4.70) the first order approximation of $\left|u^{(1)}\right|$ at $\varepsilon = 1$, $\gamma = 1$ and $\alpha, \rho_1, \rho_2 = 1, T = 10$ with considering only one term on the series (M=1).

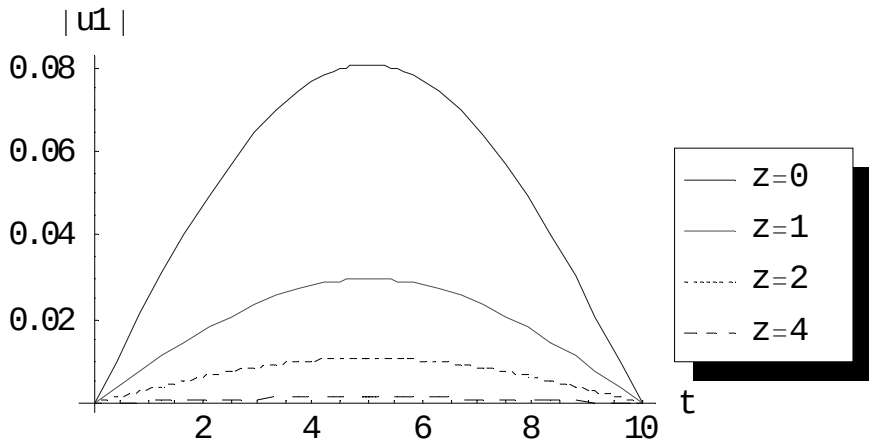

Fig. (4.71) the first order approximation of $\left|u^{(1)}\right|$ at $\varepsilon = 0.2, \gamma = 1$ and $\alpha, \rho_1, \rho_2 = 1, T = 10, M = 1$ for different values of z.

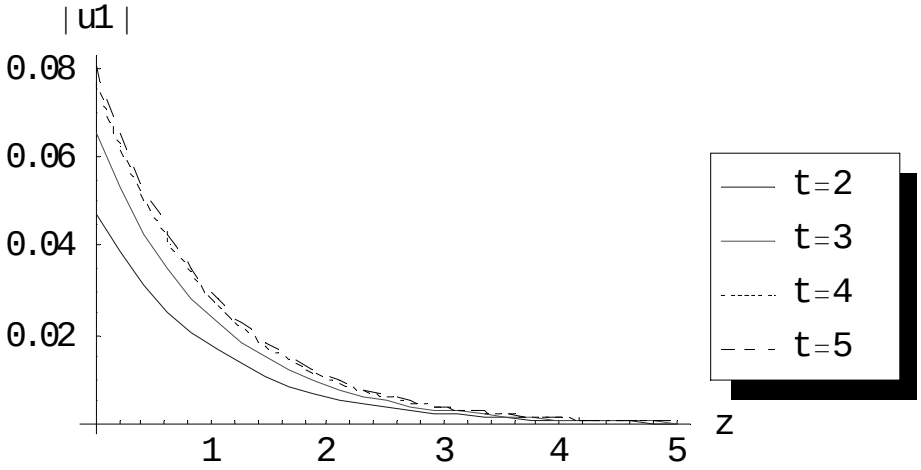

Fig. (4.72) the first order approximation of $\left|u^{(1)}\right|$ at $\varepsilon = 0.2, \gamma = 1$ and $\alpha, \rho_1, \rho_2 = 1, T = 10, M = 1$ for different values of t.

Note: we calculated till first order only taking M=10 for both $\gamma = 0$ and $\gamma = 1$ and we cannot calculate more since the machine gives "MATHEMATICA KERNEL OUT OF MEMORY".

4.6 Comparison between Perturbation & Picard Approximation

We are here giving both perturbation method and Picard approximation results in the same graph for some selected cases to compare between the two methods.

4.6.1 Case study 1

Taking the case $f_1(t) = \rho_1, f_2(t) = \rho_2$, the following selected results are obtained.

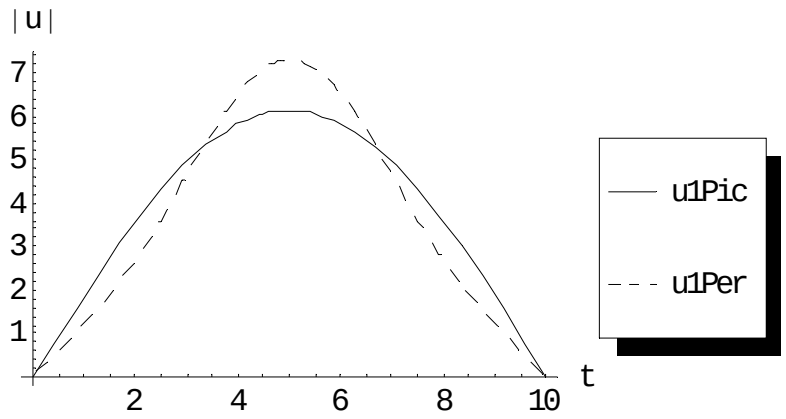

Fig. (4.73) comparison between Picard approximation and Perturbation method for first order at $\varepsilon = 0.2, \gamma = 0$ and $\alpha, \rho_1, \rho_2 = 1, T = 10, z = 5$.

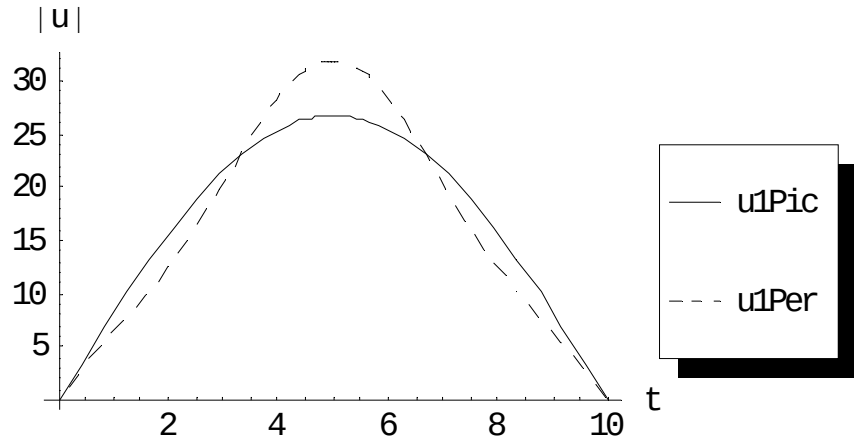

Fig. (4.74) comparison between Picard approximation and Perturbation method for first order at $\varepsilon = 1, \gamma = 0$ and $\alpha, \rho_1, \rho_2 = 1, T = 10, z = 5$.

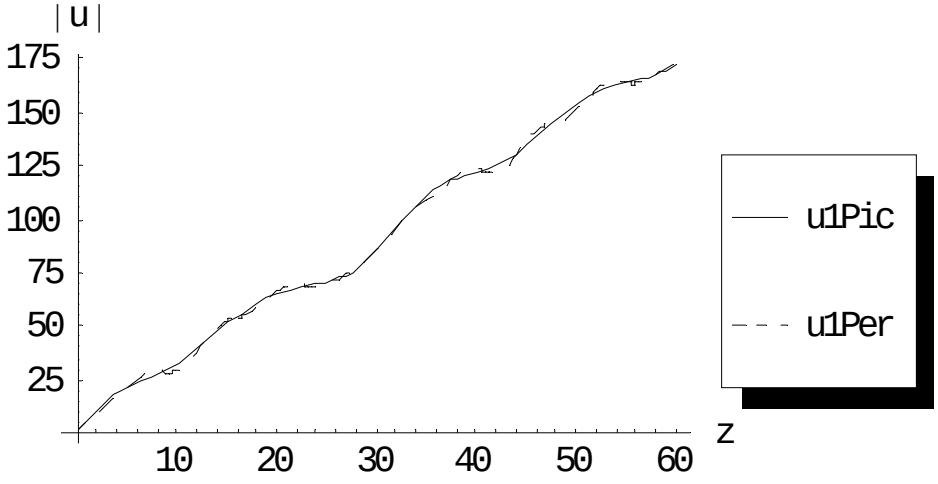

Fig. (4.75) comparison between Picard approximation and Perturbation method for first order at $\varepsilon = 1, \gamma = 0$ and $\alpha, \rho_1, \rho_2 = 1, T = 10, t = 3$.

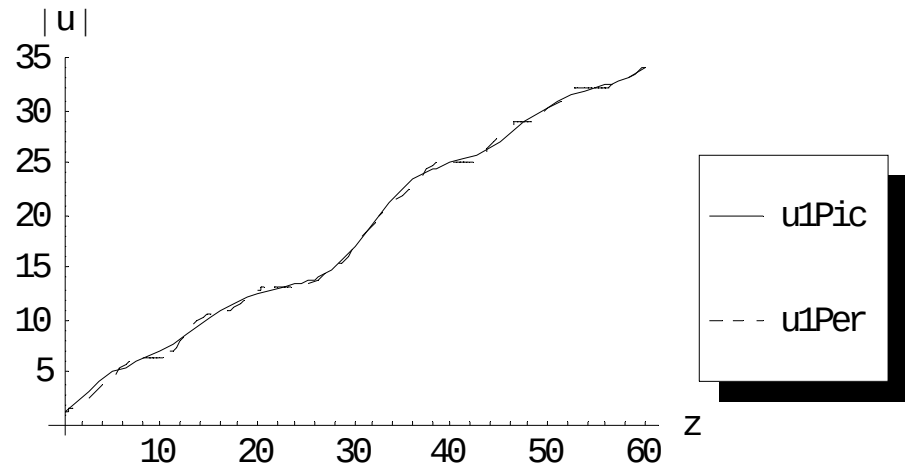

Fig. (4.76) comparison between Picard approximation and Perturbation method for first order at $\varepsilon = 0.2, \gamma = 0$ and $\alpha, \rho_1, \rho_2 = 1, T = 10, t = 3$.

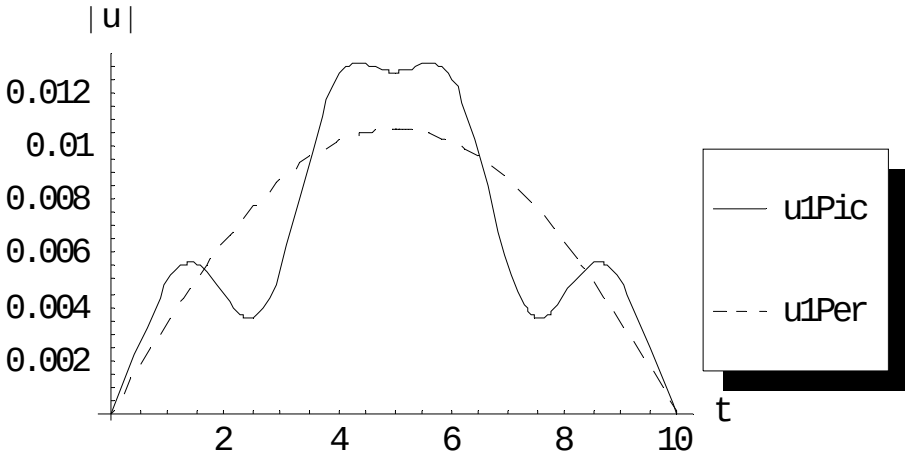

Fig. (4.77) comparison between Picard approximation and Perturbation method for first order at $\varepsilon = 0.2, \gamma = 1$ and $\alpha, \rho_1, \rho_2 = 1, T = 10, z = 5$.

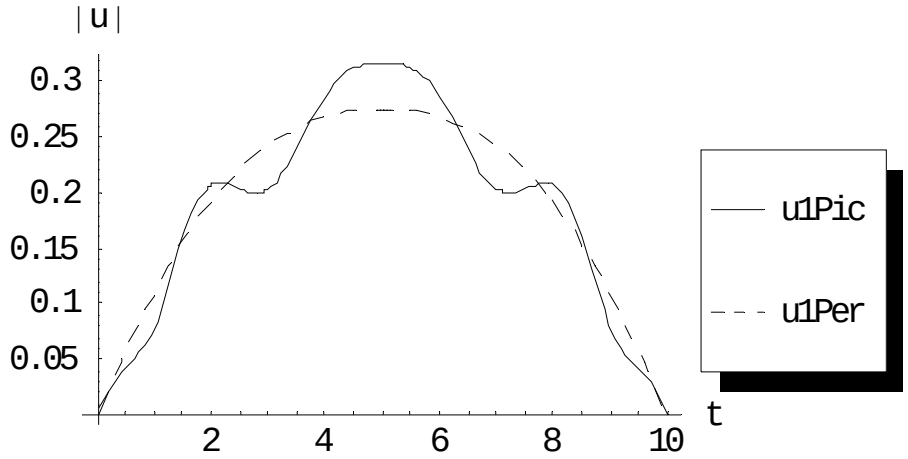

Fig. (4.78) comparison between Picard approximation and Perturbation method for first order at $\varepsilon = 1, \gamma = 1$ and $\alpha, \rho_1, \rho_2 = 1, T = 10, z = 2$.

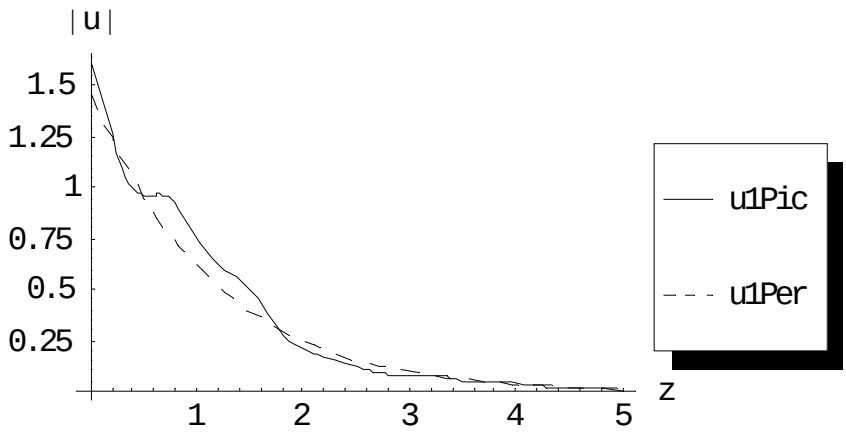

Fig. (4.79) comparison between Picard approximation and Perturbation method for first order at $\varepsilon = 1, \gamma = 1$ and $\alpha, \rho_1, \rho_2 = 1, T = 10, t = 3$.

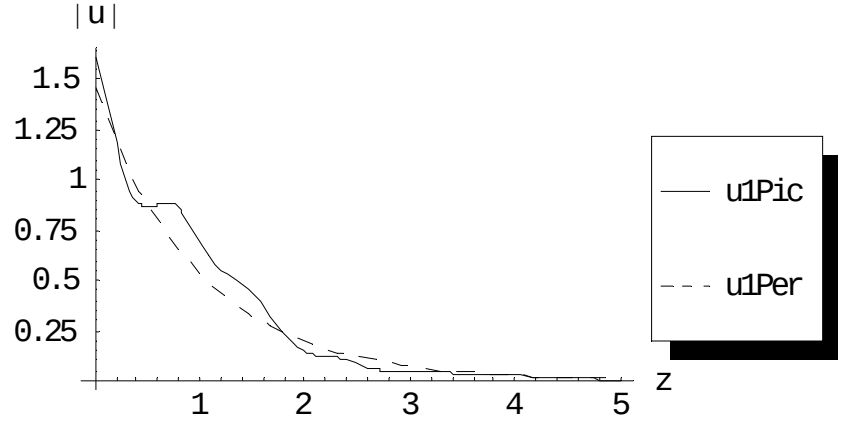

Fig. (4.80) comparison between Picard approximation and Perturbation method for first order at $\varepsilon = 0.2, \gamma = 1$ and $\alpha, \rho_1, \rho_2 = 1, T = 10, t = 3$.

4.6.2 Case study 2

Taking the case $f_1(t) = \rho_1, f_2(t) = \rho_2 \sin\left(\frac{m\pi}{T}\right) t$, the following selected results are obtained.

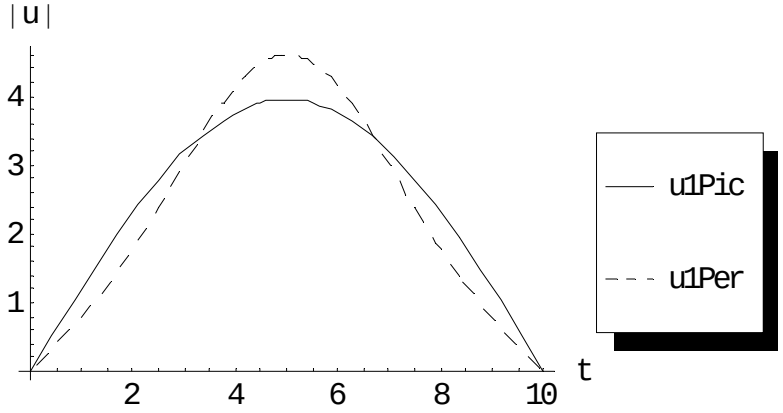

Fig. (4.81) comparison between Picard approximation and Perturbation method for first order at $\varepsilon = 0.2, \gamma = 0$ and $\alpha, \rho_1, \rho_2 = 1, T = 10, z = 5$.

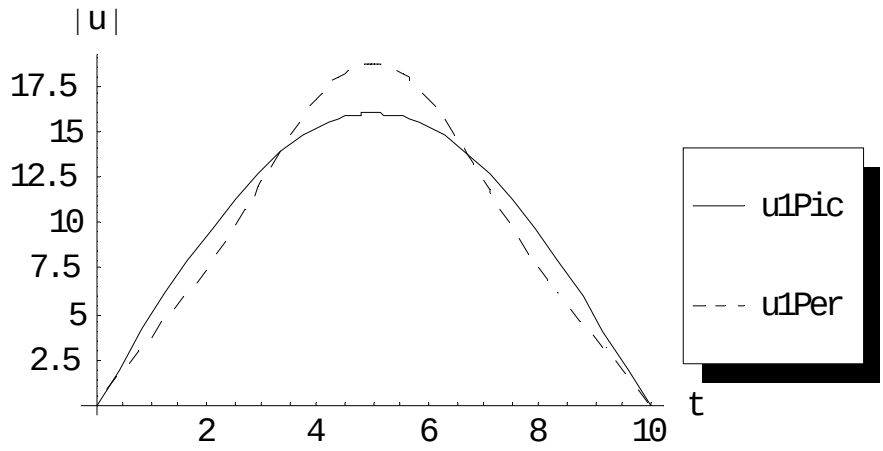

Fig. (4.82) comparison between Picard approximation and Perturbation method for first order at $\varepsilon = 1, \gamma = 0$ and $\alpha, \rho_1, \rho_2 = 1, T = 10, z = 5$.

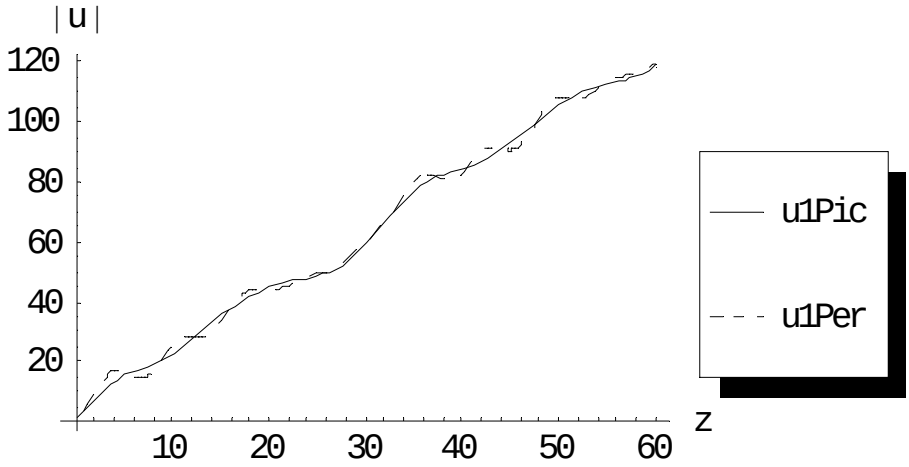

Fig. (4.83) comparison between Picard approximation and Perturbation method for first order at $\varepsilon = 1, \gamma = 0$ and $\alpha, \rho_1, \rho_2 = 1, T = 10, t = 6$.

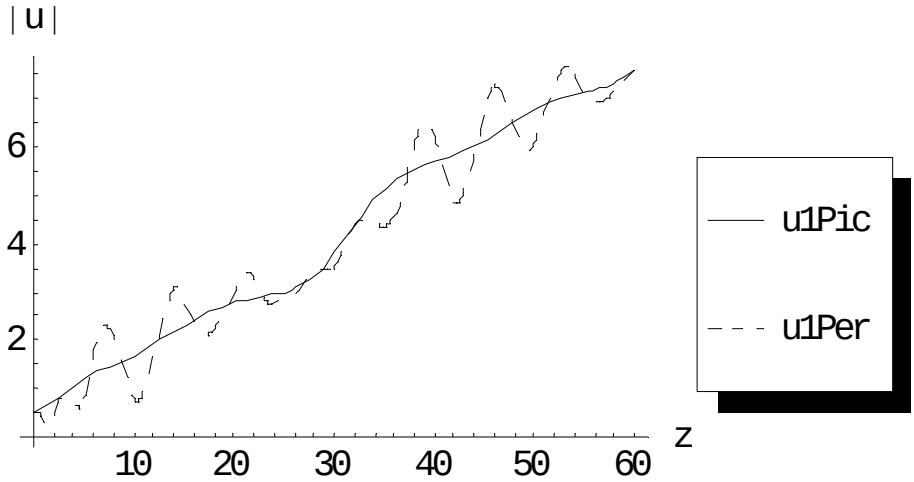

Fig. (4.84) comparison between Picard approximation and Perturbation method for first order at $\varepsilon = 1, \gamma = 0$ and $\alpha, \rho_1, \rho_2 = 1, T = 10, t = 9$.

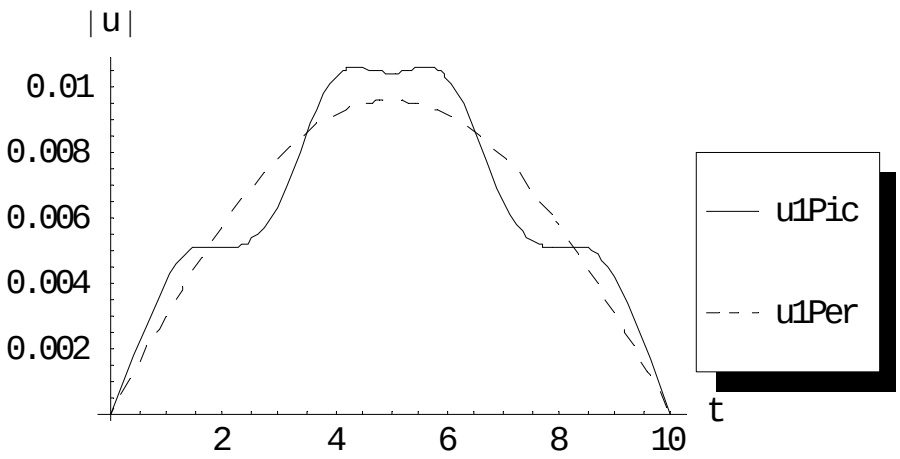

Fig. (4.85) comparison between Picard approximation and Perturbation method for first order at $\varepsilon = 0.2, \gamma = 1$ and $\alpha, \rho_1, \rho_2 = 1, T = 10,\ z = 5$.

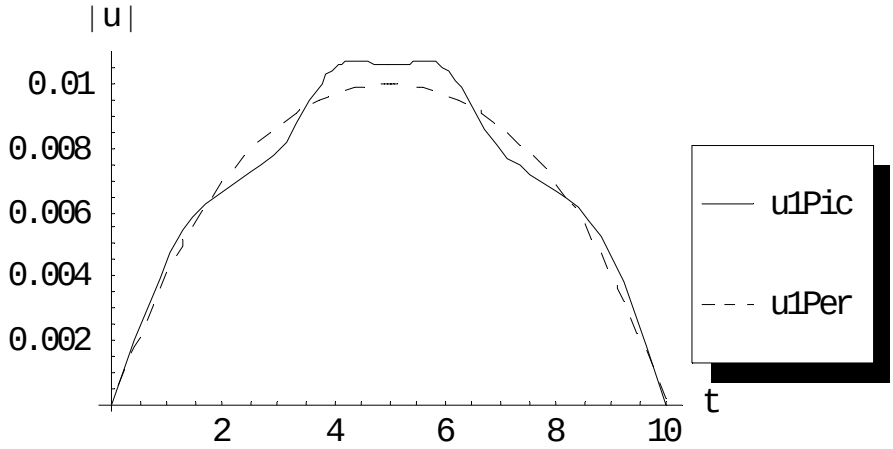

Fig. (4.86) comparison between Picard approximation and Perturbation method for first order at $\varepsilon = 1, \gamma = 1$ and $\alpha, \rho_1, \rho_2 = 1, T = 10,\ z = 5$.

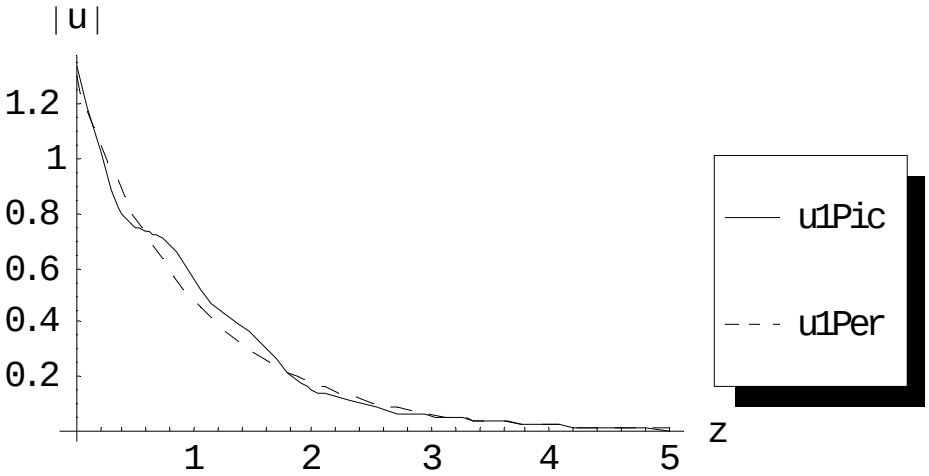

Fig. (4.87) comparison between Picard approximation and Perturbation method for first order at $\varepsilon = 1, \gamma = 1$ and $\alpha, \rho_1, \rho_2 = 1, T = 10,\ t = 3$.

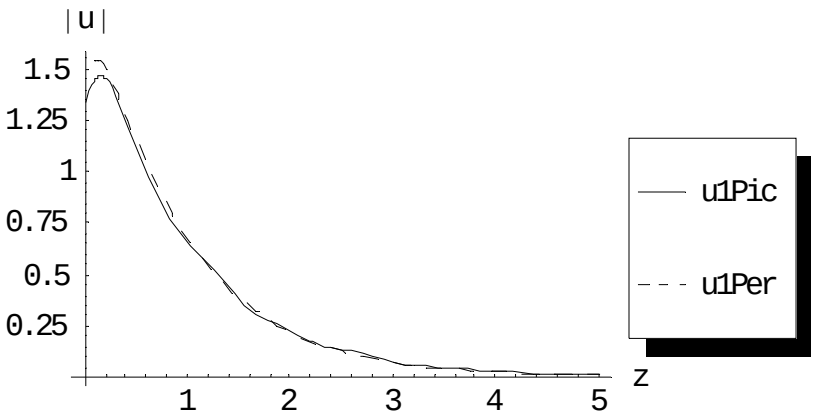

Fig. (4.88) comparison between Picard approximation and Perturbation method for first order at $\varepsilon = 0.2, \gamma = 1$ and $\alpha, \rho_1, \rho_2 = 1, T = 10,\ t = 6$.

4.6.3 Case study 3

Taking the case $f_1(t) = \rho_1 e^{-t}, f_2(t) = \rho_2 e^{-t}$, the following selected results are obtained.

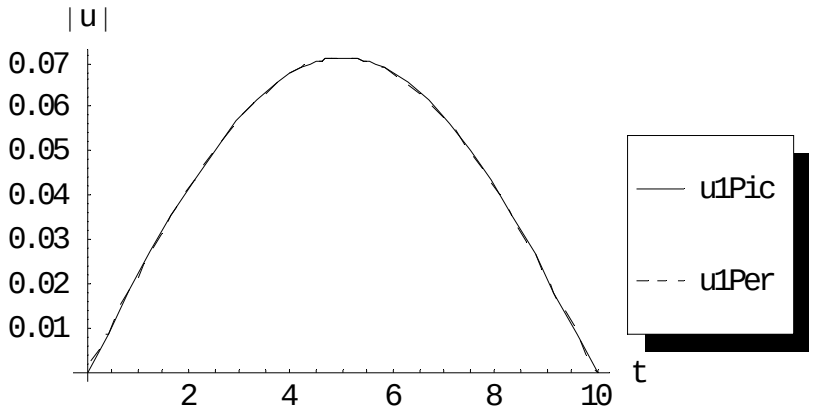

Fig. (4.89) comparison between Picard approximation and Perturbation method for first order at $\varepsilon = 1, \gamma = 0$ and $\alpha, \rho_1, \rho_2 = 1, T = 10,\ z = 5$.

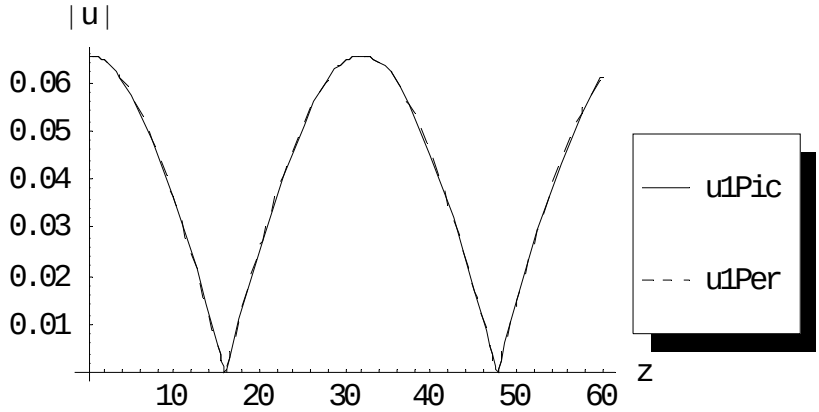

Fig. (4.90) comparison between Picard approximation and Perturbation method for first order at $\varepsilon = 0.2, \gamma = 0$ and $\alpha, \rho_1, \rho_2 = 1, T = 10,\ t = 3$.

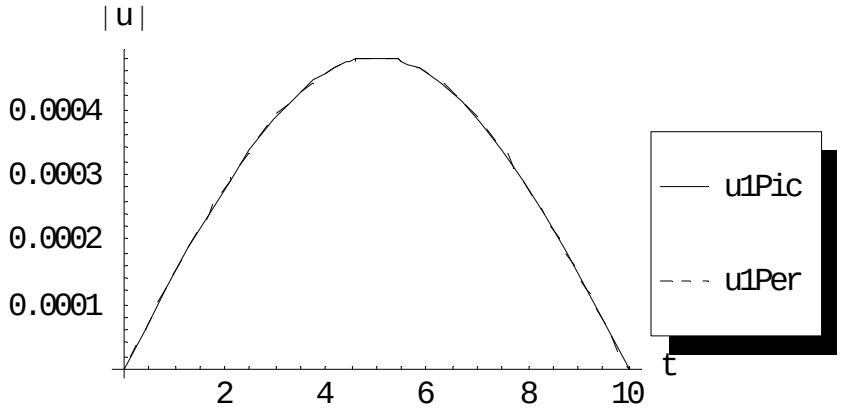

Fig. (4.91) comparison between Picard approximation and Perturbation method for first order at $\varepsilon = 0.2, \gamma = 1$ and $\alpha, \rho_1, \rho_2 = 1, T = 10,\ z = 5$.

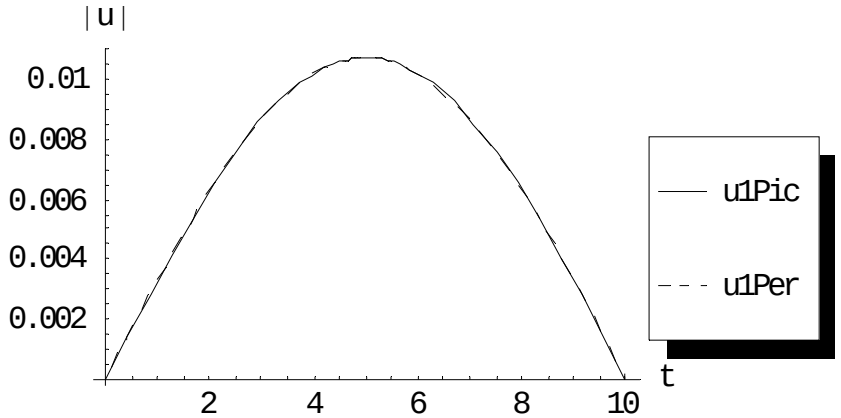

Fig. (4.92) comparison between Picard approximation and Perturbation method for first order at $\varepsilon = 1, \gamma = 1$ and $\alpha, \rho_1, \rho_2 = 1, T = 10,\ z = 2$.

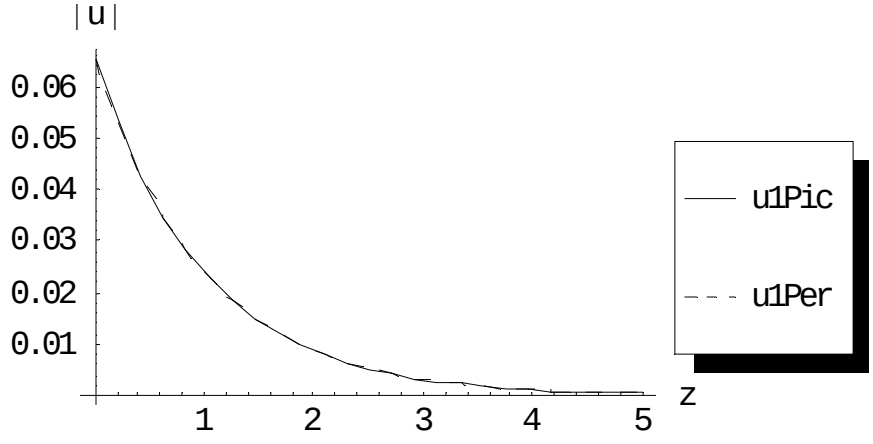

Fig. (4.93) comparison between Picard approximation and Perturbation method for first order at $\varepsilon = 1, \gamma = 1$ and $\alpha, \rho_1, \rho_2 = 1, T = 10,\ t = 3$.

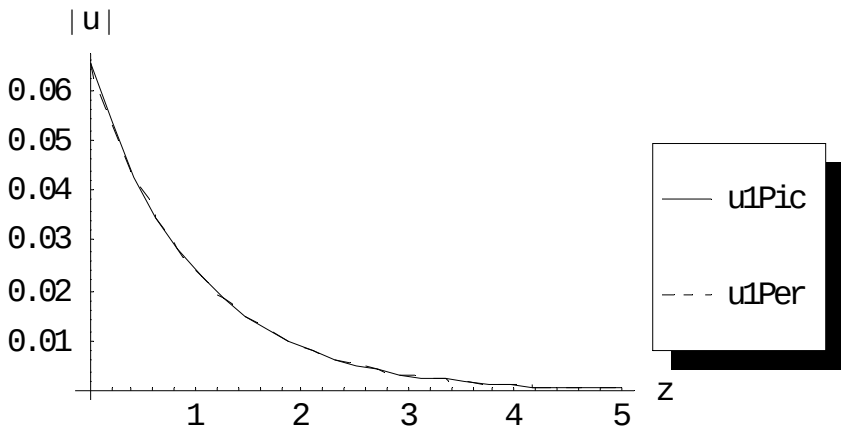

Fig. (4.94) comparison between Picard approximation and Perturbation method for first order at $\varepsilon = 0.2, \gamma = 1$ and $\alpha, \rho_1, \rho_2 = 1, T = 10,\ t = 3.$

4.7 T – Study

We are here examining the behavior of Perturbation method and Picard Approximation against different values of T through case studies on the same graph.

4.7.1 Case Studies, Perturbation

4.7.1.1 Case study 1

Taking the case $f_1(t) = \rho_1, f_2(t) = \rho_2$ where ρ_1 & ρ_2 are constants and following the algorithm, the following selected results for the first and second order approximations are got:

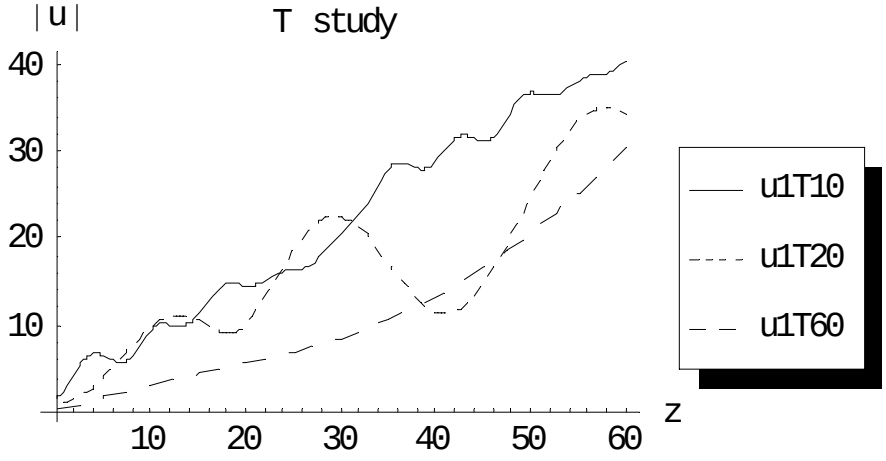

Fig. (4.95) the first order approximation of $\left|u^{(1)}\right|$ at $\varepsilon = 0.2$, $\gamma = 0$ and $\alpha, \rho_1, \rho_2 = 1, M = 10, t = 4$ for different values of T =10, 20 and 60 respectively.

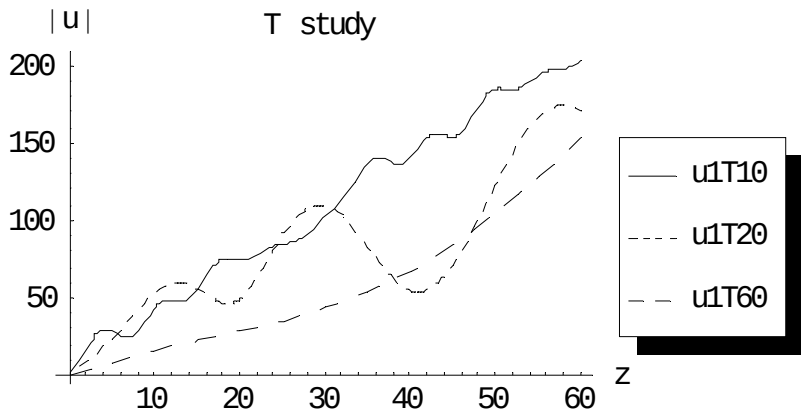

Fig. (4.96) the first order approximation of $\left|u^{(1)}\right|$ at $\varepsilon = 1$, $\gamma = 0$ and $\alpha, \rho_1, \rho_2 = 1, M = 10, t = 4$ for different values of T =10, 20 and 60 respectively.

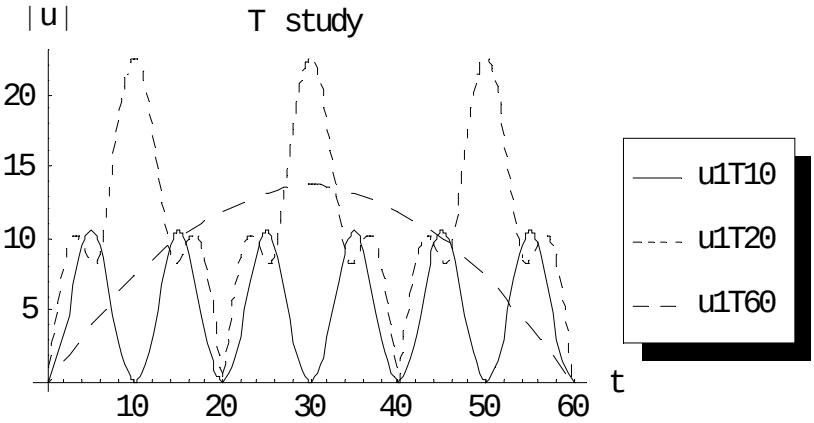

Fig. (4.97) the first order approximation of $\left|u^{(1)}\right|$ at $\varepsilon = 0.2$, $\gamma = 0$ and $\alpha, \rho_1, \rho_2 = 1, M = 10, z = 10$ for different values of T =10,20 and 60 respectively.

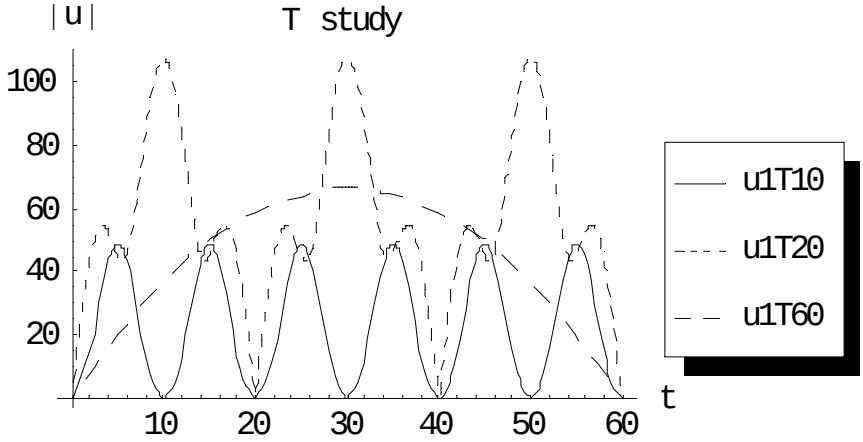

Fig. (4.98) the first order approximation of $\left|u^{(1)}\right|$ at $\varepsilon = 1$, $\gamma = 0$ and $\alpha, \rho_1, \rho_2 = 1, M = 10, z = 10$ for different values of T =10,20 and 60 respectively.

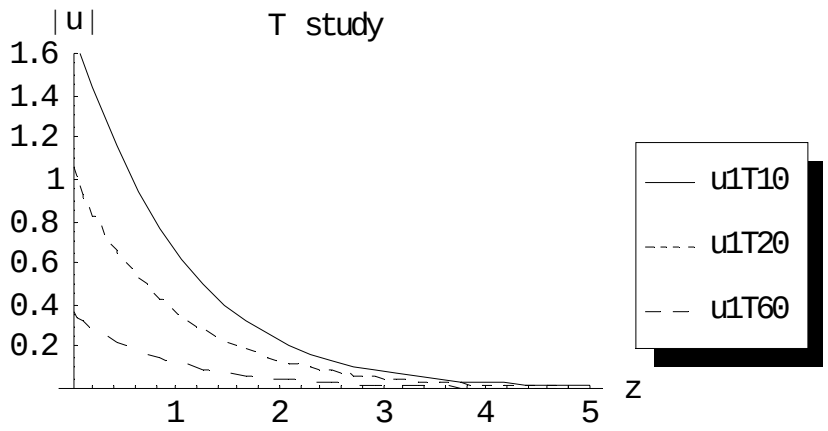

Fig. (4.99) the first order approximation of $\left|u^{(1)}\right|$ at $\varepsilon = 0.2$, $\gamma = 1$ and $\alpha, \rho_1, \rho_2 = 1, M = 10, t = 4$ for different values of T =10, 20 and 60 respectively.

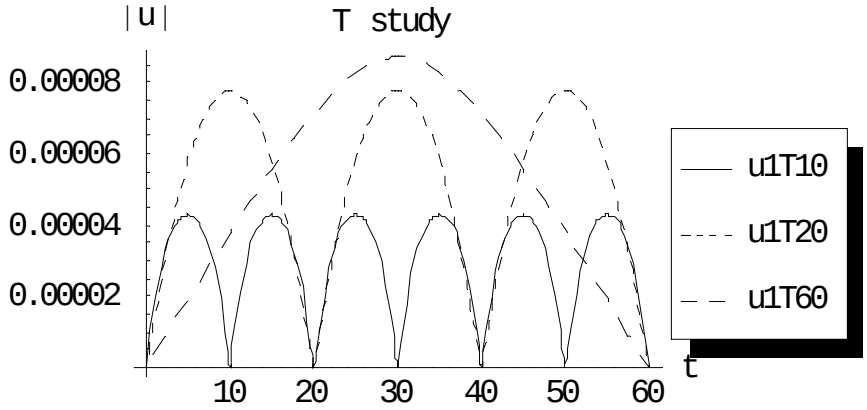

Fig. (4.100) the first order approximation of $\left|u^{(1)}\right|$ at $\varepsilon = 0.2$, $\gamma = 1$ and $\alpha, \rho_1, \rho_2 = 1, M = 10, z = 10$ for different values of T =10,20 and 60 respectively.

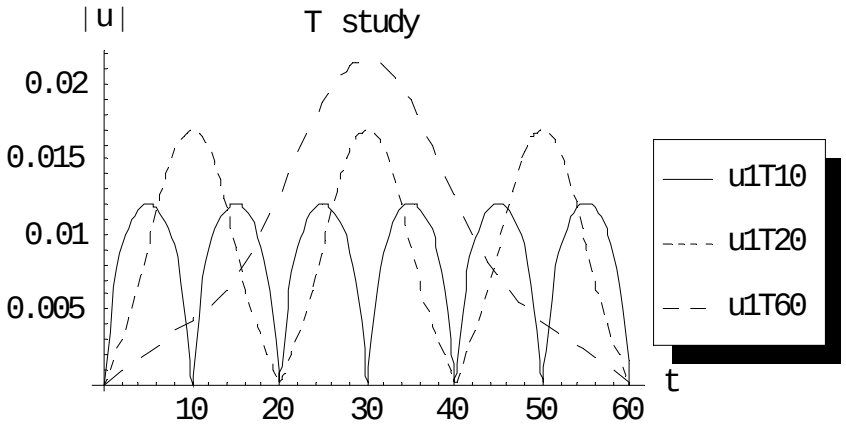

Fig. (4.101) the first order approximation of $\left|u^{(1)}\right|$ at $\varepsilon = 1$, $\gamma = 1$ and $\alpha, \rho_1, \rho_2 = 1, M = 10, z = 5$ for different values of T =10, 20 and 60 respectively.

4.7.1.2 Case study 2

Taking the case $f_1(t) = \rho_1, f_2(t) = \rho_2 \sin\left(\frac{m\pi}{T}t\right)$, and following the algorithm, the following selected results for the first and second order approximations are got:

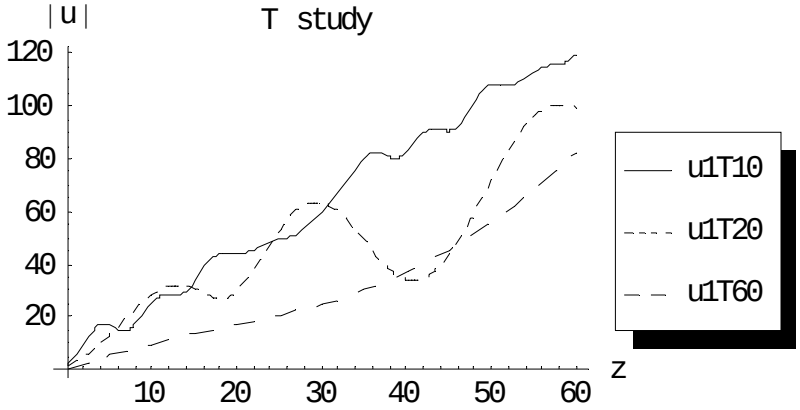

Fig. (4.102) the first order approximation of $\left|u^{(1)}\right|$ at $\varepsilon = 0.2$, $\gamma = 0$ and $\alpha, \rho_1, \rho_2 = 1, M = 10, t = 4$ for different values of T =10, 20 and 60 respectively.

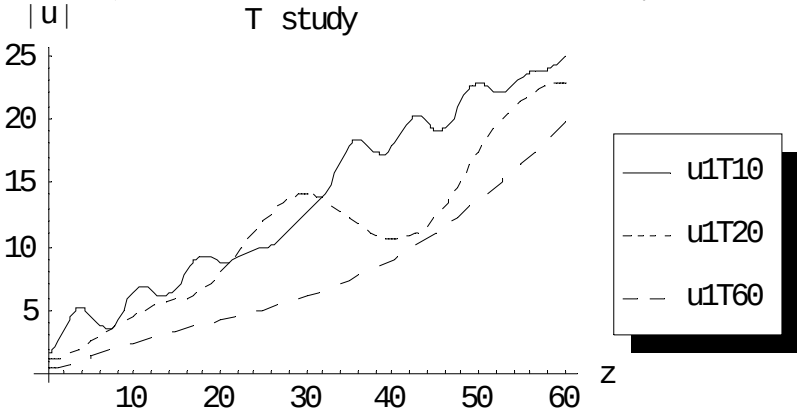

Fig. (4.103) the first order approximation of $\left|u^{(1)}\right|$ at $\varepsilon = 1$, $\gamma = 0$ and $\alpha, \rho_1, \rho_2 = 1, M = 10, t = 5$ for different values of T =10, 20 and 60 respectively.

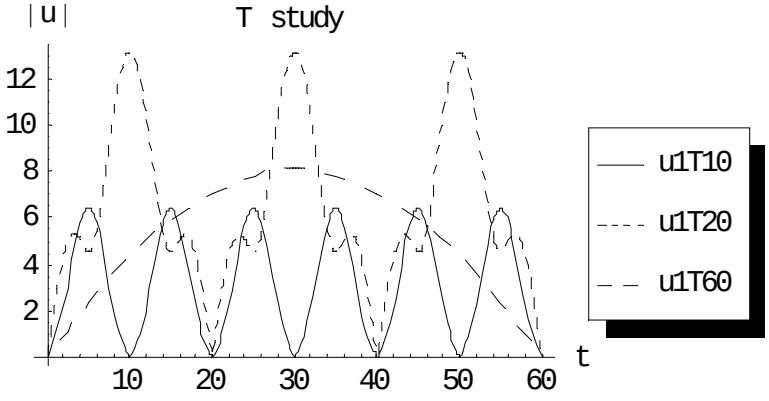

Fig. (4.104) the first order approximation of $\left|u^{(1)}\right|$ at $\varepsilon = 0.2$, $\gamma = 0$ and $\alpha, \rho_1, \rho_2 = 1, M = 10, z = 10$ for different values of T =10,20 and 60 respectively.

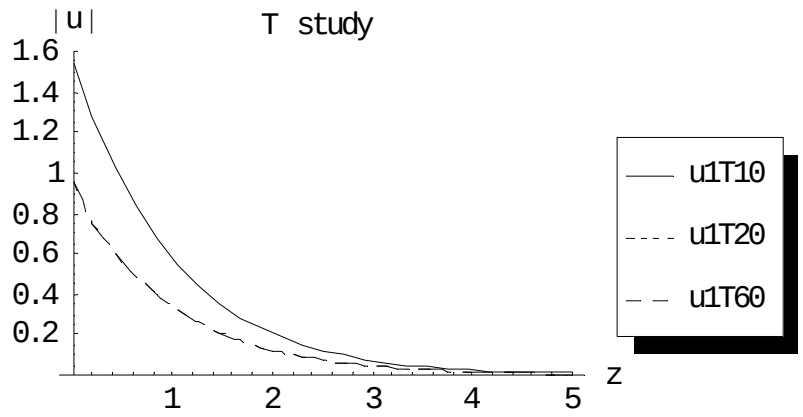

Fig. (4.105) the first order approximation of $\left|u^{(1)}\right|$ at $\varepsilon = 0.2$, $\gamma = 1$ and $\alpha, \rho_1, \rho_2 = 1, M = 10, t = 4$ for different values of T =10, 20 and 60 respectively.

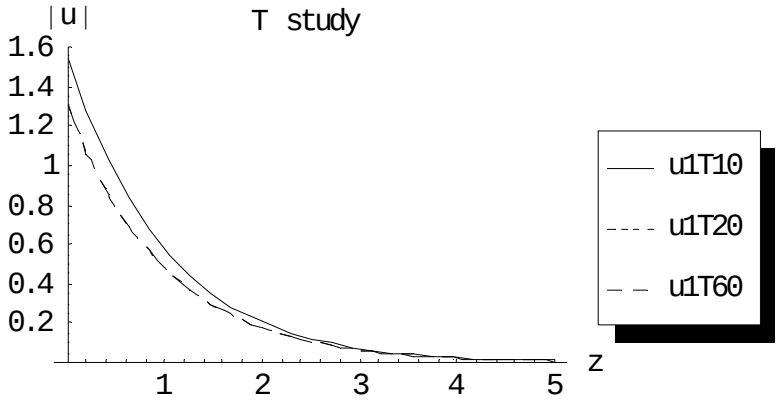

Fig. (4.106) the first order approximation of $\left|u^{(1)}\right|$ at $\varepsilon = 1$, $\gamma = 1$ and $\alpha, \rho_1, \rho_2 = 1, M = 10, t = 6$ for different values of T =10, 20 and 60 respectively.

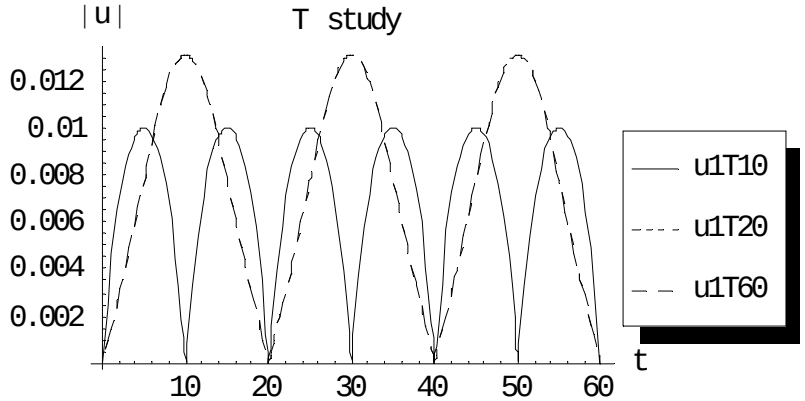

Fig. (4.107) the first order approximation of $\left|u^{(1)}\right|$ at $\varepsilon = 1$, $\gamma = 1$ and $\alpha, \rho_1, \rho_2 = 1, M = 10, z = 5$ for different values of T =10, 20 and 60 respectively.

4.7.1.3 Case study 3

Taking the case $f_1(t) = \rho_1 e^{-t}, f_2(t) = \rho_2 e^{-t}$ and following the algorithm, the following selected results for the first and second order approximations are got:

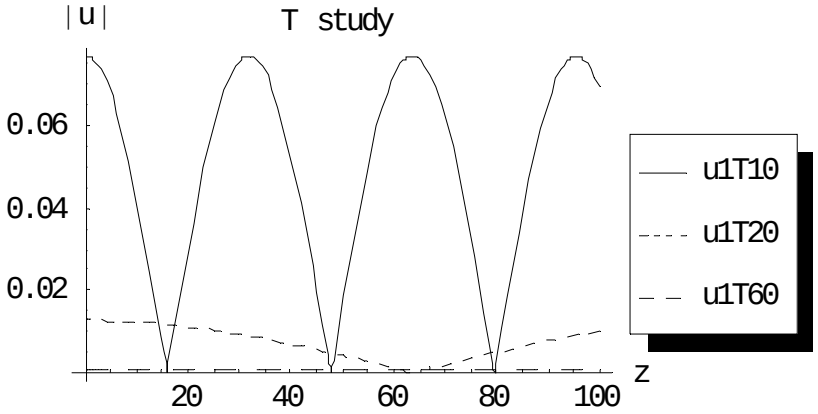

Fig. (4.108) the first order approximation of $\left|u^{(1)}\right|$ at $\varepsilon = 0.2$, $\gamma = 0$ and $\alpha, \rho_1, \rho_2 = 1, M = 10, t = 4$ for different values of T =10, 20 and 60 respectively.

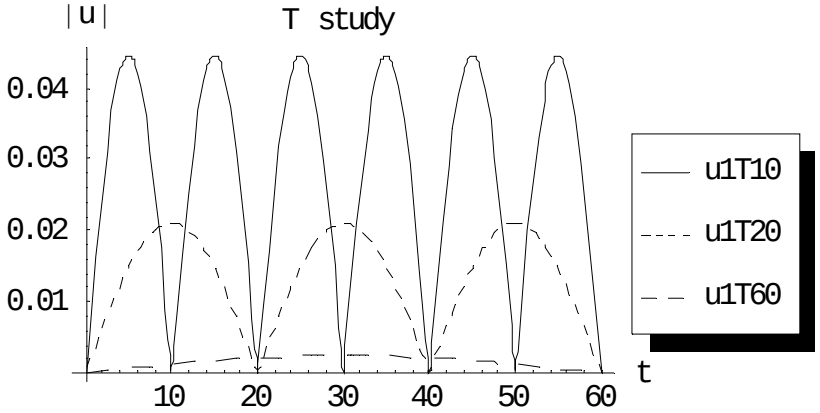

Fig. (4.109) the first order approximation of $\left|u^{(1)}\right|$ at $\varepsilon = 0.2$, $\gamma = 0$ and $\alpha, \rho_1, \rho_2 = 1, M = 10, z = 10$ for different values of T =10,20 and 60 respectively.

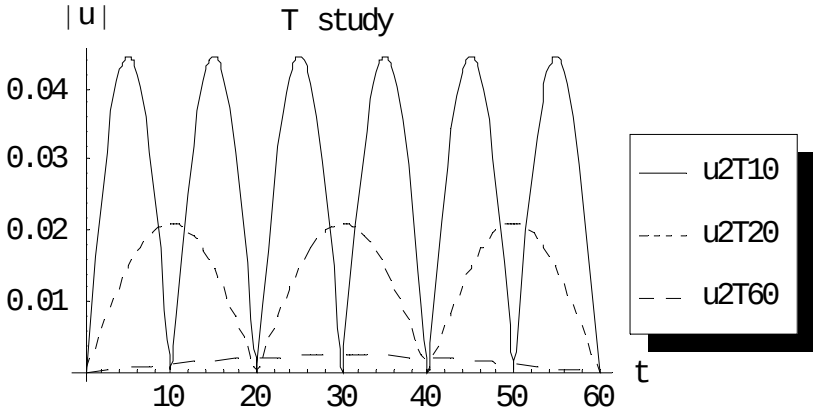

Fig. (4.110) the first order approximation of $\left|u^{(1)}\right|$ at $\varepsilon = 1$, $\gamma = 0$ and $\alpha, \rho_1, \rho_2 = 1, M = 10, z = 10$ for different values of T =10,20 and 60 respectively.

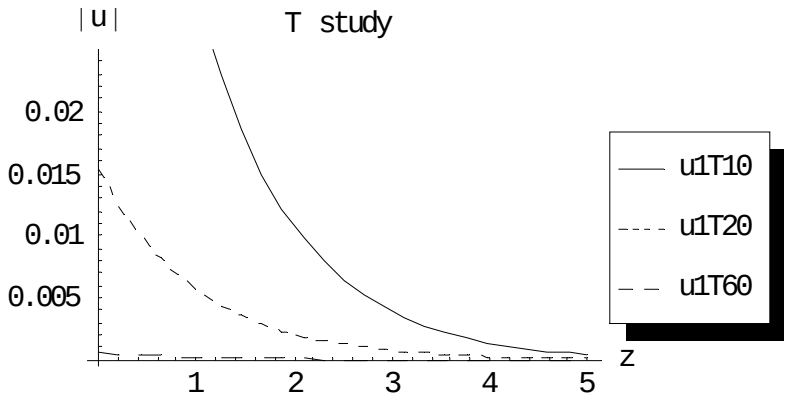

Fig. (4.111) the first order approximation of $\left|u^{(1)}\right|$ at $\varepsilon = 1$, $\gamma = 1$ and $\alpha, \rho_1, \rho_2 = 1, M = 10, t = 6$ for different values of T =10, 20 and 60 respectively.

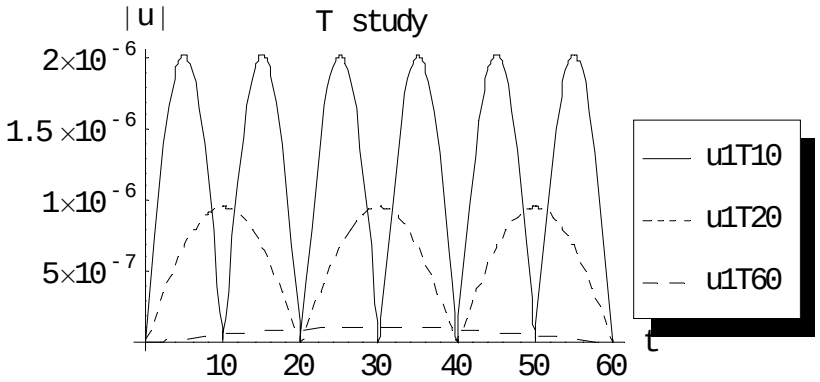

Fig. (4.112) the first order approximation of $\left|u^{(1)}\right|$ at $\varepsilon = 0.2$, $\gamma = 1$ and $\alpha, \rho_1, \rho_2 = 1, M = 10, z = 10$ for different values of T =10,20 and 60 respectively.

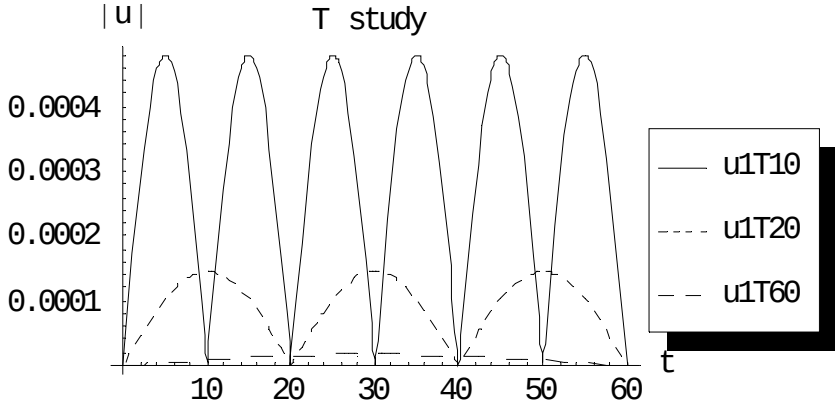

Fig. (4.113) the first order approximation of $\left|u^{(1)}\right|$ at $\varepsilon = 1$, $\gamma = 1$ and $\alpha, \rho_1, \rho_2 = 1, M = 10, z = 5$ for different values of T =10, 20 and 60 respectively.

4.7.2 Case Studies, Picard

4.7.2.1 Case study 1

Taking the case $f_1(t) = \rho_1, f_2(t) = \rho_2$ and following the algorithm, the following selected results for the first and second order approximations are got:

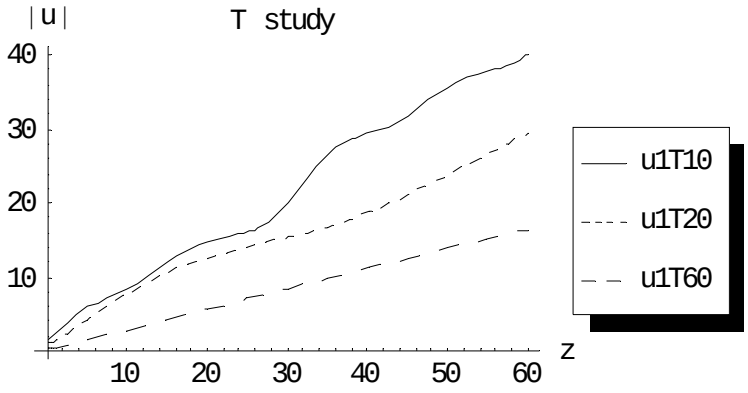

Fig. (4.114) the first order approximation of $\left|u^{(1)}\right|$ at $\varepsilon = 0.2$, $\gamma = 0$ and $\alpha, \rho_1, \rho_2 = 1, M = 1, t = 4$ for different values of T =10, 20 and 60 respectively.

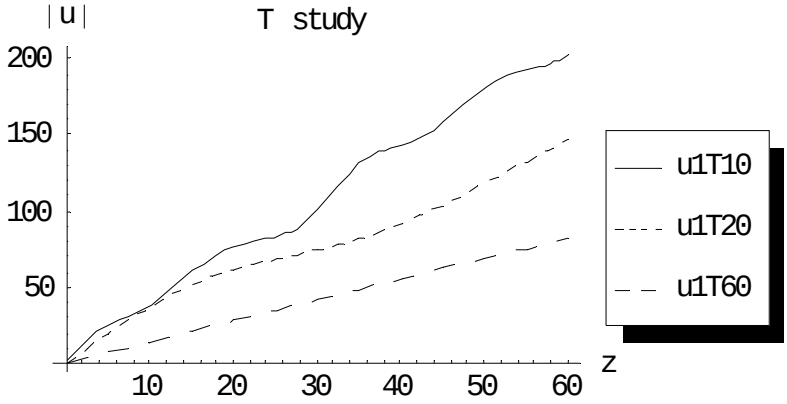

Fig. (4.115) the first order approximation of $\left|u^{(1)}\right|$ at $\varepsilon = 1$, $\gamma = 0$ and $\alpha, \rho_1, \rho_2 = 1, M = 1, t = 4$ for different values of T =10, 20 and 60 respectively.

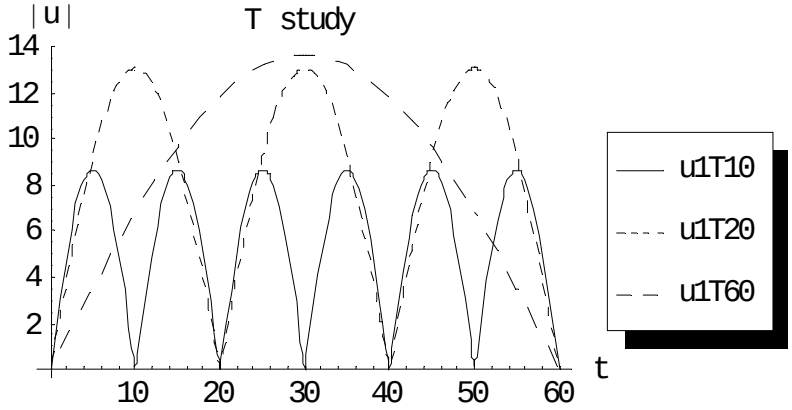

Fig. (4.116) the first order approximation of $\left|u^{(1)}\right|$ at $\varepsilon = 0.2$, $\gamma = 0$ and $\alpha, \rho_1, \rho_2 = 1, M = 1, z = 10$ for different values of T =10, 20 and 60 respectively.

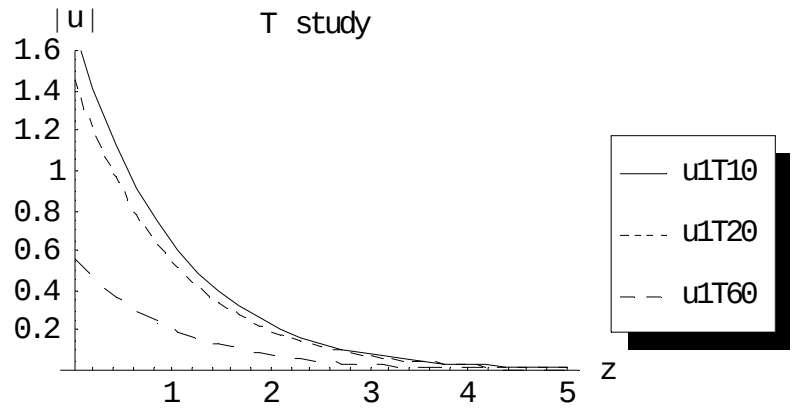

Fig. (4.117) the first order approximation of $\left|u^{(1)}\right|$ at $\varepsilon = 0.2$, $\gamma = 1$ and $\alpha, \rho_1, \rho_2 = 1, M = 10, t = 6$ for different values of T =10, 20 and 60 respectively.

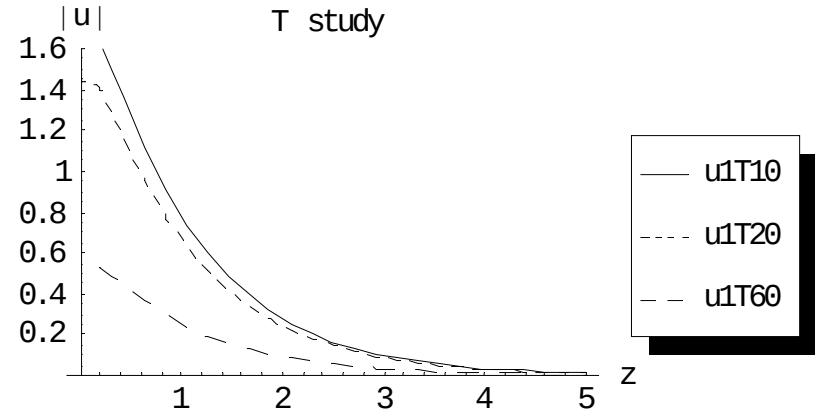

Fig. (4.118) the first order approximation of $\left|u^{(1)}\right|$ at $\varepsilon = 1$, $\gamma = 1$ and $\alpha, \rho_1, \rho_2 = 1, M = 10, t = 6$ for different values of T =10, 20 and 60 respectively.

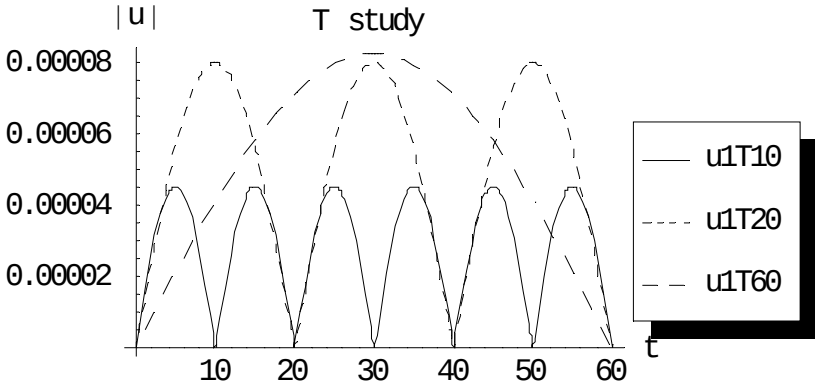

Fig. (4.119) the first order approximation of $\left|u^{(1)}\right|$ at $\varepsilon = 0.2$, $\gamma = 1$ and $\alpha, \rho_1, \rho_2 = 1, M = 10, z = 10$ for different values of T =10,20 and 60 respectively.

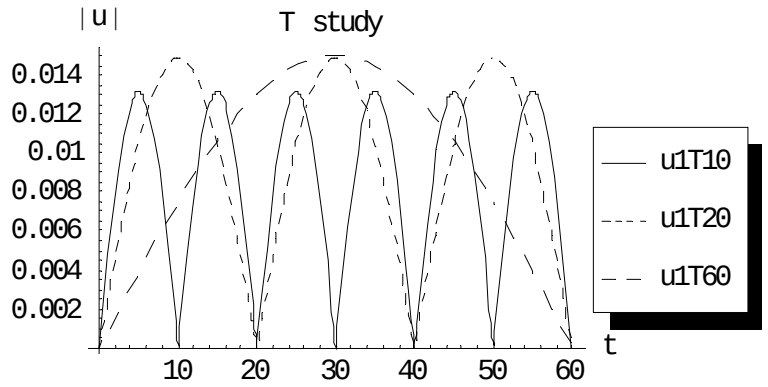

Fig. (4.120) the first order approximation of $\left|u^{(1)}\right|$ at $\varepsilon = 1$, $\gamma = 1$ and $\alpha, \rho_1, \rho_2 = 1, M = 10, z = 5$ for different values of T =10, 20 and 60 respectively.

4.7.2.2 Case study 2

Taking the case $f_1(t) = \rho_1, f_2(t) = \rho_2 \sin\left(\frac{m\pi}{T}t\right)$ and following the algorithm, the following selected results for the first and second order approximations are got:

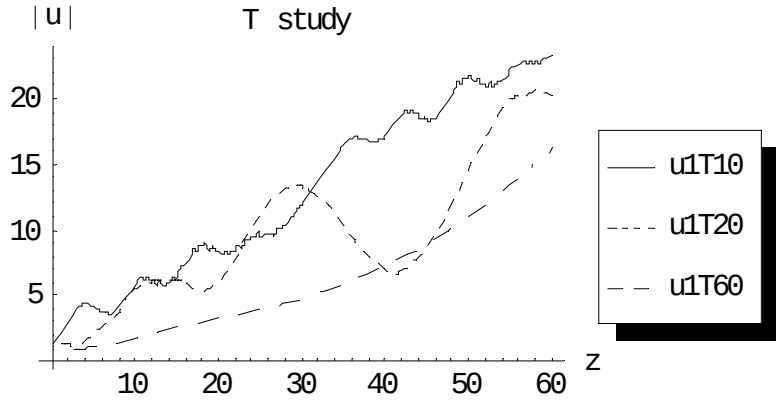

Fig. (4.121) the first order approximation of $\left|u^{(1)}\right|$ at $\varepsilon = 0.2$, $\gamma = 0$ and $\alpha, \rho_1, \rho_2 = 1, M = 1, t = 4$ for different values of T =10, 20 and 60 respectively.

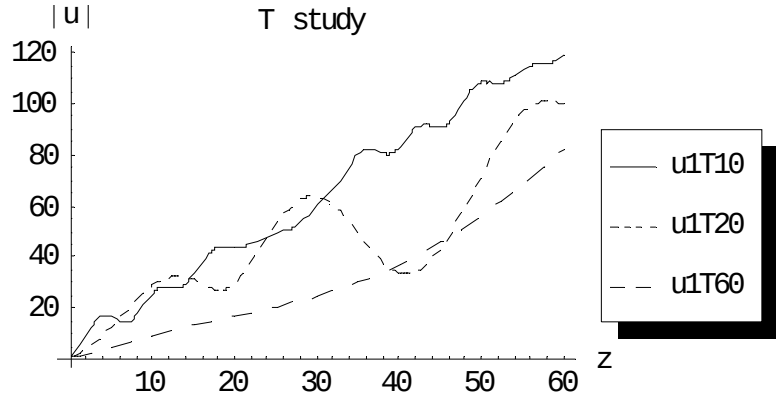

Fig. (4.122) the first order approximation of $\left|u^{(1)}\right|$ at $\varepsilon = 1$, $\gamma = 0$ and $\alpha, \rho_1, \rho_2 = 1, M = 1, t = 4$ for different values of T =10, 20 and 60 respectively.

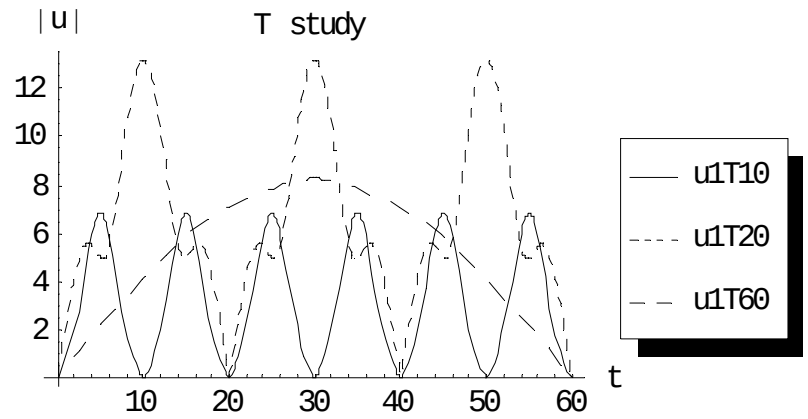

Fig. (4.123) the first order approximation of $\left|u^{(1)}\right|$ at $\varepsilon = 0.2$, $\gamma = 0$ and $\alpha, \rho_1, \rho_2 = 1, M = 1, z = 10$ for different values of T =10, 20 and 60 respectively.

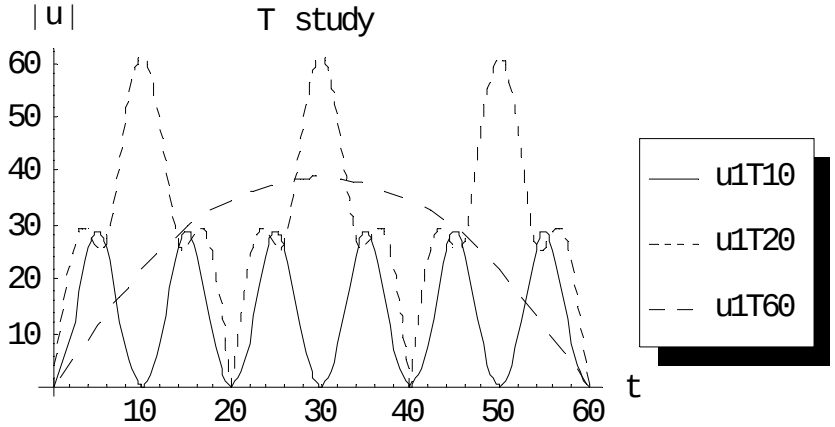

Fig. (4.124) the first order approximation of $\left|u^{(1)}\right|$ at $\varepsilon = 1$, $\gamma = 0$ and $\alpha, \rho_1, \rho_2 = 1, M = 1, z = 10$ for different values of T =10, 20 and 60 respectively.

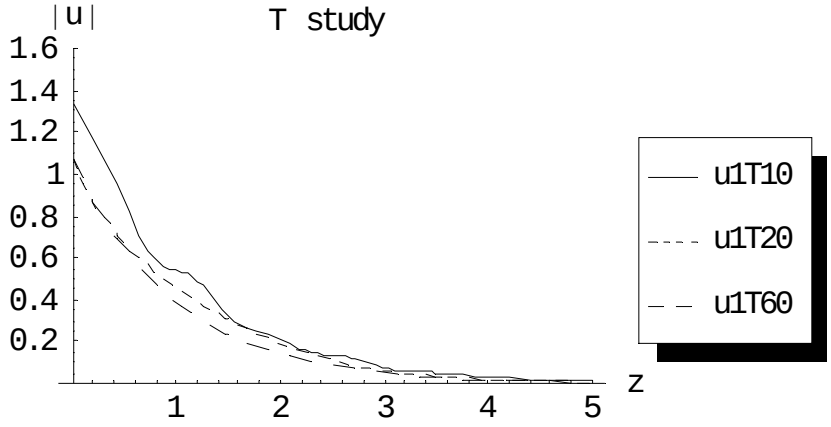

Fig. (4.125) the first order approximation of $\left|u^{(1)}\right|$ at $\varepsilon = 0.2$, $\gamma = 1$ and $\alpha, \rho_1, \rho_2 = 1, M = 10, t = 4$ for different values of T =10, 20 and 60 respectively.

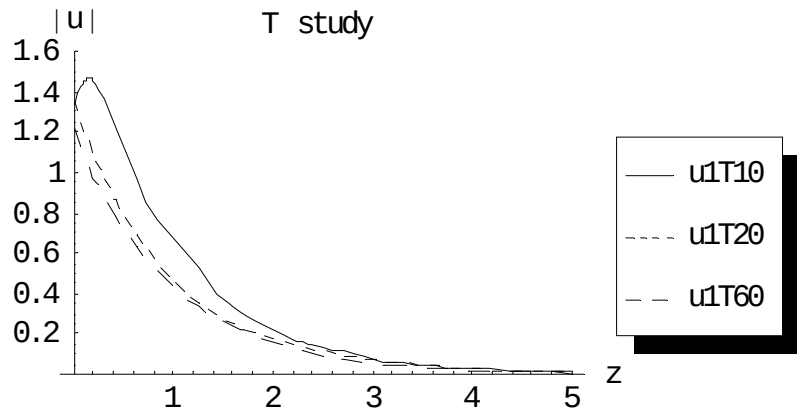

Fig. (4.126) the first order approximation of $\left|u^{(1)}\right|$ at $\varepsilon = 1$, $\gamma = 1$ and $\alpha, \rho_1, \rho_2 = 1, M = 10, t = 6$ for different values of T =10, 20 and 60 respectively.

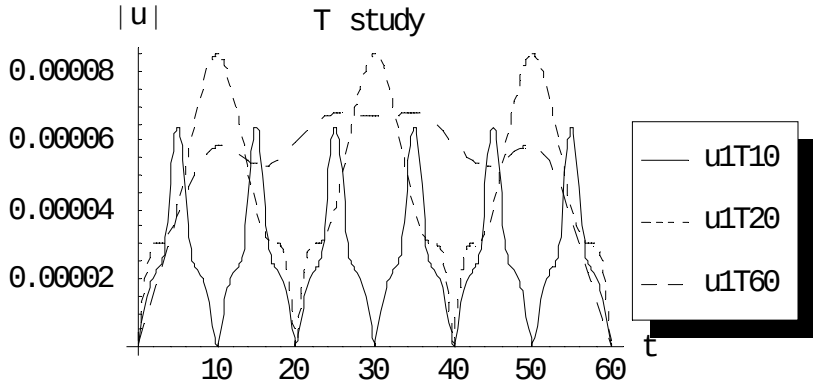

Fig. (4.127) the first order approximation of $\left|u^{(1)}\right|$ at $\varepsilon = 0.2$, $\gamma = 1$ and $\alpha, \rho_1, \rho_2 = 1, M = 10, z = 10$ for different values of T =10,20 and 60 respectively.

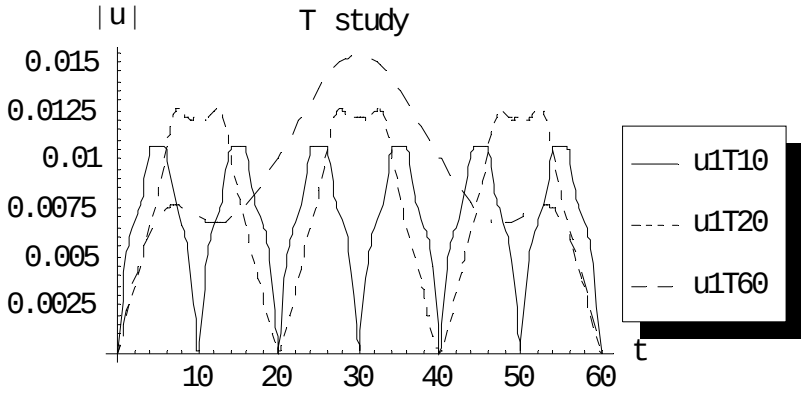

Fig. (4.128) the first order approximation of $\left|u^{(1)}\right|$ at $\varepsilon = 1$, $\gamma = 1$ and $\alpha, \rho_1, \rho_2 = 1, M = 10, z = 5$ for different values of T =10, 20 and 60 respectively.

4.7.2.3 Case study 3

Taking the case $f_1(t) = \rho_1 e^{-t}, f_2(t) = \rho_2 e^{-t}$ and following the algorithm, the following selected results for the first and second order approximations are got:

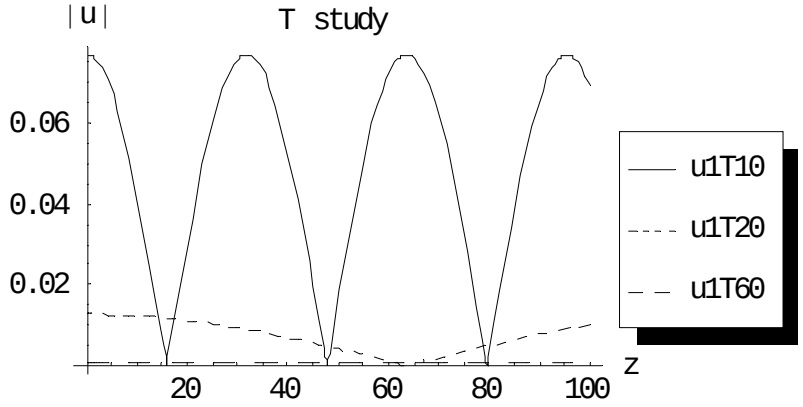

Fig. (4.129) the first order approximation of $\left|u^{(1)}\right|$ at $\varepsilon = 0.2$, $\gamma = 0$ and $\alpha, \rho_1, \rho_2 = 1, M = 1, t = 4$ for different values of T =10, 20 and 60 respectively.

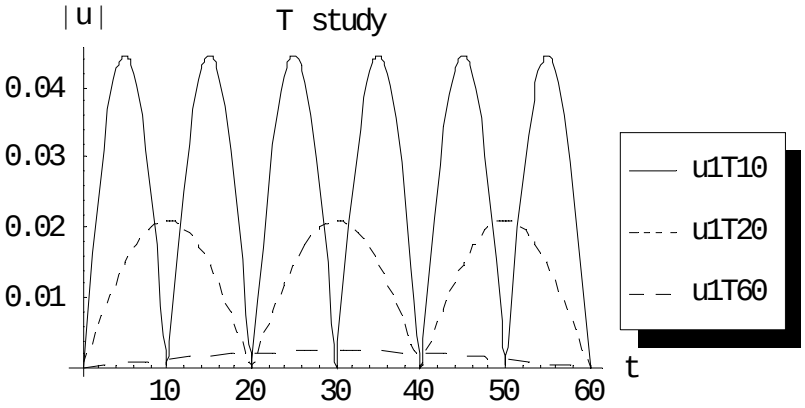

Fig. (4.130) the first order approximation of $\left|u^{(1)}\right|$ at $\varepsilon = 0.2$, $\gamma = 0$ and $\alpha, \rho_1, \rho_2 = 1, M = 1, z = 10$ for different values of T =10, 20 and 60 respectively.

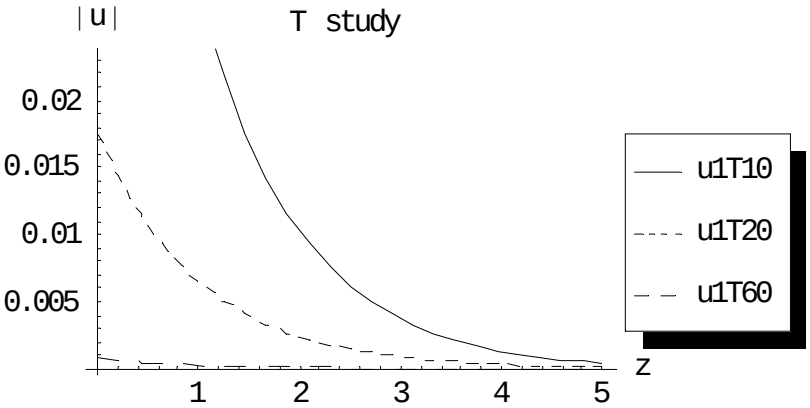

Fig. (4.131) the first order approximation of $\left|u^{(1)}\right|$ at $\varepsilon = 0.2$, $\gamma = 1$ and $\alpha, \rho_1, \rho_2 = 1, M = 10$, $t = 6$ for different values of T =10, 20 and 60 respectively.

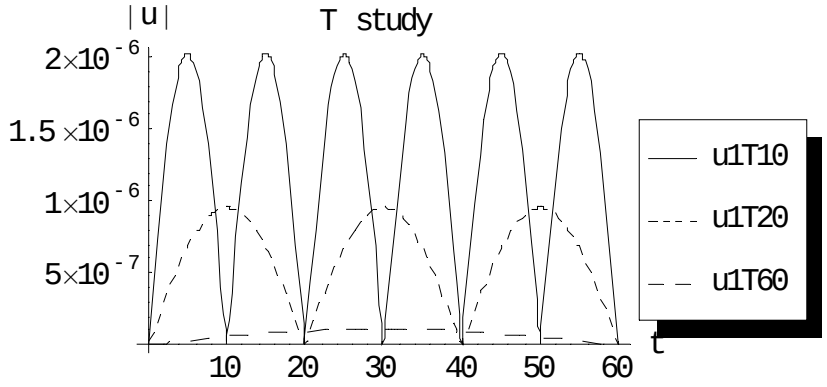

Fig. (4.132) the first order approximation of $\left|u^{(1)}\right|$ at $\varepsilon = 0.2$, $\gamma = 1$ and $\alpha, \rho_1, \rho_2 = 1, M = 10$, $z = 10$ for different values of T =10,20and 60 respectively.

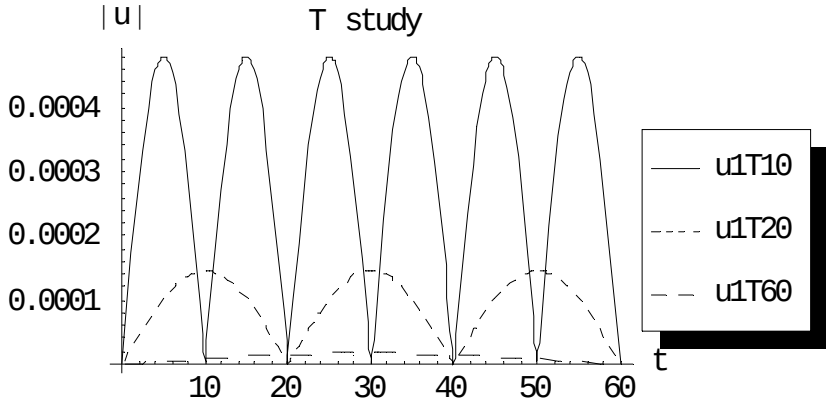

Fig. (4.133) the first order approximation of $\left|u^{(1)}\right|$ at $\varepsilon = 1$, $\gamma = 1$ and $\alpha, \rho_1, \rho_2 = 1, M = 10$, $z = 5$ for different values of T =10, 20 and 60 respectively.

Chapter 5 Summary and Conclusion

5.0 Summary

We demonstrated in this thesis that both Perturbation Method and Picard approximation can be used to solve both cubic and quintic Nonlinear Schrodinger equation. Through different case studies, we can find that the results for both methods are near enough; however, in Perturbation method we obtained higher order approximations than Picard approximation. As, an example in cubic homogeneous case, we obtained up to third order approximation, while by using Picard approximation for the same equation with same initial and boundary conditions, we obtained up to second order approximation.

In Appendix A, we showed in details the steps of solution for the general linear case. This solution is considered as zero order approximation for both perturbation method and Picard approximation.

In chapters 2, 3 and 4, we used the perturbation method and Picard approximation to solve the Cubic Homogeneous, the Cubic Non-Homogeneous and the Quintic Homogeneous nonlinear Schrodinger equations, respectively and illustrated the solution through different case studies. We compared between results of both methods on the same graph. Also, we studied the solution change for both methods; perturbation and Picard approximation at different values of time.

In chapter 3, we studied the effect of non homogeneous term; $F_1(t,z) + iF_2(t,z)$ and we found that in case of zero initial conditions; $f_1(t,z) + if_2(t,z) = 0$ the change of non homogeneous term from constant (ρ_1), exponential ($\rho_1 e^{-t}$) or sinusoidal ($\rho_1 \sin(\frac{m\pi}{T}t)$ has no spatial effect on the solution.

5.1 Conclusions

- For cubic and quintic homogeneous nonlinear Schrodinger equations:
    - We found that the stability of the solution of the nonlinear homogeneous Schrodinger equation is highly affected in the absence of gamma (γ) term.
    - The perturbation as well as the Picard methods introduce approximate solutions for such problems where second or third order of approximations can be obtained from which some

parametric studies can be achieved to illustrate the solution behavior under the change of the problem physical parameters.

- The use of Mathematica, or any other symbolic code, makes the use of the solution algorithm possible and can develop a solution procedure which can help in getting some knowledge about the solution.
- The results for both perturbation and Picard methods are quite nearer in the presence of gamma (γ) term.
- With the existence of gamma (γ) term, the magnitude of solution ($|u|$) decreases as time increases.

- For cubic non-homogeneous nonlinear Schrodinger equation:
  Same conclusions as cubic and quintic Homogeneous nonlinear Schrodinger equations cases, while, we found the following:

  - In the case of zero initial conditions, we found that the change of non homogeneous term did not affect on the solution; both constant ($F1 = \rho_1$), exponential ($F1 = \rho_1 e^{-t}$) and sinusoidal ($F1 = \rho_1 \sin(\frac{m\pi}{T} t)$) had the same solutions.
  - Due to non homogeneous term, we can not calculate more than second order approximation at ($\gamma = 0$) and first order approximation at ($\gamma = 0$).

- Part of the work of chapter 2 was published in TOAMJ [Magdy El-Tawil, H. El Zoheiry and Sherif E. Nasr, 2010] and we are arranging to send cubic non-homogeneous and quintic cases; chapter 3 and 4 respectively for publishing on the nearest future

Hopefully, with high capabilities of computers, we can reach to higher order approximations and solve quintic non-homogeneous nonlinear Schrodinger equation.

Appendix A The general Linear Case

We introduce here the general solution of linear Schrodinger equations

A.1 The general linear case

Consider the non homogeneous linear Schrodinger equation:

$$i\,\frac{\partial u(t,z)}{\partial z}+\ \alpha\,\frac{\partial^2 u(t,z)}{\partial t^2}+i\,\gamma u(t,z)=F_1(t,z)+\ i\,F_2(t,z),$$

$$(t,z)\in(0,T)\,x\,(0,\infty) \qquad (A.1)$$

where $u(t,z)$ is a complex valued function which is subjected to:

$$I.Cs.: u(t,0)=\ f_1(t)+\ i\,f_2(t) \qquad (A.2)$$

$$B.Cs.: u(0,z)=\ u(T,z)=0 \qquad (A.3)$$

Let $u(t,z)=\psi(t,z)+\ i\,\phi(t,z),\ \psi,\phi$ are real valued functions.

Let $\psi(t,z)=e^{-\gamma z}W(t,z)$ and $\phi(t,z)=e^{-\gamma z}V(t,z)$. The following coupled equations are got as follows:

$$\frac{\partial V(t,z)}{\partial z}=\ \alpha\,\frac{\partial^2 W(t,z)}{\partial t^2}+\ G_1(t,z), \qquad (A.4)$$

$$\frac{\partial W(t,z)}{\partial z}=\ \alpha\,\frac{\partial^2 V(t,z)}{\partial t^2}+\ G_2(t,z) \qquad (A.5)$$

where,
$W(t,0)=f_1(t), V(t,0)=f_2(t), G_1(t,z)=-e^{\gamma z}F_1(t,z),\ G_2(t,z)=e^{\gamma z}F_2(t,z),$
and all corresponding other I.C. and B.C. are zeros.

Eliminating one of the variables in equations ($A.4$) and ($A.5$), one can get the following independent equations:

$$\frac{\partial^4 W(t,z)}{\partial t^4}+\frac{1}{\alpha^2}\frac{\partial^2 W(t,z)}{\partial t^2}=\frac{1}{\alpha^2}\tilde{\psi}_1(t,z), \qquad (A.6)$$

$$\frac{\partial^4 V(t,z)}{\partial t^4}+\frac{1}{\alpha^2}\frac{\partial^2 V(t,z)}{\partial t^2}=\frac{1}{\alpha^2}\tilde{\psi}_2(t,z) \qquad (A.7)$$

where,

$$\tilde{\psi}_1(t,z) = \frac{\partial\, G_2(t,z)}{\partial z} - \alpha \frac{\partial^2 G_1(t,z)}{\partial t^2} \qquad (A.8)$$

$$\tilde{\psi}_2(t,z) = \alpha \frac{\partial^2 G_2(t,z)}{\partial t^2} + \frac{\partial\, G_1(t,z)}{\partial z} \qquad (A.9)$$

Using the eigenfunction expansion technique, the following solution expressions are obtained:

$$\psi(t,z) = e^{-\gamma z} \sum_{n=0}^{\infty} T_n(z) \sin\left(\frac{n\,\pi}{T}\right) t \qquad (A.10)$$

$$\phi(t,z) = e^{-\gamma z} \sum_{n=0}^{\infty} \tau_n(z) \sin\left(\frac{n\,\pi}{T}\right) t \qquad (A.11)$$

where $T_n(z)$ and $\tau_n(z)$ can be got through the applications of initial conditions and then solving the resultant second order differential equations using the method of variational of parameter [Staliunas,1994]. The final expressions can be got as the following :

$$T_n(z) = \left(C_1 + A_1(z)\right) \sin \beta_n z + \left(C_2 + B_1(z)\right) \cos \beta_n z \qquad (A.12)$$

$$\tau_n(z) = \left(C_3 + A_2(z)\right) \sin \beta_n z + \left(C_4 + B_2(z)\right) \cos \beta_n z \qquad (A.13)$$

where,

$$\beta_n = \alpha \left(\frac{n\,\pi}{T}\right)^2 \qquad (A.14)$$

$$A_1(z) = \frac{1}{\beta_n} \int \tilde{\psi}_{1n}(z\,;n) \sin(\beta_n z)\, dz \qquad (A.15)$$

$$B_1(z) = \frac{-1}{\beta_n} \int \tilde{\psi}_{1n}(z\,;n) \sin(\beta_n z)\, dz \qquad (A.16)$$

$$A_2(z) = \frac{1}{\beta_n} \int \tilde{\psi}_{2n}(z\,;n) \cos(\beta_n z)\, dz \qquad (A.17)$$

$$B_2(z) = \frac{-1}{\beta_n} \int \tilde{\psi}_{2n}(z\,;n) \cos(\beta_n z)\, dz \qquad (A.18)$$

in which,

$$\tilde{\psi}_{1n}(z\,;n) = \frac{2}{T}\int \tilde{\psi}_1\,(t\,,z)\sin\left(\frac{n\,\pi}{T}t\right)dt \qquad (A.19)$$

$$\tilde{\psi}_{2n}(z\,;n) = \frac{2}{T}\int \tilde{\psi}_2\,(t\,,z)\sin\left(\frac{n\,\pi}{T}t\right)dt \qquad (A.20)$$

The following conditions should also be satisfied:

$$C_2 = \frac{2}{T}\int_0^T f_1(t)\sin\left(\frac{n\,\pi}{T}t\right)dt - B_1(0) \qquad (A.21)$$

$$C_4 = \frac{2}{T}\int_0^T f_2(t)\sin\left(\frac{n\,\pi}{T}t\right)dt - B_2(0) \qquad (A.22)$$

finally the following solution is obtained:

$$u(t\,,z) = \psi(t\,,z) + \,i\,\phi(t\,,z) \qquad (A.23)$$

Or

$$|u(t\,,z)|^2 = \psi^2(t\,,z) + \;\phi^2(t\,,z) \qquad (A.24)$$

The general linear case solution is considered at $\varepsilon = 0$ as zero order approximation for cubic nonlinear homogeneous, cubic nonlinear non homogeneous Schrodinger equations and quintic nonlinear homogeneous Schrodinger equations.

References

[1] A. Degasperis, “The nonlinear Schrödinger Hierarchy in perturbation theory”. Physica D: Nonlinear Phenomena (1995),87(1-4): 151-154.

[2] Abdullaev F. and Granier J. Solitons in media with random dispersive perturbations. Physica D (1999), 134: 303-315.

[3] Ablowitz MJ and Ladik JF, *J Math Phys* (1975), 16: 598 .

[4] Ablowitz MJ and Ladik JF, J Math Phys (1976), 17: 1011 .

[5] Ablowitz MJ, Segur H, J Fluid Mech (1979), 92: 691 .

[6] Ablowitz MJ, Segur H, Solitons and the Inverse Scattering Transform, SIAM (1981) , 4.

[7] Ablowitz MJ and Clarkson PA, Solitons, Nonlinear Evolution Equations and Inverse Scattering, London Math Soc Lecture Notes Series, Cambridge Univ Press (1991), 149.

[8] Ablowitz MJ, Biondini G, Chakravarty S, Jenkins RB, Optics Letters (1996), 21: 1646 .

[9] Ablowitz MJ, Biondini G, Blair S, Phys Lett A (1997), 236: 520 .

[10] Ablowitz MJ and Biondini G, Optics Letters (1998), 23: 1668 .

[11] Ablowitz MJ, Ohta Y, Trubatch AD, Phys Lett A (1999), 253: 287 .

[12] Ablowitz MJ, Biondini G, Blair S, Phys Rev. E (2001a), 63: 046605 .

[13] Ablowitz MJ, Hirooka T and Biondini G, Optics Letters (2001b), 26: 459 .

[14] Ablowitz MJ and Hirooka T, *JOSAB* (2002), 19: 425 .

[15] Ablowitz MJ, Hirooka T and Inoue T J. Opt. Soc. Am. B (2002b), 19: 2876 .

[16] Ablowitz MJ, Biondini G, Chakravarty S, Horne RL, J. Opt. Soc. Am. B (2003), 20: 831 .

[17] Ablowitz MJ, Docherty A and Hirooka T, Optics Letters (2003b), 28: 1191

[18] Ablowitz MJ, Musslimani Z, *Phys. Rev. E* (2003), 67: 025601(R) .

[19] Ablowitz MJ, Prinari B, Trubatch AD, “Continuous and Discrete Nonlinear Schrodinger systems”, London Math Soc Lecture Notes Series, Cambridge Univ. Press (2004), 302.

[20] Ablowitz MJ, Prinari B, Trubatch AD, Inv Probl (2004), 20: 1217 .

[21] Ablowitz MJ, Bakirtas I, Ilan B, Physica *D* (2005), 207: 230 .

[22] Agrawal GP, “Nonlinear Fiber Optics”, Third Edition. Academic Press, New York (2001).

[23] Anastassiou C, Segev M, Steiglitz K, Giordmaine MA, Mitchell M, Shih M, Lan S, Martin J, Phys. Rev. Lett. (1999), 83:2332 .

[24] Bartosz Reichel, Sergey Leble, “On convergence and stability of a numerical scheme of Coupled Nonlinear Schrödinger Equations”. Computers & Mathematics with Applications (2008), 55(4):745-759 .

[25] Belokolos ED, Bobenko AI, Enolski VZ, Its AR, Matveev VB, " Algebro-geometric approach in the theory of integrable equations" Springer, Berlin (1994).
[26] Benney DJ, Newell AC, J Math Phys (1967), 46: 133 .
[27] Benney DJ, Roskes GJ, Studies App Math (1969), 48: 377 .
[28] Biswas A. and Milovic D. Bright and dark solitons of generalized Schrodinger equation. Communications in nonlinear Science and Numerical Simulation. To appear.
[29] Bruneau C., Menza L., and Lehner T. "Numerical resolution of some nonlinear Schrodinger – like equations in plasmas". Numer. Math. PDEs (1999), 15: 672-696 .
[30] Calogero F, Degasperis A Spectral Transform and Solitons. I Amsterdam: North-Holland, (1982) .
[31] Carretero R., Talley J.D., Chong C. and Malomed B.A. Multistable solitons in "the cubic-quintic discrete nonlinear Schrodinger equation". Physics letter A (2006), 216: 77-89 .
[32] Cazenave T. and Lions P. "Orbital stability of standing waves for some nonlinear Schrodinger equations". Commun. Math. Phys. (1982),85: 549-561 .
[33] Chaoqing Dai, Yueyue Wang, Caijie Yan, "Chirped and chirp-free self-similar cnoidal and solitary wave solutions of the cubic-quintic nonlinear Schrödinger equation with distributed coefficients". Optics communications, In Press, Corrected Proof, Available online (2009)
[34] Corney J.F. and Drummond P. Quantum noise in Optical fibers.II.Raman Jitter in soliton communications. J. Opt.Soc.Am.B (2001), 18 :153-161 .
[35] Chen M, Tsankov MA, Nash JM and Patton CE, Phys. Rev. *A* (1994), 49: 12773 .
[36] Chiao RY, Garmire E, Towner CH, Phys Rev Lett (1964), 15: 479 .
[37] Christodoulides DN and Joseph RI, Optics Lett (1988), 13: 794 .
[38] D.Cai and D.W. McLaughlin ''Chaotic and turbulent behavior of unstable One-dimensional nonlinear dispersive waves", J. MATH. Phys. (2000), 41: 4125-4153 .
[39] Davey A, Stewartson K, *Proc Royal Soc Lon Series A* (1974), 338: 101
[40] Davydov AS, *J Theor Biol* (1973), 38: 559 .
[41] Debussche A. and Menza L. "Numerical resolution of stochastic focusing NLS equations". Applied mathematics letters (2002), 15: 661-669 .
[42] Debussche A. and Menza L. "Numerical simulation of focusing stochastic nonlinear Schrodinger equations". Physica D (2002), 162 :131-154 .
[43] Efremidis NK, Christodoulides DN, Fleischer JW, Cohen O, Segev M, Phys. Rev. Lett. (2003), 91: 213906 .

[44] Eilbeck JC, Lomdhal PS, Scott AC, Phys Rev B (1984), 30: 4703 .
[45] Eilbeck JC, Lomdhal PS, Scott AC, Physica *D* (1985), 16: 318 .
[46] Eilbeck JC, Johansson M, Proceedings of the Third Conference "Localization and Energy Transfer in Nonlinear Systems"*, Edts. Vasquez* et al*, World Scientific Pu.Co.* (2003), *p. 44* .
[47] Eisenberg HS, Silberberg Y, Morandotti R, Boyd AR, and Aitchison JS, *Phys Rev Lett* (1998), 81: 3383
[48] El-Tawil A. and El-Hazmy A. "Perturbative nonlinear Schrodinger equations under variable group velocity dissipation". Far East Journal math. Sciences (2007), 27 : 419 – 430 .
[49] El-Tawil A. and El Hazmy A. ''On perturbative cubic nonlinear Schrodinger equations under complex non-homogenities and complex intial conditions". Journal Differential Equations and Nonlinear Mechanics (2009), Article ID 395894: doi:10.1155/2009/395894 .
[50] Emmanuel Yomba, "Generalized hyperbolic functions to find soliton-like solutions for a system of coupled nonlinear Schrodinger equations". Physics Letters A (2008), 372(10): 1612-1618 .
[51] F. Azzouzi, H. Triki, K. Mezghiche and A. El Akrmi "Solitary wave solutions for high dispersive cubic-quintic nonlinear Schrodinger equation". Chaos, Solitons & Fractals, (2009), 39: 1304-1307 .
[52] Faddeev LD, Takhtajan LA "*Hamiltonian Methods in the Theory of Solitons"* Springer Verlag (1987) .
[53] Faris W.G. and Tsay W.J. Time delay in random scattering. SIAM J. on applied mathematics (1994), 54: 443-455 .
[54] Farlow S., "Partial Differential Equations for scientists and engineers". John Wiely & sons. N.Y. (1982) .
[55] Gabitov IR, Turitsyn SK, *Opt Lett* , (1996), 21: 327 .
[56] Gesztesy F and Holden H, "*Soliton Equations and Their Algebro-Geometric Solutions".* Cambridge Univ Press (2003), 79 .
[57] Ginibre J and Velo G, *J Func Anal* (1979), 32: 1 .
[58] Ginzburg VL, *Sov Phys JETP* (1956), 2: 589 .
[59] Ginzburg VL, Landau LD, *Sov Phys JETP* (1950), 20: 1064 .
[60] Ginzburg VL, Pitaevskii LP, *Sov Phys JETP* (1958), 7: 858 .
[61] Gordon JP, Haus HA *Opt Lett* (1986), 11: 665 .
[62] Gordon JP, Mollenauer LF *Opt Lett* (1990), 15: 1351 .
[63] Green, P.D., Milovic, D.M., Lott D.A., and Biswas, A. "Dynamics of Gaussian optical solitons by collective variables method". Applied Mathematics & Information Sciences, (2008), 2: 259-273 .
[64] Hasegawa A, Tappert F, App Phys Lett (1973a), 23: 142 .
[65] Hasegawa A, Tappert F, App Phys Lett (1973b), 23: 171 .

[66] Hasegawa A, Kodama Y, *Solitons in Optical Communciations* Oxford (1995).
[67] Haung D. and et al. Explicit and exact traveling wave solution for the generalized derivative Schrodinger equation. Chaos, Solitons and Fractals (2007), 31: 586-593 .
[68] Jia-Min Zhu, Zheng-Yi Ma, "Exact solutions for the cubic–quintic nonlinear Schrödinger equation". Chaos, Solitons & Fractals (2007), 33(3): 958-964 .
[69] Jin-Liang Zhang, Bao-An Li, Ming-Liang Wang ,"The exact solutions and the relevant constraint conditions for two nonlinear Schrödinger equations with variable coefficients". Chaos, Solitons & Fractals, (2009), 39: 858-865 .
[70] Jun Hirata, "A positive solution of a nonlinear Schrödinger equation with G-symmetry". Nonlinear Analysis: Theory, Methods & Applications (2008), 69(9): 3174-3189 .
[71] Juan Belmonte-Beitia, Gabriel F. Calvo ,"Exact solutions for the quintic nonlinear Schrödinger equation with time and space modulated nonlinearities and potentials". Physics Letters A, (2009), 373: 448- 453 .
[72] Juan Belmonte-Beitia, Vladimir V. Konotop, Víctor M. Pérez-García, Vadym E. Vekslerchik, " Localized and periodic exact solutions to the nonlinear Schrödinger equation with spatially modulated parameters: Linear and nonlinear lattices". Chaos, Solitons & Fractals (2009), 41(3): 1158-1166 .
[73] L. F. Mollenauer and K. Smith, ''Demonstration of soliton transmission over more than 4000km in fiber with loss periodically compensated by Raman gain", Optics Letters,(1988),13: 8 .
[74] Laedke EW, Spatschek KH, Turitsyn SK, Phys Rev Lett (1994), 73: 1055 .
[75] Lott, D.A., Henriques, A., Sturdevant, B.J.M., and Biswas, A. A numerical study of optical soliton-like structures resulting from the nonlinear Schrodinger's equation with square-root law nonlinearity. Applied Mathematics and Computation, (2009), 207: 319-326 .
[76] Lott, D.A., Antman, S.S., Szymczak, W.Z., The quasilinear wave equation for antiplane shearing of nonlinearly elastic bodies, J. Comp. Phys., (2001) 171:201-226 .
[77] Lushnikov PM, *Opt. Lett.* (2001), 26: 1535 .
[78] Ismail M.S., "Numerical solution of coupled nonlinear Schrödinger equation by Galerkin method". Mathematics and Computers in Simulation (2008), 78(4): 532-547 .
[79] El-Tawil A. Magdy, El Zoheiry H. and Nasr E. Sherif "Nonlinear Cubic Homogeneous Schrodinger Equations with Complex Intial Conditions, Limited Time Response", The Open Applied mathematics Journal, (2010), 4: 1-12
[80] Manakov SV, *Sov Phys JETP*(1974), 38: 248 .
[81] Mañas M, *J Phys A: Math Gen*(1996), 29: 7721 .

[82] Matveev VB, Salle MA, *Darboux transformations and solitons*, Berlin (1991).
[83] Menyuk CR, *IEEE J Quant Elect* (1987), 23: 174 .
[84] Menyuk CR, *J Eng Math.* (1999), 36: 113 .
[85] Merle F and Raphael P, *Inventiones Mathematicae* (2004), 156: 165 .
[86] Mezentsev VK, Musher SL, Ryzhenkova IV, Turitsyn SK, *JETP Lett*(1994), 60: 29 .
[87] Molleneauer LF and Gordon JP *Solitons in Optical Fibers: Fundamental and Applications to Telecommunications* Academic Press, London, (2006) .
[88] Molleneauer LF, Stolen RH, Gordon JP *Phys Rev Lett* (1980), 45: 1095 .
[89] Novikov SP, Manakov SV, Pitaevskii LP, Zakharov VE *Theory of Solitons. The Inverse Scattering Method* New York: Plenum, (1984) .
[90] Papanicolaou GC, Sulem C, Sulem PL, Wang XP, *Physica D* (1994), 72: 61
[91] Parsezian K. and Kalithasan B. Cnoidal and solitary wave solutions of the coupled higher order nonlinear Schrodinger equations in nonlinear optics. Chaos, Solitons and Fractals (2007), 31: 188-196 .
[92] Pethick CJ and Smith H "*Bose- Einstein Condensation in Dilute Gases"*, Cambridge University Press (2002) .
[93] Pipes L. and Harvill L. "Applied mathematics for engineers and physicists", McGraw –Hill, Tokyo (1970) .
[94] Prinari B, Ablowitz MJ, Biondini G, *J Math Phys* (2006), 47: 063508 .
[95] R. Beech, F. Osman, ''Effects of Higher Order Dispersion Terms in the Nonlinear Schrödinger Equation", American J. App. Sci., (2005), 2: 1356-1369 .
[96] R. Jordan, B. Turkington, and C. Zirbel, ''A mean field statistical theory for the nonlinear Schrodinger equation'', Physica D (2000), 137:353–378 .
[97] R. Moussa, S. Goumri-Said, H. Aourag, "Unperturbed and perturbed nonlinear Schrödinger system for optical fiber solitons". Physics Letters A (2000), 266(2-3): 173-182 .
[98] Roskes GJ, *Stud App Math* (1976), 55: 231 .
[99] Ruiyu Hao, Lu Li, Zhonghao Li, Wenrui Xue, Guosheng Zhou, "A new approach to exact soliton solutions and soliton interaction for the nonlinear Schrödinger equation with variable coefficients". *Optics Communications (2004), 236(1): 79-86 .*
[100] Wolfram S. "The Mathematica Book", 4th Edition, ISBN:0521643147, Cambridge University Press, (1999) .
[101] Seenuvasakumaran P., Mahalingam A. and Porsezian K. "Dark solitons in N-coupled higher order nonlinear Schrodinger equations". Communications in nonlinear science and numerical simulation (2008), 13: 1318-1328 .
[102] Sakaguchi H. and Higashiuchi T. Two- dimensional dark soliton in the nonlinear Schrodinger equation. Physics letters A (2006), 39: 647-651.

[103] Soljacic M, Steiglitz K, Sears SM, Segev M, Jakubowski MH, Squier R, *Phys Rev Lett* (2003), 90 :254102 .
[104] Staliunas K. "Vortices and dark solitons in the two-dimensional nonlinear Schrodinger equation". Chaos, Solitons and Fractals (1994), 4: 1783-1796 .
[105] Sturdevant, B.J.M., Lott, D.A., and Biswas, A. "Topological solitons in 1 + 2 dimensions with time-dependent coefficients". Progress In Electromagnetics Research Letters, (2009), 10: 69-75 .
[106] Su WP, Schieffer JR and Heeger AJ, *Phys Rev Lett* (1979), 42: 698 .
[107] Sulem C, Sulem PL, "*The nonlinear Schrodinger equation - Self-focusing and Wave Collapse".* Applied Mathematical Sciences (1999), 139 .
[108] Sun J. and et al. "New conservation schemes for the nonlinear Schrodinger equation". Applied mathematics and computation (2006), 177: 446-451 .
[109] Sweilam N."Variation iteration method for solving cubic nonlinear Schrodinger equation". J. of computational and applied mathematics (2007), 207(1): 377-427.
[110] Talanov VI, Radiophysics (1964), 7: 254 .
[111] Talanov VI, Sov Phys JETP Lett (1965), 109: 138 .
[112] Tsuchida T, Ujino H, Wadati M, J Phys A (1999), 32: 2239 .
[113] Vladyslav Prytula, Vadym Vekslerchik, Víctor M. Pérez-García, " Collapse in coupled nonlinear Schrödinger equations: Sufficient conditions and applications" Physica D: Nonlinear Phenomena (2009), 238(15): 1462-1467 .
[114] Vlasov F, Petrishchev V, Talanov V, Radiophys. Quant. Elec. (1971),14: 1070.
[115] Wang M. and et al, "Various exact solutions of nonlinear Schrodinger equation with two nonlinear terms". Chaos, Solitons and Fractals (2007), 31: 594-601 .
[116] Weinstein MI, *Nonlinearity* (1999), 12: 673 .
[117] Wei-Zhong Zhao, Yong-Qiang Bai, Ke Wu, "Generalized inhomogeneous Heisenberg ferromagnet model and generalized nonlinear Schrödinger equation". Physics Letters A (2006), 352(1-2): 64-68 .
[118] Woo-Pyo Hong, "Modulational instability of optical waves in the high dispersive cubic–quintic nonlinear Schrödinger equation". *Optics Communications (2002), 213: 173-182 .*
[119] Xiang-Jun Chen, Hui-Li Wang, Wa Kun Lam ,"Two-soliton solution for the derivative nonlinear Schrödinger equation with nonvanishing boundary conditions".Physics Letters A, (2006), 353: 185-189 .
[120] Xiao-feng Pang, "The dynamic natures of microscopic particles described by nonlinear Schrödinger equation". Physica B: Condensed Matter (2009), 404(16): 353-2358 .
[121] Xing Lü, Bo Tian, Tao Xu, Ke-Jie Cai and Wen-Jun Liu, . Analytical study of nonlinear Schrodinger equation with an arbitrary linear-time potential in

quasi one dimensional Bose-Einstein condensates. Annals of Physics (2008), 323: 2554-2565 .
[122] Xu L. and Zhang J. “Exact solutions to two higher order nonlinear Schrodinger equations”. Chaos, Solitons and Fractals (2007), 31: 937-942 .
[123] Li Y. and McLaughlin D. W., ‘‘Morse and Melnikov functions for nonlinear Schrodinger equation’’, Commun. Math. Phys. (1994), 162: 175–214 .
[124] Li Y., ‘‘Smale horseshoes and symbol dynamics in perturbed nonlinear Schrodinger equations’’, J. Nonlinear Sci. (1998), 9: 363–415 .
[125] Zai-Dong Li, Qiu-Yan Li, Xing-Hua Hu, Zhong-Xi Zheng, Yubao Sun, “ Hirota method for the nonlinear Schrödinger equation with an arbitrary linear time-dependent potential”. Annals of Physics (2007), 322(11): 2545-2553 .
[126] Zakharov VE, *Sov Phys J App Mech Tech Phys* (1968), 4: 190 .
[127] Zakharov VE, *Sov Phys JETP*(1972), 35: 908 .
[128] Zakharov VE, Shabat AB, *Sov Phys JETP* (1972), 34: 62.
[129] Zakharov VE, Shabat AB, *Sov Phys JETP* (1973), 37: 823 .
[130] Zhu S. “Exact solutions for the high order dispersive cubic- quintic nonlinear Schrodinger equation by the extended hyperbolic auxiliary equation method”. Chaos, Solitons and Fractals (2006), 30: 960-779 .
[131] Zvedzin AK, Popkov AF, *Sov Phys JETP* (1983), 57: 350 .
[132] Zwillinger D. “Handbook of differential Equations”, Third edition. Acadimic Press (1997).

ملخص الرسالة

فى هذه الرسالة ومن خلال تحليل كمى تم إيجاد حلول تقريبية لمعادلات شرودنجر من الدرجتين الثالثة و الخامسة بإستخدام طريقتين مختلفتين- طريقتى الإضطراب وبيكارد - (Perturbation Technique and Picard Approximation). فى البداية تم إثبات أن الحل (إن وجد) سيكون فى صورة متسلسلة قوى فى المتغير (ε). بإستخدام برنامج (Mathematica 5.1) ، تم إيجاد الحلول التقريبية حتى الدرجة الثالثة فقط و ذلك نظراً للحسابات الكثيفة المعقدة من تفاضلات و تكاملات .

تم دراسة تأثير تغيير قيمة الدوال المركبة الخاصة بالشروط الإبتدائية (complex initial conditions) و الحدود المركبة غير المتجانسة (complex nonhomogenity) فى كلٍّ من الحالات التاليه:الدوال الثابتة و الاسية والجيبية.

تم عمل مقارنات بين النتائج التى تم الحصول عليها من الطريقتين (Perturbation Technique and Picard Approximation) على نفس الشكل البيانى و تم توضيح تقارب الحلول و خاصة فى وجود معامل الفقد جاما (γ Dissipation Term) .

تم دراسة تأثير تغير الفترة الزمنية (T) عند ١٠ ، ٢٠ ، ٦٠ وحدة زمنية عند حالات مختلفة كثيرة وتبين استقرار و ثبات الحلول فى وجود معامل الفقد(γ) مع زيادة الفترة الزمنيه (T) .

فى الفصل الأول تم عمل مسح علمى (scientific survey) على بعض أنواع من معادلات شرودنجر غير الخطية و الطرق المختلفة لحلها مع توضيح أهمية هذا النوع من المعادلات و تطبيقاتها المختلفة فى مجالات مختلفة على سبيل المثال: الإتصالات بإستحدام الألياف (Fiber Optic Communications) و الإلكترونيات(Electronics) و الكيمياء الحديثة (Modern Chemistry) و الميكانيكا غيرالخطية (Nonlinear Mechanics) .

فى كلٍّ من الفصل الثانى و الثالث و الرابع تم حل معادلات شرودنجر من الدرجة الثالثة المتجانسة و غير المتجانسة و الدرجة الخامسة المتجانسة على الترتيب باستخدام كلتا الطريقتين (Perturbation Technique and Picard Approximation) مع عمل مقارنات بين النتائج التى تم الحصول عليها من الطريقتين عند حالات دراسة متعددة . فى نهاية كل فصل من هذه الفصول تم دراسة تغيير الفترة الزمنية (T) على الحلول فى كلتا الطريقتين .

فى الفصل الخامس تم تلخيص و إبراز النتائج التى تم التوصل اليها فى كلٍّ من الفصل الثانى و الثالث والرابع مع نبذة مختصرة عن العمل المستقبلى المتعلق بهذا الموضوع .

تحليل كمى لمعادلات شرودنجرالغيرخطية من الدرجة الثالثة و الخامسة

إعداد

مهندس/ **شريف عيد نصر**

رسالة مقدمة الى كلية الهندسة، جامعة القاهرة

كجزء من متطلبات الحصول على درجة الدكتوراه

فى

الريـاضيات الـهندسية

تحت إشراف

أ.د. مجدى عبد العاطى الطويل

أ.د. حنفى الزهيرى **أ.د. لبيب إسكندر**

قسم الرياضيات والفيزيقا الهندسية

كليه الهندسة - جامعة القاهرة

كلية الهندسة، جامعة القاهرة

الجيزة، جمهورية مصر العربية

أبريل ٢٠١٠

تحليل كمى لمعادلات شرودنجرالغيرخطية
من الدرجة الثالثة و الخامسة

إعداد

مهندس/ **شريف عيد نصر**

رسالة مقدمة الى كلية الهندسة، جامعة القاهرة

كجزء من متطلبات الحصول على درجة الدكتوراه

فى

الريـاضيات الـهندسية

كلية الهندسة، جامعة القاهرة

الجيزة، جمهورية مصر العربية

أبريل ٢٠١٠